Magnetic Nanoparticles: Design and Characterization, Toxicity and Biocompatibility, Pharmaceutical and Biomedical Applications

ARTICLE *in* CHEMICAL REVIEWS · OCTOBER 2012

Impact Factor: 46.57 · DOI: 10.1021/cr300068p · Source: PubMed

4 AUTHORS, INCLUDING:

Julien Nicolas
Université Paris-Sud 11
92 PUBLICATIONS **3,759** CITATIONS
SEE PROFILE

Patrick Couvreur
Université Paris-Sud 11
581 PUBLICATIONS **25,582** CITATIONS
SEE PROFILE

CHEMICAL REVIEWS

Review

pubs.acs.org/CR

Magnetic Nanoparticles: Design and Characterization, Toxicity and Biocompatibility, Pharmaceutical and Biomedical Applications

L. Harivardhan Reddy,[†,‡] José L. Arias,[§] Julien Nicolas,[†] and Patrick Couvreur*[,†]

[†]Laboratoire de Physico-Chimie, Pharmacotechnie et Biopharmacie, Université Paris-Sud XI, UMR CNRS 8612, Faculté de Pharmacie, IFR 141, 5 rue Jean-Baptiste Clément, F-92296 Châtenay-Malabry, France

[§]Departamento de Farmacia y Tecnología Farmacéutica, Facultad de Farmacia, Campus Universitario de Cartuja s/n, Universidad de Granada, 18071 Granada, Spain

[‡]Pharmaceutical Sciences Department, Sanofi, 13 Quai Jules Guesdes, F-94403 Vitry-sur-Seine, France

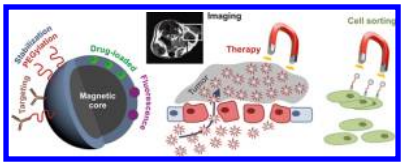

CONTENTS

1. Introduction 5819
2. Design of Magnetic Colloids 5819
2.1. Synthesis Strategies 5819
2.1.1. Electron Beam Lithography 5819
2.1.2. Gas-Phase Deposition 5819
2.1.3. Sol−Gel Method 5819
2.1.4. Oxidation Method 5820
2.1.5. Chemical Coprecipitation 5820
2.1.6. Hydrothermal Method 5821
2.1.7. Flow Injection Method 5822
2.1.8. Electrochemical Method 5822
2.1.9. Aerosol/Vapor-Phase Method 5822
2.1.10. Sonochemical Decomposition Method 5822
2.1.11. Supercritical Fluid Method 5823
2.1.12. Synthesis Using Nanoreactors 5823
2.1.13. Microbial Method 5823
2.1.14. Synthesis of Metal-Doped Iron Oxide Nanoparticles 5823
2.2. Stabilization Procedures 5824
2.2.1. Use of Stabilizing Surface Coating Materials 5824
2.2.2. Encapsulation into Polymeric Shells 5826
2.2.3. Encapsulation into Liposomes 5827
3. Physicochemical Properties and Physicochemical Characterization 5827
3.1. Geometry 5827
3.2. Structure 5827
3.3. Surface Charge 5828
3.4. Surface Thermodynamics 5828
3.5. Magnetism 5829
3.6. Colloidal Stability 5830
4. Pharmacokinetics, Biodistribution, And Biological Fate 5830
4.1. Influence of the Size 5831
4.2. Influence of the Surface Charge 5832
4.3. Influence of the Administration Route 5832
4.4. Factors Influencing the Tissue/Cell Penetration 5833
5. Toxicity and Biocompatibility 5834
5.1. In Vitro Evaluation of the Toxicity 5834
5.1.1. Influence of the Surface Coatings 5834
5.1.2. Influence of the Size 5834
5.1.3. Influence of the Surface Charge 5834
5.2. In Vivo Evaluation of the Toxicity 5835
5.2.1. Toxicity after Intravenous Administration 5835
5.2.2. Toxicity after Intraperitoneal Administration 5836
5.2.3. Toxicity after Subcutaneous Administration 5837
6. Disease Therapy 5837
6.1. Construction of Magnetically Guided Nanoparticles for Drug Delivery 5837
6.2. Chemotherapy 5838
6.2.1. Systemic Chemotherapy 5838
6.2.2. Local Chemotherapy 5842
6.2.3. Oral Delivery 5844
6.2.4. Stimuli-Sensitive Drug Delivery 5844
6.2.5. Miscellaneous Applications 5844
6.3. Magnetofection (Gene Delivery) 5845
6.3.1. In Vitro Magnetofection 5846
6.3.2. In Vivo Magnetofection 5846
6.4. Magnetically Guided Radioimmunotherapy 5847
6.5. Magnetically Guided Photodynamic Therapy 5847
6.6. Magnetic Fluid Hyperthermia 5848
6.6.1. Preclinical Evaluation of Magnetic Fluid Hyperthermia 5848
6.6.2. Clinical Evaluation of Magnetic Fluid Hyperthermia 5850
7. Magnetic Resonance Imaging 5850
7.1. Organ/Tissue Imaging 5850
7.1.1. Lymph Node Imaging 5851
7.1.2. Imaging of Atherosclerotic Plaques 5851
7.1.3. Imaging of Inflammatory Response in Central Nervous System Disorders 5852
7.1.4. Imaging of Macrophage Infiltration in Transplanted Organs 5852
7.1.5. Imaging of Macrophage Infiltration in Knee Joints 5853
7.1.6. Imaging Using Ligand-Functionalized Superparamagnetic Iron Oxide Nanoparticles 5853

Received: February 16, 2012
Published: October 9, 2012

   dx.doi.org/10.1021/cr300068p | *Chem. Rev.* 2012, 112, 5818−5878

8. Cell Labeling and Imaging 5853
8.1. Imaging of Transplanted Stem Cells 5854
8.2. Imaging of Transplanted Pancreatic Islet Cells 5855
8.3. Imaging of Dendritic Cells 5855
8.4. Imaging of Apoptotic Cells 5855
9. Tissue Engineering 5856
9.1. Engineering of Heterotypic Cell/Tissue Constructs 5856
9.2. Scaffold-Based Tissue Engineering 5856
9.3. Scaffold-Free Engineering of Three-Dimensional Tissue Constructs 5857
10. Miscellaneous Applications 5857
10.1. Cell Separation and Cell Sensing 5857
10.1.1. Separation of Bacterial Cells And Mammalian Cells 5858
10.1.2. Separation of Viruses 5859
10.1.3. Magnetic-Relaxation Switches 5859
10.2. Separation of Biochemicals 5859
10.3. Enzyme/Protein Immobilization 5860
10.4. Bioanalysis and Immunoassays 5861
10.5. Separation of Heavy Metal Contaminants from Mixtures 5863
11. Conclusions 5863
Author Information 5864
Corresponding Author 5864
Notes 5864
Biographies 5864
Acknowledgments 5865
Abbreviations 5865
References 5867

1. INTRODUCTION

In recent years, considerable efforts have been spent in the development of magnetic nanoparticles (MNPs), the understanding of their behavior, and the improvement of their applicability in many different areas.[1,2] Precise control over the synthesis conditions and surface functionalization of MNPs is crucial because it governs their physicochemical properties, their colloidal stability, and their biological behavior/fate. For pharmaceutical and biomedical purposes, magnetic platforms should possess very small size and narrow size distribution together with high magnetization values. Additionally, these nanoparticles (NPs) must combine high magnetic susceptibility for an optimum magnetic enrichment and loss of magnetization after removal of the magnetic field. Finally, their optimal surface coating is desired in order to ensure tolerance and biocompatibility, as well as specific localization at the biological target site. MNPs possessing appropriate physicochemistry and tailored surface properties have been extensively investigated for various applications such as drug delivery, hyperthermia, magnetic resonance imaging (MRI), tissue engineering and repair, biosensing, biochemical separations, and bioanalysis. In the field of disease therapy, the development of "theranostics", which facilitates simultaneous drug delivery and imaging, represents an important breakthrough of MNP technology.[3] Currently, various clinical trials are in progress to investigate the potential of different magnetic nanosystems for pharmaceutical and biomedical applications.[1,4,5]

This review will comprehensively describe the synthesis of MNPs, their physicochemical characterization, and their biopharmaceutical performances, including pharmacokinetics, biodistribution, and toxicity. A particular emphasis will be given to their applications in therapy, diagnosis, tissue engineering, and other biomedical applications such as sensing and separation of cells, bacteria and viruses, and analysis of biochemicals and heavy metals.

2. DESIGN OF MAGNETIC COLLOIDS

2.1. Synthesis Strategies

The ferrite colloids, magnetite (Fe_3O_4) and maghemite (γ-Fe_2O_3), are the main representatives of the MNPs, which have received so far considerable attention in the medical and pharmaceutical fields, due to their biocompatibility and their biodegradability.[1,5] These ferrite colloids are characterized by a spinel crystal structure with oxygen ions forming a close-packed cubic lattice and iron ions located at the interstices. The magnetization of Fe_3O_4 arises from antiferromagnetic coupling (superexchange though oxygens) between the Fe^{3+} ions in octahedral and tetrahedral interstices, leaving the magnetic moments of the Fe^{2+} ions (in octahedral positions) as responsible for the magnetization of the unit cell.

The main synthesis pathways proposed for the preparation of Fe_3O_4 NPs are reported as follows:

(1) Physical methods, such as gas-phase deposition and electron beam lithography. These methods, however, suffer from their inability to control the particle size down to the nanometer scale.[6−9]

(2) Wet chemical preparation methods, such as sol−gel synthesis,[10,11] oxidation method,[12,13] chemical coprecipitation,[14,15] hydrothermal reactions,[16,17] flow injection synthesis,[18] electrochemical method,[19,20] aerosol/vapor-phase method,[21,22] sonochemical decomposition reactions,[23,24] supercritical fluid method,[25,26] and synthesis using nanoreactors.[27,28]

(3) Microbial methods, which are generally simple, versatile, and efficient with appreciable control over the composition and the particle geometry of the resulting material.[29−31]

Alternatively, great interest has been recently devoted to the development of metal-doped iron oxides with enhanced magnetic properties. As a consequence, various methods have been proposed for the synthesis of these spinel metal ferrites (MFe_2O_4, where M can be Mn, Fe, Zn, Ni, Co, etc.).[32−34]

2.1.1. Electron Beam Lithography. This physical method frequently involves the conversion of iron particles into iron oxides (i.e., Fe_3O_4) under exposure to a beam of electrons. The electron beam (e-beam) is emitted in a patterned fashion across a surface covered with a film of iron particles, thus leading to the formation of nanosized iron oxide nanoparticles (IONPs).[6−8]

2.1.2. Gas-Phase Deposition. The synthesis procedure leads to one-dimensional iron oxide nanostructures and is based on a catalyst-assisted chemical vapor deposition process of molecular precursors, $[Fe(OBu^t)_3]_2$ or $Sn(OBu^t)_4$, on gold-decorated alumina substrates (Figure 1).[9] The existence of gold particles on the substrate surface catalyzes the one-dimensional growth of the IONPs. The thermal fragmentation of Fe^{3+} species under low pressure partially reduces Fe^{3+} to Fe^{2+} and leads to the formation of nanostructured Fe_3O_4 films at elevated temperatures.[35]

2.1.3. Sol−Gel Method. The sol−gel method, also known as chemical solution deposition, is based on the hydroxylation

dx.doi.org/10.1021/cr300068p | Chem. Rev. 2012, 112, 5818−5878

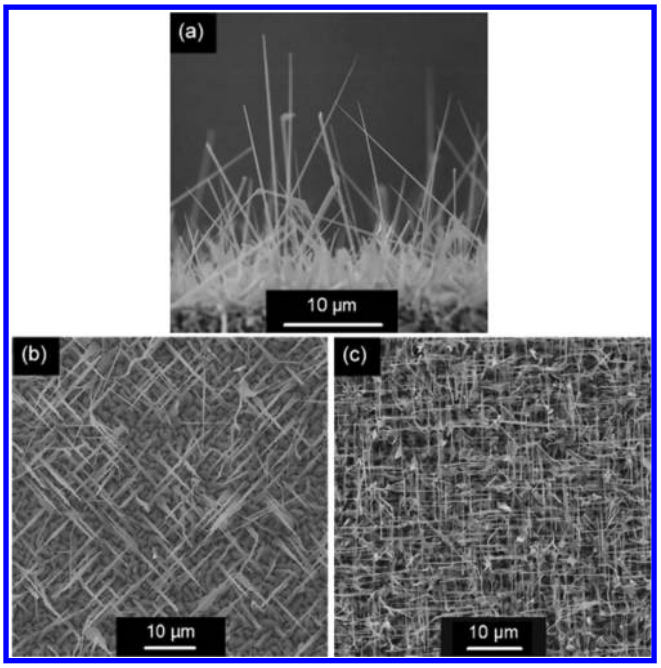

Figure 1. Scanning electron microscopy (SEM) images of 1D Fe_3O_4 nanostructures on polycrystalline alumina (a) and single-crystal MgO substrates grown at 825 °C (b) and 800 °C (c). Reprinted with permission from ref 9. Copyright 2008 Wiley.

and condensation of precursors in a solution phase to yield a sol of nanosized particles. Condensation and inorganic polymerization of the sol lead to the formation of a gel made of a three-dimensional metal oxide network. The crystalline state will be obtained then upon heat treatment of the gel.[10,11] The control over the characteristics and structure of the gel can be easily obtained by fixing the hydroxylation and condensation conditions, as well as the kinetics of the growing process. In particular, the pH, the temperature, the nature and concentration of the salt precursors, and the nature of the solvent have been described to influence the synthesis process.[11,36,37] The main advantages of this method rely on the achievement of a good control of both the particle structure and size (with low particle size distributions) (Figure 2).

The optimization of the synthesis procedure can be easily carried out by the incorporation of surfactants in the solution phase. As a result, nucleation and crystal growth will be adequately controlled, the aggregation of the insoluble metal will be avoided, and the resulting NP dispersion will be stabilized. However, the use of surfactants may alter the surface morphology and surface charge of the NPs, even though the crystal structure is not altered.[38] Alternatively, the use of polyols (e.g., ethylene glycols such as mono-, di-, tri-, and poly(ethylene glycol), propylene glycol, etc.) was suggested to control the particle growth, to ensure a high degree of crystallinity of the so-formed NPs, and to prevent interparticle aggregation. Practically, NP formation occurs when the metal precursor is suspended in polyol and heated up to its boiling point, under stirring. Polyols generally offer attractive properties: they act as solvents for inorganic compounds due to their high dielectric constants, and they offer a wide operating-temperature range for preparing inorganic compounds owing to their relatively high boiling point.[39−41] Finally, the addition of small amounts of Pt or Ag salts facilitates the formation of small-sized particles which then favors a heterogeneous nucleation.[42,43]

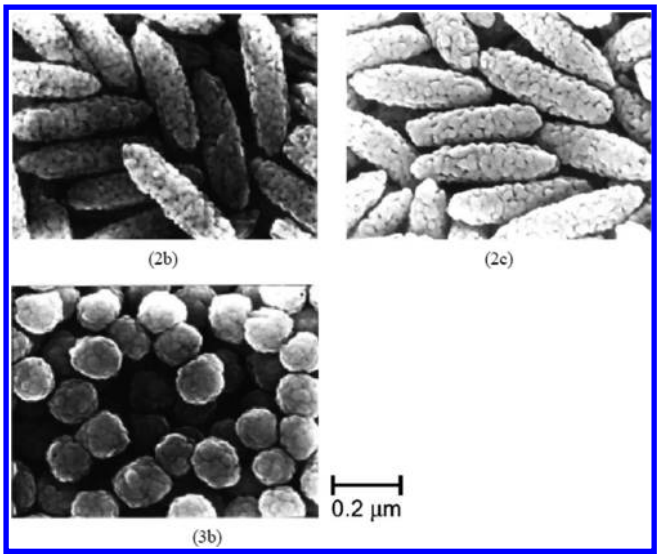

Figure 2. SEM photographs of ellipsoidal polycrystal Fe_3O_4 (2b) and γ-Fe_2O_3 (2c) particles, as well as of spherical Fe_3O_4 particles (3b). Reprinted with permission from ref 11. Copyright 2003 Elsevier.

2.1.4. Oxidation Method. This wet chemical preparation method for the synthesis of small-sized ferrite colloids (i.e., Fe_3O_4) by crystallization starting from the ferrous hydroxide gels involves partial oxidation of the Fe(II) hydroxide suspensions with different agents (e.g., nitrate ions).[12,13,44−46] The synthesis of monodisperse γ-Fe_2O_3 NPs can be achieved by oxidizing Fe_3O_4 NPs at 90 °C in a solution of ferric nitrate.[47]

2.1.5. Chemical Coprecipitation. The coprecipitation process in aqueous solution is perhaps the simplest and the most efficient chemical pathway to synthesize superparamagnetic iron oxide nanoparticles (SPIONs) (average diameters are typically below 50 nm) (Figure 3).[48,49]

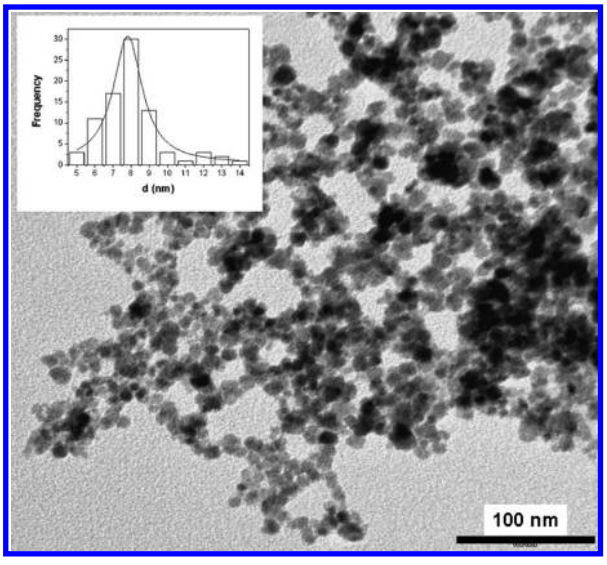

Figure 3. Transmission electron microscope (TEM) picture of nanometer Fe_3O_4 particles obtained by coprecipitation in solution. Insert: size histogram. Bar length: 100 nm. Reprinted with permission from ref 49. Copyright 2007 Elsevier.

dx.doi.org/10.1021/cr300068p | *Chem. Rev.* 2012, 112, 5818−5878

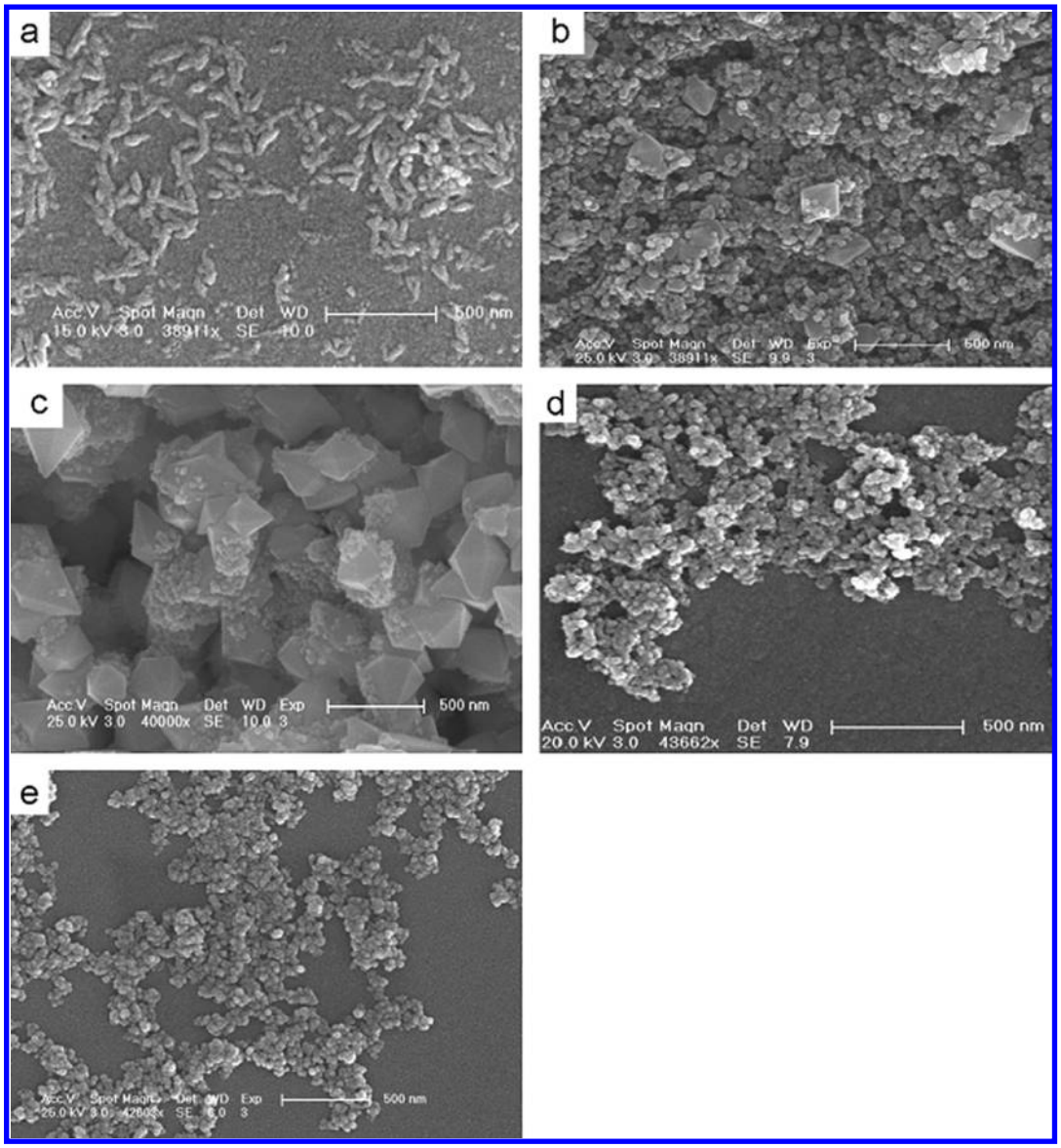

Figure 4. SEM images of magnetic nanocrystals obtained at (a) 180 °C, 5 h; (b) 180 °C, 15 h; (c) 120 °C, 10 h; (d) 80 °C, 10 h; and (e) 180 °C, 10 h, ethanol as the reaction medium. Reprinted with permission from ref 17. Copyright 2008 Elsevier.

The method is based on the chemical reactions carried out in an aqueous monophasic liquid medium, allowing both the nucleation and growth of iron hydroxide nuclei to be controlled.[14,15,48,49] The synthesis procedure consists of the precipitation of ferric and ferrous hydroxides by addition of a base (e.g., NH_4OH or NaOH) to a solution of Fe(III) and Fe(II) salts (eq 1). Then, the gelatinous iron hydroxide precipitate is isolated by magnetic decantation or centrifugation and treated with concentrated base or acid solutions to electrostatically stabilize the ferrofluid. Alternatively, the iron hydroxide precipitate can be sterically stabilized to the resulting Fe_3O_4 or other ferrites by heating in the presence of a suitable surfactant, e.g., oleic acid (OA).

$$Fe^{2+} + 2Fe^{3+} + 8OH^- \rightarrow Fe_3O_4 + 4H_2O \quad (1)$$

Depending on the stoichiometric mixture of ferrous and ferric salts in the aqueous medium and on other experimental conditions [e.g., ionic strength and pH of the medium, presence of oxygen, injection fluxes, nature of the salts (perchlorates, chlorides, sulfates, or nitrates), temperature, nature and concentration of the alkali medium, or nature of the surfactant], iron oxide particles with suitable diameter, magnetic responsiveness, and surface properties can be obtained.[14]

2.1.6. Hydrothermal Method. The hydrothermal synthesis method is used to synthesize MNPs in aqueous media in reactors or autoclaves at high temperature (i.e., >200 °C) and high pressure (i.e., >13 790 kPa).[16,17,50] High temperatures result in rapid nucleation and faster growth of the newly formed particles, leading to the formation of small-sized NPs. Two main routes were adopted for achieving NPs under hydrothermal conditions: (i) hydrolysis and oxidation and (ii) neutralization of mixed metal hydroxides. With the hydrothermal techniques, it is possible to control the geometry of the NPs after optimization of the experimental parameters such as the reaction time, the temperature, the reactants concentration and stoichiometry, the nature of the solvent, the precursors, the complexing strength, and the addition of seeding agents (Figure 4).

A wrap−bake−peel process has also been developed for the synthesis of IONPs using the thermal hydroxylation technique,

dx.doi.org/10.1021/cr300068p | *Chem. Rev.* 2012, 112, 5818−5878

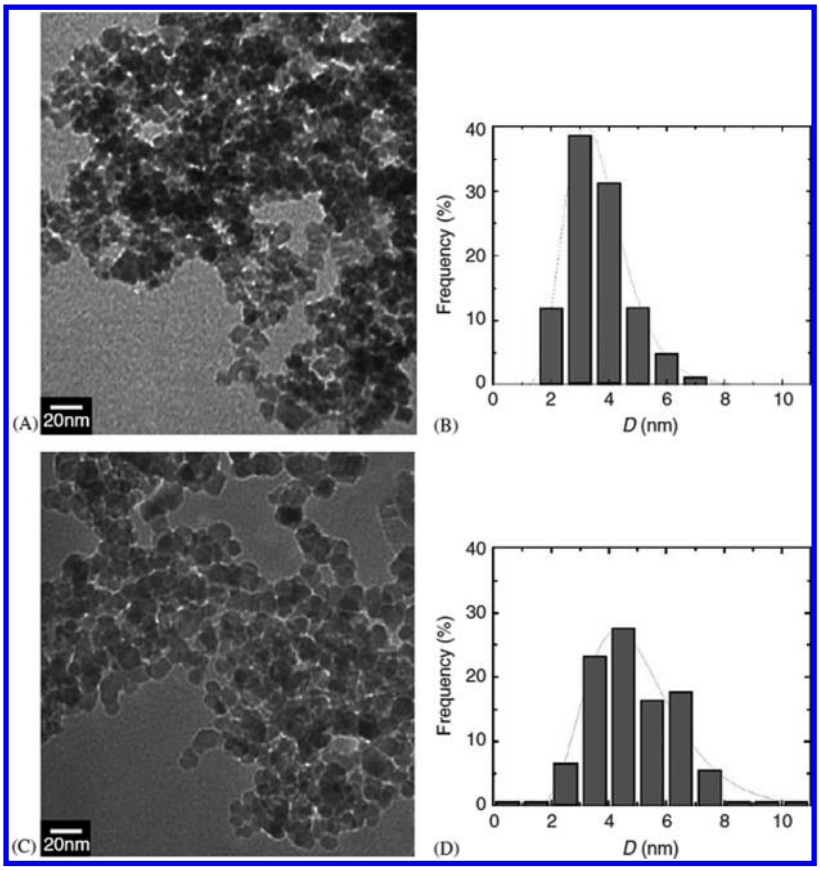

Figure 5. TEM pictures and respective particle size distribution diagrams for IONPs prepared by continuous flow injection (A and B) and batch methods (C and D). Reprinted with permission from ref 18. Copyright 2006 Elsevier.

based on the principle of transformation of material phases at increased temperatures. The fabrication process sequentially involved the following steps: (i) synthesis of akaganeite (β-FeOOH) NPs by heating (at 80 °C) a 0.02 M $FeCl_3$ aqueous solution under mechanical stirring for 12 h; (ii) coating of thin silica (SiO_2) shell onto the NPs to obtain β-FeOOH/SiO_2 core/shell NPs; and (iii) calcination of the core/shell structure in air followed by heat treatment, and then etching of the SiO_2 shell by sonication in a NaOH solution to obtain hollow nanocapsules. During the fabrication, the coated SiO_2 shell served to prevent particle aggregation as well as to avoid the collapse of the surface pores formed during the formation of the nanocapsules. Depending on the heat treatment conditions, hollow nanocapsules of either haematite (α-Fe_2O_3) or Fe_3O_4 could be produced.[51]

2.1.7. Flow Injection Method. Flow injection synthesis consists of continuous or segmented mixing of reagents under a laminar flow regime in a capillary reactor.[18] This technique exhibits significant advantages such as a good reproducibility and a high mixing homogeneity together with a precise control of the process. Fe_3O_4 NPs having a narrow size distribution in the range of 2−7 nm were obtained using this method (Figure 5).

2.1.8. Electrochemical Method. The electrochemical method carried out under oxidizing conditions can also be used to synthesize IONPs.[19,20] For instance, γ-Fe_2O_3 and Fe_3O_4 particles of 3−8 nm have been prepared from an iron anode and platinum foil as cathode, by using a solution of tetraoctylammonium bromide in *N*,*N*-dimethylformamide as the supporting electrolyte. Finally, the resulting NPs were stabilized by a cationic surfactant. The control of the particle size could be successfully achieved by varying the current density.[52]

2.1.9. Aerosol/Vapor-Phase Method. This method involves the vaporization onto a substrate of an organic solution containing ferric salts and a reducing agent (also known as spray pyrolysis).[21,22,53,54] The resulting fine droplets are transformed into NPs (whose size depends on the droplet size), following the evaporation of the organic solvent. Alternatively, a laser may be used to heat a gaseous mixture of iron precursor (e.g., iron pentacarbonyl). This route is also known as laser pyrolysis. The reaction is performed continuously into generators in order to reach high yields. For instance, magnetic composites of Fe-based NPs encapsulated into carbon/SiO_2 or carbon matrices have been formulated by laser-induced pyrolysis of aerosol.[55]

2.1.10. Sonochemical Decomposition Method. The so-called sonolysis technique facilitates the formation of IONPs with narrow particle size distribution starting from an organometallic precursor.[23,24,56−60] Basically, 10-nm-sized Fe_3O_4 particles can be synthesized from iron(II) acetate [$Fe(C_2H_3O_2)_2$] in double distilled deoxygenated water. The IONPs are obtained by irradiating the solution with a high-intensity ultrasonic horn under 1.5 atm of argon at room temperature for at least 3 h.[61] The control of the particle size can be achieved by changing the metal precursor used for the NP formation or by varying the temperature. In the latter case, the MNPs can be generated by subjecting a $Fe(CO)_5$ [or $Co_2(CO)_8$] solution in hydrocarbons (e.g., toluene) to a very high temperature (thermal decomposition process), resulting in

dx.doi.org/10.1021/cr300068p | *Chem. Rev.* 2012, 112, 5818−5878

hot spots generated by the rapid collapse of the sonically generated cavities. This allows the conversion of the ferrous salt into MNPs. In this approach, oleylamine and OA are used as stabilizers that additionally permit the surface functionalization of the NPs with hydrophilic (or amphiphilic) polymers.[62]

2.1.11. Supercritical Fluid Method. Supercritical fluid (SCF) technology has also been proposed for manufacturing IONPs in a controlled fashion with desired geometry.[26,63] A SCF is a substance that exists as a single phase above its critical pressure and temperature. Some examples of SCFs being used in nanomaterial production are trifluoromethane, chlorodifluoromethane, acetone, carbon dioxide, diethyl ether, propane, nitrous oxide, and water.[25,38] However, the nontoxic and nonflammable nature of supercritical carbon dioxide, along with the mild critical conditions needed in its use (i.e., ~8300 kPa and ~35 °C), determine its extensive use in pharmaceutical processing.[26,64] Alternatively, supercritical H_2O has also been used in the preparation of α-Fe_2O_3 and Fe_3O_4. In this case, the critical conditions to be fixed are ~22.11 MPa and ~374.3 °C.[26,65]

Employing the SCF method for the synthesis of IONPs allows the use of organic solvents to be avoided, thus representing a green chemistry approach. This technique yields efficient control of the particle size by maintaining the appropriate molar ratio of the starting material [i.e., $Fe(NO_3)_3$] to the surface modifier (i.e., decanoic acid, OA, or hexaldehyde).[38,65]

2.1.12. Synthesis Using Nanoreactors. Nanoreactors have been employed to synthesize MNPs of well-defined dimensions. In these confined-space conditions, the particle growth can be perfectly controlled.[27,28] For instance, water-in-oil emulsions have served as nanoreactors to synthesize SPIONs with a narrow size range and uniform physical properties. This template is formed by well-defined nanodroplets corresponding to the internal aqueous phase of the emulsion, stabilized by a surfactant in the continuous oil/hydrocarbon phase. The main advantage of this approach is the possibility to precisely control the NP size by monitoring the diameter of the inner aqueous droplets, the pH, the surfactant, and the reducing agents used, as well as the concentration and type of metal ions employed.[4] Other attempts to obtain IONPs of well-defined size include the use of amphoteric surfactants (which form water-swollen reversed micellar structures in nonpolar solvents),[66] cyclodextrins,[67] dendrimers,[68] phospholipid membranes (which form vesicles),[69] and apoferritin protein cages,[70] serving here as solid supports.[1] This route also allows the preparation of iron, ferrites, Fe alloys, and also metal (Fe, Co) NPs coated by layers of noble metals (e.g., gold), in order to protect the cores from oxidation and to functionalize their surface for further biomedical applications.[71−73]

2.1.13. Microbial Method. Large-scale production of Fe_3O_4 NPs employing microbial processes has recently been demonstrated.[29−31] This approach ensures high yield, good reproducibility, and good scalability, as well as low cost, but requires low temperature and low energy (Figure 6), contrary to the previously described methods. Fe(III)-reducing bacteria such as *Thermoanaerobacter* species (i.e., *Thermoanaerobacter ethanolicus* strain TOR 39) and *Shewanella* species (e.g., Shewanella loihica strain PV-4) possess the ability of synthesizing Fe_3O_4 NPs under anaerobic conditions.[30] The fermentation is carried out by incubation of a β-FeOOH precursor ($M_xFe_{1-x}OOH$, where M is a metal) with the bacteria while

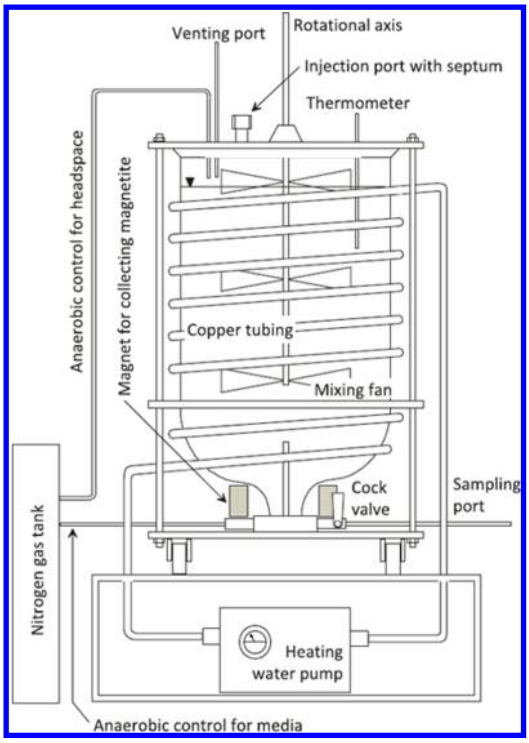

Figure 6. Schematic representation of the 35 L reactor for large-scale fermentative production of Fe_3O_4 NPs. Reprinted with permission from ref 31. Copyright 2010 Springer.

maintaining the temperature at 65 °C from several days up to 3 weeks by intermittent addition of electron donors such as glucose. The microbial process is capable of producing 5−90-nm-sized particles.

2.1.14. Synthesis of Metal-Doped Iron Oxide Nanoparticles. The development of metal-doped iron oxides with enhanced magnetic properties is currently under extensive investigation. Various methods have been proposed for the synthesis of MFe_2O_4 (where M can be Mn, Fe, Zn, Ni, Co, etc.).[32−34,74] For instance, a high-temperature, nonhydrolytic reaction between the divalent metal chloride and the iron tris-2,4-pentadioate in the presence of surfactants, and further coating with 2,3-dimercaptosuccinic acid (DMSA), resulted in the formation of single-crystalline, monodisperse NPs exhibiting high colloidal stability under a broad range of pH (pH 6−10) and also in serum.[74] Another class of MNPs, namely, heterodimer MNPs (e.g., heterodimer NPs of FePt−Au), have been synthesized by successive heating at different temperatures (up to 300 °C) a mixture of $Pt(acetylacetone)_2$, $Fe(CO)_5$, OA, and oleylamine, followed by ethanol treatment to obtain FePt NPs. These NPs were then mixed with AuCl and hexadecylamine and heated up to 70 °C followed by precipitation in ethanol to obtain FePt−Au NPs. Further coating of these particles with dihydrolipoic acid−poly(ethylene glycol)−OH opened an avenue to surface functionalization with biomolecules such as neutravidin or HmenB1 antibody (selective to prostate-specific antigen) for imaging applications.[75] Different functionalities were given to these nanosystems: (i) catalytic effects of FePt for heteroepitaxial Au growth; (ii) high aqueous solubility and biocompatibility through versatile ligand chemistry of Au−S linkages; (iii) Au for chip-based biosensing; and (iv) magnetic resonance contrast effects of superparamagnetic FePt. Likewise, NPs of iron carbides, wrapped in multilayered graphitic sheets (carbon

dx.doi.org/10.1021/cr300068p | *Chem. Rev.* 2012, 112, 5818−5878

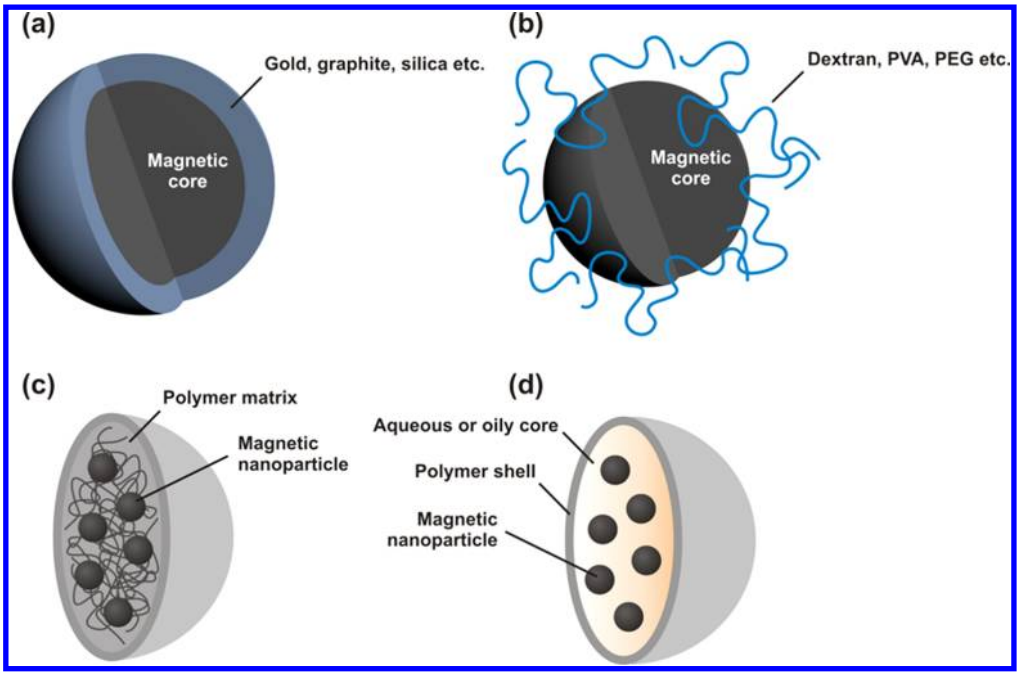

Figure 7. Schematic representation of the stabilization of MNPs by surface coating with inorganic (a) or organic materials (b) or by encapsulation into nanospheres (c) or nanocapsules (d).

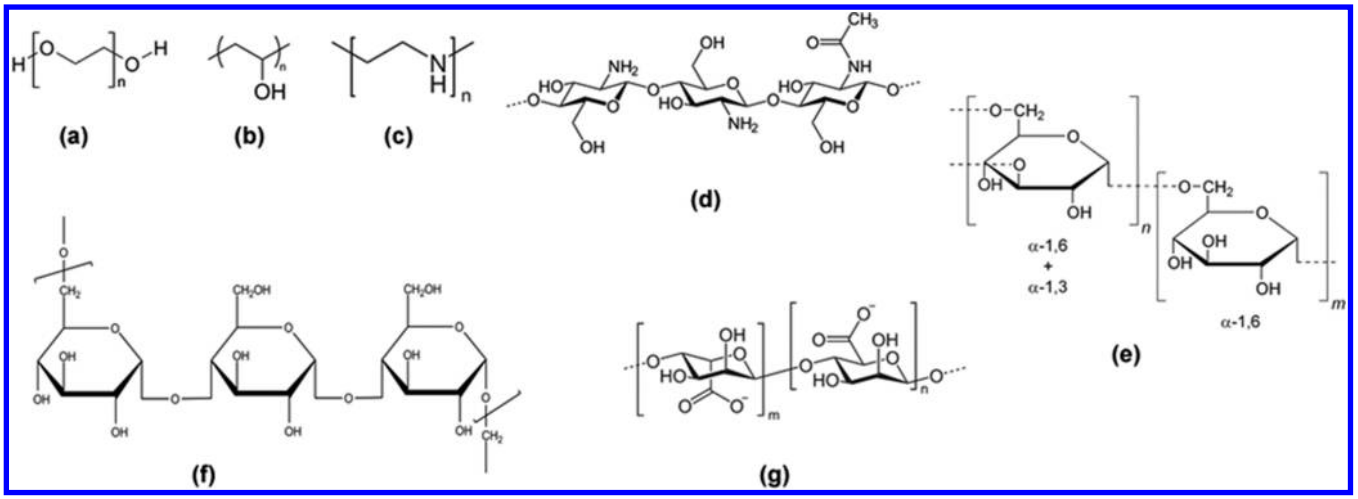

Figure 8. Structure of polymeric stabilizers of MNPs: PEG (a), PVA (b), PEI (c), chitosan (d), dextran (e), pullulan (f), and alginate (g).

nanocapsules)[76] or synthesized via a simple chemical vapor deposition process,[77] have been suggested recently for drug delivery applications.

2.2. Stabilization Procedures

Finely divided iron is extremely reactive toward oxidizing agents and in the presence of water or humid air. Thus, protection of MNPs is of prime importance for obtaining physically and chemically stable colloidal systems. Such protection can be achieved by surface coating of the MNPs (Figure 7). In addition, the surface coating may improve both the colloidal and physical stability of the particles, increase their water-dispersibility, and provide functionalization for further conjugation with bioactive molecules or targeting ligands, and for obtaining multifunctional NPs.[78−82] Such stabilization can be achieved by the following:

(1) By surface coating using appropriate polymeric stabilizers/surfactants, e.g., dextran,[83,84] carboxydextran,[85] poly(vinyl alcohol) (PVA),[86] or poly(ethylene glycol) (PEG);[87,88] or by deposition of a few atomic layers of inorganic metals (e.g., gold),[89] nonmetals (e.g., graphite),[90] or oxide surfaces (e.g., SiO_2).[91]

(2) By generating polymeric shells that avoid cluster growth after nucleation and hold the particle domains apart against attractive forces. In this case, composite particles prepared from monomers or preformed polymers may consist of either a polymer matrix (i.e., nanosphere)[45,92,93] or a reservoir system in which an aqueous or an oily core is surrounded by a polymeric shell (i.e., nanocapsule).[94]

(3) By the formation of lipid-like coatings (e.g., liposomes/lipid NPs) around the magnetic core.[95−99]

2.2.1. Use of Stabilizing Surface Coating Materials. Stabilizers such as surfactants or polymers are usually added during the synthesis of MNPs to stabilize the newly formed

dx.doi.org/10.1021/cr300068p | Chem. Rev. 2012, 112, 5818−5878

surfaces and hence to prevent both in vitro and in vivo aggregation.[1,86,88] The type of the surface coating and its geometric arrangement onto the magnetic core not only determine the overall size of the colloid but also play a significant role regarding its biological fate (i.e., pharmacokinetics and biodistribution; see section 4).[91,100−102] Surface stabilization is usually achieved using nonpolymeric stabilizers based on organic monomers bearing functional groups like carboxylate, phosphate, or sulfate, e.g., alkanesulphonic and alkanephosphonic acids,[103,104] OA,[58,105−107] lactobionic acid,[108] lauric acid,[105,109] dodecylphosphonic and hexadecylphosphonic acids,[105] or phosphonates;[110] or polymeric stabilizers, i.e., dextran,[111] PEG,[88] PVA,[86] alginate,[112] chitosan,[113] pullulan,[114] or poly(ethylene imine) (PEI)[115] (Figure 8).

When polymeric materials are employed as stabilizers, the adsorption of polymers onto the MNPs confers protective steric repulsion and acts as a barrier against the interaction between the particles,[5] thereby maintaining the particles apart from one another. Such protection is the most efficient when using amphiphilic copolymers bearing a hydrophilic segment with a tendency to spread into the aqueous medium and a hydrophobic segment anchoring onto the particle surface. If the polymer chains are charged, an additional electrostatic repulsion may occur, thus conferring a combined ionic and steric (electrosteric) stabilization effect. In other words, polymeric coatings can tailor the surface properties (chemical functionality and surface charge) of the MNPs and constitute an excellent barrier for preventing aggregation, leading to physically and chemically stable magnetic nanoformulations. Concerning the vascular administration [intravenous (i.v.) or intra-arterial] of MNPs, the gravitational settling in the blood flow can be considered as negligible, thanks to these polymer coatings that generally decrease the mean density of the magnetic cores. However, prior to considering biomedical applications, some key characteristics of the polymer must be taken into consideration: length and molecular weight, chemical structure (biodegradability and hydrophobic/hydrophilic character), conformation, degree of surface coverage, and attachment mechanism to the particle surface (covalent, hydrophobic, or ionic binding). The conformation of the polymer onto the NP surface contributes to their effective hydrodynamic size and antifouling properties, which are important factors for minimizing the rapid blood clearance of NPs after i.v. administration, due to immunological recognition (see section 4). To facilitate the efficient attachment of the polymers onto the surface of the MNPs, several functional molecules such as DMSA,[116] biphosphonates,[103] or alkoxysilanes[117,118] may be employed.

Remarkably, coating MNPs with hydrophilic polymers [usually polysaccharides like dextran, PEG, starch, or polyvinylpyrrolidone (PVP)] or with proteins (e.g., lactoferrin or ceruloplasmin) may increase their plasma half-life from a few minutes to several hours or even up to days in some cases, as a result of the *stealth* properties conferred by the polymer shell.[119−122] Among the above-mentioned hydrophilic polymers, PEG is by far the most widely used polymer for NP coating in nanomedicine[123−125] due to its nontoxic and impressive steric repulsive properties. Various strategies have been proposed for attaching PEG to MNPs, such as polymerization at the NP surface,[88,126] modification through the sol−gel approach,[127] or silane grafting onto the oxide surfaces.[87,128,129] The development of bifunctional PEG-silanes capable of forming self-assembled monolayers that increase the polymer packing onto the NPs provides covalent linkages to surfaces and allows controlling the polymer conformation.[130−133] For instance, it has been demonstrated that the coating of Fe_3O_4 NPs by the protein-resistant copolymer poly(3-(trimethoxysilyl)propyl methacrylate-*co*-poly(ethylene glycol)methacrylate) [poly(TMSMA-*co*-PEGMA)] composed of silane-anchoring moieties and PEG branches assured an improved accumulation of this magnetic system into the mice tumor xenografts.[134]

Apart from PEG, the polysaccharide dextran has also been widely used to design the surface coatings of MNPs for in vivo imaging applications.[100,135−137] To generate amino groups and to facilitate further attachment of biomolecules onto the NP surface, the dextran coat can be cross-linked with epichlorohydrin followed by a treatment with ammonia.[138,139]

Inorganic metals such as gold are other useful coating materials. Gold provides the possibility of depositing monolayers of alcohol or carboxylic acid-terminated thiols onto the NP surface, which further provides the opportunity for surface functionalization with ligands of interest.[140,141] However, some difficulty in the formation of the shell over the MNP surface may arise from the chemical inertness of gold.[142] Gold-coated IONPs are generally stable under acidic and neutral pH in aqueous media.[143]

Coatings with nonmetallic materials such as graphite have also improved the solubility and stability against oxidation of FeCo colloids in aqueous media. A single-layered graphitic shell deposited onto the FeCo nanocrystals not only provides the chemical stability but also offers near-infrared optical properties to the nanocrystals. This interesting property may be useful for the heat-induced therapy of cancers leading to the destruction of tumor cells[90] (for details, see section 6.6).

SiO_2 coatings onto MNPs, combined with the incorporation of surface-reactive groups such as functional alkoxysilanes (e.g., tetraethoxysilane and 3-aminopropyltriethoxysilane) may also facilitate NP stability and allow the design of multifunctional NPs for different applications.[144−147] The advantage of using SiO_2 as coating material relies on its ease of synthesis and stability in aqueous medium.[2] For instance, a core/shell NP made of iron oxide/SiO_2 (iron oxide core of 10 nm diameter, and SiO_2 shell of 10−15 nm thickness) exhibiting superparamagnetic and luminescent properties has been constructed by coating the MNP core with SiO_2 as a primary shell and then doping an organic dye, tris(2,2′-bipyridine) ruthenium [Ru(bpy)], inside a second SiO_2 shell to provide luminescence (Figure 9). It is noteworthy that the primary SiO_2 shell on the iron oxide core prevented the luminescence quenching by minimizing the interaction between the magnetic core and the dye.[79]

Attaching crystalline shells of Fe_3O_4 to the iron particles has also been reported and ensured a robust protective coating against deep oxidation in comparison to amorphous coatings.[148] These coatings can be easily obtained by a nanocluster deposition methodology allowing the control of the core sizes (in a range of ∼2−100 nm) and of the shell thickness (in a range of ∼2.5−5 nm) via an accurate tuning of the cluster growth parameters.[149] The chemical instability and aggregation tendency of iron has been considerably minimized by encapsulation into iron oxide shell using CO_2 laser pyrolysis technique. Thus, iron/iron carbide core and iron oxide shell (Fe/γ-Fe_2O_3) NPs of ∼15 nm diameters have been directly obtained using the above technique equipped with a filter to separate the aggregates formed during the process. The

dx.doi.org/10.1021/cr300068p | *Chem. Rev.* 2012, 112, 5818−5878

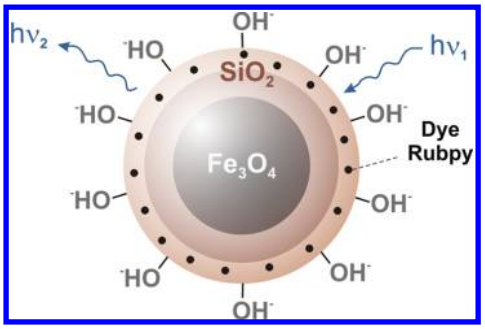

Figure 9. Representation of an iron oxide/SiO_2 core/shell NP with superparamagnetic and luminescent properties.

resulting NPs were found to be discrete, and very few particle aggregates were formed.[150]

In addition, inorganic matrices such as hydrotalcite or zeolite have also been used to coat the magnetic metals (e.g., Co, Fe, FeCo-alloy, or magnetic ferrites such as Fe_3O_4 and γ-Fe_2O_3, as well as barium ferrite).[59,151−156] Particularly, the use of zeolite appears very promising due to its high capacity to load inorganic or organic molecules, which may be an added value for drug-delivery purposes. However, the safety and biocompatibility of these inorganic coatings needs to be clarified if pharmaceutical applications are envisioned.

2.2.2. Encapsulation into Polymeric Shells. Surface coating of the MNPs with polymeric materials has been described to improve the water dispersibility as well as the physical and chemical stability of the colloid (as described in section 2.2.1). More interestingly, the polymeric shell can provide functional groups such as terminal amine or carboxyl moieties at the NP surface for further conjugation with bioactive molecules and/or targeting ligands, as a route toward multifunctional MNPs. In this way, a large number of natural and synthetic biodegradable polymers, e.g., human serum albumin,[157] polyaspartate,[158] polysaccharides,[159] gelatin,[160] starch,[161,162] alginate,[163] poly(acrylic acid),[164] PEG,[126,165,166] poly(D,L-lactide) (PLA),[167−169] PEG−poly(aspartic acid),[170] poly(PEG monomethacrylate),[171] PLA-*b*-PEG,[172,173] poly(D,L-lactide-*co*-glycolide) (PLGA),[174−178] poly(alkyl cyanoacrylate) (PACA),[45,92,179−184] chitosan,[93,113,162,185,186] chitosan-L-glutamic acid,[187] and poly(ε-caprolactone) (PCL),[188,189] and nonbiodegradable polymers, e.g., ethylcellulose,[190,191] polystyrene (PS),[157,192] polymethylmethacrylate (PMMA),[193] and poly[2-(methacryloxyloxy)ethyl phosphoryl choline],[194] are currently under evaluation as shells for the encapsulation of MNPs.

For instance, PS/Fe_3O_4 core/shell NPs of very small size (<10 nm) and narrow size distribution have been obtained by the polymerization of styrene at the surface of the NPs.[195] The monomer-to-initiator ratio and the chemical structure of the initiator were found to play an important role in achieving NPs with the desired properties. In another instance, in situ fabrication of magnetic particles in the presence of gelatin resulted in the formation of magnetic sponge-like hydrogel systems (also called ferrosponges).[196] These ferrosponges, which possess an interconnected nanopore structure, may readily serve as a drug reservoir for drug delivery applications (Figure 10). The high swelling capacity of the ferrosponges, coupled to their excellent elasticity and hydrophilicity, make them able to efficiently respond to an external oscillating magnetic field by a rapid and repeatable swelling and deswelling process. This makes the release of the encapsulated drug sensitive to the magnetic stimulus.

Hybrid magnetic carriers consisting of alginate/SiO_2 nanocomposite shell loaded with Fe_3O_4 NPs and prepared by spray-drying technique were found to exhibit a superparamagnetic behavior.[197] These NPs were internalized by cultured fibroblasts. Furthermore, selective intracellular alginate degradation was observed, suggesting that these nanodevices may have some potential for drug-delivery purposes.

Copolymers were also employed for the design of IONP shells. For example, magnetic nanocomposite particles were synthesized by encapsulating nanosized Fe_3O_4 with an acrylate-based cationic copolymer made of methyl methacrylate (MMA), *n*-butyl acrylate (BA), and 8-quinolinyl methacrylate (8-QMA). The cationic charge was provided to the copolymer by functionalization with 2-(methacryloyloxy)ethyl trimethyl ammonium chloride, and further surface stabilization of the nanocomposites was accomplished with methoxyPEG methacrylate (MePEGMA).[198] The positive charge generated on the Fe_3O_4/copolymer NPs provided the possibility to noncovalently load negatively charged drugs, such as acetylsalicylic acid, by electrostatic interaction. Other examples of copolymers include amphiphilic block copolymers such as maleimide-

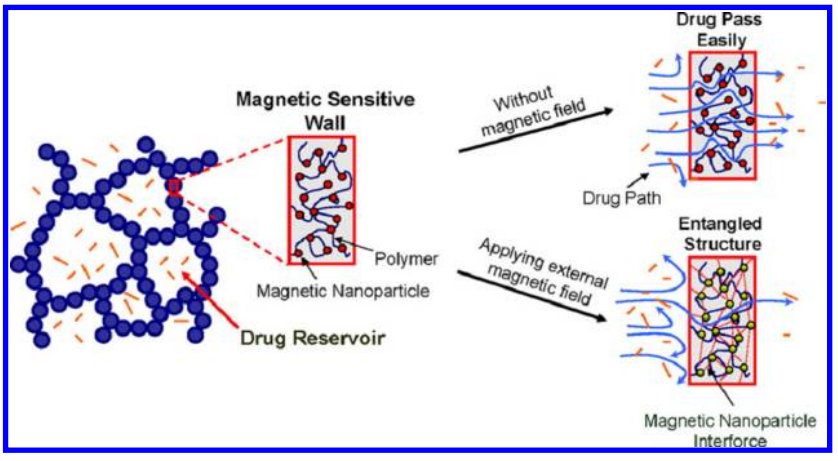

Figure 10. Schematic drawing of drug release from the magnetic-sensitive ferrosponges with and without applying an external magnetic field. Reprinted with permission from ref 196. Copyright 2007 Elsevier.

dx.doi.org/10.1021/cr300068p | *Chem. Rev.* 2012, 112, 5818−5878

terminated PEG-*b*-PLA and methoxy-terminated PEG-*b*-PLA.[173]

However, it should be noted that, in some cases, the presence of polymers or copolymers during magnetic nanocrystal nucleation and growth may induce imperfections in the crystal structure that, consequently, may alter the magnetic properties of the IONPs.[199] Various other studies have also demonstrated that the encapsulation into polymer shells may negatively influence the magnetic properties of the MNPs.[200,201] Thus, great caution has to be exercised during the selection of polymeric materials for the stabilization of magnetic colloids.

2.2.3. Encapsulation into Liposomes. Liposomes (phospholipid bilayer vesicles) have been shown to encapsulate high concentrations of magnetic colloids. The advantage of liposomal magnetic systems (also known as magnetoliposomes) is that the surface functionalization may be achieved using the usual liposomal methodologies without any chemical modification of the encapsulated Fe_3O_4 colloids.[202] Long-circulating magnetic fluid-loaded liposomes (~200 nm) (liposomes surface-equipped with hydrophilic polymers such as PEG) made from egg phosphatidylcholine and phospholipid−PEG derivative distearoyl phosphatidyl ethanolamine ($DSPE\text{-}PEG_{2000}$) can be obtained by extrusion[203] or by film-hydration technique coupled with sequential extrusion techniques, which facilitates the encapsulation of $\gamma\text{-}Fe_2O_3$ nanocrystals within these unilamellar vesicles.[204]

Magnetoliposomes having an average diameter of ~35 nm were also obtained from magnetotactic bacteria, i.e., *Magnetospirillum gryphiswaldense*. These extracted magnetic particles are also called bacterial magnetosomes (BMs) because they are isolated from the intracellular organelles of the bacteria. In a typical preparation procedure, the bacteria are disrupted with a French Press and the cell contents are washed with phosphate-buffered saline (PBS) and submitted to ultrasonication before subsequent magnetic purification.[205−207] The magnetoliposomes may be considered as promising candidates for various biomedical applications such as MRI, targeted drug and gene delivery, tumor hyperthermia, and magnetic cell separation.[81,95,97,98,206,208−210] These systems have also served as a template for promoting the self-assembly of viral protein cage to build up virus-like particles with high magnetic susceptibility.[211]

3. PHYSICOCHEMICAL PROPERTIES AND PHYSICOCHEMICAL CHARACTERIZATION

3.1. Geometry

Size and shape are the key features that govern the physical stability of MNPs, both in vitro and in vivo. The size strongly influences the magnetic moment of the particles and their subsequent response to the magnetic fields. For instance, magnetization measurements have demonstrated that the saturation magnetization of iron oxide particles decreased with a decrease in size. A decrease of the particle size results in an increase of the surface area, which may have important implications on the noncrystalline character of the particles and consequently on their magnetic moment.[5,212] However, MNPs at the very low size range can exhibit superparamagnetism, which determines greater magnetization capabilities compared to paramagnetic materials (see section 3.5 for further details). Interestingly, particle size has also been described to control the signal (i.e., transverse relaxation T_2/T_1) in MRI of iron oxides, which can have consequences concerning the quality of the diagnosis.[213,214]

The size and the shape of iron oxide particles are mainly characterized by using high-resolution transmission electron microscopy (HRTEM) and field-emission scanning electron microscopy (FeSEM).[190,215,216] These techniques have the ability to resolve the atomic arrangement in the nanosized particles and are thus employed for the investigation of interfacial NP structures. Additional techniques that are generally employed for the determination of mean particle size and size distributions include photon correlation spectroscopy (PCS, also named dynamic light scattering, DLS), quasi-elastic light scattering (QELS),[216,217] and X-ray diffraction and Mössbauer spectroscopy.[218,219]

3.2. Structure

The appropriate mineralogical purity and the degree of crystallinity of iron oxides define their magnetic properties. X-ray diffraction (using both conventional and synchrotron radiation sources), thermal analysis, and Mössbauer and infrared spectroscopy can be considered the most important techniques to elucidate the NP structure.[217] However, these methodologies usually require sample drying, which may result in irreversible particle aggregation. Consequently, the results obtained may not accurately reflect the nature of the species in the liquid dispersion formulated for pharmaceutical purposes. The above issue may be solved by the characterization of the particles as a liquid suspension using small-angle X-ray scattering (SAXS), small-angle neutron scattering (SANS),[220] angular dispersive X-ray diffraction (ADXD), or energy-dispersive X-ray diffraction (EDXD).[212,217,221] In some cases, HRTEM has also been employed for investigating the crystallography (i.e., lattice vacancies and defects, lattice fringes characteristic, glide plane, and screw axis) of iron oxide particles.[222,223] The combination of these various characterization techniques may be advantageous to analyze the crystal structure of less-ordered magnetic systems, like SPIONs (average size < 20 nm), despite the limited number of cubic cell units.[212]

The structures of composite particles made of iron oxide and organic molecules such as ligands as well as the nature of the interactions between the iron oxide core and the associated molecular structures within the composite (e.g., chemical association and/or physical adsorption) have been investigated using thermogravimetric and differential thermogravimetric analysis (TGA), differential scanning calorimetry (DSC), and further by coupling these data with the Fourier transform infrared spectroscopy (FTIR) and statistic secondary ion mass spectra (SSIMS).[111,218,224] The mechanism of surface adsorption of such organic/inorganic moieties onto the iron oxide core can be further analyzed by conductometric measurements and adsorption isotherm curves.[225]

Several techniques such as atomic and chemical force microscopy (AFM and CFM, respectively) allow the morphological changes occurring on the surface of IONPs upon exposure to a coating material to be investigated.[104,226] In this context, the electrophoretic mobility (u_e) determinations are useful in evaluating the effect of the coatings on the zeta potential (ζ), while interfacial tension measurements (contact angle techniques) can be employed to inspect the interfacial hydrophilic character of the coated magnetic particles.[45,92,187,190,216] This has been illustrated with magneto-responsive squalenoyl gemcitabine (SQdFdC, or SQgem)

dx.doi.org/10.1021/cr300068p | *Chem. Rev.* 2012, 112, 5818−5878

composite NPs for potential application in cancer therapy (Figure 11).[216]

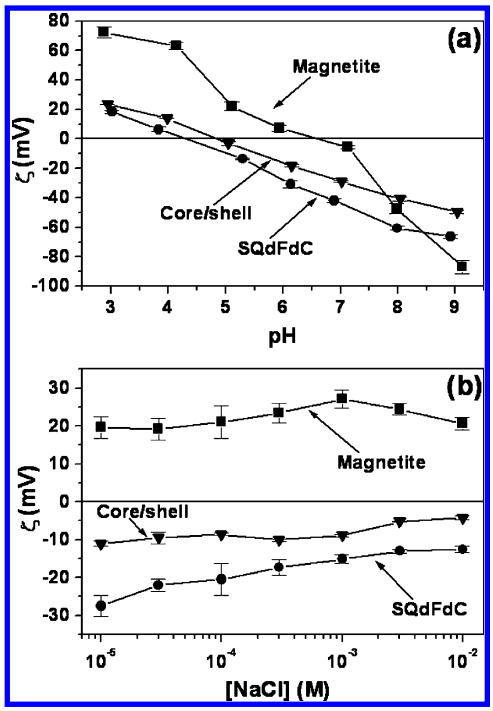

Figure 11. ζ values of Fe_3O_4, SQdFdC, and Fe_3O_4/SQdFdC (core/shell) composite NPs as a function of pH in the presence of 10^{-3} M NaCl (a) and as a function of the NaCl concentration at pH = 5.6 (b). Reprinted with permission from ref 216. Copyright 2008 American Chemical Society.

3.3. Surface Charge

Following intravenous (i.v.) injection, MNPs encounter a slightly basic physiological pH (pH 7.4) and a relatively high ionic strength (~140 mEq/L). These conditions, along with the magnetic attractive forces, typically lead to particle aggregation (mainly by van der Waals and/or magnetic dipole−dipole attractive interactions). Therefore, in vitro and in vivo stability of magnetic particles are only possible if these effects are compensated by the (i) electrostatic repulsion between adequately charged surfaces; (ii) hydrophilic particle−particle interactions; and (iii) existence of an adequate shell (steric barrier) onto the particle surface (see also section 2.2).[5,227]

Usually, solid particles acquire a surface charge when they are in contact with an aqueous electrolyte solution.[228] Electroneutrality requirements determine a compensation of the charge by an ion distribution in the area surrounding the particles, resulting in the electrical double layer.[5,227,229] Unfortunately, it is difficult to gain experimental access to the surface charge of a MNP. To some extent, the problem can be resolved by using experimental methodologies based on the electrokinetic phenomena. These techniques rely on the hypothesis that close to the solid/liquid interface exists an ideal surface/plane that separates the electrical double-layer region adhered to the particle surface (the shear layer) from the region that can move with respect to it upon application of an external field (the diffuse layer, which is involved in the stability of colloids, particularly the hydrodynamic motion of the suspended particles).[5,227,230] The potential at that plane is usually named electrokinetic or zeta potential (ζ), which is considered a function of the surface charge density, the shear plane location, and the surface structure and may dramatically influence the in vitro and in vivo stability of the NPs.

ζ can be calculated indirectly from the experimental techniques (streaming current or potential, electrophoretic mobility, and electric conductivity) using theoretical approaches.[231−233] Alternatively to these methods, the ultrasound technique could be advantageous because it is able to characterize concentrated samples without the need of dilution,[234] unlike with the light-based methods that require extreme dilution of suspensions to make the sample sufficiently transparent for the measurement. Nevertheless, it has been demonstrated that the ζ values for the same charged interface, measured using different techniques, are hardly comparable, and the standardization of these techniques is far to be achieved.[217,235]

Of the above, the usually employed methodology involves the measurement of electrophoretic mobility, u_e. It is accepted that ζ data can be calculated from u_e by using the Smoluchowski equation.[5,232,235,236] Unfortunately, despite the fact that this equation may be the one most largely used, it cannot be applied to small particles, i.e., SPIONs, or high surface potentials. Alternative equations have also been proposed to indirectly calculate ζ from u_e. However, the consistency of the ζ data depends upon the applicability of such equations to the system investigated. For instance, Henry's equation can correct the size limitations but is still valid only for low potentials. On the contrary, the O'Brien and White general theory have resulted in significant help to the problem, even if high surface potentials are considered.[231] In addition, the theory by Ohshima proposing analytical expressions covering the wide range of parameters involved in the electrokinetic phenomena (i.e., the particle size and the surface potentials) can definitively be considered of great help when calculating ζ from u_e.[237−239]

Electrokinetic determinations have also been of great help in the formulation of nanocomposites consisting of magnetic nuclei surface coated with an organic or inorganic shell. Indeed, ζ determinations were found to be very useful in the evaluation of the coating of iron oxides or iron particles by biodegradable polymers or lipidic systems (as mentioned in section 3.2). There are other instances in which the ζ of magnetic drug carriers is a useful determination. A noticeable one is the qualitative follow-up of the drug loading onto the magnetic carrier, thanks to the sensitivity of electrokinetic determinations to even minute changes in the surface concentration of species responsible for charge generation. In such cases, the drug molecules need to possess charge to allow their detection onto the magnetic particles.[180−182]

3.4. Surface Thermodynamics

The significance of particle wettability and the phenomena associated to particle−particle interactions in the aqueous medium determine the tendency of MNPs to remain dispersed or to aggregate by reducing their interfacial surface area. In aqueous media, hydrophobic magnetic particles will tend to attract each other because of the hydrophobic attraction energy, whereas a hydrophilic character will definitively lead to a better thermodynamic stability. Such interfacial interactions can be easily quantified using the well-known model of van Oss.[5,240] Following this model, the determination of the surface free energy components of a magnetic nanomaterial may be useful

dx.doi.org/10.1021/cr300068p | Chem. Rev. 2012, 112, 5818−5878

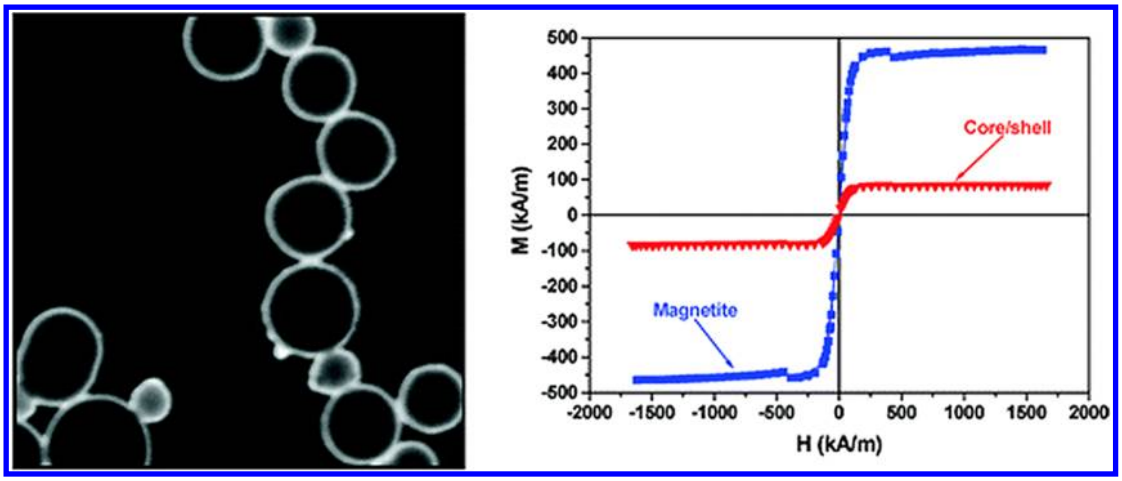

Figure 12. Dark-field HRTEM photograph of magnetic core/shell NPs obtained by the nanoprecipitation of SQdFdC around Fe_3O_4 NPs (left), and hysteresis cycles of Fe_3O_4 and composite core/shell NPs (right). Reprinted with permission from ref 216. Copyright 2008 American Chemical Society.

for the quantification of its thermodynamic stability (based on wettability considerations) in aqueous suspensions. Practically speaking, these components can be experimentally determined, e.g., by contact angle measurements.[5,45,92,167,180] Knowledge of these quantities helps in the evaluation of the van der Waals interaction between the magnetic particles, which could induce their flocculation if not balanced by a comparable repulsion. If hydrophobic aggregation occurs, then the solid/liquid interface disappears, and the surface free energy change (per unit area) quantity (ΔG_{SLS}) will be negative. On the contrary, hydrophilic repulsion will correspondingly be associated to the positive values of ΔG_{SLS}, where the magnetic particles tend to stay dispersed.

As previously indicated in the case of electrophoretic measurements (see section 3.3), the thermodynamic analysis of magnetic particles would be of great interest for the determination of the efficiency of the surface engineering of NPs with organic or inorganic materials. In fact, contact angle determinations have helped in the evaluation of the changes in the interaction free energy displayed by these magnetic cores when a hydrophobic shell (made of a biodegradable polymer or of a lipid) is deposited onto their surface.[5] For example, it should lead to a shift from hydrophilic iron oxide to hydrophobic composite (core/shell) magnetic particles upon complete coating.[45,92,180,190]

Finally, the hydrophilic/hydrophobic nature of the magnetic particles further determines their interaction with the plasma proteins (opsonization process) in biological conditions. In general, this process occurs more rapidly with the hydrophobic particles than with the hydrophilic ones.[5,241] This further emphasizes the importance of the characterization of surface thermodynamics of MNPs.

3.5. Magnetism

The magnetic properties of iron oxide particles can be described by the dependence of the magnetic induction (B) on the magnetic field (H). For most of the materials there is a linear relationship between B and H: $B = \mu \times H$, where μ is the magnetic permeability of the particles. Iron oxide particles exhibit paramagnetism if $\mu > 1$ and diamagnetism if $\mu < 1$. The magnetic susceptibility $\chi = \mu - 1$ is also considered in the characterization of these NPs: paramagnetic NPs have $\chi > 0$, and diamagnetic materials have $\chi < 0$. The characterization of the hysteresis cycle of magnetic particles is widely used to define their magnetism and magnetic responsiveness [i.e., magnetic remanence and intrinsic magnetization (magnetic moment)] (Figure 12).[5,92,179,180,216] Furthermore, the magnetization curves have been proposed to investigate the iron oxide crystal size and the width of the crystal size distribution. These parameters are also useful for the evaluation of the contrast efficacy of an iron oxide formulation.[242]

Particles whose unpaired electrons spins align themselves spontaneously so that they can exhibit magnetization without being in a magnetic field are called ferromagnetic particles. When these ferromagnetic particles are removed from the magnetic field, they exhibit permanent magnetization. In contrast to ferromagnetism, no permanent magnetization remains in the paramagnetic materials when they are removed from the magnetic field. Paramagnetism can be understood by postulating permanent atomic magnetic moments, which can be reoriented in a magnetic field.[1,5]

On the other hand, ferromagnetic materials, which are size-reduced to particle dimensions smaller than a particular domain, are no longer ferromagnetic but exhibit superparamagnetism. Interestingly, the magnetization of SPIONs is quite similar to that of ferromagnetic materials, and thus greater than the one of paramagnetic particles. As a result, superparamagnetic nanomaterials can be easily tracked in a magnetic field without losing the advantage of a stable colloidal suspension.[241] In fact, the null or negligible remnant magnetization of superparamagnetic particles is an interesting property that avoids their aggregation, both during storage and after i.v. administration. Upon suppressing the magnetic field, the particles no longer show magnetic interaction (negligible remanence and coercivity), and thus agglomeration (as well as the potential embolization of capillary vessels) is avoided.[137,241]

Additional benefits of the superparamagnetic particles come from their (i) heating behavior, the result of the Néel relaxation mechanism when they are under the influence of an alternating magnetic field (AMF);[241,243] and (ii) powerful enhancement of the proton relaxation times T_1 and T_2.[100] Because of this behavior, such materials are also used as magnetic storage media[244] or as magnetic inks for jet printing.[245] Unfortunately, the reduced size of superparamagnetic particles easily results in pronounced surface effects (due to the enhanced surface-to-

dx.doi.org/10.1021/cr300068p | Chem. Rev. 2012, 112, 5818–5878

volume ratio, i.e., spin-canting, spin-glass-like behavior, and noncollinear spin), which can alter their magnetic properties.[246]

3.6. Colloidal Stability

Colloidal stability in adequate media is an essential feature for medical applications of the MNPs. As already mentioned before, thanks to their moderate average density, MNPs exhibit negligible gravitational settling in the blood flow. In the absence of an applied magnetic field, the stability of the particles mainly depends on the balance between attractive forces (dipole−dipole van der Waals interactions) and repulsive forces (steric and electrostatic interactions) acting between the magnetic particles.[247−250] The former interactions depend on the particle nature, while electrostatic particle−particle interactions are sensitive to external experimental parameters, such as the electrolyte concentration and the pH of the media (see section 3.3). Both forces could be properly controlled by an adequate engineering of the magnetic particles.

Concretely, in order to avoid the aggregation of the particles in vitro and in vivo, it is required that[5,235,248,249,251] (i) particles are protected against irreversible aggregation by van der Waals forces, taking advantage of the protective electrostatic and/or steric (electrosteric) repulsion conferred by the adsorbed biocompatible materials (e.g., PEG and dextran); and (ii) remnant magnetization of the particles is almost negligible or null. When sufficient amount of stabilizing agent is located onto the particle surface, steric stabilization provides reasonable stability even at higher electrolyte concentrations and in a wide range of pH values.[252] Regarding the second requisite, it implies that the magnetic particles must be superparamagnetic or, instead, soft ferro- or ferri-magnetic materials. This is the case for the materials typically employed as drug carriers (e.g., Fe_3O_4, γ-Fe_2O_3, iron), that, despite the fact that they are magnetically multidomain particles (diameter $\geq$ 50 nm), possess a narrow hysteresis cycle and, consequently, a small remnant magnetization.[5,48,49,253]

A typical experimental method to investigate the colloidal stability is based on the study of the time evolution of the hydrodynamic particle size using the DLS technique, for instance, as a function of the ionic strength and/or pH.[254,255] It is also possible to investigate the stability of MNPs by measuring the aggregation kinetics via turbidity measurements.[248,256]

However, due to the tendency of DLS to overweigh large particles, great care must be taken to choose appropriate experimental settings (e.g., the angle of scattered light, generally 90° but could be varied, and the delay between the measurements, especially when different batches have to be compared).[252]

4. PHARMACOKINETICS, BIODISTRIBUTION, AND BIOLOGICAL FATE

In the targeted drug-delivery field, the intravenously injected MNPs follow three successive steps: (i) they are magnetically guided to the targeted tissue; (ii) they are immobilized in the tissue while the drug is released, using an external magnetic field; and (iii) they undergo clearance from the body. The transport of the intravenously injected MNPs through the blood vessels is favored by the hydrodynamic forces of the blood flow. Soon after i.v. injection, an immediate interaction between the MNPs and the plasma proteins (opsonins) occurs. This interaction results in the adsorption of plasma proteins onto the magnetic colloids, a process termed as opsonisation. Such an adsorption process plays a key role in the biological fate of the MNPs (i.e., biodistribution and elimination).[257] Once these opsonic proteins approach the MNPs surface, interactions including van der Waals, electrostatic, and hydrophilic/hydrophobic balance would facilitate the opsonin binding onto the NP surface. In general, opsonization of the hydrophobic particles occurs more rapidly compared to that of the hydrophilic particles.

The opsonised NPs undergo rapid clearance from the vascular compartment, as a result of their capture by the macrophages of the liver (i.e., Küpffer cells), of the spleen, and of the bone marrow, which are tissues belonging to the so-called reticuloendothelial system (RES).[258−260] Such accumulation of the opsonised NPs into the RES organs may be considered favorable when these organs are the intended target sites. Hence, in order to deliver the MNPs to tissues other than the RES organs, minimizing the rapid systemic clearance of the NPs becomes essential. As previously commented (see section 2.2), this could be achieved by coating the MNPs to create nonfouling shells on the particle surface and provide shielding effect (also called as "stealth" property).[100,137,261,262] To date, PEG is by far considered to be the most appropriate and the most widely used hydrophilic polymer to prevent the intravenously injected NPs from rapid systemic clearance by the RES. The chain length and packing density of PEG retard the NP opsonisation by steric hindrance effect and thereby prolong the systemic circulation time of the NPs.[130,263] PEG of chain lengths starting from 2 kDa molecular weights is the most suitable for this purpose, as demonstrated with various nanoparticulate systems developed for drug-delivery applications.[119,264,265] Although significant literature exists showing the prolongation of systemic circulation time by PEGylated nanosized particles, it was important to investigate whether the repeated injection of the PEGylated particles could have an impact on their pharmacokinetic profile. Although, some early preclinical reports showed that repeated injections of PEGylated liposomes (~100 nm size) had no effect on pharmacokinetic profile when tested in rats (at a spacing of 24 or 48 h)[266] or in rabbits (at a spacing of 6 weeks),[267] the later studies have oppositely reported the phenomenon of "accelerated blood clearance" (ABC) following the repeated injections of PEGylated liposomes in rats.[268,269] ABC involved a decrease in systemic circulation time of the second and/or subsequent doses of PEGylated liposomes, possibly due to the induction of anti-PEG-IgM (by the first dose), which binds to the subsequent injected doses of liposomes, leading to the activation of complement and resulting in the rapid systemic elimination of liposomes.[269] The ABC phenomenon was reported to be dependent on the injected lipid dose (limited or no effect at high lipid dose) and PEG surface density (no effect at high density, i.e., beyond 5 mol %).[270] Additionally, the ABC phenomenon was not observed with doxorubicin-encapsulated PEGylated liposomes (Caelyx), with the proposed reason being the negative impact of doxorubicin on the phagocytic activity of the macrophages.[268,271] The ABC phenomenon was also reported for PEGylated PLA NPs (50 μg/rat first dose followed by subsequent significantly higher dose of 1000 μg/rat) with an associated increase of anti-PEG-IgM, while the increase in systemic clearance and also the anti-PEG-IgM values were not linear with the spacing time of the second dose. Additionally, contrary to PEGylated liposomes, the PEG content of the PEGylated NPs did not influence the ABC phenomenon.[272] Noteworthy is the fact that the use of

hydrophilic polymers such as PVP (conjugated to PLA) did not induce the ABC phenomenon, although the prolongation of systemic circulation time of PVP−PLA NPs was lower than that of PEG−PLA NPs.[273] Although the ABC phenomenon was reported for PEGylated liposomes and PEGylated polymeric NPs, a consistent description of the factors (e.g., physicochemical, dose, and effect of spacing time) responsible for the induction of this phenomenon is not yet available. Overall, these reported observations have to be taken into account when a new PEGylated nanosized particle system is developed.

In the case of tumors, the long circulating NPs may reach the diseased area by passive extravasation, taking advantage of the increased tumor permeability resulting from the leaky tumor vasculature. This is the so-called enhanced permeability and retention (EPR) effect.[274,275] Alternatively, MNPs may be actively accumulated into the tumor tissues by guidance with an external magnetic field of suitable strength (Figure 13). To avoid the NPs getting rapidly cleared from the targeted tissue, the magnetic force must be higher than the hydrodynamic blood flow (arteries > 10 cm/s, capillaries = 0.05−0.1 cm/s). The efficacy of MNP immobilization also depends on particle size.[5,45,276] Practically, the field induction should be ≥1 T for efficient immobilization of the MNPs against the Brownian and hydrodynamic forces acting in the blood flow.[277] In general, the small particles in normal vessels are captured only at distances <0.5 cm close to the skin, for extracorporeally applied magnetic fields. However, in the case of tumor vessels, capture can occur up to 1.5 cm because of the leaky vasculature. With larger particles under stronger magnetic forces, the capture distances increase notably, reaching up to 6 cm for the healthy vessels and up to 10 cm for the diseased ones.[5]

The Food and Drug Administration (FDA) has established that the magnets inducing fields up to 8 T do not present any significant physiological risk for the adults. Fields ≈ 1 T can be readily obtained using external devices with electromagnets or powerful permanent magnets based on neodymium−iron (Nd−Fe) alloys (for ∼15 cm depths in the body) or by implanting the magnets internally by minimal invasive surgery (for larger depths).[5,261]

4.1. Influence of the Size

The size of the NPs is one of the important parameters influencing the pharmacokinetic and biodistribution of the intravenously injected NPs. The adsorption of plasma proteins (opsonins) onto the NPs surface (resulting in their recognition by macrophages and systemic clearance) depends on the size of the particles. For instance, it has been shown that the quantity of plasma protein adsorbed was lower for the smaller NPs (6% protein adsorbed onto 80-nm-sized particles), whereas it was significant for the NPs of relatively bigger size (23% and 34% adsorbed protein onto 171-nm- and 240-nm-sized particles). As a result, the systemic clearance of the smaller particles was slower than that of the bigger NPs.[278] In addition, the NPs of size >200 nm undergo filtration in the spleen, resulting in spleen uptake, whereas particles of size < 50−100 nm have a high probability of getting trapped into the hepatic parenchyma. Moreover, the particles > 4 μm diameter are mainly captured and withheld in lungs and may lead to the risk of embolism.[3,279] Thus, the size and the size distribution of the NPs should be tailored depending on the desired pharmacokinetic and distribution.

In the case of the clinically approved dextran-coated IONPs, Ferumoxide (80−150 nm diameter) and Ferumoxtran-10 (20−40 nm diameter), the larger particle size of Ferumoxide led to rapid systemic clearance resulting in a shorter systemic half-life (8−30 min), while Ferumoxtran-10 exhibited a significantly longer half-life (25−30 h). Ferumoxide was found to mainly accumulate in the liver (>80% of the injected dose 24 h postinjection), whereas Ferumoxtran-10 showed lower accumulation in the liver but higher lymph node uptake (∼20% of the injected dose).[280−282] Similarly, the impact of the size of IONPs on their biodistribution was analyzed in mice, using Fe_3O_4−dextran NPs of different diameter. The results revealed that the plasma half-life of the NPs decreased with increasing NP size,[283] while the hepatic uptake was augmented with an increase of the particle diameters. At 20 min postinjection (2 mg Fe/kg), the hepatic uptake of NPs was 22% of the injected dose for the smaller NPs of ∼30 nm diameter, whereas 42%

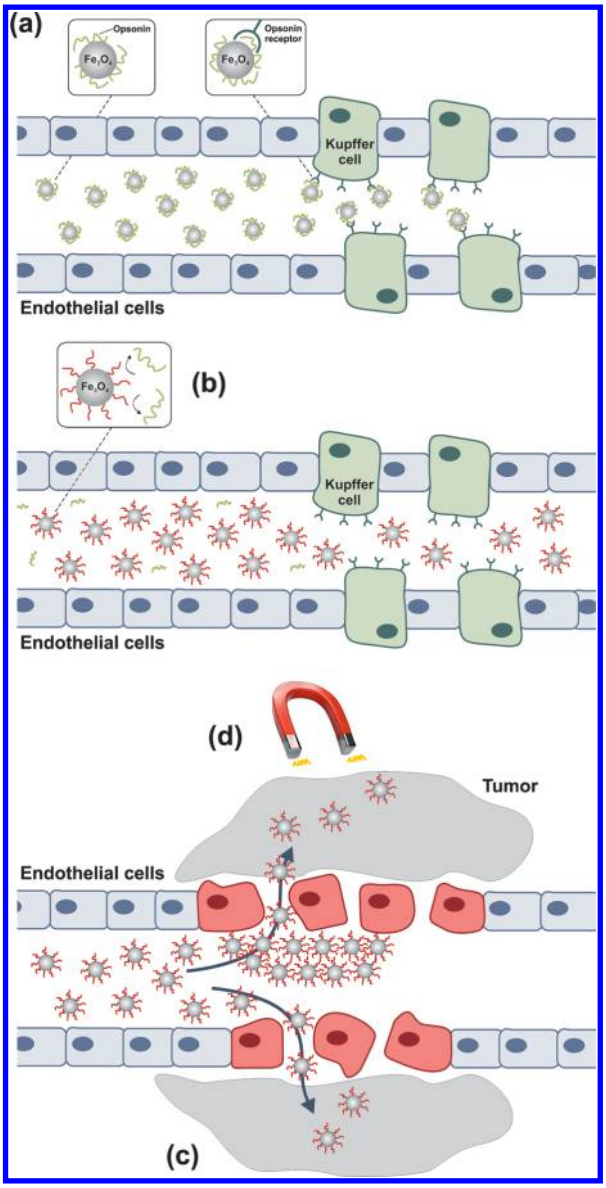

Figure 13. Representation of the in vivo fate of MNPs depending on their surface coating and on the use or not of magnetic guidance. Opsonisation and clearance of uncoated MNPs by Küpffer cells (a), escape from the Küpffer cells by means of PEGylation (b), accumulation of PEGylated NPs in tumor cells via the enhanced permeability and retention (EPR) effect (c), and active accumulation in tumor cells by the use of magnetic guidance (d).

dx.doi.org/10.1021/cr300068p | Chem. Rev. 2012, 112, 5818−5878

hepatic uptake was observed with the larger particles of ~100 nm diameter. This was assigned to the increased phagocytosis and sequestration of the bigger particles by the hepatic macrophages as a result of the opsonization process.[5,284] Similar size-dependence on biodistribution was also observed by Iannone and co-workers[285] with intravenously injected dextran-coated IONPs of 40 and 200 nm size fractions, as measured by electron spin resonance spectroscopy. The results revealed a rapid clearance of the 200 nm particles and a slow clearance of the 40 nm particles, clearly indicating the particle size influence on the NP biodistribution.

4.2. Influence of the Surface Charge

Surface charge of NPs may also have an important control on their biodistribution following i.v. injection. Neutral charge interacts minimally with the plasma proteins (less opsonization) and thus contributes to the extended circulation time of the NPs, whereas a high surface charge (positive or negative) enhances the phagocytosis process.[100,137] Unlike generally expected effect that the overall negative charge density on the cell membrane limits the efficient electrostatic interactions between the cell surface and anionic NPs, it was reported that anionic MNPs efficiently interacted with the cells and were internalized by adsorptive endocytosis.[286,287] Indeed, the anionic DMSA-coated IONPs (having 8.7 nm core diameter) were found to efficiently and nonspecifically bind to the surface of HeLa human ovarian tumor cells and RAW264.7 mouse macrophages at the cationic sites of the cell membrane, and they were internalized through endocytosis.[286] When compared to the dextran-coated IONPs, the uptake of anionic NPs was ~3-fold higher by the HeLa cells. Such nonspecific NP−cell membrane interactions may have negative implications from the toxicological standpoint, because of the risk associated with distribution and accumulation of NPs in cell/tissue in a nonspecific manner (Figure 14). The nonspecific binding of these anionic DMSA-coated IONPs to the HeLa cells was reduced by surface coating with albumin. Interestingly, it enhanced the NP uptake by the macrophages, thus indicating that the NPs interact differently with the HeLa and macrophage cell types.[288]

The influence of the surface charge on the biodistribution of IONPs has been further demonstrated by a study carried out on mice, using dextran-coated Fe_3O_4 NPs with neutral, negative (− 30 mV), or positive (+ 20 mV) surface charge. Hepatic uptake of the NPs was up to 3-fold lower for the electrically neutral particles than that for the charged particles.[283] Strong negative surface charges on the particles increased their hepatic uptake,[283] whereas positively charged particles tend to nonspecifically stick to the cells.[289] Another in vivo study revealed that the cationic poly-L-lysine-coated IONPs were rapidly cleared (within a few minutes) from the systemic circulation in comparison to the neutral ones (up to 2−3 h).[290]

4.3. Influence of the Administration Route

In addition to the physicochemical characteristics of the IONPs, the administration route may also influence their biodistribution. When injected locally (e.g., subcutaneously or intratumorally) at the diseased site, small magnetic particles undergo passive infiltration into the interstitial spaces around the injection site and are gradually absorbed by the lymphatic capillary system. For this reason, locally injected NPs (≤60 nm) are used for lymphatic targeting (e.g., chemotherapy or imaging of lymphatic tumors). In this case, magnetism may not be a prerequisite but may be a useful property to immobilize the particles in place for a longer time or to enable hyperthermia (see section 6.6).

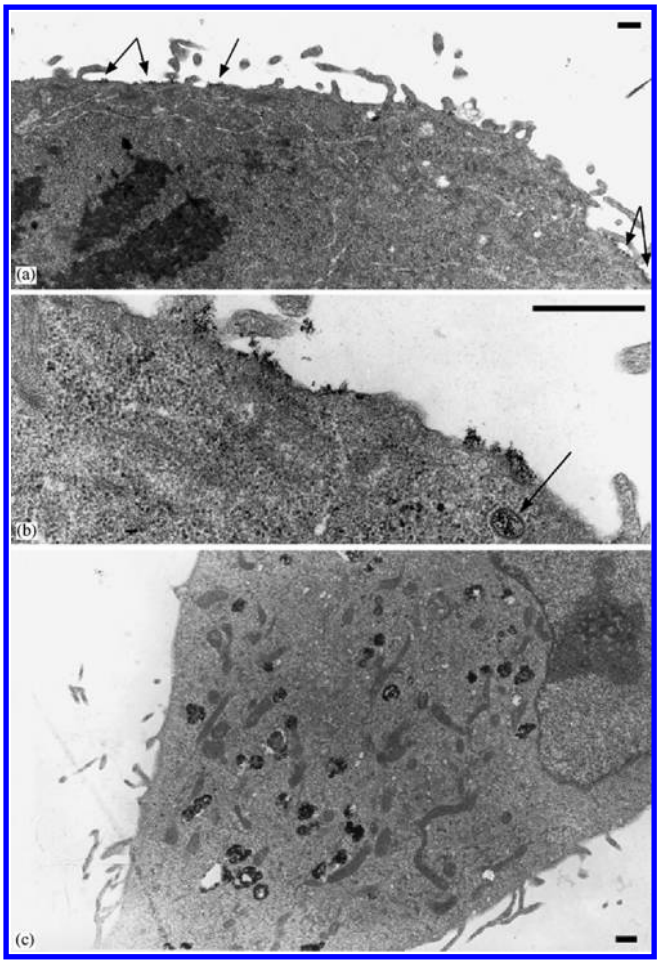

Figure 14. TEM photographs of a HeLa cell (a) fixed after 1 h incubation with anionic γ-Fe_2O_3 nanoparticles (AMNPs) at 4 °C ([Fe] = 20 mM). One observes the adsorption of NPs onto the plasma membrane mainly on the form of clusters (arrows). (b) TEM photographs of a HeLa cell fixed after 1 h incubation with AMNPs at 4 °C ([Fe] = 20 mM) and 10 min chase at 37 °C: particles are present within invaginations of the cell membrane and within (eventually clathrin-coated) early endosomes (arrow). (c) TEM photographs of a HeLa cell fixed after 1 h incubation at 4 °C with AMNPs ([Fe] = 20 mM) and 1 h chase at 37 °C: the anionic NPs are densely confined into numerous late endosomes and lysosomes. Bar lengths: 1 mm. Reprinted with permission from ref 288. Copyright 2003 Elsevier.

PVP-stabilized and fluorescent-tagged MNPs (50 nm mean diameter) administered by inhalation route to mice, through the nose for 4 weeks, accumulated considerably into the liver followed by testis, spleen, lung, and brain, as evaluated by fluorescence imaging and MRI. Only limited accumulation was observed locally in the nasal cavity as well as in heart and kidney.[291] Thus, the inhaled NPs could cross the tight barriers such as the pulmonary epithelium or the blood−brain and blood−testis endothelium.

Intraperitoneally injected (25−100 mg/kg dose for 4 weeks) SiO_2-coated MNPs (PVP-stabilized, fluorescent-tagged, 50 nm mean diameter) were found distributed at high concentrations into liver and spleen, followed by kidneys, heart, testes, and uterus, while a very low accumulation was observed in lungs.[292] In-depth investigation concerning the accumulation in the brain tissue revealed that these particles penetrated into the brain and

dx.doi.org/10.1021/cr300068p | Chem. Rev. 2012, 112, 5818−5878

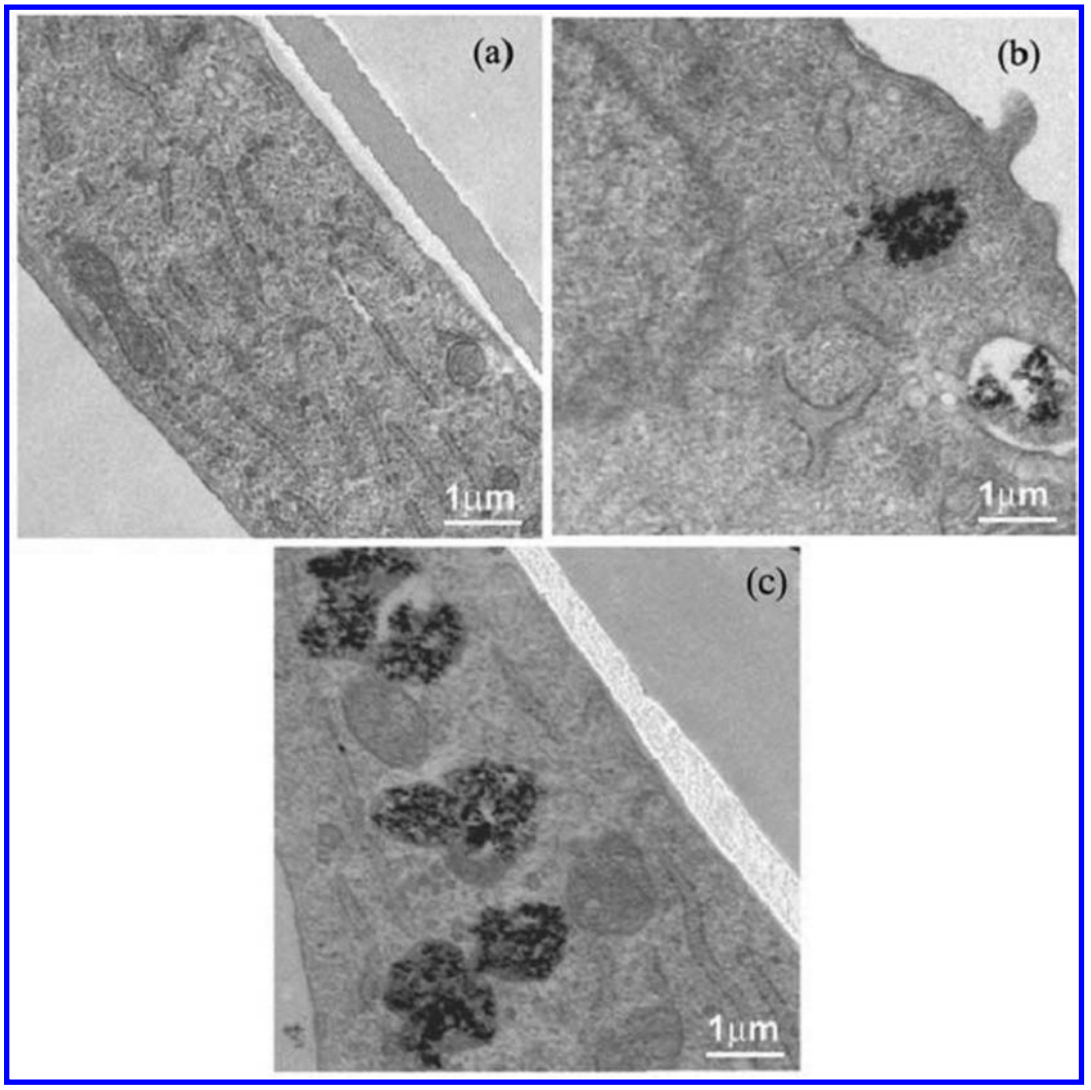

Figure 15. TEM pictures of human fibroblasts incubated with MNPs: (a) control, (b) uncoated, and (c) PEGylated. Reprinted with permission from ref 78. Copyright 2004 Springer.

were taken up specifically by the neuronal cells without structurally and functionally disturbing the blood−brain barrier (BBB).

4.4. Factors Influencing the Tissue/Cell Penetration

Concerning the tissue diffusion of NPs, an average diameter larger than 10 nm usually impedes their diffusion through the small vascular pores of the normal/healthy endothelium.[243,293] On the contrary, if the endothelial barrier is temporarily compromised by artificial means (e.g., heating or radiation) or as the result of specific pathologic conditions (e.g., inflammation or tumor infiltration), NPs up to ~700 nm could penetrate freely through the endothelium.[279] In addition to the particle size, the coating material also influences the degree of uptake of IONPs by the tissue, as well as their clearance from the tissue, especially in the case of the liver. For instance, despite the similar mean particle size of the NC100150 IONPs (methoxyPEG phosphate-coated, 12 nm diameter) (Clariscan) and of the fractionated SHU 555A IONPs [carboxydextran-coated, fractionated from SHU 555A (Ferucarbotran, Resovist, 59 nm mean diameter) by ultrafiltration to obtain 12-nm-diameter particles], their hepatic uptake at 3 days after i.v. injection (16% for NC100150 and 34% for fractionated SHU 555A) and their hepatic half-lives (29 h for NC100150 and 10 days for fractionated SHU 555A) were considerably different, as determined by relaxometry and induced coupled plasma-atomic emission spectroscopy.[85] The above differences may also suggest different degradation rates of these NPs in the liver. It is noteworthy that the degradation of iron oxide particles is influenced by the accessibility of the particle surface to water, which may vary depending on the coating layer. IONPs with similar coating materials but with different particle sizes exhibited similar rates of degradation in the liver. For instance, the 58-nm-sized SHU 555A and 12-nm-sized fractionated SHU 555A NPs having similar carboxydextran coating, injected i.v. at 5 mg Fe/kg, showed similar rates of degradation in the liver. A comparable observation was made concerning the metabolization in the liver of Ferumoxide and Ferumoxtran-10.[85] It has to be noted that, if the clearance of IONPs by hepatic tissue is not regulated by differences in particle size, the extent of particle uptake may, in turn, influence the rate of clearance.[294−296]

At the cellular level, the mechanism of penetration of the NPs is dramatically influenced by their size.[297] Larger NPs are only captured by the cells capable of phagocytosis, whereas smaller NPs (<150 nm) could have cellular access through

dx.doi.org/10.1021/cr300068p | Chem. Rev. 2012, 112, 5818−5878

pinocytosis.[298] Following cellular entry, the IONPs are clustered within the lysosomes, and the degradation into iron and oxygen is presumed to occur under the influence of low pH and of a variety of hydrolytic enzymes participating in the iron metabolism. One of the key advantages of IONPs relies in the fact that Fe ions, deriving from the biodegradation, are further reused by the cells via normal biochemical pathways of the Fe metabolism[299] (see also the review by Singh and co-workers).[300]

5. TOXICITY AND BIOCOMPATIBILITY

The biocompatibility of a drug nanocarrier is linked to both the immune system response following its administration and to the intrinsic toxicity of the carrier and/or of its biodegradation metabolites. Importantly, when associated with a nanocarrier, the toxicity profile of the drug itself may be increased or decreased as a consequence of a modification of its cell/tissue biodistribution and clearance/metabolization. Accumulation may, indeed, occur in biological sanctuaries where the drug cannot diffuse when administered alone.

From the toxicological standpoint, the colloids and their degradation products must be cleared from the body in the shortest time after the drug release has occurred. Obviously, the toxicity of magnetic particles may depend on numerous factors including the dose, chemical composition, size, structure, solubility, surface chemistry, route of administration, biodegradability, pharmacokinetics, and biodistribution.[261]

5.1. In Vitro Evaluation of the Toxicity

As already mentioned, the NP−cell interaction primarily depends on the nature of the NP surface. The prerequisite for improved drug delivery, improved diagnostic performance, and other applications of IONPs is the efficacy of their cell uptake and internalization. Incubation of the NPs with the cells may, however, alter the nature of cell adhesion, which may further affect the morphology, cytoskeleton, proliferation, differentiation, migration, and survival.[301,302]

5.1.1. Influence of the Surface Coatings. The biocompatibility of IONPs, surface-coated or not with PEG, was analyzed using in vitro cultured primary human fibroblasts (hTERT-Bj1).[78] The uncoated IONPs (~50 nm diameter) caused a significant decrease (by ~64%) in cell adhesion compared to that of the control cells, whereas PEG-coated NPs did not cause notable change. The uncoated NP-incubated cells were found to exhibit numerous vacuoles in the cytoplasm with disorganized cytoskeleton, cell membrane abnormalities, and disruption. However, the cells treated with PEGylated MNPs maintained their fibroblast cytoskeleton, although they underwent an increased cell uptake compared to the uncoated NPs. This could be attributed to different NP/cell interaction depending on the presence of PEG on the particle surface, whereas the kinetics of NP metabolism may also vary (Figure 15).

Incubation of dextran-coated IONPs (~10 nm diameter) with hTERT-BJ1 primary human fibroblasts caused cytotoxicity and apoptosis similar to that of the uncoated NPs.[303] The cell uptake of both dextran-coated and uncoated NPs was similar, but the former caused a greater decrease in cell motility and disruption of the cell membrane. On the opposite, the albumin-coated IONPs did not reduce cell viability unlike dextran-coated and uncoated NPs.[84,304] The albumin-coated NPs caused only a slight membrane disruption, probably because of the interaction of albumin with membrane phospholipids/fatty acids. However, overall, the toxicity of these NPs was considerably lower than that of the uncoated and dextran-coated NPs. Noteworthy is the fact that the cell internalization rate of the albumin-coated NPs was lower than that of the uncoated and dextran-coated particles, which suggests a possible influence of the different intracellular particle concentrations on the NP toxicity described above. However, it has been recently demonstrated that, even at concentrations as high as 1 mg/mL, Ferumoxtran-10 was not toxic to cells but showed a slight toxicity only at 10 mg/mL. Moreover, Ferumoxtran-10 did not activate human monocyte macrophages to produce pro-inflammatory cytokines or superoxide anions and did not interfere with Fc-receptor-mediated phagocytosis,[305] which highlighted the safety of these MNPs. Therefore, if the nature of the surface coating may significantly influence the cytotoxicity of IONPs, the same coating (i.e., dextran) onto different cores (i.e., 50 nm-sized IONPs as opposed to 20 nm-sized Ferumoxtran-10) may also have different toxicological implications due to the contribution of other parameters such as size, as discussed below.

5.1.2. Influence of the Size. The particle size may, indeed, have different effects on cells in vitro. For instance, 30-nm-sized IONPs showed relatively higher toxic effects as compared to that of 0.5-μm-sized particles.[306] When incubated with the A549 alveolar epithelial cell line, a size-dependent and dose-dependent influence on cell damage was observed. For instance, 30-nm-sized Fe_3O_4 particles caused higher oxidative DNA damage compared to 0.5-μm-sized particles, at a 80 μg/mL concentration, whereas at lower concentrations, such as 40 μg/mL, none of these particles were toxic, as assessed using comet assay. Additionally, at 80 μg/mL concentration, both 30-nm- and 0.5-μm-sized Fe_3O_4 particles showed mitochondrial depolarization, suggesting a mitochondrial damage with subsequent cell death induced by apoptosis.

The in vitro cytotoxicity of MNPs may also be linked to some cell culture modifications induced by NP incubation.[307] For instance, bare (uncoated) iron oxides are often negatively charged in water due to the adsorption of OH^- ions onto their surface. The resulting electric field may attract counterions and hence promote protein adsorption. Moreover, the Cl^- ions that may be present in the cell culture medium may also competitively bind to the Fe, thus altering the pH of the medium together with the surface characteristics of the NPs. Such interactions with the cell culture medium, resulting in alterations such as variations in the ionic concentration and protein function, may cause cell detachment and subsequently may lead to cell death. However, the surface-coated MNPs show, in general, minimal interaction with the components of the cell culture media, probably due to the availability of fewer sites for protein adsorption on the particle surface.[307]

5.1.3. Influence of the Surface Charge. The surface charge of IONPs may also influence the cell morphology and function. It was observed that the coating of 10-nm-sized IONPs with DMSA (anionic charge) enhanced endocytosis by various cell types[287,288] and caused a concentration-dependent decrease in cell adhesion as well as a reduction in the viability of the PC12 pheochromocytoma clonal cell line.[308] After a 48 h exposure to nerve growth factor (NGF), the spherical PC12 cells generally differentiate into neuronal cells and begin to form mature neuritis, which extends to the periphery. However, after incubation with anionic NPs, damages to the cytoskeleton occurred that hampered the neurite maturation and considerably decreased the number of neurite formation per cell as

dx.doi.org/10.1021/cr300068p | Chem. Rev. 2012, 112, 5818−5878

well as the length of the neuritis. Additionally, a decrease in expression of GAP-43 protein related to axonal sprouting and neuronal function was observed at the tested concentrations, suggesting a dose-dependent toxicity of these anionic MNPs (Figure 16).

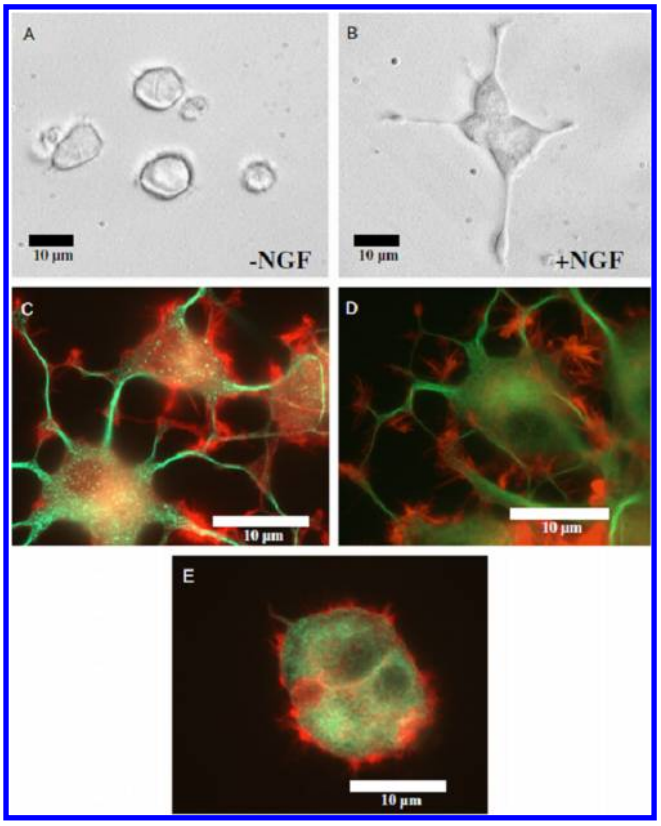

Figure 16. Phase-contrast images of PC12 cells, 48 h in culture (A) without nerve growth factor (NGF) and (B) with NGF (+NGF). PC12 immunofluorescence for tubulin (green) and actin (red) at 6 days after AMNPs exposure and 5 days after NGF exposure to a Fe concentration of 0 mM (C, control cells), 0.15 mM (D), and 15 mM (E). Control cells form more actin microfilaments throughout the entire cell and produce more mature neurites than cells exposed to AMNPs. Reprinted with permission from ref 308. Copyright 2007 Elsevier.

However, cytotoxicity of anionic IONPs was observed to depend on the nature of the surface coating: DMSA, citric acid, or lauric acid showed different cytotoxicity on SK-MEL-37 human melanoma cell line. The IC_{50} (half-maximal inhibitory concentration) values for DMSA-coated, citric acid-coated, and lauric acid-coated NPs were 2260, 433, and 254 μg Fe/mL, respectively. At very high concentrations such as 840 μg Fe/mL, lauric acid-coated NPs caused cellular apoptosis as indicated by morphological features typical of apoptosis pattern, such as surface blebbing, intense vacuolization, and chromatin condensation.[309] Thus, the surface coatings, even if providing similar surface charge to the resulting NPs, may importantly alter their cytotoxicity in a dose-dependent manner. A case-by-case evaluation of the cytotoxicity is therefore required regarding the intended application.

Even if the in vitro toxicity measurements of MNPs on various cell lines may reveal preliminary information concerning the safety of the NPs, these assays may have limited relevance, as they do not represent the real in vivo conditions. Noteworthy is the fact that the cytotoxicity may, however, be more pronounced in vitro than in vivo because in cell culture conditions the NPs and/or their degradation products (which can affect cell viability) remain in close contact with the cells and may act as a depot showing continuous effect. On the contrary, NPs are in vivo continuously eliminated from the body providing they are biodegradable.[284] Thus, it is obvious that the assessment of in vivo safety of the MNPs is essential for pharmaceutical applications.

5.2. In Vivo Evaluation of the Toxicity

As discussed previously, intravenously injected IONPs are mainly cleared from the systemic circulation by macrophages residing in the reticuloendothelial organs.[310] These NPs are taken up by the cells via receptor-mediated endocytosis and are presumably metabolized in the lysosomal compartment, which has low pH, hydrolytical enzymes, and proteins that participate in the iron metabolism.[311] The released free iron is then incorporated into the iron stores of the body, then gradually found as hemoglobin and in part bound to transferrin, and is mostly eliminated slowly via faecal route.[299,312] This was demonstrated for Ferumoxide and Ferumoxtran-10.[97] The total body iron store is ~4000 mg in a normal male adult. As a consequence, the injection of small quantities of iron may not pose iron-linked toxicity issues, but the injection of higher amounts may lead to an increased plasmatic iron concentration as a result of the surpassed transferrin iron binding capacity, which may lead to oxidative stress and various toxicities including cardiac and hepatic toxicity.[313] Thus, the toxicity of MNPs has been evaluated after different routes of administration such as i.v., intraperitoneal, and subcutaneous.

5.2.1. Toxicity after Intravenous Administration. IONPs stabilized with OA and pluronic F-127 coatings have been evaluated for safety following i.v. injection into rat at a dose of 10 mg Fe/kg (Figure 17).[314] Although ~55% of the injected iron accumulated in the liver at 6 h postinjection, such accumulation did not result in any notable or long-term alteration of serum biomarker levels such as alanine aminotransferase, aspartate aminotransferase, and alkaline phospha-

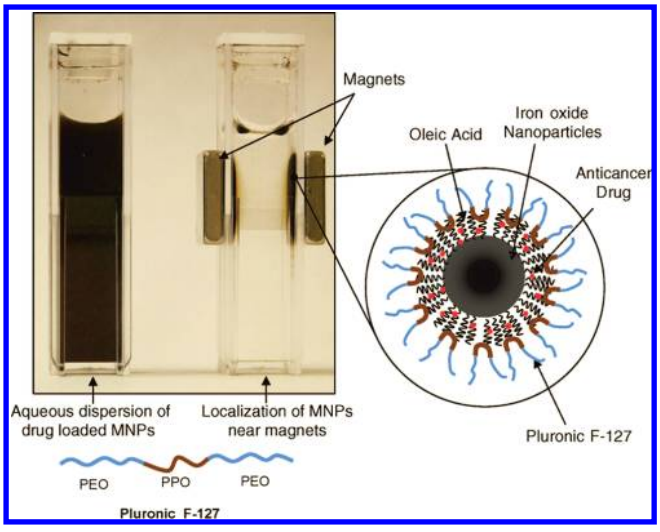

Figure 17. Schematic of oleic acid (OA)−Pluronic-coated iron oxide MNPs. Hydrophobic drugs can be partitioned in the OA layer around the iron oxide core. Pluronic F-127 anchored onto OA provides aqueous dispersibility. Reprinted with permission from ref 314. Copyright 2008 American Chemical Society.

dx.doi.org/10.1021/cr300068p | Chem. Rev. 2012, 112, 5818−5878

tase, which are indicative of the liver functionality. As iron overload in tissues may cause oxidative injury to the phospholipidic cell membrane, the lipid hydroperoxide levels were estimated to measure the oxidative effect induced by IONPs. The differences observed in lipid hydroperoxide levels were found to be tissue-dependent. In fact, they were slightly higher for liver, spleen, and kidney than for the other organs (i.e., lungs, brain, and heart). However, the higher lipid hydroperoxide levels did not affect tissue morphology and cellular integrity even up to 1 week postinjection, indicating that the oxidative stress was minor and insignificant at the injected dose. This suggests the importance of the dose and dosing interval of MNPs for their safe use as discussed below.

The MNPs showed, indeed, a satisfactory safety profile in different animal species but depending on the dose administered. For instance, Ferumoxtran-10 at a dose of 2.6 mg Fe/kg i.v. injection was safe in rats with no changes in hemodynamic parameters whereas 13 mg Fe/kg dose caused a slight increase in aortic blood flow, but no arrhythmia, no disturbance in electrocardiogram, and no respiratory toxicity were observed.[282] The treatment-related clinical signs, which lasted for 24 h postinjection, were observed in rats only at very high single doses such as 126 mg Fe/kg and 400 mg Fe/kg Ferumoxtran-10. However, repeated i.v. dosing of 17.9 mg Fe/kg Ferumoxtran-10 in rats (3−5 doses) caused moderate changes in body weight and hematological parameters. No maternal toxicities were observed in rats up to 15 mg Fe/kg/day nor in repeated injections (in rabbits up to <50 mg Fe/kg/day), and Ferumoxtran-10 was not mutagenic.[282] In dogs, Ferumoxtran-10 did not show any treatment-related cardiovascular and renal toxicities up to 20 mg Fe/kg i.v. injection, whereas at higher doses such as 200 mg Fe/kg (a dose 75 times higher than that used in human as a MRI contrast agent), slight cardiovascular toxicity, decrease in blood pressure, increase in respiratory rate, increase in cardiac output, and moderate increase in urine output and urinary sodium excretion were noticed. In monkeys, single doses up to 25 mg Fe/kg did not show any notable signs of cardiovascular toxicity or blood counts. After injection, the serum iron was found noticeably increased in rat, dog, and monkey, but normal levels were recovered after the treatment withdrawal. Overall, the toxicity of IONPs could be considered dose-dependent while, at the high dose, the nature of the toxicological events was similar in the different animal species tested.

A comparative acute toxicity study (i.v. single dose) carried out in mice using IONPs either uncoated or coated by different substances such as dextran, PEG, albumin, and PLA revealed IC_{50} values of 355, 355, 232, and 559 mg/kg, respectively. These results suggest that the PLA coating improved the tolerability of the NPs compared to the other coating materials tested. Pathological investigation on the dead animals revealed lung toxicity, heart filled black matter, and mild splenomegaly.[315] However, the particle size of these different NPs and the coating extent were not described in this report so that their impact on the NP toxicity cannot be overlooked. After oral feeding, the median lethal dose (LD_{50}) values of the above NPs were found to be >2000 mg/kg, suggesting a higher tolerability after oral feeding compared to the i.v. injection. IONPs stabilized by anhydroglucose polymer (50−150 nm diameter) were also found to be biocompatible after i.v. administration because no clinical signs of toxicity were observed in rats and mice.[316] Furthermore, a good tolerance was observed with dextran-stabilized IONPs (AMI-25, Feridex) in rats and dogs up to 3000 μmol Fe/kg, which corresponded to a dose that is almost 150 times higher than that required for diagnostic liver MRI purpose,[310] suggesting a broad safety margin of these NPs.

In human cancer patients, intravenously injected IONPs (100-nm-sized particles coated with anhydroglucose polymer) were found to be well-tolerated. These NPs (total iron injected per therapy session ranging from 132 to 468 mg) were loaded with the anticancer drug doxorubicin (Dox). A transient elevation of the serum iron levels was observed but without any toxic symptoms, while the urine iron concentrations were found to be in the normal range. In this clinical investigation, a magnetic field was applied at the skin surface where only a slight skin surface discoloration was observed without any other toxicological event.[317,318] Similarly, Ferucarbotran intravenously injected (5−40 μM Fe/kg) was found to be safe except a transient decrease in clotting factor XI activity, which did not lead to any clinically relevant adverse effects. Also, no cardiovascular changes related to blood pressure and heart rate were detected.[319−322] In another study, some minor side effects related to the central nervous system (CNS), including a lowered or increased spontaneous locomotor activity, rearing, exophthalmos, or mydriasis have also been observed.[323] It was mentioned in the literature that the chronic iron toxicity (cirrhosis or hepatocellular carcinoma) in humans may occur after administration of high doses of iron leading to hepatic iron concentrations over 4 mg Fe/g liver wet weight.[100]

The surface properties of NPs, such as surface charge, were found to influence the interactions of NPs with the biological system and, in turn, their safety. In general, the neutral and negatively charged NPs show lower interaction with plasma proteins than positively charged NPs that interact strongly with blood components, undergo nonspecific binding, and can cause cell lysis. Positively charged NPs also undergo relatively rapid clearance from systemic circulation, leading to nonspecific tissue uptake.[324,325]

5.2.2. Toxicity after Intraperitoneal Administration. The toxicity of $MnFe_2O_4$ NPs prepared as ionic NPs (charge-induced by Fe^{3+} and Mn^{2+}) (10 nm diameter) was compared to that of citrate-coated NPs (generated by chemisorption of citrate ions on the NP surface) after intraperitoneal injection in mice (0.5−0.0005 M concentration range).[326] Parameters such as LD_{50} and side effects were assessed, and cytogenetic analysis of the isolated peritoneal macrophages and bone marrow cells was carried out. The citrate-coated IONPs resulted in the death of ∼30% of mice, whereas the ionic IONPs and the free citrate control were well-tolerated. It was observed that the citrate-coated NPs considerably increased the mitotic index of the peritoneal macrophages as compared to the ionic NPs and thus stimulated the immune reaction. Both types of NPs induced inflammatory response by increasing the lymphocyte frequency in the peritoneal cell population. Moreover, higher concentrations of these ionic or citrate-coated NPs have considerably damaged the nuclei of both neutrophils and lymphocytes, indicating that both types of NPs were toxic following intraperitoneal administration that may represent a sort of local administration.

Intraperitoneally injected (25−100 mg/kg dose for 4 weeks) SiO_2-coated MNPs (stabilized using PVP, fluorescent-tagged) of 50 nm mean diameter were found to be safe and did not elicit any visible toxicity as assessed by tissue histology and body weight measurements in mice. These NPs did not show any mutagenic potential. Unexpectedly, some of these intraperitoneally injected NPs were detected in mouse brain,

dx.doi.org/10.1021/cr300068p | Chem. Rev. 2012, 112, 5818−5878

suggesting that these particles penetrate the BBB but without disturbing the structure and function of the barrier, as assessed by the BBB permeability measurements.[292] The mechanism by which these NPs could enter the brain deserves, however, further clarification.

5.2.3. Toxicity after Subcutaneous Administration. The subcutaneous injection of dextran-coated IONPs (15 nm mean size) was found to be safe up to 3150 mg/kg but induced mortality at 4500 mg/kg dose.[327] The LD_{50} was evaluated to be 4410 mg/kg. However, the causes of mice mortality were not investigated in this report. When 3150 mg/kg dose was subcutaneously injected, no changes in blood counts and in serum parameters (e.g., alanine aminotransferase and aspartate aminotransferase) were observed, indicating no liver toxicity. The subcutaneously injected IONPs (30 nm mean diameter) were reported to be well-tolerated in healthy mice, at 100 mg/kg dose, after single dose as well as after 10 repeated doses for 10 successive days.[328]

Overall, the IONPs may be considered as biocompatible, but their safety may vary with the composition, physicochemical properties, and route of administration, whereas the determination of the dose range and the dose schedule are key factors to avoid side effects and toxicity. Thus, as already pointed out, the IONPs safety should be evaluated case-by-case based on the intended medical and pharmaceutical applications. It has to be noted that not much information concerning the toxicity of the MNPs following oral feeding was found in the literature.

6. DISEASE THERAPY

Conventional drug delivery is often limited by poor specificity to the site of action and reduced drug diffusion through biological barriers, leading to a suboptimal pharmacological activity and high incidence of adverse effects.[329] These limitations could be potentially overcome by encapsulation and delivery of drugs using nanodevices. Carrier-mediated drug delivery has received significant attention in recent decades, because this approach has often resulted in improved pharmacokinetics and pharmacodynamics of the drugs, translating into an improved pharmacological efficacy and safety.[330,331] Drug encapsulation into stealth (i.e., plasma protein repulsive) nanocarriers (polymeric, lipidic, or inorganic) with an ability to minimize the drug distribution to macrophage-rich organs (such as the liver and the spleen) has resulted in prolonged systemic circulation of the carried drugs with possible specific translocation into diseased inflammatory tissues (the so-called EPR effect; see section 4). Consequently, the half-life and the exposure of the NP-encapsulated drug increase, and as a result, an improved therapeutic activity can be expected. For those drugs/NPs that do not cross the biological barriers by passive accumulation or those which need to be specifically delivered to the diseased cells, the so-called "active targeting strategy" must be employed. Stimuli-sensitive carriers, as a part of the active drug-targeting strategies, allow selective drug delivery to cells, organs, or tissues. These colloidal systems are engineered to be able to change their physical properties under exposure to an external stimulus (i.e., temperature, pH, ionic strength, or a magnetic gradient in the specific case of magnetic targeting), leading to the enhancement of drug accumulation at the intended site of delivery.

In this context, MNPs are promising stimuli-sensitive drug carriers because of their magnetic field responsiveness: an applied extracorporeal magnetic field can concentrate these nanodevices at the desired site, keeping them in place for a given period of time until the encapsulated drug is released, thereby minimizing the drug-associated side effects due to nonspecific distribution.[261,276,332−340] Alternatively, the heat generation property of the MNPs under the influence of an external AMF may contribute to an additional therapeutic mechanism called hyperthermia. Generally, the NPs smaller than 100 nm exhibit better tissue permeability properties and hence are suitable for heat-generating purposes, whereas the larger particles are suitable for magnetic targeting due to their higher sensitivity to magnetic guidance.[341]

6.1. Construction of Magnetically Guided Nanoparticles for Drug Delivery

Noteworthy is the fact that the use of MNPs as drug carriers requires the synthesis of composite particles capable of loading a sufficient amount of drug per unit volume of the carrier. Often the drug loading by surface adsorption is, however, insufficient to reach the therapeutic drug concentration necessary at the targeted site.[93,180−182] Thus, organic or inorganic shell-forming matrices have to be conceived to achieve sufficient drug payload. Usually, as stated before, magnetic drug-delivery systems are made of a magnetic core and a biodegradable organic or inorganic shell. Typically, the magnetic core allows magnetic accumulation of the NPs at the target site, whereas the shell acts as a drug reservoir able to release the drug as a consequence of the shell biodegradability. Additionally, the shell may provide surface functionality for decorating the MNPs with agents (i.e., specific ligands) that still improve the tissue/cell specificity.

The drug loading into the MNPs is usually carried out by dissolving the drug in either an organic phase (nonaqueous phase) in which the shell material is dissolved or in the aqueous phase containing the MNPs.[5,93,180−182,342] The core/shell NPs may be obtained by different techniques: (i) the nanoprecipitation technique in which the water-miscible organic phase (e.g., ethanol, acetone, and tetrahydrofuran) containing the dissolved shell material is added into the aqueous phase containing the IONPs followed by the evaporation of the organic solvent; and (ii) the emulsification/evaporation technique in which the water-immiscible organic phase (e.g., ethyl acetate and dichloromethane) containing the dissolved shell material is emulsified into an aqueous phase holding the IONPs and the stabilizer, before organic solvent evaporation. The size reduction may be achieved using a microfluidizer or a high-pressure homogenizer. The size and polydispersity of the NPs are the main controls for ensuring batch-to-batch uniformity.

Because, as mentioned previously, the drug payload and the drug-release rate are essential parameters, special attention has to be paid to the preparation procedures and to the drug and coating material interactions. Drugs whose therapeutic doses are low, but having strong electrostatic affinity toward MNPs, can be loaded just by adsorption onto the NP surface. In contrast, those exhibiting high therapeutic doses must be incorporated into the organic/inorganic shell formed over the magnetic core. In this case, the drug should have strong affinity for the shell (selected for its encapsulation properties) to avoid quick release, leading to a pharmacokinetic/pharmacodynamic profile similar to that of the free drug. Generally, the drug release from the intravenously injected NP matrix depends on the drug's partitioning coefficient (K) between the NP matrix and the biological medium. A high K value indicates high affinity of the drug toward the NP matrix and hence requires

dx.doi.org/10.1021/cr300068p | Chem. Rev. 2012, 112, 5818−5878

higher dilution volumes for inducing the drug leakage from the NP, resulting in a sustained drug release. Thus, a rational selection of the shell matrix based on the physicochemical properties of the drug to be incorporated is needed to allow (i) retention of the drug in the NP until it reaches the biological target (a property essential for targeting application) and (ii) further drug release at the target site.

The efficacy of the magnetic guidance may depend on (i) the ability to minimize the rapid systemic clearance of the NPs by the liver and the spleen to the detriment of the targeted tissue and (ii) the ability to efficiently cross the barriers at the tissue level (e.g., vascular endothelium in the case of i.v. administration). Therefore, the MNPs must possess sufficient magnetic susceptibility whereas the force fields acting on them must be strong enough to ensure the transport of the drug carrier to the target site before and during release.[5] At the site of action, the drug release may occur by simple diffusion from the NP matrix or through other mechanisms such as enzymatic/chemical degradation or pH-, temperature-, or electromagnetic-triggering.[261,343,344]

When using an external magnetic field for drug-targeting purpose, the therapeutic efficacy is determined by the location of the magnet (as close as possible to the targeted tissue) and by the physiology of the host (body weight, organ function, blood volume, cardiac output, and peripheral resistance of the circulatory system).[243,345] To solve the issues related to the penetration depth of the externally applied magnetic field,[346] it is now possible to use permanent neodymium iron boron (Nd−Fe−B) magnets in combination with SPIONs.[347] The use of an implanted magnet is another promising strategy that would optimize the delivery of MNPs to the selected biological areas.[348−350] For instance, it has been reported that the insertion by laparoscopy in the rabbit of a small permanent magnet in the lower pole of the kidney significantly enhanced the accumulation of Dox-loaded iron−carbon particles in the kidney containing the magnetic implant (by comparison with the control kidney without magnetic implant; Figure 18).[351]

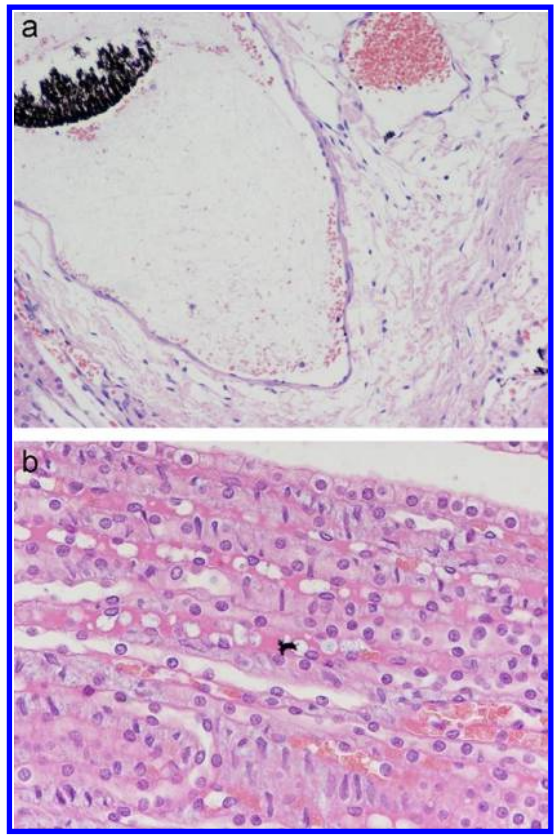

Figure 18. Histopathology analysis. (a) Image of left kidney in which a magnet has been inserted (hematoxylin and eosin stain, 200× magnification): the NPs are clearly visible and oriented in the direction of the magnetic field gradient. (b) Right control kidney (400× magnification): practically no particles are observed. Reprinted with permission from ref 351. Copyright 2007 Elsevier.

6.2. Chemotherapy

6.2.1. Systemic Chemotherapy. *6.2.1.1. Preclinical Studies.* IONPs coated with polymeric, lipidic, or inorganic shells were used as drug-delivery carriers for systemic administration of anticancer agents. For instance, superparamagnetic Fe_3O_4/PCL core/shell NPs (∼160 nm diameter) containing the anticancer drug gemcitabine (Gem, loaded into the polymeric matrix) is an excellent illustration of efficient magnetic drug targeting after i.v. injection.[352] Under the influence of an external magnetic field (generated by fixing the magnets on the skin around the tumor area in mice with subcutaneously implanted human pancreatic adenocarcinoma), these magnetically guided NPs showed significant antitumor activity at a dose 15-fold lower than that of free Gem. The magnetic targeting was evidenced by staining the iron particles accumulated into the tumors, using the Prussian blue staining technique.

Similarly, epirubicin-loaded MNPs (50−150 nm diameter) have been successfully used for the treatment of mice with subcutaneously implanted colon carcinoma or hypernephroma.[317] The drug loading was done by adsorption onto NPs stabilized by anhydroglucose. In this study, permanent rare earth magnets with magnetic field strengths up to 500 mT were fixed around the tumor site and the NP formulation was injected intravenously. Following this treatment, both the colon and the renal carcinomas were found to shrink and disappeared after a few days, thus evidencing an efficient antitumor activity compared to the same treatment but in the absence of an extracorporeal magnetic field or to the treatment with the free drug.

Recently, cross-linked (trimethoxysilyl)propyl methacrylate-γ-PEG methacrylate-coated SPIONs bearing carboxyl groups onto which the positively charged Dox was electrostatically loaded were synthesized (Figure 19).[353] Following i.v. administration and in the absence of any extracorporeal magnetic field, this NP formulation underwent already significant extravasation into the tumors and less accumulation than the free drug into nontarget organs such as the liver. A remarkable antitumor activity at 8-fold lower dose than the free drug (0.64 mg/kg for the NP formulation and 5 mg/kg for free Dox) was obtained on subcutaneously implanted Lewis lung carcinoma bearing mice. Toxicological evaluation revealed that the therapeutically active dose of free Dox induced hepatic impairment, lymphatic damage, and reduced white blood cell count, whereas the NP formulation was found to be nontoxic. Because no magnetic field was used in this study, the superior efficacy of the MNP formulation may only be assigned to the long-circulating properties of these particles allowing passive accumulation into the tumors. In this study, the use of a magnetic core may not bring any additional therapeutic benefit over the traditional nonmagnetic long-circulating NPs, but it allowed for the performance of MRI of the tissues (Figure 19).

Magnetic liposomes have also been used as stimuli-sensitive nanodevices under the influence of a magnetic field;[354] with

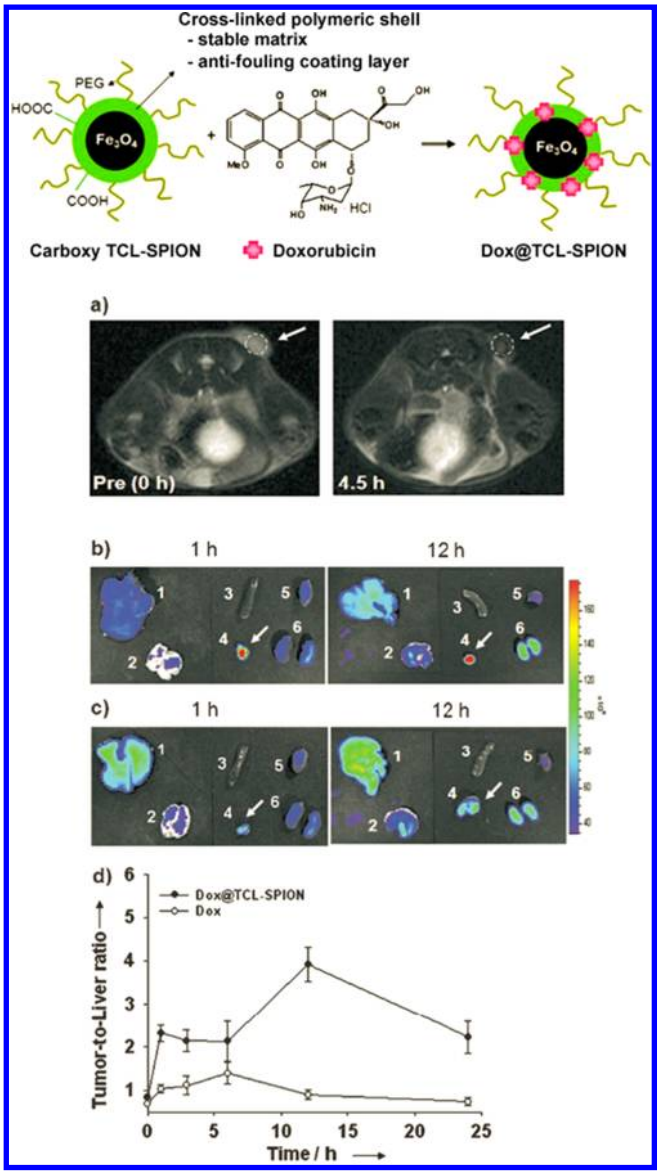

Figure 19. (Upper part) Formation of Dox-loaded thermally cross-linked SPION (Dox@TCL-SPION). (Lower part) (a) T_2-weighted fast-spin echo images (time of repetition/time of echo: 4200 ms/102 ms) taken at 0 and 4.5 h after injection of Dox@TCL-SPION at the level of Lewis lung carcinoma (LLC) tumor on the right back of the mouse. The dashed circle with white arrow indicates the allograft tumor region. (b and c) Optical fluorescence images of major organs and allograft tumors: 1, liver; 2, lung; 3, spleen; 4, tumor; 5, heart; 6, kidney. The images were taken after i.v. injection of (b) Dox@TCL-SPION (equivalent to 4 mg of Dox) and (c) free Dox (4 mg) into tumor-bearing mice (n = 3); mice were euthanized after 1 h and 12 h. (d) The ratio of fluorescence intensities of tumor to liver for Dox@TCL-SPION (closed circles) and free Dox (open circles) as a function of time. Reprinted with permission from ref 353. Copyright 2008 Wiley.

such a nanodevice, the combination of drug-delivery and imaging purposes (i.e., "multifunctional" liposomes) is another exciting approach.[355,356] Liposomes have been intensively explored as drug carriers due to their excellent biocompatibility, ability to incorporate both hydrophobic and hydrophilic compounds, acceptable stability, and ease of surface functionalization to achieve prolonged circulation and molecular targeting properties.[357] Magnetic liposomes may be constructed either by incorporation of magnetic cores into the phospholipid bilayer or into the aqueous compartment, depending upon the type of manufacturing technique employed.[95] They have been used to deliver drugs for various therapeutic indications (i.e., muscle relaxation, tumor treatment using photosensitizers and anticancer agents, etc.). It was observed that uptake of magnetic fluid-loaded liposomes by human prostatic adenocarcinoma cells was significantly improved by guidance in the near vicinity of the cells by means of a 0.29 T external magnet developing a magnetic field gradient close to 30 mT/mm. Double detection of lipids by fluorescence tracking and of iron oxide by magnetophoresis showed excellent correlation, demonstrating that magnetic liposomes associated with tumor cells as intact vesicle structures which conserve their internal IONP content.[358]

Intravenously injected muscle relaxants diadony- or diperony-loaded magnetic liposomes showed 3−5 times higher efficacy (reduction in nerve muscle stimulation) under the influence of an external magnetic field (applied to the leg muscle of cats), as compared to the control treatment in the absence of any magnetic field.[95]

The tumor targeting of phthalocyanin-based photosensitizers (such as Photosense and Teraphthal) is another application of magnetic liposomes subject to the application of a magnetic field: once the vesicles accumulated in the tumor tissue, the photosensitizers were activated by laser irradiation or catalytic activation by ascorbic acid to elicit the therapeutic activity.[95]

Magnetic liposomes have also been used for efficient liver targeting with and without inhibition of the RES using gadolinium (Gd^{3+}) chloride as a RES blocker. It was demonstrated that the magnetically guided vesicles could accumulate into the liver even when the RES was inhibited, indicating that the observed hepatic accumulation was due to the external magnetic field rather to the unspecific macrophage uptake.[359]

6.2.1.2. Clinical Studies. MNPs of ∼100 nm in diameter stabilized by anhydroglucose, at the surface of which the anticancer agent epirubicin was adsorbed, have been tested in cancer patients.[317,360] In this clinical investigation, the tumor of the patients was exposed to an external magnetic field and the NP formulation was perfused during 15 min. An increased accumulation of the NPs into the tumors was observed by MRI. Of the 14 patients treated with the NP formulation, 4 patients showed slight tumor reduction, while constant tumor size or tumor progression was observed in the remaining patients. Although this study was performed on a small number of patients with interindividual variations and limited anticancer efficacy, it provided encouraging results for magnetic tumor targeting in humans.

6.2.1.3. Functionalization with Targeting Ligands. Targeting of NPs to specific organ/tissue or cells in the body could be classified as "passive targeting" and "active targeting". As discussed before, passive targeting is a phenomenon by which the accumulation of NPs occurs into the organ/tissue, owing to their physicochemical characteristics, such as size and surface properties; whereas in the case of active targeting, the NPs are enabled to accumulate in the intended organ/tissue or cells by using either stimuli-responsive or surface-functionalized nanodevices with homing moieties.[330,331,361−363] In the case of cancer, the surface conjugation involves specific ligands possessing high affinity toward the unique molecular signatures found on malignant cells or on endothelial cells lining the tumor neovasculature.[330,364]

dx.doi.org/10.1021/cr300068p | Chem. Rev. 2012, 112, 5818−5878

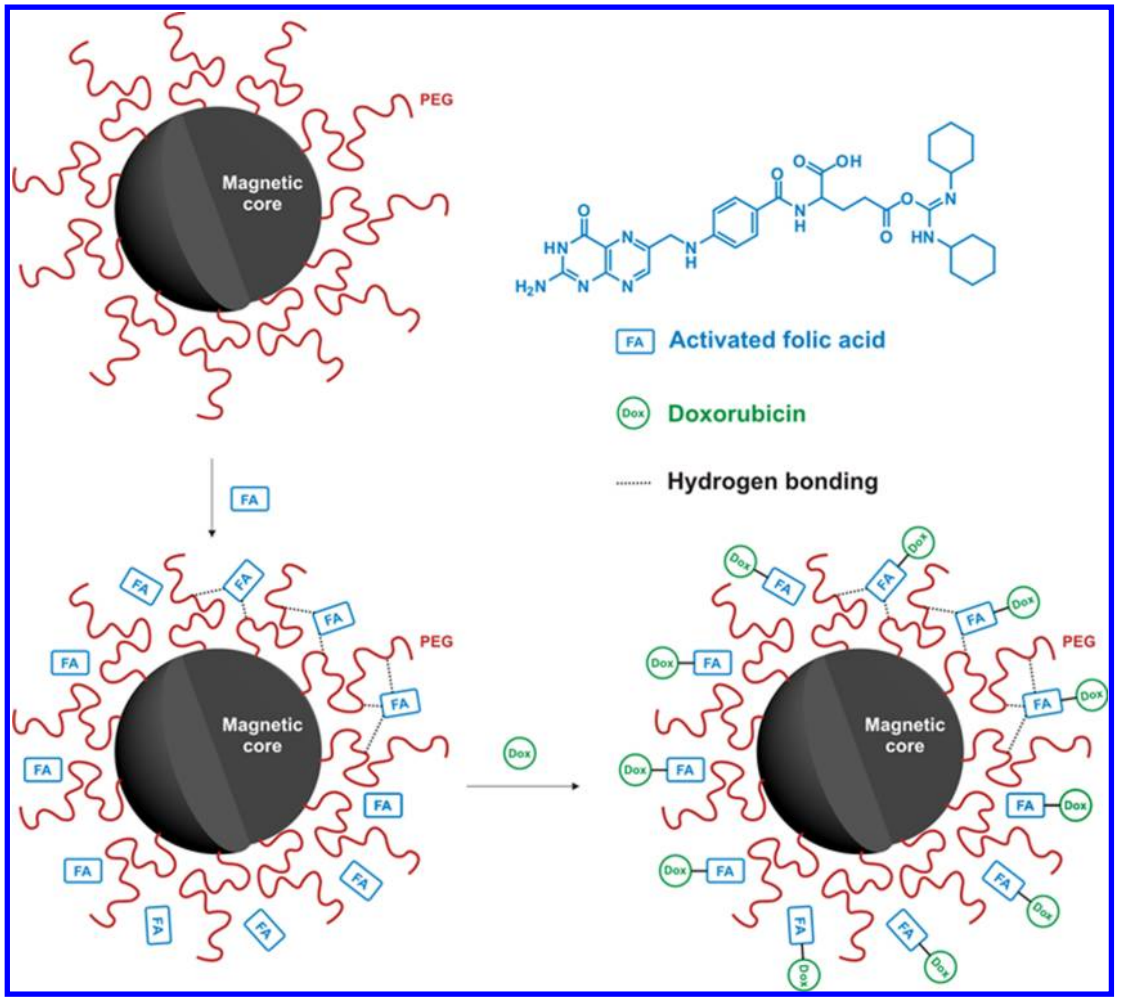

Figure 20. Synthesis of FA-modified and PEG-coated Fe_3O_4 NPs conjugated with Dox. Reprinted with permission from ref 384. Copyright 2008 Elsevier.

In general, various categories of targeting ligands have been employed for tissue-specific targeting of drug nanocarriers: (i) peptides such as RGD (arginine-glycine-aspartate sequence), which recognizes and binds to $\alpha_v\beta_3$ integrins that are overexpressed on a variety of angiogenic tumor endothelial cells;[365] (ii) proteins such as transferrin that target the transferrin receptors overexpressed on a variety of tumor cells[366] and annexin V, which recognizes and binds to the phosphatidyl serine receptors expressed on the apoptotic cell surface;[138] and (iii) aptamers that target specific antigen types expressed/overexpressed on the cancer cells (e.g., prostate-specific membrane antigen).[367−371] Monoclonal antibodies (MAb's) have also been used to deliver MNPs,[83,372−377] despite their large size, inherent immunogenicity, and a somewhat poor diffusion through the biological barriers.[378] For specific targeting of hepatocytes, sugar molecules were exploited such as galactose moieties that can bind to the asialoglycoprotein receptors overexpressed by the hepatocytes.[379] For instance, amino-functionalized SPIONs (ASPIONs) and lactose-derivatized galactose-terminal-ASPIONs have been reported for the specific targeting of the asialoglycoprotein receptors overexpressed at the surface of the hepatocytes.[379] Small molecule targeting ligands, such as anisamide, which is specific of the sigma receptors overexpressed on certain cancer cell types,[380] or folic acid (FA), which targets the folate receptors overexpressed in ovarian cancers,[381] may also be employed as homing devices for tumor targeting. These small molecular ligands offer the possibility of increasing the affinity of MNPs toward the cancer cells through multivalent attachment. In addition, they have a better chemical stability than proteins and peptides, thus reducing the risk of loss of functionality during the synthesis of the ligand-functionalized MNPs.[382,383] Especially FA has been extensively applied for the surface decoration of IONPs. For example, FA-functionalized and PEG-coated IONPs were used as carriers to deliver Dox to the tumor cells (Figure 20).[384]

Similarly, folate−PEG−PCL copolymeric micelle system (75 nm diameter) noncovalently loaded with Dox and SPION showed improved targeting toward folate-overexpressing KB human oral squamous carcinoma cell line.[385] The in vitro cell uptake was additionally enhanced when subjected to an external magnetic field. Although these in vitro results deserve interest, the in vivo demonstration of the synergic effect between folate targeting and magnetic guidance would have represented an important added value.

The functionalization of IONPs by cell penetrating agents such as the transactivator of transcription (TAT)-peptide has also been proposed for improved intracellular penetration.[139,386−388] For example, TAT-functionalized magnetic polymer/lipid hybrid particles were used to enhance the penetration of drugs through the blood−spinal cord barrier.[389] Practically, these TAT-conjugated PEGylated MNPs (83 nm

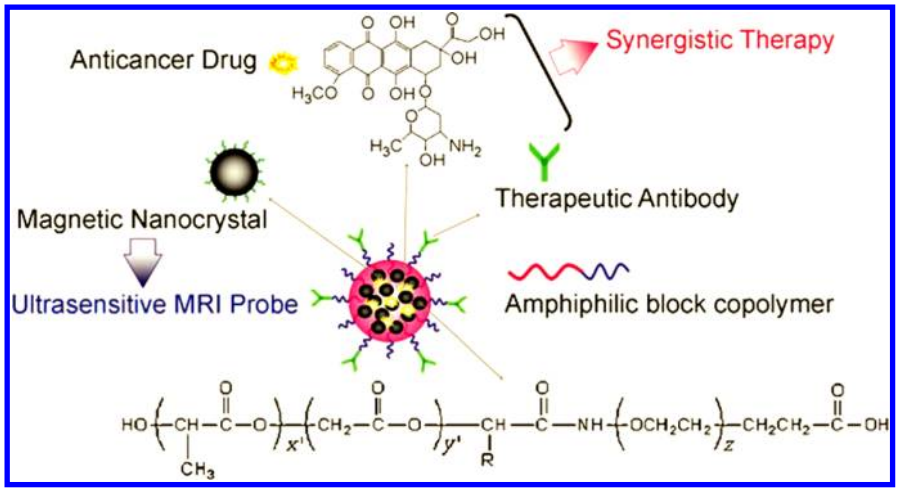

Figure 21. PEGylated PLGA-coated MNPs functionalized with herceptin for targeted detection and synergistic therapeutic effects on breast cancer. Reprinted with permission from ref 400. Copyright 2007 Wiley.

mean diameter) were synthesized using PEGylated amphiphilic octadecyl quaternized carboxymethyl chitosan, cholesterol, and SPION. Following i.v. injection in an experimental rat model, considerable accumulation of the magnetic polymer/lipid hybrid NPs occurred around the spinal cord injury site and inside the nerve cells, as compared to the nontargeted magnetic hybrid NPs (i.e., without TAT), suggesting the potential of this approach for delivering drugs across the blood−spinal cord barrier. However, in this experiment, no magnetic field was used for guiding the MNPs, and hence the rationale for using a magnetic core containing PEGylated polymer/lipid hybrid NP instead of a simple PEGylated polymer/lipid hybrid NP is not clear.

6.2.1.4. Theranostics. Nanodevices possessing both therapeutic and diagnostic features (i.e., "nanotheranostics") represent the "holy grail" for scientists in the pharmaceutical world. Ideally, the intravenously injected theranostic nanomedicine must be capable of addressing the chemotherapy agent toward the target tissue/cell, simultaneously allowing the monitoring/visualization of the response to the treatment (e.g., the visualization of the tumor volume decrease).[390] A variety of recent studies have reported the development of theranostic systems, either magnetic[173,391−394] or nonmagnetic.[395,396] Noteworthy is the fact that most of the reports on MNPs for theranostic purposes have verified the proof-of-concept only in vitro in cell cultures rather than in vivo. For instance, iron oxide encapsulated poly(acrylic acid) core/shell NPs derivatized with FA and noncovalently loaded with a fluorescent agent and the anticancer molecule paclitaxel (Ptx) have been used for drug delivery and simultaneous dual optical and MRI applications. The ability of this NP formulation to deliver the encapsulated Ptx together with dual imaging capability was demonstrated in vitro on normal cardiomyocytes and folate overexpressing A549 lung tumor cells.[392] Also reported was the design of multifunctional mesoporous SiO_2 NPs (~50 nm diameter) consisting of a single Fe_3O_4 nanocrystal core and a mesoporous SiO_2 shell surface-functionalized with PEG and exhibiting both MRI and fluorescence imaging capabilities. Dox was noncovalently loaded to the SiO_2 overcoat, whereas the fluorescent dye (e.g., fluorescein isothiocyanate or rhodamine B isothiocyanate) was covalently linked to this shell to permit fluorescence imaging. The proof-of-concept of this approach for combined drug delivery and imaging was verified in vitro using MCF-7 breast tumor cell line.[397] Similarly, Dox-loaded cRGD-functionalized IONPs coated with a PEG-*b*-PLA shell were used for targeting the integrins overexpressing SLK endothelial cells in vitro, simultaneously allowing MRI of the NPs accumulation into the cells.[173]

One of the very few examples of an in vivo theranostic approach consists of the use of PEGylated PLGA-coated MNPs functionalized with herceptin (trastuzumab). HER2 is a human epidermal growth factor receptor-2 overexpressed at the surface of breast and ovarian tumors that has been correlated with a poor prognosis.[398,399] Herceptin is a mAb that recognizes and binds selectively to HER2. The PEGylated PLGA-coated MNPs functionalized with herceptin and loaded with Dox have demonstrated their ability to address the drug to the cancer tissue in vivo with simultaneous MRI. Following i.v. injection, this nanoformulation showed an improved antitumor activity on the NIH3T6.7 subcutaneously grafted tumor in mice, compared to the control NPs conjugated with an irrelevant antibody, or to the free drug, or to a physical mixture of the free drug and herceptin. Thus, these herceptin-functionalized NPs were able to combine therapeutic and diagnostic capabilities (Figure 21).[400]

Similarly, fumagillin (an antiangiogenic drug)-loaded MNPs surface-functionalized with RGD for in vivo targeting of $\alpha_5\beta_1(\alpha_v\beta_3)$ or $\alpha_v\beta_3$ integrins in MDA-MB-435 tumors were used for simultaneous drug delivery to tumor angiogenesis and imaging.[401] In both of the above examples, no external magnetic field was employed for tumor targeting, and thus the magnetic core was used only as a contrast agent for MRI.

Gang and co-workers[352] developed MNPs coated with a PCL shell into which the anticancer drug Gem was encapsulated. In this experiment, the tumor targeting was obtained in vivo by employing an extracorporeal magnetic field. The intravenously injected magnetically targeted NPs showed antitumor efficacy similar to free Gem but at a 15-fold lower dose. Here, it is interesting to note that the NPs did not contain PEG functionality, and hence, inclusion of PEG may be expected to further enhance the amount of particles reaching the tumor, due to the minimized RES uptake and systemic clearance.

Recently, Couvreur and co-workers reported a novel nanotheranostic platform in which the theranostic particles have been constructed by coating IONPs with a lipidic prodrug (i.e., a drug conjugated to squalene, a natural and biocompatible

dx.doi.org/10.1021/cr300068p | *Chem. Rev.* 2012, 112, 5818−5878

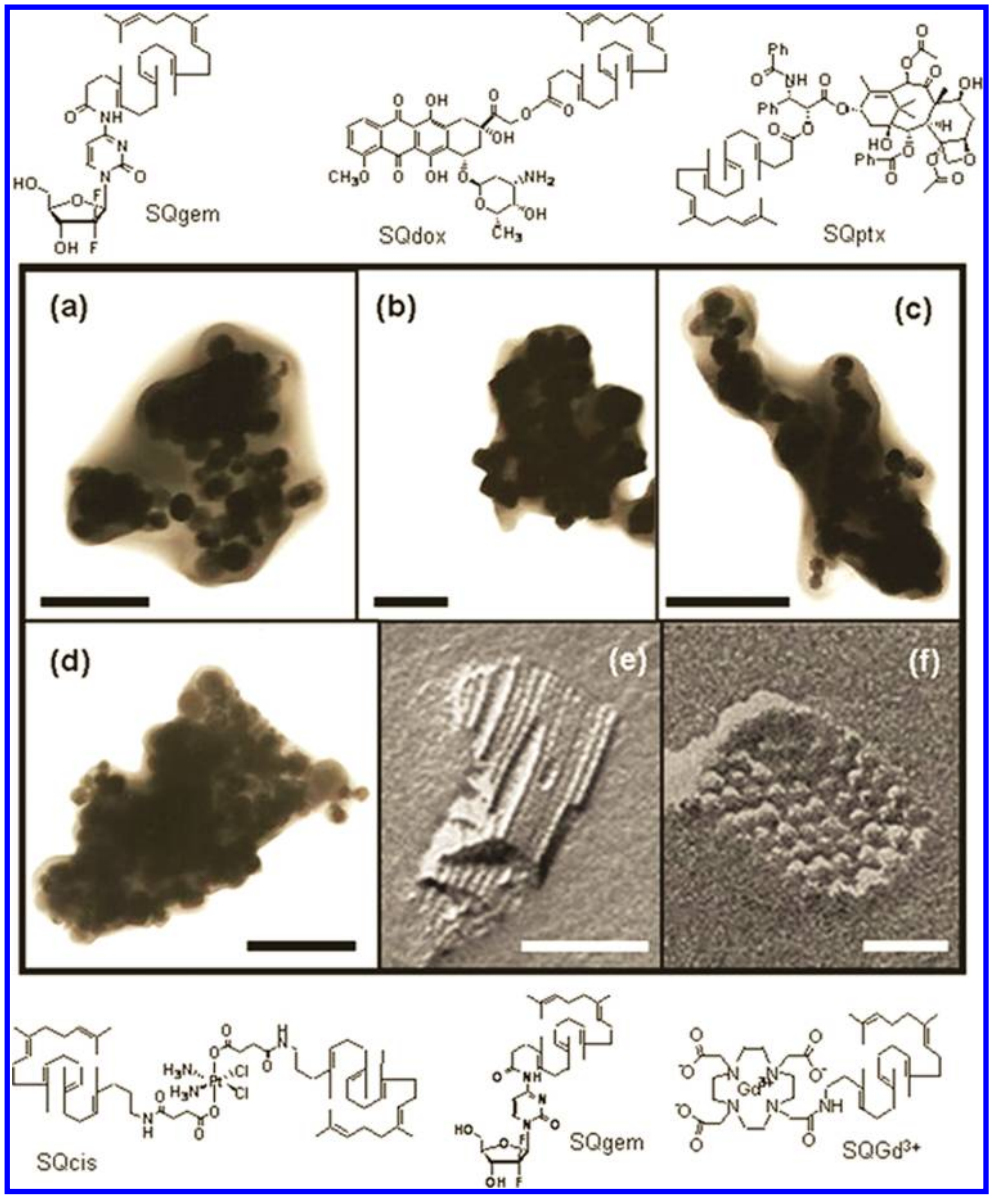

Figure 22. HRTEM photographs of SPIONs coated with the squalenoyl gemcitabine (SQgem) bioconjugate (SPION/SQgem) (a), SPIONs coated with the squalenoyl doxorubicin bioconjugate (SPION/SQdox) (b), SPIONs coated with the squalenoyl paclitaxel bioconjugate (SPION/SQptx) (c), and SPIONs coated with the squalenoyl cisplatin bioconjugate (SPION/SQcis) (d). Freeze-fracture TEM photographs (FF-TEM) of SPION/SQgem (e) and composite NPs made of SQgem and squalenoyl gadolinium bioconjugate (SQgem/SQGd^{3+}) (f). Bar lengths: 100 nm (a–e) and 50 nm (f). Reprinted with permission from ref 394. Copyright 2011 American Chemical Society.

lipid) (Figure 22).[216,394] When these NPs were intravenously injected into the tumor-bearing mice and guided using an extracorporeal magnetic field, an impressive anticancer activity was obtained with very low doses of the anticancer drug (i.e., Gem at 5 mg/kg). Because of the embedded IONPs, the tumor collapse could be easily visualized by MRI (Figure 23). This concept has also been enlarged to other anticancer compounds [e.g., Dox, Ptx, cisplatin (Cis), etc.] using also T_1 SQGd^{3+} instead of the iron oxide cores for imaging. The major benefits of this nanoparticulate platform are (i) very high drug loading; (ii) sustained drug release linked to the prodrug nature of the anticancer agent; and (iii) ability to magnetically address the drug to the tumor tissue despite the absence of homing device.

6.2.2. Local Chemotherapy. In preclinical studies, locoregional administration of MNPs close to the tumor sites has been shown to efficiently treat various experimental cancers. The advantage of this approach is that the locoregional injection limits the biodistribution of the NPs and facilitates rapid access of the NPs to the tumor site in the direction of the blood flow to the tumor, as opposed to the overall biodistribution of the NPs after i.v. injection. When subjected to an extracorporeal magnetic field, the proportion of tumor-accumulated NPs is expected to be still dramatically increased in locoregional injection versus i.v. injection. For instance, intra-arterially injected, methotrexate-loaded, starch-coated SPIONs (100 nm diameter) exposed to an extracorporeal magnetic field have demonstrated remarkable antitumor activity with complete remission of the experimentally induced VX-2 squamous cell carcinoma in rabbits.[402] In another report,[403] intracarotid arterial injection followed by magnetic guidance of drug-free PEI-modified MNPs (110 nm diameter) toward an orthotopic glioma model in mice resulted in a 30-fold enhanced tumor

dx.doi.org/10.1021/cr300068p | Chem. Rev. 2012, 112, 5818–5878

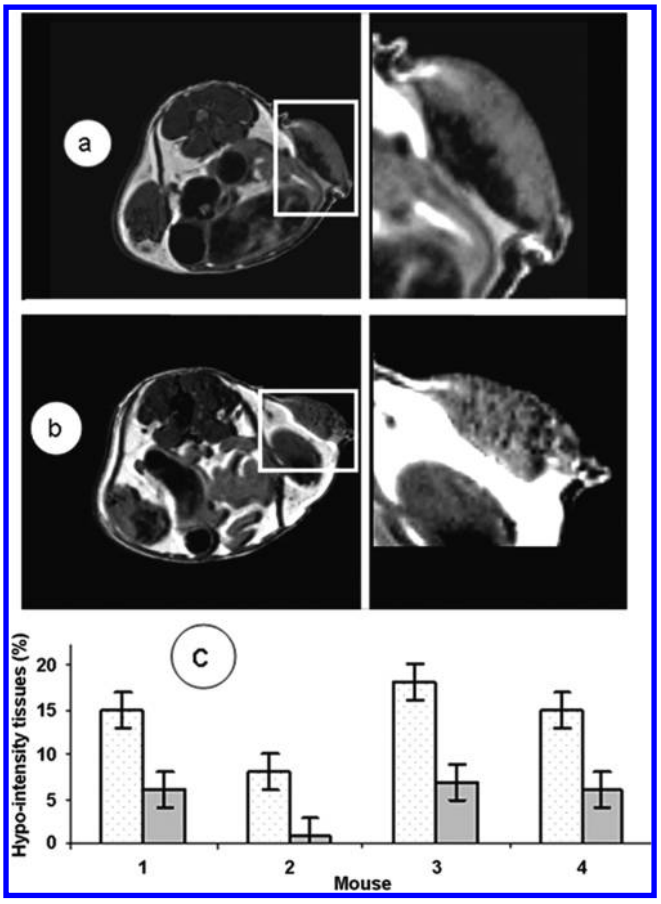

Figure 23. T_2-weighted images of the tumors obtained at 2 h postinjection of SPION/SQgem NPs (a) in the absence of an external magnetic field and (b) guided by an external magnetic field (1.1 T); (c) percentage of the hypo-intensity tissues with T_2 < 36 ms (white column) and with T_2 < 20 ms (gray column). Mouse 2 was injected with nanocomposites without exposition to magnetic field. Mice 1, 3, and 4 were injected with SPION/SQgem NPs with 2 h exposure to 1.1 T magnetic field. Reprinted with permission from ref 394. Copyright 2011 American Chemical Society.

accumulation as compared to a single i.v. injection of the same NPs, suggesting the potential of locoregional infusion for therapeutic drug delivery to brain tumors.

In a pioneer study, magnetic albumin NPs of larger size (~1 μm mean diameter) loaded with adriamycin have been employed for the treatment of subcutaneously implanted Yoshida sarcoma in rat tail. The placebo magnetic particles (particles without drug) injected intra-arterially proximal to the tumor and maintained under the influence of an external magnetic field have shown important accumulation in the tumor and were rapidly endocytosed by the tumor cells (as early as 10 min after administration).[404] When adriamycin was loaded into the above-mentioned particles, a remarkably higher anticancer activity was observed than with the free drug or with drug-loaded MNPs without exposure to the external magnetic field. All the nontarget tissues showed much lower drug concentrations after treatment with the magnetically guided NPs and hence the incidence of adverse effects was found to be much lower.[405]

BMs have also been attempted for the delivery of therapeutic substances through locoregional administration. This crystalline structure is present in the intracellular organelles of the magnetotactic bacteria *Magnetospirillum gryphiswaldense*[406,407] or *Magnetospirillum magnetotacticum*.[408] BMs have been extensively characterized for magnetic applications due to their nanosize (~50 nm diameter) and paramagnetic properties.[409−411] These magnetosomes have been used as carriers for drugs and DNA.[412,413] For instance, the antitumor effect of Dox-loaded BMs (Dox-BMs) was studied on EMT-6 and HL60 hepatocellular carcinoma cell lines and on the corresponding in vivo tumor models. Dox-BMs showed similar cytotoxicity and in vivo antitumor activity on H22 hepatic tumor-bearing mice as free Dox after subcutaneous injection close to the tumor site. From a toxicological standpoint, Dox-BMs showed less cardiotoxicity compared to free Dox as assessed by histology evaluation, probably due to a different biodistribution profile of the NP formulation. However, as no magnetic field was applied in this study, the BMs acted only as a conventional drug carrier rather than through their magnetic properties,[413] although they may also exhibit application in imaging.

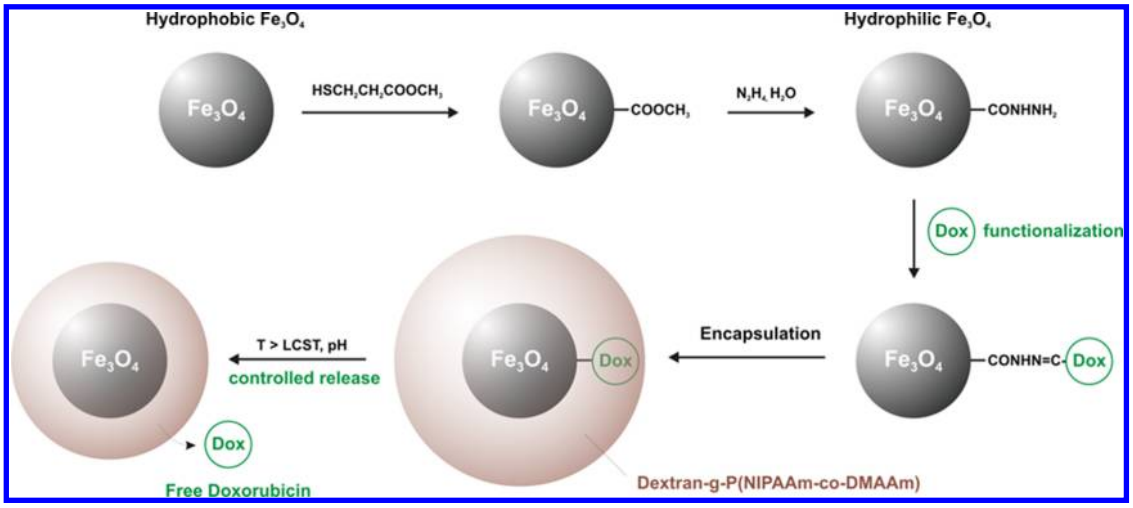

Figure 24. Schematic representation of the sequence of steps in the synthesis of the core/shell dextran-*g*-P(NIPAAm-*co*-DMAAm) magnetic carrier. Also illustrated is the drug-release process through a collapse mechanism at a temperature greater than the lower critical solution temperature (LCST), which resulted in rapid release of the drug.

dx.doi.org/10.1021/cr300068p | *Chem. Rev.* 2012, 112, 5818−5878

6.2.3. Oral Delivery. It has been suggested in a few studies that MNPs could also be used for the oral delivery of therapeutic agents. For instance, a magnetic liposomal formulation administered orally to mice with the intestine exposed to an external magnetic field resulted in an increased retention of the formulation in the intestine, followed by oral absorption and hepatic accumulation, as compared to the oral administration in the absence of magnetic field.[414] Although this study offers some hope for magnetic field-mediated oral delivery, it is important to ensure the liposome stability in the gastrointestinal tract. Moreover, because no drug candidate was employed in the above study, the real potential of this approach remains to be verified.

6.2.4. Stimuli-Sensitive Drug Delivery. MNPs encapsulated into stimuli-sensitive polymeric shells have been proposed as stimuli-sensitive drug-delivery systems. For example, a Dox-loaded MNP formulation exhibiting stimuli-sensitive drug-release property in response to temperature and pH changes has been designed by the encapsulation of MNPs within the thermosensitive dextran-*g*-poly(*N*-isopropylacrylamide-*co*-*N*,*N*-dimethylacrylamide) [dextran-*g*-P(NIPAAm-*co*-DMAAm)] copolymer (Figure 24).[415] This formulation (8 nm diameter) was composed of 5-nm-sized Fe_3O_4 particles conjugated with Dox through an acid-labile hydrazone bond as a core, which was then embedded into the thermosensitive polymer matrix (3 nm diameter). This copolymer exhibited a lower critical solution temperature (LCST) of ∼38 °C, which allowed an on−off trigger drug-release mechanism. When the temperature was below the LCST, the drug release was slow, whereas when the temperature was above the LCST, the drug release was biphasic with an initial burst release followed by a sustained release up to >40 h. The drug release following temperature increase was triggered successively by (i) the collapse of the thermosensitive polymer at the temperature above the LCST, leading to the exposure of the Dox conjugated magnetic core; and (ii) further cleavage of the acid-labile hydrazone linkage between Dox and the magnetic core. Such acid-sensitive drug-release behavior potentially protects the NP formulation from drug release as long as it is in the systemic compartment, but when the NPs reach the tumor, supplying mild heat to the tumor tissue causes temperature-mediated degradation of the polymer matrix. This may further result in the exposure of acid-labile bonds to the lower intracellular pH, leading to drug release. Noteworthy, if this hypothesis has been verified in vitro, in buffer solutions at different pH values (pH 5.3 and 7.4, representing acidic and physiological pH, respectively), the in vivo proof-of-concept remains to be demonstrated. In a subsequent report, the dextran moiety of the polymer has been replaced by chitosan in order to overcome the potential impact of the high solubility of dextran on the drug release, because chitosan, unlike dextran, exhibits pH-dependent solubility. In addition, the cationic nature of chitosan could be expected to promote the cell-adhesion properties of the NPs.[416]

Similarly, hydroxypropyl cellulose (LCST = 41 °C) conjugated to MNPs has been proposed as a thermoresponsive delivery system. At the LCST, the cellulose undergoes structural deformation as a result of coil-to-globule transition and exposes the encapsulated material.[417] PEI-modified poly(ethylene oxide)-*b*-poly(propylene oxide)-*b*-poly(ethylene oxide) copolymer-coated MNP is another example of a thermoresponsive magnetic drug-delivery system.[80] Under the influence of an external magnetic field, such nanodevices hold promise for targeting and stimuli-responsive intratumoral drug release.

6.2.5. Miscellaneous Applications. *6.2.5.1. Chemoembolization.* Chemoembolization is an approach by which a chemotherapeutic agent loaded into particles is injected into a tumoral artery in order to cause the blockade of the vessel inducing tumor hypoxia, followed by drug release into the tumor.[418] It was hypothesized that the use of magneto-responsive particles may provide the opportunity to enhance the retention time of the injected particles into the tumor vessels, leading to a prolonged therapeutic activity. For example, the i.v. injection of IONPs (∼100 nm mean diameter) into the femoral vein of rats under the influence of an external magnetic field (exposure time was ∼10 min) induced the formation of a thrombus within the capillary bed of the muscle.[345] Similarly, if mice bearing tumors in the dermal portion of the ear surface were exposed to an external magnetic field, tumor embolization occurred successfully after i.v. injection of epirubicin (an anticancer agent)-loaded IONPs. However, further collateral circulation development may occur in some cases around the tumor-feeding arteriole, resulting in unpredictable results. Thus, if tumor embolization using MNPs may be an interesting approach, direct targeting of the diseased area may remain the most efficient alternative.[345]

MNPs guided by an external magnetic field were used as carriers of thrombolytics for dissolution of clots formed in the arteries. For instance, the intra-arterially injected recombinant tissue plasminogen activator (rt-PA)-loaded MNPs coated with dextran were magnetically guided to the location of an artificially implanted thrombus in the artery of rat, facilitating their on-site accumulation. The therapeutic agent released from the NPs at the thrombus site maintained high local concentration and promoted efficient thrombolytic activity. On the contrary, NP retention was not observed in the artery not exposed to the magnetic field, indicating the superiority of magnetic targeting.[419] Intravenously injected MNP formulations have also resulted in appreciable clot degradation following i.v. injection of streptokinase-loaded MNPs in a dog model, upon exposure to an external magnetic field. The magnetic targeting resulted in accumulation of the NPs at the thrombus site, making the streptokinase available in sufficient concentrations for efficient thrombolytic activity.[420]

6.2.5.2. Drug Delivery to the Articular Joints. Generally, arthritis treatment needs frequent drug administration either via systemic route or after local delivery, probably due to the low drug residence time at the disease site leading to patient noncompliance.[421] In this context, magnetic targeting may have potential as a tool for drug delivery to the articular joints.[422,423] For instance, intravenously injected ∼2.4-μm-sized particles, prepared by encapsulating the magnetic microspheres into gelatin loaded with the anti-inflammatory agent diclofenac sodium, have been delivered into rabbit's knee joints by focusing the external magnetic field to the knee articular joint (the target area). This treatment resulted in higher accumulation of the drug delivery system in the femoral artery and knee synovium and also led to prolonged drug release with significant drug concentrations at the target site, at least up to 24 h postinjection. Interestingly, only negligible accumulation occurred in the unexposed knee joint to the magnetic field.[160] This example indicates the promise of systemically administered MNPs for guidance toward the articular space, which can be considered beneficial when the intra-articular injection causes pain and discomfort to the patients.[424]

dx.doi.org/10.1021/cr300068p | *Chem. Rev.* 2012, 112, 5818−5878

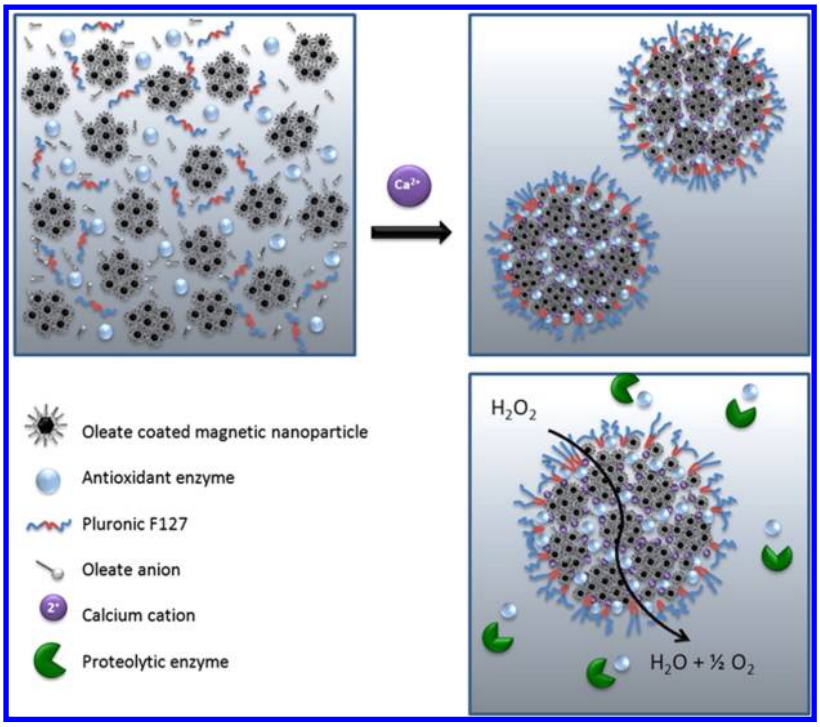

Figure 25. Representation of a biocompatible magnetic nanocarrier system suitable for efficient encapsulation of antioxidant enzymes, superoxide dismutase, and catalase, with preserved biological activity. Reprinted with permission from ref 426. Copyright 2010 Elsevier.

6.2.5.3. Drug Delivery against Oxidative Stress-Mediated Diseases. MNPs have also been employed to deliver proteins or antioxidant enzymes to the desired site of action. In various pathological conditions, especially cardiovascular diseases such as stroke and myocardial infarction, an increased production of reactive oxygen species (ROS) occurs, which further leads to oxidative stress-mediated cell/tissue damage.[425] Delivery of therapeutically effective concentrations of antioxidant enzymes to the site of ROS-mediated injury may enable efficient treatment of the disease. In one instance, antioxidant enzymes (such as catalase or superoxide dismutase)-loaded calcium oleate-coated IONPs (300−400 nm mean diameter) stabilized using pluronic F-127 showed considerable accumulation in aortic endothelial cells in vitro, under the influence of an external magnetic field (Figure 25). This has induced effective protection of the cells from the hydrogen peroxide-induced oxidative stress-mediated cell death. On the contrary, in the absence of magnetic field, oxidative damages remained because MNPs did not internalize appreciably into the cells.[426] Although encouraging, these results were only obtained in vitro. Now, the in vivo proof-of-concept needs to be established in relevant animal models in order to demonstrate the applicability of this approach in the clinic.

6.2.5.4. Magnetic Implant-Mediated Drug Delivery. An interesting approach in the area of magnetic targeted drug delivery is the introduction of a magnetizable implant into the desired site of the body, followed by the injection of the drug-loaded MNPs. The local magnetic field generated by the implant may attract the magnetic particles and facilitate drug release at the desired site, thereby providing a localized drug effect and minimizing systemic drug distribution and potential side effects.[427] However, as such an approach may alter the endogenous iron circulation or iron stores, the implants intended for such a purpose should be weakly magnetizable so that the magnetic field generated is sufficient for attracting particles passing close to the implants but the overall exposure of the body to the magnetic field must be considerably low. This approach has been employed recently for coronary restenosis drug delivery.[428] Coronary restenosis is the narrowing of the coronary arterial vessel occurring after vascular injury.[429] Employing the NPs for targeting the drugs directly to the restenosis site may provide high local drug concentrations for efficient treatment.[430] For instance, a weakly magnetizable implant installed into the artery may generate high local magnetic fields, resulting in the accumulation of the intravenously injected therapeutic agent loaded into MNPs with subsequent drug release at the local site in the artery. Such systems could be employed for the treatment of both vascular and local pathologies.[431]

Such an approach has been used to deliver PLA-based MNPs loaded with the restenosis-inhibiting agent Ptx.[432] The PLA layer served to facilitate the sustained drug release owing to its slow and progressive biodegradation. Practically, the stents were placed in the artery of the rat restenosis model and magnetized using an external magnetic field.[432] After i.v. injection, the MNPs were found to be efficiently directed toward the magnetized stent, placed in the restenosis affected artery. As a consequence, the MNPs significantly inhibited the restenosis compared to the control-treated rats in the absence of magnetic field.

6.3. Magnetofection (Gene Delivery)

Magnetofection is the term used for the delivery of nucleic acids [e.g., DNA, antisense oligodeoxynucleotides (AODN), and small interfering ribonucleic acids (*si*RNA)] into the cells by means of a magnetic field. The delivery of nucleic acids using viral vectors is called transduction, whereas the delivery using nonviral vectors is termed transfection.[433] AODNs are single-stranded deoxyribonucleotide sequences, whereas *si*RNAs are double-stranded ribonucleotides. The site of action of AODNs may be either the cell cytoplasm (complementary sequence of

dx.doi.org/10.1021/cr300068p | *Chem. Rev.* 2012, 112, 5818−5878

*m*RNA) or nucleus (DNA), whereas for *si*RNAs the site of action is only the cell cytoplasm (*m*RNA). The transfer of AODNs or *si*RNAs into the cells is complicated by their susceptibility to degradation by extracellular nucleases and by their hydrophilicity and negative charges, which dramatically hinder their intracellular penetration.[434,435] To address those limitations, chemical modification of the nucleic acids or the use of nanovectors based on polymers (see reviews by Toub and co-workers[436] and Fattal and Barratt[437]) or lipids[438] has been widely investigated. Nucleic acid incorporation into these carriers has been accomplished by different ways such as ionic interactions by complexation with cationic substances (forming polyplexes or lipoplexes) or by entrapment within the carrier. The transfection of cells using nonviral vectors of nucleic acids may be further enhanced by maintaining high local concentrations of nucleic acids at the proximity of the cells, so that the incubation and transfection times could be significantly reduced.[439] This has been achieved via magnetofection, whereby the nucleic acids were associated with a magnetic core either through ion pairing with a cationic polymer or a lipid (see review by Plank and co-workers)[440] or by means of antigen−antibody or avidin−biotin interactions.[441,442]

Magnetofection comprises the following steps: (i) formulation of the DNA-loaded MNPs; (ii) in vitro incubation with cultured cells or in vivo systemic injection via the bloodstream or even local injection into the target tissue; and (iii) application of an external magnetic field in order to guide the vector toward the target cells or tissue to allow transfection.[122,443,444]

The efficient physical adsorption of the nucleic acids (negatively charged) onto the magnetic core could be achieved by bridging the magnetic core and the nucleic acid with cationic substances such as PEI or protamine sulfate.[445] PEI is the most frequently employed cationic polymer for nucleic acid delivery because it binds to DNA and leads to its condensation owing to the presence of a large number of secondary amines on the polymer backbone.[446] After intracellular capture, PEI facilitates the lysosomal escape of the so-formed polyplex via the "proton sponge" mechanism.[447,448]

6.3.1. In Vitro Magnetofection. The transfection efficacy of magnetic nucleic acid NPs was found to be dramatically increased when the cell culture was subjected to a magnetic field, by placing magnets under the cell culture plates. This resulted in enhanced particles concentration near to the cells (due to magnetic sedimentation), which, in turn, promoted cell endocytosis and enhanced transfection.[115,439] Similarly, retrovirus coated-MNPs constructed using avidin−biotin interaction have increased the infection of HeLa cells under the influence of a magnetic field positioned in a similar way.[442]

MNPs coated with PEI have been used as *si*RNA carriers in HeLa cells stably transduced with the green fluorescent protein (GFP) reporter gene. Transfection using the above magnetic nanoconstruction containing anti-GFP *si*RNA has resulted in a considerable silencing in GFP expression (up to >70% at low *si*RNA concentrations).[449]

It is noteworthy that, when the nucleic acid molecules are just adsorbed onto the particle surface, exposure to the external environment may lead to their partial degradation. Thus, the encapsulation of nucleic acids into nanocarriers is generally preferred to improve their protection until intracellular delivery. This has been done with reporter *Lac Z* and *e*GFP genes encapsulated into magnetic cationic liposomes (MCLs) [Fe_3O_4 loaded liposomes of 64 nm diameter, made of 1,2-dioleoyl-3-trimethylammonium propane (DOTAP) and 1,2-dioleoyl-3-*sn*-phosphatidyl ethanolamine (DOPE)].[450,451] After incubation with osteoblasts or the He99 lung tumor cell line, the liposomal formulation subjected to the magnetic field showed enhanced transfection efficiency compared to the controls (i.e., in the absence of magnetic field and the liposome-free gene). Likewise, MCLs prepared with *N*-(*α*-trimethylammonioacetyl)-didodecyl-*d*-glutamate chloride, dilauroylphosphatidylcholine (DLPC), and DOPE, loaded with plasmid DNA of humanized recombinant GFP (*hr*GFP), showed higher transfection efficiency (on NIH/3T3 mouse fibroblasts and normal human epidermal keratinocytes) than cationic liposomes without a magnetic core. The percentage of *hr*GFP-expressing cells transfected in the presence of the magnetic field was ∼7 times higher than that without magnetic field.[452]

MNPs made by the coating of Fe_3O_4 with dimethyldioctadecylammonium bromide and a lipid composition of soy phosphatidylcholine and cholesterol has been used as a nanocarrier for the delivery into KB tumor cells and F98 rat glioma cells of the plasmid pcDNA3-CMV-luc (*p*DNA) encoding firefly luciferase. The *p*DNA preliminarily associated with PEI through ionic interactions was then adsorbed onto the lipid-coated MNPs before transferrin was physically overcoated. In the presence of a magnetic field, the resulting magnetic electrostatic complexes showed *a* > 200-fold higher transfection efficiency than in the absence of magnetic field and *a* > 300-fold higher transfection than the PEI−*p*DNA polyplex or single cationic liposome−*p*DNA (i.e., liposomes prepared using the above-mentioned lipid composition), indicating the effectiveness of the magnetofection comparatively to the use of simple polyplexes or lipoplexes.[453]

Core/shell iron oxide/polymeric NPs have also been proposed as vectors for magnetofection. For instance, hexanoyl chloride-modified, chitosan-stabilized IONPs were used for delivering the viral gene (Ad/*Lac Z*) via magnetofection to K562 human leukemia cells.[454]

Finally, magnetofection has been exploited for genetic manipulation of stem cells without adversely affecting their proliferation or self-renewal capacity.[455] Magnetofection of murine embryonic stem cells with the *e*GFP reporter gene associated with MNPs has resulted in a significantly higher transfection efficacy (45%) of stem cells than that with the standard FuGENE 6 reagent (15%). The transfected stem cells retained the ability to form embryoid bodies and differentiated in vitro into cells of the three germ layers. Moreover, the *e*GFP expression was found to be sustained during stem cell proliferation and differentiation. Therefore, magnetofection was found to be an efficient and reliable method for the introduction of foreign DNA into embryonic stem cells.

6.3.2. In Vivo Magnetofection. Although the magnetofection has been extensively demonstrated in vitro, there are only a few reports describing in vivo achievements. *Cy*3 fluorescently labeled AODN-surface-loaded Fe_3O_4 NPs were injected in the femoral artery of mice, and the testes of the mice were exposed to an external magnetic field.[456,457] A significant fluorescence was observed in the cremaster muscle of the testes exposed to the field, contrary to the control experiment, thus indicating the specific delivery of ODN by magnetofection.

Magnetofection has also been investigated for veterinary applications. For instance, PEI-coated MNPs physically adsorbed with the feline granulocyte-macrophage colony-stimulating factor (feGM-CSF) were injected intratumorally

into the feline fibrosarcoma of cats whose tumors were exposed to an external magnetic field. The antitumor efficacy has been evaluated in a phase I study. About 50% of the cats receiving the treatment became free of local tumors, whereas the recurrence of local tumors or even of metastasis was observed for the remaining cats.[458,459]

6.4. Magnetically Guided Radioimmunotherapy

Radioimmunotherapy involves low doses of radioactive isotopes conjugated to MAb's for cancer treatment. The antibody is expected to target and accumulate the radionuclide into the tumors and further kill the malignant cells by its continuous emission of radiation. Radioimmunotherapy represents a major breakthrough in the field of cancer therapy especially for the treatment of hematological malignancies, as illustrated by the clinical success and commercialization of ^{90}-Ibritumomab tiuxetan (Zevalin) and ^{131}I-tositumomab (Bexxar). However, for the treatment of solid tumors, radioimmunotherapy has been less impressive, probably due to their poor accessibility and radiosensitivity.[460]

Magnetic engineering of radioimmunoparticles has shown some promise in preclinical studies by improving the tumor delivery of radioimmunoconjugates and by enhancing their therapeutic efficacy. For instance, recombinantly generated antibody fragment ^{111}In-di-scFv-c was coupled onto 20-nm-sized IONPs for radioimmunotherapy of MUC-1-expressing HBT3477 breast and DU-145 prostate cancers. Biodistribution and autoradiography studies carried out after i.v. injection in mice and exposure of the tumor to an external magnetic field revealed effective tumor targeting of the NPs.[461] The efficacy of dextran−Fe_3O_4 NPs surface functionalized with a radioimmunoconjugate (i.e., ^{131}I-antivascular endothelial growth factor mAb) has been investigated on a human hepatic xenografted mice model following i.v. injection.[462] The objective was to achieve antitumor activity by a double-punch effect (i.e., by combining the antiangiogenic effect of the antibody with the radionuclide's internal radiation effect). The NPs were magnetically guided to the tumor site, causing considerable accumulation into tumors together with a higher anticancer activity as compared to ^{131}I-NP, ^{131}I-antibody, and ^{131}I alone used as controls.

MNPs have also served as a tool for combined radioimmunoconjugate delivery and thermal ablation of the neoplasic tissue. For instance, IONPs of 20 and 100 nm were compared regarding their ability to deliver radioimmunoconjugates to tumors as well as to induce magnetic thermal ablation. Dextran- and PEG-coated IONPs were surface functionalized with ^{111}In-DOTA-chimeric L6 antibody for targeting the subcutaneously implanted HBT 3477 breast tumor in mice. Following i.v. injection, the 20-nm-sized NPs exhibited longer circulation time and higher tumor accumulation as compared to their 100-nm-sized analogues. However, the latter were 6 times more efficient for causing thermal ablation, likely due to a better AMF absorption rate. Thus, if the goal is to achieve antitumor activity with combined modalities of radiation and thermal ablation, 100-nm-sized NPs were found to be more beneficial.[463] Overall, the modality of combinatorial radioimmunotherapy in addition to magnetic thermal ablation may have considerable potential for efficient targeted antitumor therapy, with potentially limited toxicity.

6.5. Magnetically Guided Photodynamic Therapy

Photodynamic therapy is an emerging treatment of solid tumors. It involves the administration of a light-activatable nontoxic drug (photosensitizer) followed by laser illumination of the tumor.[464] Upon absorption in the visible region (600−800 nm) of the illuminated light radiation, the photosensitizer transfers its energy of excitation to the surrounding oxygen atoms, leading to the generation of ROS and free radicals that cause necrosis of the tumor tissue and tumor cell death.[465,466] However, the conventional photodynamic therapy suffers from certain limitations such as the poor solubility of a variety of photosensitizers and an insufficient specificity to the tumor tissue. Thus, IONPs guided by an external magnetic field have been employed as a tool for addressing the photosensitizer to the tumor site and in some cases for combined tumor targeting and MRI applications. The photosensitizer can be either physically associated or chemically conjugated to the IONPs. For instance, IONPs loaded into a phospholipid emulsion have been used for the delivery of photosensitizers to a skin cancer.[467] Practically, the photosensitizers such as zinc phthalocyanine[466] or temoporfin (Foscan)[467] were dissolved in an oily phase and the IONPs were dispersed in an aqueous phase containing poloxamer 188 as the surfactant. Mixing of both phases allowed a magnetically responsive emulsion to be obtained, although the efficacy of this approach has not been demonstrated (Figure 26).

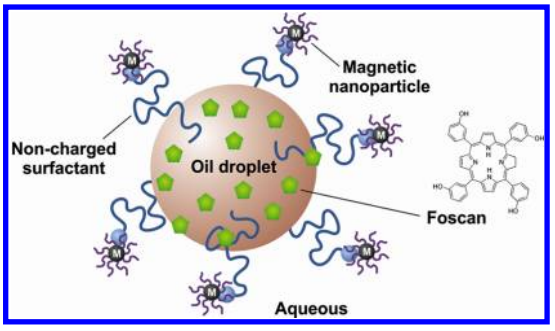

Figure 26. Schematic representation of the o/w magnetic nanoemulsion droplet containing Foscan as a photosensitizer for photodynamic therapy. Inset: chemical structure of Foscan.

IONPs were also used for guiding the photosensitizer to the tumor and for simultaneous MRI.[468] The photosensitizer chlorine e6 was covalently coupled to IONPs (20 nm diameter) using silane as a coupling agent. When injected intravenously into mice bearing subcutaneously grafted MGC803 gastric tumor and guided by an external magnetic field, the NPs gradually accumulated into the tumor tissue. Activation of the photosensitizer using 632.8 nm laser for 10 min resulted in a considerable antitumor activity as assessed by tumor volume measurement. This combined magnetic targeting and photodynamic therapy led to a superior antitumor activity compared to the photodynamic therapy alone and to the magnetic targeting alone. The tumor accumulation of IONPs has also facilitated MRI of the tumor, allowing monitoring of the efficacy of the treatment. Various other photosensitizers that have been coupled to MNPs include hematoporphyrin and 5-aminolevulinic acid,[465] 2-[1-hexyloxyethyl]-2-devinyl pyropheophorbide-a (HPPH),[469] methylene blue,[146] *meso*-tetra(4-sulfonatophenyl) porphyrin dihydrochloride (TSPP),[470] and porfimer sodium (Photofrin).[471] Multifunctional core/shell NPs (~30 nm diameter) made of Fe_3O_4, 2,7,12,18-tetramethyl-3,8-di-(1-propoxyethyl)-13,17-bis-(3-hydroxypropyl) porphyrin (PHPP) as the photosensitizer, and SiO_2 have even been designed for combined magnetic targeting, photodynamic

dx.doi.org/10.1021/cr300068p | *Chem. Rev.* 2012, 112, 5818−5878

therapy, and magnetic thermal ablation.[472] A SiO_2 coating was here employed to facilitate the slow release of the photosensitizer and/or the resultant singlet oxygen from the NPs into the tumor tissue. The proof-of-concept of this approach has been shown in vitro by demonstrating the photodynamic activity on a cell culture of irradiated human SW480 colon carcinoma.

Recently, Fe_3O_4/SiO_2 core/shell NPs functionalized with phosphorescent iridium (Ir) complexes have been designed as a new tool for photodynamic therapy. The Fe_3O_4/SiO_2(Ir) nanocomposite was versatile in facilitating MRI, enhancing the spin−orbit coupling in the Ir complex, thereby making it suitable for phosphorescent labeling and simultaneous generation of oxygen singlets for provoking the apoptosis of tumor cells.[473] Similarly, micellar structures (~35 nm diameter) made of diacylphospholipid−PEG and IONPs (8 nm diameter), in which the photosensitizer HPPH was dispersed, have been designed for magnetically guided photodynamic therapy to tumors.[469] Photodynamic activity of these micellar structures has been demonstrated in vitro on tumor cells, whereas the in vivo demonstration has not yet been reported.

Core/shell-type iron oxide/gold NPs surface coupled with anti-HER2 antibody have also been developed as bimodal-imaging agents (MRI and optical) and photothermal therapeutic agents.[474] Following incubation with SKBR3 breast tumor cells, these NPs selectively destroyed the tumor cells only in the region that was illuminated by the near-infrared laser (owing to the photothermal nature of the gold surface plasmon resonance effect), while the tumor cells devoid of near-infrared-absorbing NPs were spared. Thus, such NPs hold potential for multimodal local tumor therapy and for minimizing potential side effects.

6.6. Magnetic Fluid Hyperthermia

The magnetic fluid hyperthermia (MFH) involves the injection of a magnetic fluid into a tissue with its subsequent exposure to an AMF, allowing heat generation. When MNPs are subjected to an AMF of low or moderate frequency (generally ~250 kHz), heat is generated due to the magnetic hysteresis loss. Thus, the MNPs accumulated in a tumor tissue may warm up to a temperature that depends on their magnetic properties, on the strength and nature of the magnetic field, on the frequency of oscillation, and on the cooling capacity of the blood flow in the tumor.[475−479] The heat released will then diffuse to the adjacent tissue environment as a consequence of the oscillation of the magnetic moment inside the NPs exposed to the magnetic field.[243] The heating efficiency is governed by the mechanisms of magnetic energy dissipation for single-domain particles (Brown and Néel relaxations), which are highly sensitive to the crystal size, the solvent (carrier fluid viscosity), and, in general, the properties of any magnetic materials.[117,480,481]

6.6.1. Preclinical Evaluation of Magnetic Fluid Hyperthermia. *6.6.1.1. Magnetic Fluid Hyperthermia Alone.* MFH has been extensively investigated and applied for cancer treatment, because the tumor cells heated at temperatures in the range of 42−45 °C are irreversibly damaged.[475,482−485] It has been evidenced that local heating of tumor for ~30 min is sufficient to destroy the tumor tissue.[486] Importantly, if temperature exceeds 56 °C, it results in thermoablation (i.e., coagulation, necrosis, and carbonization of the tissue).[482,487]

Hyperthermia has been tested either by using MNPs coated with stabilizers or by using encapsulated MNPs into delivery nanocarriers, such as liposomes.[476,488,489] The promise of hyperthermia as a minimal invasive treatment of malignant brain tumors has been demonstrated by a systematic analysis of its effects on a glioblastoma rat model.[490] Two hyperthermia treatments (on days 4 and 6) in a rat model (in which RG-2 rodent glioblastoma was implanted in the brain) were carried out by intratumoral injection of carboxydextran-coated iron oxide (3 nm mean diameter) or aminosilane-coated iron oxide (15 nm mean diameter) NPs, as well as subsequent exposure to AMF. This revealed that the carboxydextran-coated NPs failed to generate temperatures greater than 39 °C and hence led to a poor antitumor response, whereas the aminosilane-coated NPs maintained high temperature and resulted in a significant anticancer activity as illustrated by the 4.5-fold increase in survival of so-treated rats, compared to the untreated control animals. The autopsy revealed no iron deposits in the brain tissue after injection of carboxydextran-coated NPs contrary to aminosilane-coated NPs. Although no clear explanation was given, these data suggested the important impact of the surface chemistry (i.e., particle size and chemical nature of the coating) on the NP retention in the brain tissue.

MNPs encapsulated into cationic liposomes have been tested for MFH. The intratumoral injection of MCLs [prepared by encapsulating Fe_3O_4 into a lipid mixture made of *N*-(α-trimethylammonioacetyl) didodecyl-*d*-glutamate chloride, dilauroylphosphatidylcholine, and dioleoylphosphatidylethanolamine] into the MM46 mammary tumor-bearing mice with subsequent exposure of the tumors to the AMF (30 min) caused an increase of temperature up to ~45 °C at the surface of the tumor, resulting in tumor regression. The tumor response was found to be still improved after repeated cycles of hyperthermia.[476] Unexpectedly, the repeated hyperthermia treatment had also generated antitumor immunity because these animals resisted the tumor challenge consisting of successive subcutaneous inoculation of the tumor cells. This may be explained by the fact that, when subjected to repeated cycles of hyperthermia, the tumor cells (and not the normal cells) upregulated heat shock proteins (HSPs) such as HSP70 or HSP72, which are engaged in the immune cascade reactions.[491] In addition, HSP70-mediated induction of antitumor immunity has been demonstrated in a T-9 rat glioma experimental model.[492,493] MFH treatment using MCLs has resulted in necrosis of the tumors, which correlated with the expression of HSP70. Such antitumor immunity induction was observed in the case of mice bearing either small or large tumors.[493]

In another investigation, the therapeutic effect of MFH has been studied on an experimental model of human hepatocellular carcinoma xenograft.[494] The MFH treatment significantly inhibited the tumor proliferation and induced apoptosis, which was not observed in the control animals. Importantly, because MFH is based on the local administration of magnetic particles at the tumor site, this therapeutic approach may not be applicable to the treatment of metastasis where the NPs are not localized in place.

6.6.1.2. Magnetic Fluid Hyperthermia and Chemotherapy. Magnetic hyperthermia has also been used in combination with chemotherapy for obtaining a still more efficient antitumor response. For instance, combined treatment of tumor cells with Cis-loaded IONPs and hyperthermia has resulted in a synergistic effect.[495] The concept of using the heat induced by IONPs, when exposed to an AMF, for temperature-triggered drug release has been successfully tested. For instance, the

thermosensitive polymer poly(*N*-isopropylacrylamide) (PNIPAAm), which possesses a LCST, was used as a shell around the iron oxide core. The temperature increase in response to the AMF makes the PNIPAAm collapse, triggering the release of the encapsulated drug.[496] Although the in vivo proof-of-concept was not yet demonstrated, this approach may facilitate tumor treatment due to combined hyperthermia and chemotherapy.

6.6.1.3. Magnetic Fluid Hyperthermia and External Beam Radiation Therapy. Combination of MFH with external beam radiation therapy (EBRT) has been proposed because of the complementary mechanism of causing cell death following these two treatments.[497] Practically, dextran-coated IONPs (~20 nm size) having PEG−COOH groups at the surface were incubated with a human prostate cancer cell line and exposed to an externally applied AMF. Coupling MFH to EBRT resulted in a significant cell death at EBRT levels that were alone inefficient for tumor cell kill in the absence of MFH.

6.6.1.4. Targeted Magnetic Fluid Hyperthermia. Despite these promising results, MFH treatment still calls for certain improvements such as (i) selective heat induction in the tumor tissue; (ii) homogeneity of the temperature distribution into the tumor tissue; and (iii) reduction of the invasiveness of the technique. Ideally, the technique should allow the injection of a minimum quantity of magnetic fluid, while allowing for sufficient heating within the appropriate field parameters (frequencies between 0.05 and 1.2 MHz, and fields <15 kA/m).[4,486] Some of the above objectives may be achieved by enhancing the tumor distribution and tumor cell accumulation by decorating the NPs with specific tumor cell targeting ligands, e.g., MAb's,[114] FA,[498,499] or HER2 receptors,[500] which specifically bind to the tumor cells upon injection, undergo tumor cell internalization, and thereby increase the intracellular concentrations of MNPs. For more details on ligand-functionalized magnetic particles, see section 6.2.1.3. In this context, combined MFH and chemotherapy (by including the anticancer drug into the magnetic nanocarrier) may be expected to act as a double-edged sword in causing tumor cell kill. Additionally, heating the MNPs with an AMF permits controlled drug release from the NPs, in response to the magnetic stimulus (Figure 27). For instance, when the antitumor drug tamoxifen (TMX) was loaded as the inclusion complex with surface-coated β-cyclodextrin (CD) polymer onto FA-decorated SPIONs (12 nm particle diameter) and subjected to the AMF, the drug release from the CD polymer was triggered in response to the heat stimulus.[501]

6.6.1.5. Magnetic Thermal Ablation. Apart from the MFH, which uses temperatures slightly above the physiological temperatures (i.e., up to ~45 °C), the use of higher temperatures (e.g., up to ~70 °C) following exposure to AMF of high amplitude results in thermal ablation of the exposed tissues with necrosis of the tumors and intensive cell destruction. For instance, human breast adenocarcinoma-bearing mice were intratumorally injected with IONPs and exposed to an AMF of high amplitude for ~4 min. This treatment allowed a temperature of 73 °C to be reached in the center and at the periphery of the tumors, resulting in the induction of localized heat spots, in principle high enough to kill the tumor cells.[502] Even if this technique can lead to complete tumor destruction, caution should be exercised in using this approach because the ablation may cause considerable damage to the skin and to the adjacent healthy tissues due to the possible migration of some NPs to these

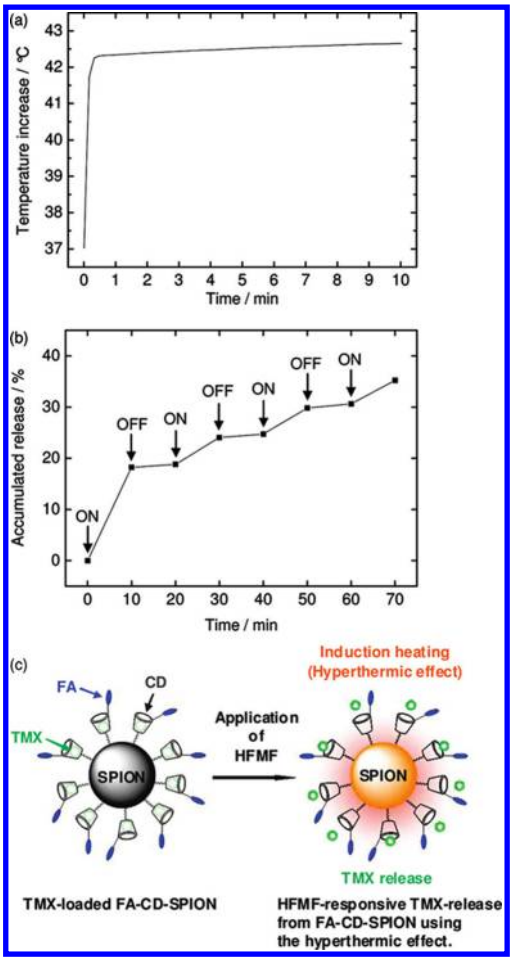

Figure 27. (a) Temperature increase of the water dispersed with 20 mg/mL of TMX-loaded FA- and CD-decorated SPIONs (FA-CD-SPIONs) under a high-frequency magnetic field (HFMF, frequency and amplitude 230 kHz and 100 Oe, respectively). (b) Controlled release of TMX from FA-CD-SPIONs by switching a HFMF *on* and *off*. (c) Schematic illustration of TMX release from FA-CD-SPIONs using the hyperthermic effect by applying a HFMF. Reprinted with permission from ref 501. Copyright 2010 American Chemical Society.

tissues. However, MFH has been demonstrated to be more effective than radiofrequency ablation (RFA) by dielectric heating.[475,503] For instance, treatment with magnetic thermal ablation of nude mice bearing BT474 human breast cancer (62 °C temperature was achieved in the center of the tumor) has resulted in a complete tumor death at 48 h post-treatment.[503]

As for MFH, efficacy and safety of the magnetic thermal ablation technique may be further enhanced by improving the tumor cell specificity using MNPs decorated with tumor-specific antibodies. For instance, PEGylated dextran-coated IONPs (20 nm diameter) surface-coupled with chimeric L6 mAb labeled with ^{111}In (^{111}In was used as a radiomarker probe) have been employed for targeting the subcutaneously grafted HBT 3477 human breast tumor after i.v. injection in mice (Figure 28). The antibody-labeled NPs exposed to AMF showed antitumor efficacy as opposed to the control treatments with IONPs using AMF alone or with ^{111}In-labeled chimeric L6 mAb alone, indicating that the observed efficacy was a combined result of tumor targeting and magnetic thermal ablation.[504]

6.6.1.6. Magnetic Fluid Hyperthermia for Presensitization of Tumor for Chemotherapy. In addition to the above-

dx.doi.org/10.1021/cr300068p | *Chem. Rev.* 2012, 112, 5818−5878

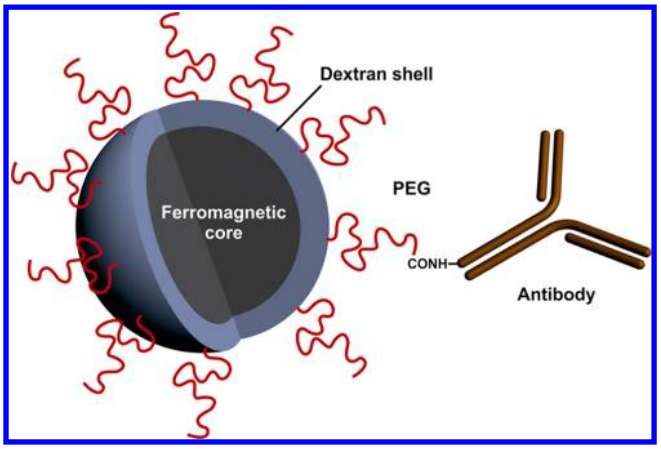

Figure 28. PEGylated dextran-coated IONPs (20 nm diameter) surface-functionalized with chimeric L6 mAb labeled with ^{111}In for AMF thermal ablation of cancer.

mentioned applications, MFH could also be used to enhance the accumulation of anticancer compounds at the neoplasic target area, by altering the local tissue permeability.[505−507] Heating the tumor increases the blood flow as well as its microvascular permeability and oxygenation.[508,509] Such modified tumor microenvironment then becomes more permeable and more accessible to drugs, drug-delivery systems, or macromolecules.[510−512] Thus, an improved tumor regression may be achieved by pretreating the tumor with MFH before systemic administration of long circulating drug-loaded nanodevices. This approach has been shown to be also appropriate for drug delivery into sanctuaries of the body, like the brain, because high temperatures such as 43 °C cause damage to the BBB.[482]

6.6.2. Clinical Evaluation of Magnetic Fluid Hyperthermia. The encouraging preclinical data obtained with MFH have prompted the evaluation of this technique in cancer patients. The first clinical study using MFH has been carried out by Johannsen and co-workers, using aminosilane-coated IONPs for the treatment of patients suffering from locally recurrent prostate cancer.[513] The next clinical studies have followed up the safety of MFH treatment and the quality of life of the patients.[514,515] Practically, MFH treatment was carried out by transperineal injection of 6 cycles of aminosilane-coated IONPs at weekly intervals followed by heating the tumor tissue using AMF. The temperatures attained in the prostate tissues were measured to be from 41.1 °C up to a maximum of 55 °C. Overall, the treatment was found to be well-tolerated, but a moderate treatment-related morbidity and temporary impairment of quality of life linked to symptoms, such as urinary problems or tiredness, were observed in some patients. However, these symptoms returned to normal a few weeks after therapy.

In another clinical trial, MFH was carried out on 22 patients with various neoplasic diseases by using a whole-body magnetic field applicator and magnetic fluid composed of aminosilane-coated IONPs.[516] The NPs were locally injected into the tumors (e.g., cervical sarcoma, ovarian, and rectal carcinomas) before exposure to an AMF using tolerable field strengths of 3.0−6.0 kA/m in the pelvis, up to 7.5 kA/m in the thoracic and neck region, or >10.0 kA/m in the head region. Specific absorption rates of 60−380 W/kg were achieved in the target tissue, leading to a 40 °C heat coverage over 86% of the target tumor volume. A moderate increase of the field of only 2 kA/m allowed for reaching temperatures up to 42 °C with coverage of the whole tumor tissue.[516] The longer retention time of the NPs in the tumor tissue, as assessed by computed tomography (CT) using the relationship between iron mass and CT density (Hounsfield unit), permitted the repetition of the hyperthermia treatment without the need of repeated NP administration.[513]

MFH has also been experienced on patients with multiforme glioblastoma. Patients received intratumoral injection of aminosilane-coated IONPs and were then exposed to AMF to induce particle heating. Again, MFH was well-tolerated by all patients with minor or no side effects. Intratumoral temperature of 44.6 °C was achieved, and signs of the control of tumor growth were observed.[517,518] In another study, radiotherapy was combined with MFH to achieve improved tumor regression and survival of the brain tumor patients.[519]

7. MAGNETIC RESONANCE IMAGING

MRI is a noninvasive imaging modality capable of providing high-resolution anatomical images. It is a widely employed method mainly for the diagnosis of soft tissue or cartilage pathologies, allowing the differentiation between malignant and healthy tissues. SPIONs are excellent MRI contrast agents[1,4,520] because of their T_2* (T = transverse relaxation) property with excellent sensitivity in T_2* and T_2 weighted images,[521] as compared to other MRI agents such as chelates of paramagnetic ions like Gd^{3+}−diethylenetriaminopentaacetic acid (Gd^{3+}−DTPA). These T_2-relaxation effects result in a signal reduction on T_2-weighted images, thus providing a dark or negative contrast due to the induction of strong magnetic susceptibility on the water protons around the particles.[522] See also section 3.5 for more details and Table 1 for details on FDA- or European-approved or proposed trials on MNPs.

7.1. Organ/Tissue Imaging

After i.v. administration, SPIONs (>50 nm in diameter) are rapidly sequestered by hepatic and splenic macrophages,

Table 1. SPION-Based Products Approved/in Clinical Trials

compound/trade name	coating agent	size (nm)	status
Ferumoxsil (AMI-121)/Lumirem (Guerbet), Gastromark (Advanced Magnetics)	dextran	300	approved
Ferumoxide (AMI-25, SHU 555A)/Endorem (Guerbet), Feridex (Advanced Magnetics)	dextran	120−180, 80−150	approved
Ferrixan (Ferucarbotran, SHU 555A)/Resovist (Schering), Cliavist (Medicadoc)	dextran	60	approved
Ferumoxtran-10 (AMI-227, BMS-180549)/Sinerem (Guerbet), Combidex (Advanced Magnetics)	dextran	20−40	late-phase clinical
Ferristene (OMP)/Abdoscan (GE-Healthcare)	sulfonated styrene−divinylbenzene copolymer	3500	approved
Feruglose (PEG-feron, NC100150)/Clariscan (GE-Healthcare)	carbohydrate−PEG coating (PEGylated starch)	20	preclinical discontinued

dx.doi.org/10.1021/cr300068p | Chem. Rev. 2012, 112, 5818−5878

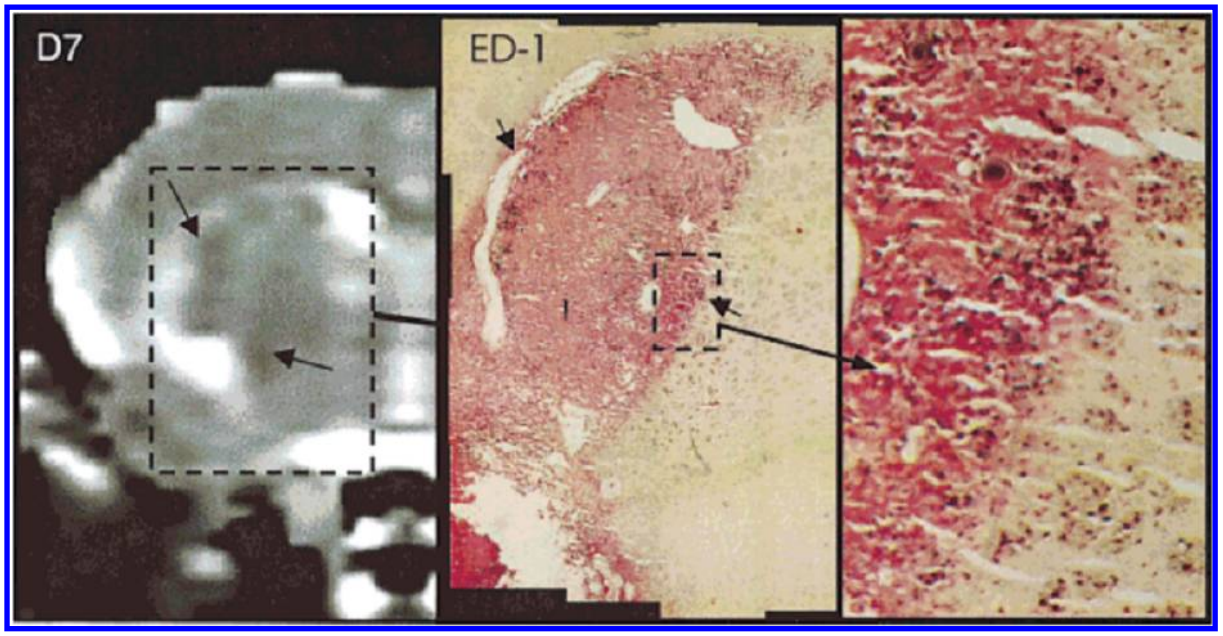

Figure 29. Comparison of transverse MRI sections 8 mm anterior to the intra-aural line of another rat with the corresponding histological analysis. Shown are the immunostained with the mAb ED1 histological sections from day 7 together with the corresponding T_2 map recorded on day 7. Areas of decreased T_2 are visible in the MR image that correspond spatially to the clusters of ED1+ macrophages (arrows). Reprinted with permission from ref 548. Copyright 2001 Wiley.

resulting in hypointense T_2-weighted images of the normal tissue. In the liver, the lack of Küpffer cells in the tumor helps to differentiate between healthy and malignant regions.[477,523−526] Therefore, SPIONs have been clinically used for imaging of liver tumors and metastases.[527,528] The commercially available SPIONs include Endorem or Feridex (manufactured by Guerbet and made of Fe_3O_4 NPs of 150 nm in diameter coated with dextran) for liver tumor imaging and Resovist (manufactured by Schering, made of Fe_3O_4 NPs with a carboxydextran coating) for imaging of focal liver lesions including metastases. Lumirem (dextran-coated iron oxide particles with a diameter of 300 nm) is another specialty manufactured by Guerbet for gastrointestinal tract imaging to facilitate the delineation of organs and the localization of lesions.

On the opposite, SPIONs with very small size (<50 nm in diameter) avoid massive uptake by liver and spleen macrophages and thus exhibit long circulating properties. In fact, after i.v. administration, such SPIONs can extravasate from the systemic circulation into the interstitial space and gain access to the deeper pathological tissues, before uptake by local inflammatory macrophages.[298,529−531] Various transport mechanisms of <50 nm-sized SPIONs toward diseased tissues have been proposed: (i) endocytosis by activated blood monocytes followed by their migration to the pathological tissues; (ii) transcytosis through vascular endothelium with further macrophages uptake in pathological tissues; and (iii) direct passage through the inflammatory leaky vasculature.[532] Thus, the very small-sized SPIONs have found application in the imaging of a wide variety of pathologies and have been tested in both preclinical experimental animal models and clinical situations. For instance, Ferumoxtran-10 (~30 nm diameter, displaying human blood half-life of 24−36 h) gains access to various diseased tissues such as abnormal lymph nodes, osteoarticular joints, brain, kidney, etc.[137,533,534]

7.1.1. Lymph Node Imaging. In lymph node imaging, the intravenously injected Ferumoxtran-10 accumulates in benign lymph nodes and causes a drop in signal intensity and homogeneous contrast. However, the presence of malignant areas leads to an abnormal pattern of NP accumulation and, in turn, disturbances in lymph flow or in nodal architecture, resulting in an intense signal. These differences are clearly detectable by MRI.[535−537] Ferumoxtran-10 offers higher diagnostic precision for the detection of lymph node metastases from various primary tumors.[538,539] These very small-sized SPIONs show T_1, T_2, and T_2* enhancing effects depending on the sequence and on their local concentration.[540] Thus, besides their T_2* property, < 50 nm-sized SPIONs also show high T_1 relaxivity at low concentrations, resulting in a T_1-enhancing effect with a positive contrast increase.[541,542]

7.1.2. Imaging of Atherosclerotic Plaques. Successful imaging of atherosclerotic plaques on the arterial wall has been done with SPIONs.[543−545] Atherosclerosis is a disease affecting arterial blood vessels in which the thickening of the arterial wall occurs as a consequence of the build up of fatty substances such as cholesterol. The macrophage invasion of the atherosclerotic plaques may affect the mechanical stability of the vessel wall, which may lead to plaque rupture and result in clot formation.[546] Ferumoxtran-10 intravenously injected to human patients at 45 μmol Fe/kg dose was found to induce a signal intensity decrease at the atheromatous plaque regions. The analysis of the plaque samples postsurgery revealed the localization of SPIONs in the activated macrophages, possibly due to the endocytosis of the SPIONs by these macrophages. Because the plaque regions have a high prevalence of these phagocytic cells, no SPIONs were found in the vascular endothelium.[532] On similar lines, various other studies have also demonstrated the accumulation of the injected SPIONs in the macrophages of the plaque regions,[545,547] predominantly in the majority of lesions that are ruptured or prone to rupture, in the human patients suffering from carotid stenosis.

dx.doi.org/10.1021/cr300068p | *Chem. Rev.* 2012, 112, 5818−5878

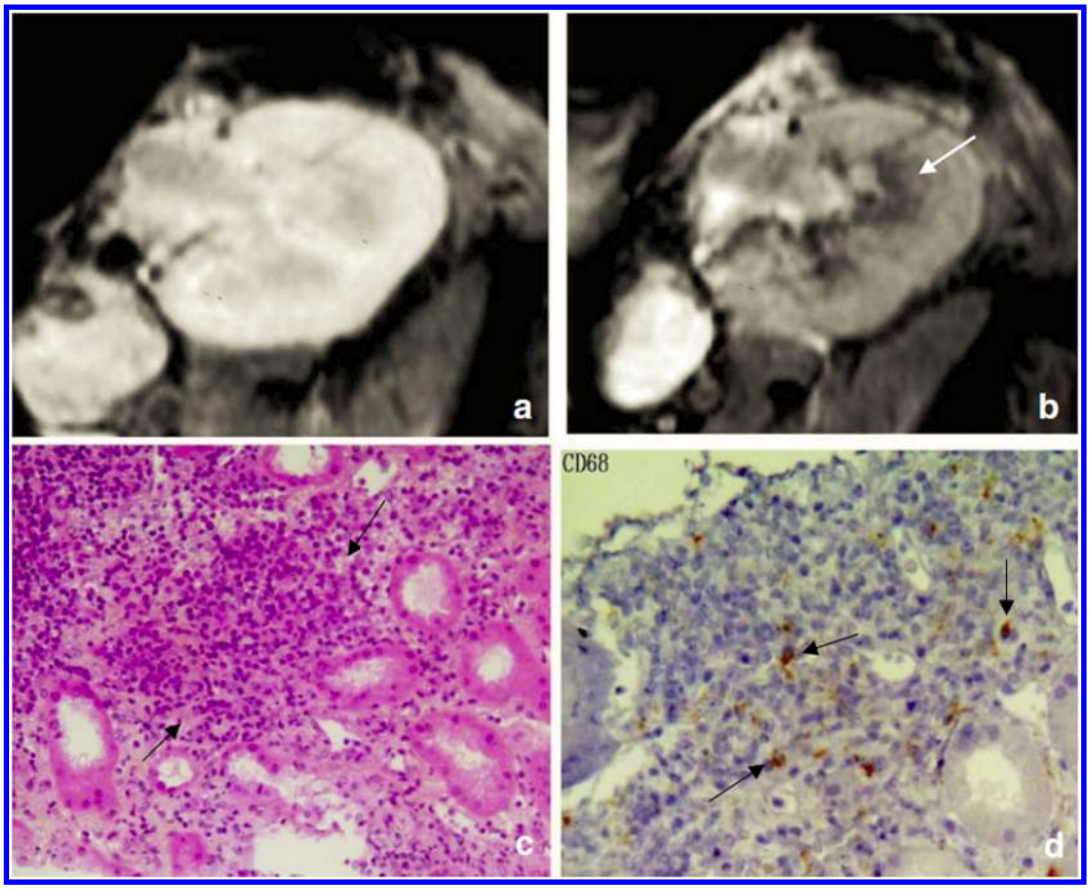

Figure 30. A 64-year-old man with acute renal failure at day 15 of renal transplantation. MRI (a) before and (b) 72 h after injection of 2.6 mg iron/kg of SPIONs shows a diffuse signal decrease in all renal compartments, more pronounced in the medulla (−51%, arrow). (c and d) Histology (magnification 100×) showed numerous interstitial CD68 cells (55/mm^2) corresponding to macrophages (arrows). Diagnosis was type Ia acute rejection according to Banff classification. Reprinted with permission from ref 533. Copyright 2007 Springer.

7.1.3. Imaging of Inflammatory Response in Central Nervous System Disorders. Imaging of the inflammatory response (i.e., recruitment of activated macrophages) by means of very small-sized SPIONs is also possible in CNS disorders, especially in the ischemic stroke lesions, cerebral inflammation, and in multiple sclerosis. It is generally believed that the intravenously injected SPIONs are captured by circulating blood monocytes before migration to the diseased site of the CNS, thus allowing MRI visualization. For instance, after i.v. injection of SPIONs to the experimental ischemic rat model developed by permanent occlusion of middle cerebral artery, hypo-intense areas on T_2* weighted images were observed. In this experiment, the SPIONs were mainly accumulated in the infarcted tissue in which the macrophages were heavily localized (Figure 29).[548]

Further, in a pilot phase II clinical study, it has been demonstrated that the SPION-enhanced MRI may provide an in vivo surrogate marker of cellular inflammation in stroke and other CNS pathologies.[549] The usefulness of very small-sized SPIONs has also been established clinically for imaging of brain tumors, as a susceptibility microvascular contrast agent to image tumor neovasculature or as a macrophage imaging agent by taking advantage of the high prevalence of macrophages in tumor pathology.[550,551] Similarly, in multiple sclerosis, which is characterized by the infiltration of macrophages across the BBB, MRI using SPIONs has been validated both in preclinical experiments using animal models[552] and in clinical trials on patients having multiple sclerotic lesions.[553]

7.1.4. Imaging of Macrophage Infiltration in Transplanted Organs. Very small-sized SPIONs have also been used for the imaging of macrophage infiltration in organ-transplant situations. For instance, the kidney transplanted rat model was imaged using SPIONs to follow macrophage infiltration into the transplanted organ and to monitor organ rejection. The rejected allografts indeed showed a decreased MR signal intensity, whereas the animals treated with immunosuppressant agents showed an absence of MR signal reduction, suggesting a negligible macrophage infiltration.[554] Encouraging observations were also made in the rat model for the detection of lung allograft rejection.[555] Following i.v. injection of SPIONs, a significant decrease in signal intensity was observed in lung-transplanted animals without immunosuppressant treatment, which was well correlated with a high grade of organ rejection, whereas the lung-transplanted animals treated with immunosuppressant showed only a minimal change in signal intensity compared to the preinjection images. Analysis of the allografts revealed significant concentration of SPIONs in the macrophages accumulated at the rejection site.

In the clinic, i.v. injection of SPIONs (30 nm diameter, coated with low molecular weight dextran) has allowed for the detection of macrophage infiltration in both native and transplanted kidneys in humans. The patients who experienced macrophage infiltration (>5 macrophages/mm^2) in the kidneys, either due to glomerulonephritis in the native kidney or due to acute rejection in transplanted kidney, showed a signal loss on T_2*-weighted MR images of the cortex region, whereas the

dx.doi.org/10.1021/cr300068p | Chem. Rev. 2012, 112, 5818−5878

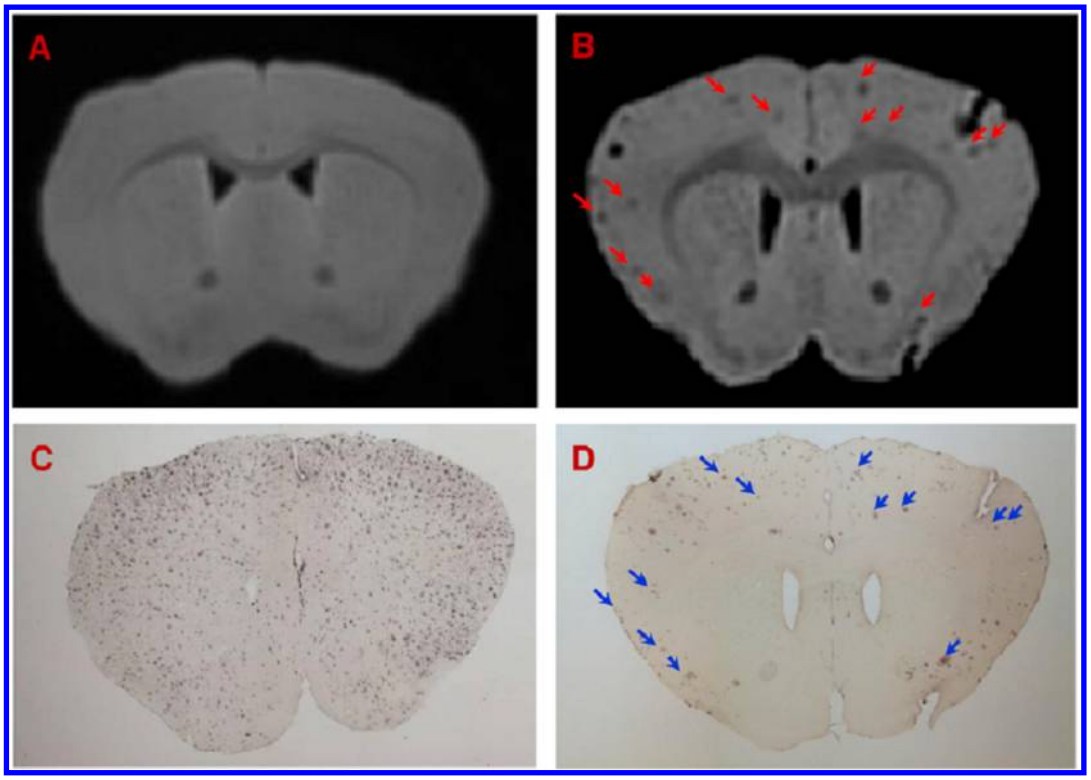

Figure 31. Amyloid plaques were detected with ex vivo T_2*-weighted μMRI after i.v. femoral injection of SPION-Aβ_{1-42} peptide with mannitol. Many plaques can be detected in APP/PS1 mice injected with SPION-Aβ_{1-42} (B). These lesions can be matched to immunostained amyloid plaques (D, arrowheads). μMRI failed to show significant numbers of amyloid plaques in a 16-month-old APP/PS1 Tg mouse (A), which was not contrast-injected but has histologically confirmed plaques (C). Reprinted with permission from ref 565. Copyright 2011 Elsevier.

patients with <5 macrophages/mm^2 did not show any signal drop (Figure 30).[533] This important clinical study indicated the promise of this imaging modality for the detection and differentiation of various kidney diseases.

7.1.5. Imaging of Macrophage Infiltration in Knee Joints. Very small-sized SPION-enhanced MRI has also been investigated for imaging macrophage infiltration in *Staphylococcus aureus*-induced knee synovial infection in the rabbit.[556] Following i.v. injection of SPIONs, signal loss was observed on T_1-, T_2-, and T_2*-weighted images of infected knees, which was not seen without knee infection, indicating the presence of SPION-loaded macrophages in the infected knee synovium. SPION-enhanced imaging has also been used as a marker of enhanced macrophage activity in experimentally induced arthritis in rabbits.[557] In addition, SPIONs were demonstrated to be a valuable contrast agent for the visualization of myocardial macrophage infiltration in healing infarcts and myocarditis.[558−561]

7.1.6. Imaging Using Ligand-Functionalized Superparamagnetic Iron Oxide Nanoparticles. Similarly to the previously mentioned therapeutic applications of the IONPs (see sectio 6.2.1.3.), the specificity toward the target tissues may be improved by NP functionalization with targeting ligands.[137,283,554] Such active targeting for imaging purposes has been considered either by using large biomacromolecules such as antibodies or peptides, e.g., herceptin for targeting HER2/neu overexpressed on breast tumors,[60] SM5-1 antibody for hepatoma detection,[562] ^{111}In-DOTA-di-scFv for anti-MUC-1-expressing cancers,[461] octreotide for targeting somatostatin receptors overexpressed on breast tumors,[563] RGD for targeting tumor angiogenesis,[564] and Aβ_{1-42} peptide for detecting the amyloid deposition in Alzheimer's disease (Figure 31),[565] or by using small ligands such as FA for tumor targeting.[566,567]

8. CELL LABELING AND IMAGING

Cellular MRI is a rapidly growing field that aims to visualize and track the cells in the living organisms. In this way, IONPs have been employed for in vivo imaging of cells transplanted into the body. This could be achieved by incubation of IONPs with the cells prior to transplantation into the body and tracking/visualization using MRI.[568−571] The advantage is that the already commercially available contrast agents can be used as markers for the short-term or long-term noninvasive MR tracking of the transplanted cells.[572]

Important challenges in the cell labeling approach include (i) achieving high labeling of the cells, which depends on the extent of uptake of the IONPs by the phagocytic and nonphagocytic cells; and (ii) ensuring the cell integrity and viability following labeling. In general, the uptake of IONPs by cells is directly proportional to the NP size. For instance, incubation of human monocytes with SPIONs (Endorem) resulted in 50 pg/cell iron concentration in comparison to only a 7 pg/cell iron concentration when incubated with SPIONs (Sinerem),[573] whereas incubation of various cell types such as murine hepatocytes, murine fibroblasts, or mesenchymal stem cells with bigger iron oxide particles (5.8 μm size) resulted in ~100 pg/cell iron concentration.[574] To enhance the labeling efficacy, various approaches have been attempted such as coating of the particles with cell internalizing antibodies[209] or translocating agents, such as the HIV-1 Tat peptide,[386,575] albumin-mediated transport into the cells,[576] or the use of transfection agents. For instance, the mAb OX-26 (murine

dx.doi.org/10.1021/cr300068p | Chem. Rev. 2012, 112, 5818−5878

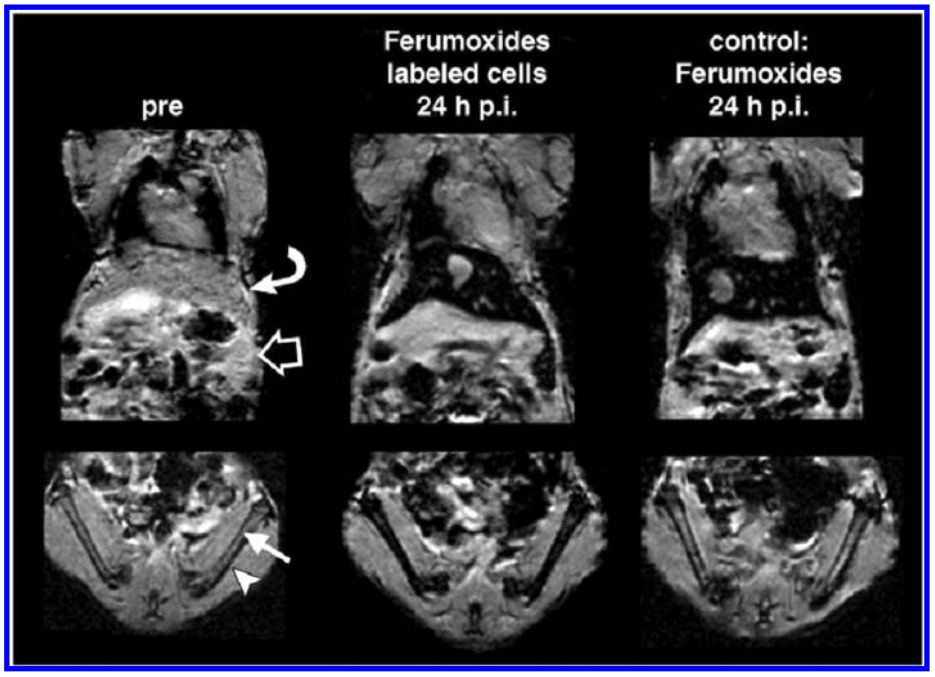

Figure 32. T_2*-weighted MR images of one Balb/c mouse before injection, as well as one Balb/c mouse at 24 h after peritoneal injection (p.i.) of 3×10^7 Ferumoxide-labeled progenitor cells and one Balb/c mouse at 24 h after injection of Ferumoxide (without cells), show that the labeled cells distribute differently than does the pure contrast agent. The amount of administered iron was 20 μg through injection of Ferumoxide-labeled cells and 25 μg through injection of the pure contrast agent (the latter applies to the usual clinical dose). MR images of the body show liver (curved solid arrow) and spleen (open arrow). Below that, MR images were reconstructed along the long axes of the femora, in which the corticalis (arrowhead) and the bone marrow (straight solid arrow) can be clearly delineated. The Ferumoxide-labeled cells caused a marked signal intensity decline in liver, spleen, and bone marrow, whereas injection of the pure contrast agent caused visible signal intensity changes in liver and spleen, but not bone marrow. Reprinted with permission from ref 586. Copyright 2005 Radiological Society of North America.

antirat transferrin mAb) coupled at the surface of very small-sized SPIONs showed efficient labeling of the rat oligodendrocyte progenitor cell line CG-4.[209] This technique was used to monitor cell grafting in the spinal cord region of a myelin deficient rat, as well as the cell survival and remyelination. Interestingly, this experimental model of demyelination is representative of physiopathological events observed in multiple sclerosis and other neurological disorders.

Combining transfection agents and IONPs has also resulted in enhanced cell labeling. Thus, lipofectamine, poly(L-lysine), poly(L-arginine), poly(L-ornithine), SuperFect (heat-activated dendrimer), protamine sulfate, etc. have been reported to significantly improve IONP labeling of the cells.[577−580] However, there are many drawbacks associated with transfection techniques: (i) It requires mixing positively charged transfection agents with the negatively charged IONPs, and the resulting loss of NP surface charge may cause NP precipitation; (ii) most of the transfection agents are more or less cytotoxic due to cell membrane perturbation; and (iii) it can result in NP adsorption onto the cell surface rather than internalization.[581] Magnetic electroporation is another method that was reported for cell labeling using IONPs. With electroporation, the cell tag is immediate, which represents a considerable advantage compared to the prolonged incubation time needed for conventional labeling techniques. With this methodology, successful labeling and preservation of cell integrity have been demonstrated using mesenchymal and neural stem cells of murine, rodent, and human origin.[582]

8.1. Imaging of Transplanted Stem Cells

Stem cell transplantation has been intensively investigated in the context of regenerative medicine, especially for the treatment of heart failure, ventricular dysfunction, vascular injury, etc. The stem cell transplantation could be done either by vascular injection and subsequent MRI verification of their guidance to the targeted organ or by direct injection.[583−585] The i.v. injection of Ferumoxide-labeled human hematopoietic progenitor stem cells into athymic mice revealed that the labeled cells distributed into liver, spleen, and bone marrow as indicated by a significant decrease of the MR signal intensity in these tissues. Interestingly, the decrease of the signal intensity in bone marrow was considerably stronger after injection of SPION-labeled cells compared to the images of control mice that received only pure SPION injections, suggesting a preferential homing of the labeled cells to the bone marrow (Figure 32). This was further confirmed by the histological examination.[586]

In another study, human embryonic stem (HES) cells labeled with dextran-coated IONPs were transplanted by direct injection into the anterior left ventricular wall of mouse myocardium and imaged using MRI. The T_2-weighted images revealed well-defined hypointense areas at the site of injection of the labeled HES cells.[587] This approach may have great potential in monitoring the fate and efficacy of HES cell-based regenerative medicine. Similarly, in vitro-expanded human neural precursor cells labeled with IONPs and transplanted into the mouse brain have been successfully tracked for at least up to 1 month.[588]

Cellular MRI has also been used to track the bone marrow-derived endothelial precursor cells.[589] The MRI following i.v. injection of the SPION-labeled cells into the glioma tumor bearing immunodeficient mice revealed that the cells migrated to the tumor tissue and were incorporated into the tumor

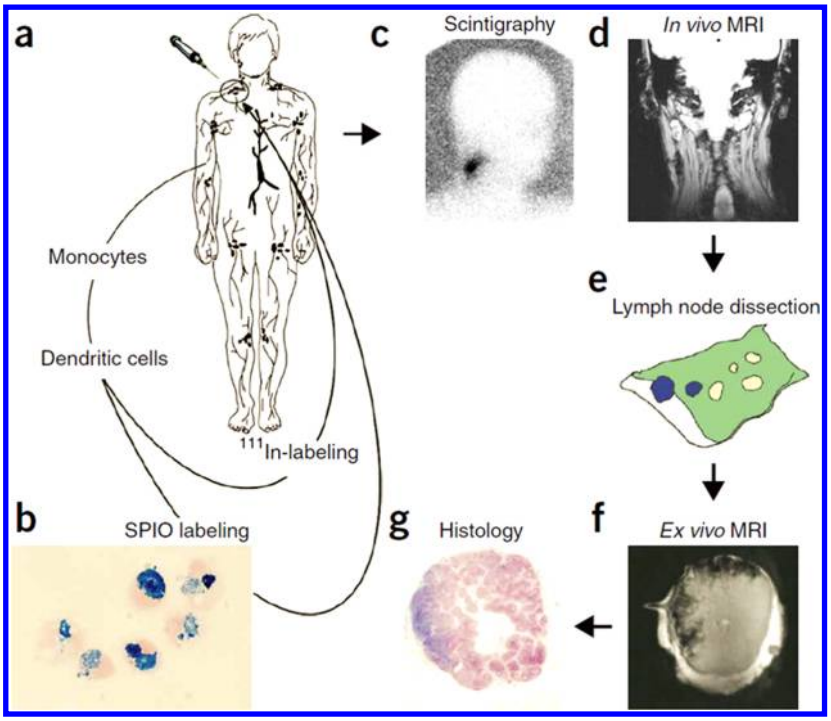

Figure 33. Imaging of dendritic cells in melanoma patients by means of MNPs for monitoring of cellular therapy. (a) Monocytes are obtained by cytopheresis from stage III melanoma patients. (b) They are cultured and labeled with SPIONs and ^{111}In. (c and d) The cells are then injected intranodally into a (either cervical, inguinal, or axillary) lymph node basin that is to be resected, and their biodistribution is monitored in vivo by γ-scintigraphy (c) and by MRI at 3 T (d). (e–g) The lymph node basis is resected, and separate lymph nodes are visualized with high-resolution MRI at 7 T (f) and histology (g). Reprinted with permission from ref 593. Copyright 2005 Nature Publishing Group.

vasculature. Thus, this technique has also been proposed for noninvasive identification of neovasculature.

8.2. Imaging of Transplanted Pancreatic Islet Cells

Since type 1 diabetes mellitus is characterized by the loss of β-cells located in the islets of Langerhans as a result of the autoimmune process, the replacement of β-cells has been considered as one possible treatment of this disease. In this view, pancreatic islet cells have been labeled with Feridex, transplanted intrahepatically into diabetic rats, and successfully in vivo monitored for the survival or rejection of the islet grafts using MRI.[590] It was demonstrated that the labeling of the pancreatic islet cells with SPIONs did not disturb the integrity of the cells. Similarly, another report revealed in vivo imaging of islet cells labeled with SPIONs modified with *Cy*5.5 dye for combining MRI and near-infrared imaging.[591] In this study, the monitoring of the transplanted islet cells was successfully achieved for 6 months. These preclinical data have encouraged subsequent clinical trials in which the feasibility and the safety of MRI-based islet graft into the liver have been demonstrated in type 1 diabetic patients.[592] Interestingly, all patients reached the state of insulin independence at least up to 15.5 months after the first infusion of the islets. Although this technique was associated with some limitations, such as the interference by the possible presence of iron background within the liver (necessitating in such case the exclusion of patients with high intrahepatic iron content), and the lack of correlation between the number of transplanted islet cells and the number of spots within the liver, it served as an important clinical proof-of-concept of the MRI-based monitoring of islet grafting.

8.3. Imaging of Dendritic Cells

Specific cell imaging has also been reported for dendritic cells that play a key role in immunotherapy by initiating endogenous host immune response against tumor cells. Following injection into the body, the dendritic cells are expected to migrate throughout the vascular and lymphatic system to present their antigens to T cells located within the lymph nodes. The challenge is, however, to deliver a sufficient amount of dendritic cells to the target tissue. Thus, accurate delivery and subsequent monitoring of the dendritic cells toward the target lymph nodes is essential to ensure effective stimulation of the immune response. Immature dendritic cells (because they are more phagocytic and, hence, take up the iron oxide label more efficiently than mature cells) were labeled with Endorem. After maturation, they were then pulsed with the melanoma peptides gp100:154-162, gp100:280-288, and tyrosinase:369-376.[593] These cells simultaneously labeled with ^{111}In-oxine were injected intranodally in patients affected by a melanoma for MRI and scintigraphy imaging (Figure 33). The MRI perfectly revealed all the lymph nodes containing dendritic cells, whereas saturated γ-scintigraphic images showed several adjacent lymph nodes as a single node. The in vivo MRI images correlated well with the ex vivo images and with the histological examination of the lymph nodes. Thus, the intranodal injection of SPION-labeled dendritic cells, followed by the migration of these cells to the adjacent lymph nodes, could be successfully monitored by MRI whereas γ-scintigraphic imaging did not allow accurate distinguishing between two nodes and also between a correct and a noncorrect intranodal injection.

8.4. Imaging of Apoptotic Cells

The detection of apoptotic cells has been achieved by surface conjugation of IONPs with annexin V, which recognizes the phosphatidyl serine receptors overexpressed on the surface of cells in apoptosis.[138] To verify the validity of this approach, Jurkat T cells were pretreated with the apoptosis-inducing drug

dx.doi.org/10.1021/cr300068p | *Chem. Rev.* 2012, 112, 5818–5878

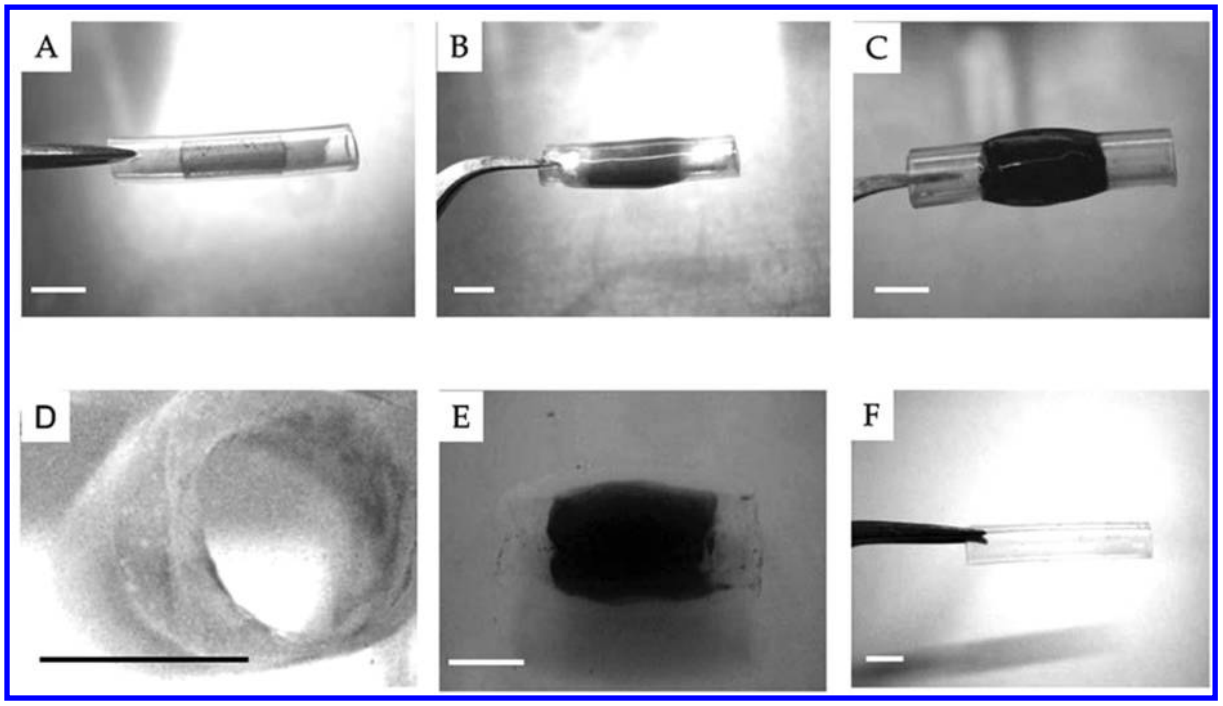

Figure 34. Bright-field micrographs of tubular constructs fabricated by magnetic force-based tissue engineering. The silicone tube containing the cylindrical magnet (A) was rolled over the magnetically labeled cell sheet, and the cell sheet (B, canine urothelial cells sheet; C, human endothelial cells, human aortic smooth muscle cells, and mouse NIH 3T3 fibroblasts) eventually covered the entire surface of the silicone tube. Collagen was then allowed to gelate around the cell sheets, and the silicone tube and the cylindrical magnet were pulled out of the construct (F), producing tubular constructs of tissue-engineered urothelial tissue (D) and vascular tissue (E). Bar length: 5 mm. Reprinted with permission from ref 604. Copyright 2005 Mary Ann Libert, Inc.

camptothecin and further incubated with annexin V-conjugated IONPs. In vitro MRI showed a significant lowering of signal intensity of the camptothecin treated-cells, which were incubated with annexin V-conjugated IONPs, compared to the untreated cells, whereas the unconjugated IONPs did not result in a considerable lowering of the signal intensity.

9. TISSUE ENGINEERING

Tissue engineering is an interdisciplinary area that integrates the principles of engineering, cell biology, and medicine aiming at the regeneration of specific cells and/or functional tissues. Tissue engineering deals with the construction of biocompatible microstructured two- or three-dimensional scaffolds on which the cells can undergo attachment, growth, differentiation, and proliferation. Cell colonization of these scaffolds can take place either ex vivo for later grafting into the body and regeneration of a damaged organ/tissue or in vivo conditions.[594] Interestingly, tissue grafts were also proposed to be used in the drug-discovery field to minimize the usage of animals for investigating the drugs' effects.

The cells to be grown are generally isolated from a tissue biopsy, cultured in vitro, and seeded into a three-dimensional porous scaffold. The challenge here is to achieve an efficient cell seeding and to ensure the effectiveness of the cell−cell interactions, especially between heterotypic cells and between cell layers. Additionally, to build up a tissue construct functioning similarly as under in vivo conditions, a three-dimensional structure is required. For this purpose, a technique known as magnetic force-based tissue engineering (Mag-TE) has been reported that utilizes magnetic nanodevices (e.g., MCLs, magnetic gelatin NPs, MNP-loaded hydroxyapatite and collagen, etc.) to provide magneto-responsive features to the cells.[595−597] Of these nanodevices, MCLs have been extensively applied.

9.1. Engineering of Heterotypic Cell/Tissue Constructs

The MCLs employed for tissue engineering were made up of SPIONs (10 nm diameter) incorporated into cationic liposomes composed of a lipid mixture of *N*-(*α*-trimethylammonioacetyl)-didodecyl-*d*-glutamate chloride, dilauroylphosphatidylcholine, and dioleoylphosphatidyl ethanolamine in a 1:2:2 molar ratio.[598] MCLs have been used to promote the adhesion of human aortic endothelial cells (HAECs) onto a rat hepatocyte layer.[595] For this purpose, the HAECs were incubated with MCLs and subsequently seeded onto a layer of rat hepatocytes before application of a magnetic field from the bottom of the culture plates for ∼24 h. The HAECs accumulated in the region where the magnetic field was focused remained adhered even after the removal of the magnetic field. On the contrary, in the absence of a magnetic field, these cells did not adhere onto the hepatocyte layer. The functionality of the obtained heterotypic construct was demonstrated by its albumin-secretion ability, whereas the hepatocyte cell culture alone failed to produce this protein. Thus, multilayered three-dimensional tissue constructs could be achieved, and their performances were found to be logically dependent on both the concentration of the magnetic particles into the cells and the intensity of the applied magnetic field.

9.2. Scaffold-Based Tissue Engineering

Scaffolds function as substrates for the local retention of cells and their further differentiation, proliferation, and tissue formation. Obviously, scaffolds for tissue engineering need to be nontoxic and biocompatible. They may be prepared with various types of materials such as sponges, biodegradable

dx.doi.org/10.1021/cr300068p | *Chem. Rev.* 2012, 112, 5818−5878

polymers, agarose, etc.[599−601] A crucial point is to reach a high cell number with sufficient packing of the cells at the interior of the scaffold. This has been addressed by (i) loading the cells with MCLs[602] or chitosan-coated MNPs;[600] (ii) hydrating the scaffold with the suspension of the cells; and (iii) applying a magnetic field. Such a protocol has resulted in the cell seeding into the deeper sites of the three-dimensional porous scaffolds, while the absence of a magnetic field did not result in efficient cell germ. The magnetic field intensity has been found to have a positive influence on the depth of the cell seeding into the scaffold.

The manufacture of the functional tissue construct able to retain cell-growth migration and differentiation properties is also very important in order to be as close as possible from the normal tissue physiology. In this context, cell patterning by which the cells can be specifically allocated with precision and control is of considerable importance. Unfortunately, conventional patterning by the sole means of a magnetic field led to destabilization and disassembling of the pattern, following cell growth and migration. This issue has been addressed by employing a cell adhesion peptide sequence, namely, RGD, in order to maintain the cells in place. Thus, MCLs surface-functionalized with the RGD sequence (RGD-MCLs) have been used as a cell-adhesion promoter for facilitating efficient cell patterning under the influence of a magnetic field.[603] The HaCaT cell line (an immortalized human keratinocyte cell line), which exhibits a high anchorage dependency and fails to show adhesion onto the hydrophilic neutral charged surface of the culture plate, has shown adhesion when incubated together with RGD-MCLs. Moreover, different patterns of the cell layers using the magnetic field may be achieved by selecting the pattern substrate and placing it between the culture plate and the magnetic field. Similarly, three-dimensional configurations with complex shapes such as tubular structures can also be constructed by employing magnetic force-based tissue engineering. For instance, MCL-incubated cells seeded onto ultralow-attachment plates formed a sheet after 24 h of culture under the influence of a magnet placed under the culture plates. When a cylindrical magnet was rolled onto this cell sheet, the latter formed a tube around it (due to magnetic attraction), which resulted in the formation of a tubular structure following removal of the magnet (Figure 34).[604]

Magnetic force-based tissue engineering therefore represents a promising approach for vascular tissue construction.[605] Encouraging results have, indeed, been reported concerning the vascular grafting of human tissues such as human smooth muscle cells and human dermal fibroblasts. The deposition of MCL-labeled cells (for grafting) onto a tubular vascular scaffold made of porcine decellularized common carotid artery, which consisted of extracellular matrix, has been successfully achieved using an external magnetic field. This has been accomplished by inserting a cylindrical magnet into the lumen of the scaffold, followed by its immersion into a suspension of labeled fibroblasts.[606] Similarly, transplantation of cultured retinal pigment epithelium cell sheet by magnetic force-based tissue engineering has shown encouraging results for the treatment of choroidal neovascularization, one of the most severe forms of age-related macular degeneration causing rapid visual loss.[607]

9.3. Scaffold-Free Engineering of Three-Dimensional Tissue Constructs

MCLs have been employed to build three-dimensional tissues without scaffolds for bone-tissue reconstruction. For instance, human mesenchymal stem cells labeled with MCLs when seeded onto an ultralow-attachment culture plate led to the formation of multilayered sheetlike structures under the influence of a magnetic field from the bottom of the plate. The so-formed sheets were harvested using an electromagnet and transplanted into experimental bone defect in the crania of the rat. Two weeks after transplantation, the formation of new bone surrounded by osteoblast-like cells in the defect area was observed by histological evaluation, whereas no bone formation was detected in the control rats without the transplant.[608,609]

In another study, Ferumoxide-loaded rabbit bone marrow-derived mesenchymal stromal cells were used to fill the bone defect, using interconnected porous calcium hydroxyapatite ceramic as a substrate.[610] Injecting the labeled cells percutaneously and concentrating them into the ceramic substrate by using an external magnetic field has resulted in the enhancement of bone formation at the defective site. Such a technique may have potential for the treatment of bone defects and bone fractures. Another report revealed successful magnetic guidance of the intra-articularly injected IONP-labeled bone marrow-derived mesenchymal stem cells to the osteochondral defects in a rabbit model.[611] Regeneration of the damaged human cartilage ex vivo has also been demonstrated using the IONP-labeled human bone marrow-derived mesenchymal stem cells.[612] Practically, the excised damaged human cartilage was incubated with labeled stem cells and subjected to the magnetic field for 6 h to concentrate the cells onto the cartilage. Culturing the cartilage for 3 weeks has resulted in the formation of a cell layer with extracellular matrix, whereas in the control group (wherein the magnetic force was not applied), cell layer failed to develop. This clearly indicated that the magnetically guided accumulation of labeled cells on the cartilage was the key success factor.

Scaffold-free multilayered three-dimensional functional cardiomyocyte sheets have also been constructed using MCLs and magnetic field for heart-tissue engineering.[613] Briefly, the MCL-labeled rat cardiomyocytes were seeded onto the hydrophilic neutral-charged surface of the culture plate, and the magnetic field was applied from the bottom of the plate. Following 24 h of culture, the cardiomyocytes formed sheets of ∼120 μm thickness, having gap junctions within the sheets, as assessed by connexin 43 antibody staining. In addition, the cells within the sheets were found to have an established electrical communication representing a functional scaffold-free cell cluster. Overall, the magnetic-based tissue engineering has shown considerable potential in the fabrication of tissue constructs and in tissue transplantation for achieving effective tissue regeneration.

10. MISCELLANEOUS APPLICATIONS

10.1. Cell Separation and Cell Sensing

Cell separation using ferro/paramagnetic substances is a widely employed technique that allows further detection of the magnetically separated cells using MRI.[4,477] MNPs intended to be used for cell separation should exhibit a good dispersibility in the separation media, an ability to distinguish and to interact with the target cells to be separated, and an ability to accumulate/concentrate under the influence of a magnetic field. MNP-mediated cell separation has been achieved by incubating the cells with NPs advantageously equipped with specific cell-recognition moieties (or not if the

dx.doi.org/10.1021/cr300068p | Chem. Rev. 2012, 112, 5818−5878

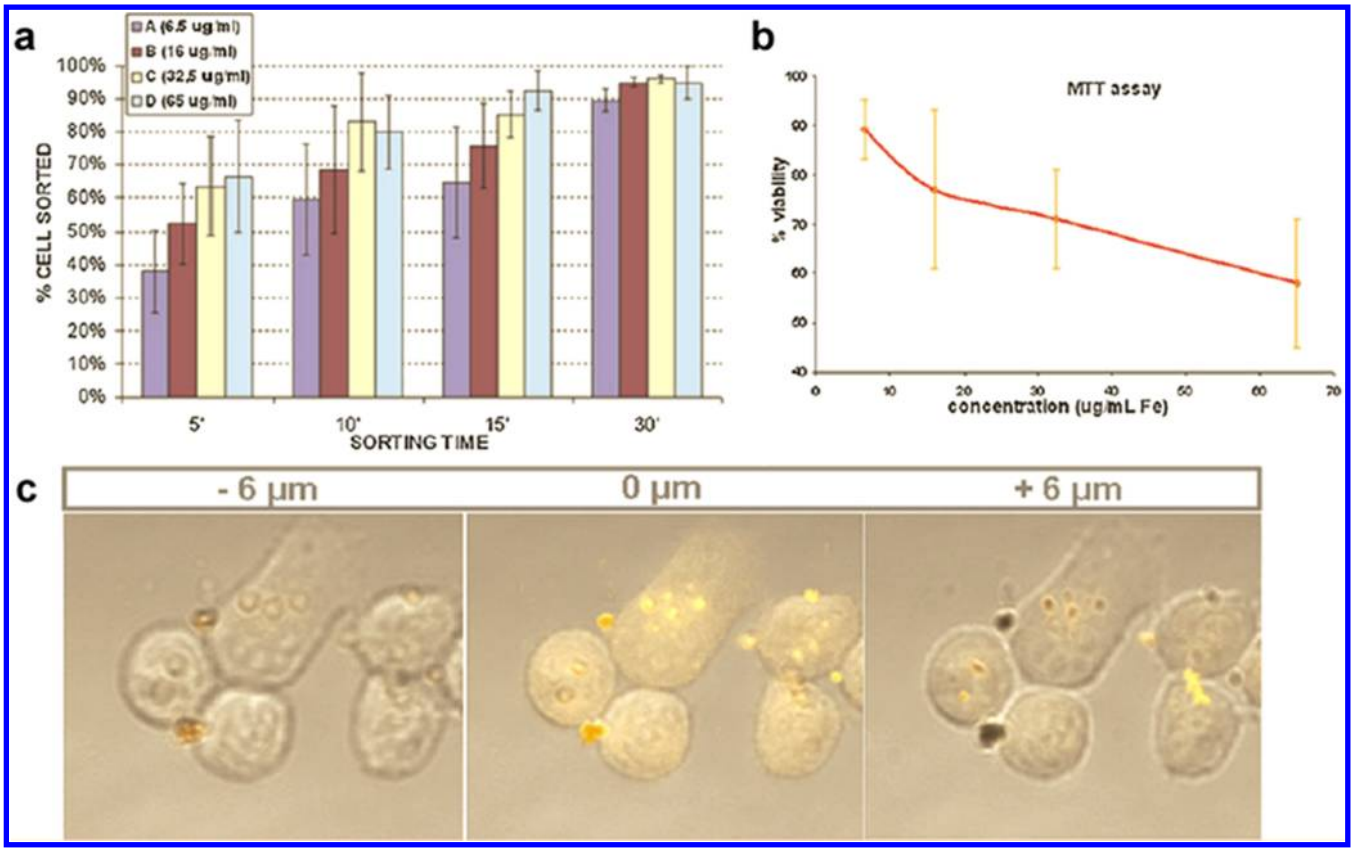

Figure 35. Results of cell-separation experiments. (a) KB cells doped with four concentrations of magneto-fluorescent NPs (6.5, 16, 32.5, and 65 $\mu g \cdot mL^{-1}$ of iron) were accumulated to the magnet at 5, 10, 15, and 30 min. The counted cells are reported versus the incubation time. (b) Cell viability test on KB cells doped with increased amounts of magneto-fluorescent NPs. (c) Sections of KB cells doped with magneto-fluorescent NPs based on oligothiophene fluorescents. Reprinted with permission from ref 616. Copyright 2009 Wiley.

NPs are able to spontaneously interact with the target cells), followed by separation using a magnetic field.

10.1.1. Separation of Bacterial Cells And Mammalian Cells. IONPs (13 nm diameter) stabilized by oleate coating have been shown to adsorb, immobilize, and separate various bacteria such as *Rhodococcus erythropolis* LSSE8-1 and *Pseudomonas delafieldii* R-8 from the culture broths under the influence of an external magnetic field.[614] The proposed mechanism of separation was the adsorption of NPs onto the bacterial surface due to hydrophobic interactions. The separation technique did not disturb the integrity of the bacteria, which could be further used for intended applications without the necessity of removing the MNPs.[615] This methodology is expected to be helpful for the separation of bacteria from consumables such as milk, or from human biological media such as blood.

MNPs encapsulated into polymeric shells have been utilized for the magnetic separation of mammalian cells from various media. For instance, iron oxide-loaded oligothiophene fluorescent-tagged amphiphilic poly(maleic anhydride-*alt*-1-octadecene) NPs (120 nm diameter) have been used for magnetic isolation of KB tumor cells (Figure 35).[616] Incubation of KB tumor cells with the NPs for 24 h, followed by the separation of the cells from the incubation medium, redispersion into a fresh medium, and subsequent exposure to the external magnetic field, has resulted in clustering and accumulation of the cells in the direction of the magnetic field. The fluorescence emitted by the fluorescent label has allowed the visualization of the magnetically separated cells.

Although the separation of cells (bacterial or mammalian) from a single cell-type suspension is usually easy, the isolation of a specific cell type from complex media or from mixtures of various cell types is more challenging. This may, however, be accomplished if the IONPs are tagged with cell-specific ligands or antibodies able to recognize specific biomolecules expressed/overexpressed at the cell surface. As for single-cell suspensions, cells may then be withdrawn from the bulk mixture thanks to the application of a magnetic field. For instance, IONPs coupled with bacteria-recognition ligands have been employed for the detection and isolation of *Mycobacterium avium* in milk and in blood.[617] Polyaniline-coated IONPs surface functionalized with mouse monoclonal anti-*Bacillus anthracis* IgG were used for recognizing *Bacillus anthracis* spores in different samples such as milk, lettuce, and ground beef. Interestingly, polyaniline was made electrically active by acidic doping, and this property was used for the detection of the NP−bacillus spore complex, formed when the samples containing bacillus were incubated with NPs, by measuring the electrical resistance signal across two electrodes.[618]

IONPs coupled with the anti-CD4 antibody have been exploited for the separation of CD4+ T cells from the human blood containing a mixed population of different cell types.[619] Practically, the CD4+ T cells were isolated by incubation of human blood with the antibody-tagged MNPs before the application of the magnetic field. The cell-purification efficacy has been confirmed by the assessment of the T cell peptide masses fingerprints using mass spectrometry. In another study, streptavidin−fluorescein isothiocyanate-conjugated IONPs

dx.doi.org/10.1021/cr300068p | *Chem. Rev.* 2012, 112, 5818−5878

have been used to efficiently bind and separate the biotin-antiCD4 antibody conjugated CD4+ T murine splenic lymphocytes from the culture.[620] In this experiment, the anti-CD4 antibody binds to lymphocytes, while the biotin is recognized by avidin functionalized onto the NPs. Again, the NP-bound complex may be further magnetically separated. Similarly, IONPs conjugated with the macrophage-specific anti-F4/80 antibody were employed for affinity-based binding and isolation of cells such as neutrophils and macrophages from peritoneal inflammatory cells in cultures.[621]

Cell-specific targeting ligands such as aptamers have also been used for binding and magnetic isolation of cancer cells using IONPs. For example, the CCRF-CEM (a human leukemia)-specific aptamer sequence was coupled onto IONPs in order to magnetically separate the CCRF-CEM leukemia cells from whole-blood samples.[369] Using the aptamer-conjugated fluorescent dye-doped IONPs has facilitated the detection of the sorted cells.[368]

The concentration of the ligands coupled onto the surface of the IONPs may considerably influence the cell recognition. For instance, a high folate density present at the surface of poly(acrylic acid) shell-based IONPs has shown a better cell recognition and separation compared to the NPs bearing a lower folate density. This approach has been demonstrated for the separation of A549 folate-expressing lung tumor cells from culture, which has potential application for the isolation of target receptor overexpressing cell types from complex samples such as blood.[622]

Recognition and magnetic separation of the apoptotic cells has also been achieved using ligand-functionalized IONPs.[623] Thus, IONPs coupled with streptavidin have been used to recognize and bind to the biotinylated annexin V-labeled apoptotic cells before magnetic separation of these cells.[624] As already mentioned before, the annexin V specifically binds to the phosphatidyl serine receptors, which are expressed on the surface of the apoptotic cells but not on the surface of the normal cells.[625] Inclusion of fluorescent agents such as propidium iodide may facilitate the visualization of the isolated apoptotic cells using methodologies such as fluorescence-activated cell sorter.

The magnetic surface-enhanced Raman spectroscopy (SERS) technique employing pathogen-specific SERS nanoprobes conjugated onto IONPs is another approach that has been exploited for the binding and detection of multiple pathogens. The proof-of-concept has been done very recently using a mixture of two bacterial pathogens: *Salmonella enterica serovar Typhimurium* and *Staphylococcus aureus*.[626]

In general, the above-mentioned conventional cell-sorting techniques are time-consuming due to the sequence of steps involved in the separation process. The processing times have, however, been considerably reduced by continuous cell sorting in a microfluidic scale device by free-flow magnetophoresis.[627] This methodology has been applied to the separation of murine macrophages and HeLa human ovarian cancer cells labeled with IONPs. In this device, a laminar flow was applied over a separation chamber, while the magnetic field was applied in the direction opposite to the laminar flow. As a result, the unlabeled cells and other nonmagnetic components present in the medium followed the direction of the laminar flow, whereas the magnetically labeled cells were attracted toward the magnetic field and collected.

10.1.2. Separation of Viruses. Separation of viral particles from virus positive biological media has been shown using the above-mentioned magnetosorption methodologies. For instance, hepatitis B viral (HBV) and hepatitis C viral (HCV) particles present in sera were adsorbed using virus-specific globulin proteins coupled onto the MNPs and then magnetically separated. The virus-sorting efficacy has been verified by analyzing the separated virus using the polymerase chain reaction technique.[628]

10.1.3. Magnetic-Relaxation Switches. Another application of interest is the use of IONPs as magnetic-relaxation switches. In this methodology, advantage has been taken from the clustering of nanomagnetic probes from independent particles into larger assemblies, which results in an enhanced dephasing of the spins of the surrounding water protons with subsequent increase of the spin−spin (T_2) relaxation, able to be detected by magnetic resonance relaxometry.[629,630] This technique has been employed for sensing different types of molecular interactions such as DNA−DNA, protein−protein, and protein−small molecule, as well as enzyme reactions, even in turbid and visually obscured biological samples. The IONPs are usually coupled with an oligonucleotide sequence or a protein that can recognize the complementary nucleic acid or protein sequence. When the binding takes place, a reversible clustering of the NPs happens. As a result, a shortening of the T_2 relaxation time occurs, compared to the NPs in an individual particle state (Figure 36).[631]

This technique has also been applied for the sensing of viruses and bacteria by conjugating IONPs with target-specific antibodies; clustering is very sensitive, allowing the detection of a few pathogen numbers in the detection medium. The application of this methodology has been practically demonstrated for the detection of viruses such as adenovirus-5, herpes simplex virus-1, etc.,[632] as well as for bacteria such as *Mycobacterium avium* spp. paratuberculosis, *Staphylococcus aureus*, etc. in complex media such as milk and blood.[617,633]

Finally, magnetic-relaxation switches were found to be efficient sensors for the investigation of the metabolic activity of bacteria, such as the consumption of specific carbohydrates in the growth medium. Such detection may be useful for the rapid and sensitive detection of bacteria, especially resistant bacteria that are characterized by specific metabolic pathways and generally identified using other very time-consuming methods.[634] For instance, magnetic-relaxation measurements were used to highlight the differences in the starch consumption by various bacteria such as *Escherichia coli*, *Serratia marcescens*, and *Shigella sonnie* in the presence or absence of the antibiotic ampicillin. The analysis was performed by incubation with IONPs functionalized with concanavalin A, which forms clusters in response to the polysaccharide concentration.

10.2. Separation of Biochemicals

Isolation of biochemicals from reaction mixtures or complex biological samples (such as cell lysates, serum, etc.) may be performed using MNPs too. For example, niobium oxide-coated MNPs have been used for the selective magnetic capture of phosphopeptides from complex peptides mixtures including tryptic digest of caseins, serum, and cell lysates. Indeed, transition metal oxides such as niobium oxide lead to strong interactions with phosphonates, thus allowing selective enrichment of phosphopeptides from the complex media.[635,636] Similarly, IONPs coupled with various other metal oxides, such as tantalum oxide,[637,638] zirconium dioxide,[639] or titanium

dx.doi.org/10.1021/cr300068p | *Chem. Rev.* 2012, 112, 5818−5878

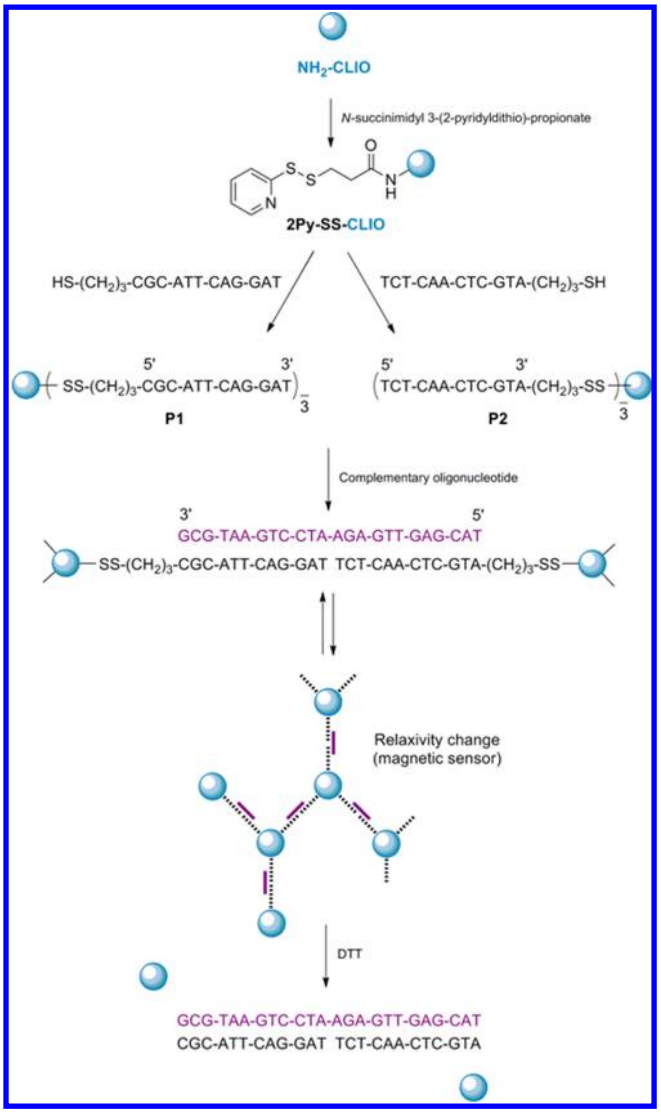

Figure 36. Alkanethio-substituted oligonucleotides were treated with *N*-succinimidyl 3-(2-pyridyldithio)propionate (SPDP)-activated NPs to form the P1 and P2 nanosensors.[631] P1 and P2 hybridize with complementary oligonucleotide sample and result in oligomerization and changes in the magnetic relaxivity. Treatment with 1,4-dithiothreitol (DTT) breaks the bond between the cross-linked iron oxide (CLIO) particles and alkanethio-substituted oligonucleotide.

dioxide,[640] have been used for phosphopeptide isolation from tryptic digest samples.

IONPs surface-conjugated with double-stranded RNA (*ds*RNA) polyinosinic/polycytidylic acid [poly(I:C)] have been employed for the recognition of the protein sponge (2-5)A synthetase of the fresh water sponge *Lubomirskia baicalensis*, thanks to the affinity of poly(I:C) for this protein.[641] Then, the NP-bound protein could be detached and isolated by treatment with urea (Figure 37).

Binding and isolation of proteins have also been carried out using PS NPs surface-conjugated with sulfonic cation-exchanger groups and combined with IONPs by spray-drying in poly(vinyl butyral) (PVB).[642] These composite NPs (~250 nm diameter), in which the PVB formed the matrix embedding the remaining components, were used to adsorb lysozyme before further magnetic separation. The nanocomposite showed lower lysozyme adsorption capacity but resulted in a considerably higher recovery compared with the PS-cation exchanger NPs devoid of IONPs. This suggests that the magnetic-separation technique has increased the protein recovery by minimizing the loss of protein associated particles that may occur during the purification step when protein-associated NPs devoid of magnetic core were used.

Another example of protein purification with MNPs is the use of iminodiacetate-functionalized SiO_2-coated IONPs. When they are surface charged with Ni^{2+}, these NPs are able to anchor to the histidine-tagged proteins. Therefore, they have been involved in the purification (from a total cell lysate) of 6 × His-tagged recombinant proteins (6 × His represents sequence specifying a string of 6−9 histidine residues).[643] Similarly, glucosaminic acid-functionalized IONPs have been used for the detection and separation of oligonucleotide sequences in aqueous medium.[644]

Separation of botanical substances has also been achieved through capture by functionalized IONPs and subsequent magnetic separation. For instance, oxovanadium(IV) acetylacetonate-coupled SiO_2-coated IONPs have been used to specifically bind and isolate 2,3-epoxygeraniol product in geraniol epoxidation reaction medium.[645]

10.3. Enzyme/Protein Immobilization

Because they allow easy and quick magnetic recovery from complex mixtures, magnetic particles are gaining increasing interest as solid support of proteins. Immobilization of enzymes/proteins may be carried out by direct conjugation onto the MNPs in the presence of carbodiimide chemistry facilitated by the presence of amphoteric hydroxyl groups on their surface.[646−648] Several enzymes have been successfully immobilized onto these magnetic nanodevices, e.g., *Candida rugosa* lipase,[649−651] horseradish peroxidase,[652] pectinase,[653] trypsin,[654] α-chymotrypsin,[654−657] cyclic adenosine monophosphate-dependent protein kinase,[658] glucose oxidase,[659−661] hexa-arginine-tagged esterase,[89] porcine pancreas lipase,[662] papain,[654] *Saccharomyces cerevisiae* alcohol dehydrogenase,[663] chitosanase,[664] triacylglycerol lipase,[665] laccase (a copper oxidoreductases from the fungal source),[666] epoxide hydrolase,[667] etc. For instance, chitosan-coated IONPs surface-coupled separately with two enzymes *S*-adenosylhomocysteine nucleosidase (Pfs) and *S*-ribosylhomocysteinase (LuxS) have been mixed and incubated with an *Escherichia coli* bacterial suspension (Figure 38). Because of its positive electrical charge, chitosan facilitated the adhesion of the NPs onto the membranes of the cells. The NP-bound cells were then isolated by magnetic separation and added to the *S*-adenosylhomocysteine (SAH) enzymatic substrate, which then reacted with Pfs and LuxS, resulting in the in situ formation of a signaling molecule termed as autoinducer-2 (AI-2) at the bacterial cell surface. The autoinducer-2 finally penetrates into the bacteria to alter their β-galactosidase expression. This procedure may have application in understanding and controlling quorum sensing (a process of coordination of gene expression by bacteria according to the local density of their population) such as biofilm formation, pathogenicity, and antibiotic resistance.[668] Moreover, the development of the next generation of antimicrobials based on the mechanism of intercepting and interrupting the quorum sensing-based signaling may benefit from this magnetic and enzyme-immobilization process.[669]

Elevated telomerase levels are often found in many types of malignancies, representing an attractive target for both diagnosis and therapy of tumors. A magnetic nanosensor

dx.doi.org/10.1021/cr300068p | *Chem. Rev.* 2012, 112, 5818−5878

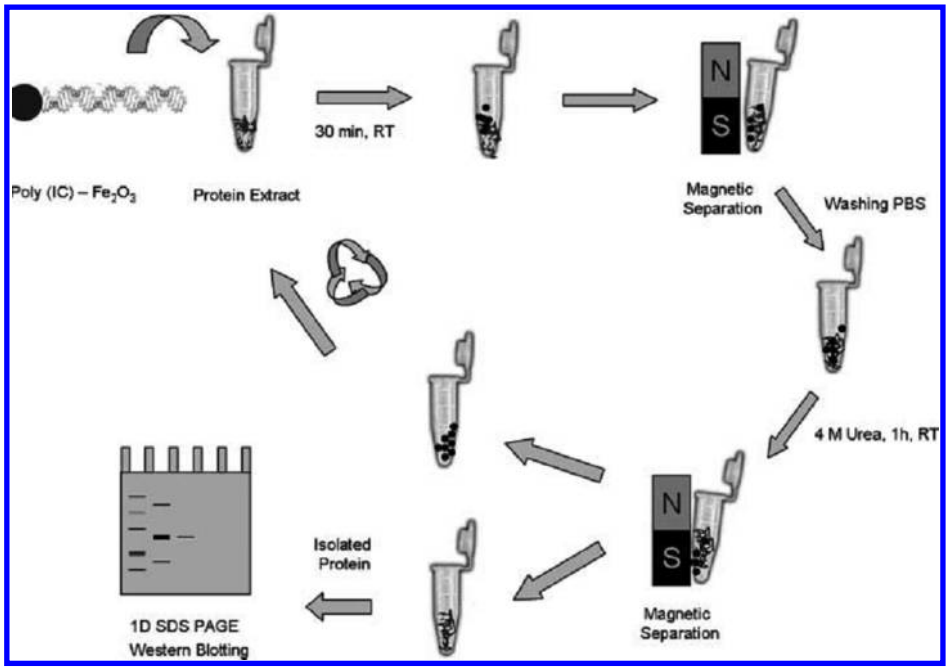

Figure 37. Isolation at room temperature (RT) of (2-5)A synthetase from sponge extract using *ds*RNA poly(I:C) functionalized superparamagnetic γ-Fe_2O_3 NPs. Reprinted with permission from ref 641. Copyright 2007 RSC Publishing.

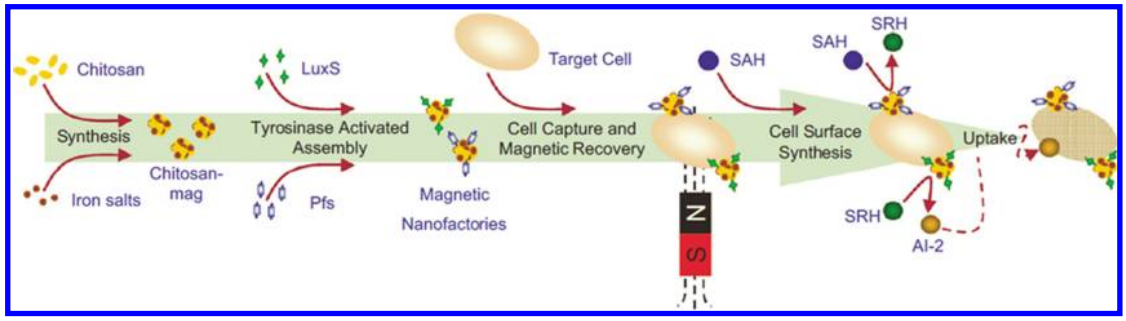

Figure 38. Overview of assembly and use of nanofactories to locally synthesize and deliver quorum signaling molecule AI-2 to a target cell. Synthesis of the magnetic carrier, chitosan-mag, by coprecipitation of iron salts and chitosan; attachment of pro-tagged Pfs and LuxS to chitosan-mag by activation using tyrosinase to assemble magnetic nanofactories; capture of target cells by the magnetic nanofactories; recovery of captured cells using an external magnet; cell-surface synthesis and delivery of AI-2 by enzymes Pfs and LuxS; uptake of AI-2 and production of cellular response (AI-2-dependent reporter). SAH, *S*-adenosylhomocysteine; SRH, *S*-ribosyl homocysteine. Reprinted with permission from ref 668. Copyright 2007 Elsevier.

based on IONPs coupled with oligonucleotide motifs complementary to the telomerase-associated amino acid repeats has been proposed for sensing of the telomerase with high sensitivity from biological samples. Since MNPs with complementary oligonucleotide motifs sense and bind to the telomerase and assemble into aggregates, it results in an increase in relaxivity quantifiable by nuclear magnetic resonance relaxometry.[670]

10.4. Bioanalysis and Immunoassays

Bioanalysis and immunoassays have taken benefit from the magnetic susceptibility and large surface area of ligand-decorated IONPs.[165,411,671−679] The differences in the magnetic fields generated by the magnetically labeled targets can indeed be detected directly by using a sensitive magnetometer.[680] In medical and clinical diagnostics, SPIONs act as solid supports for the immobilization of biomarkers to facilitate the isolation and detection of proteins,[681−688] enzymes,[689,690] and DNA,[691] which has led to the development of sensitive and efficient automated immunoassays.[243,692−694] As an example, a protein-detection procedure named "nanotechnology-based bio-barcode-amplification method" has shown superior results compared to the usually employed ELISA assay for the detection in plasma of HIV-1 p24 Gag protein, with a breadth of coverage for diverse HIV-1 subtypes.[695] The technique relied on (i) magnetic particles (~1000 nm diameter) functionalized with antibodies that specifically bind to the HIV-1 p24 Gag protein and (ii) gold NPs (15 nm diameter) functionalized with both MAb's directed to a nonoverlapping region of HIV-1 p24 Gag and barcode oligonucleotides that can sandwich the target protein captured by the MNP-bound antibodies. The resulting aggregated sandwich structures are magnetically separated from the medium and treated to isolate the sandwiched barcode DNA. The DNA barcodes (several hundreds per target) are then quantified using real-time polymerase chain reaction (PCR) and chip-based scanometric methods. This assay facilitated the detection and isolation of specific HIV-1 antigens from a mixture of diverse HIV-1 subtypes, while the detection sensitivity was as high as 0.1 pg/mL HIV-1 p24 Gag in plasma.

dx.doi.org/10.1021/cr300068p | *Chem. Rev.* 2012, 112, 5818−5878

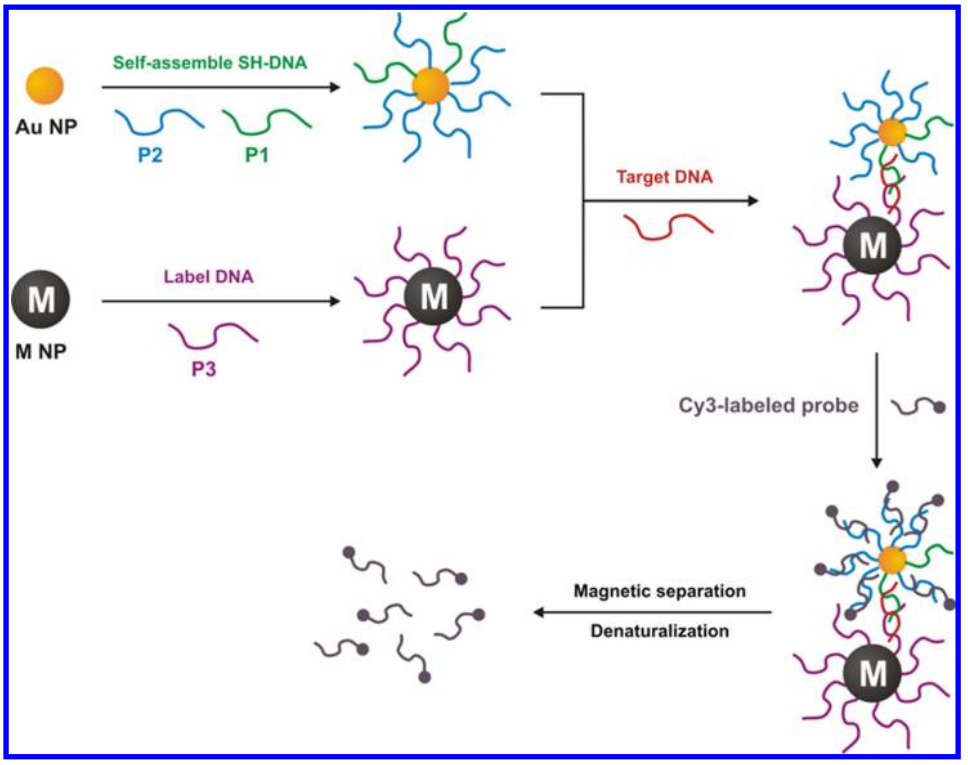

Figure 39. Schematic representation of amplified fluorescence detection of DNA based on magnetic separation.

MNP-based sandwich assays have been widely developed for the detection of DNA samples. For instance, a sandwich assay based on combined magnetic separation and amplified fluorescence detection has been recently reported.[696] In this assay, two oligonucleotide sequences, one which is complementary to one end of the target DNA and the other which is a mismatched sequence to DNA (known as barcode DNA), were conjugated onto the gold NPs (Figure 39). On the other hand, IONPs were conjugated with the oligonucleotide sequence complementary to the remaining end of the target DNA. These two NP types were then hybridized with the target DNA to sandwich it. Then, fluorescent (*Cy*3-labeled and *Cy*5-labeled) DNA probes complementary to the mismatched oligonucleotide sequence (barcode DNA) were immobilized onto the gold NPs. The sandwich complex was then isolated by magnetic separation, and the quantity of the adsorbed fluorescence on the complex was analyzed, allowing quantification of the target DNA. The detection limit was found to be as low as 1 pM, indicating the excellent sensitivity of this analytical method.

The combined use of iron oxide and gold NPs has also allowed the development of a highly specific fluoro-immunoassay for antigen detection. This assay primarily took advantage of the fluorescence-quenching property of the gold NPs for the fluorescent dyes. Thus, IONPs coated with anti-α-fetoprotein polyclonal antibodies and gold NPs coated with anti-α-fetoprotein MAb's were mixed with the samples containing the α-fetoprotein to be analyzed. The resulting sandwich immunocomplex was then magnetically separated, whereas the remaining unbound gold NP fraction was detected in the supernatant by the addition of fluorescence isothiocyanate (FITC) and subsequent measurement of fluorescence intensity (which quantitatively depended on the quenching by gold NPs). The concentration of α-fetoprotein was calculated from the concentration of gold NPs consumed for the formation of the immunocomplex. The limit of detection of the α-fetoprotein concentration was 0.17 nM.[697]

A microbead sandwich assay for P38 mitogen-activated protein kinase using surface-enhanced resonance Raman spectroscopy (SERRS) detection has been reported. A limit of detection of 9.5×10^{-12} mol/dm^3 and sensitivity to concentrations as low as 6 ng/mL have been measured (Figure 40).[698]

MNP-based immunoassay for rapid and sensitive detection of proteins using actuated magnetic particle labels has been recently described.[699] In this study, the parathyroid hormone antibody-coupled IONPs were mixed with the samples containing the parathyroid hormone to be analyzed. The NPs effectively captured the hormone, which then concentrated at the sensor surface where the particles were attracted. The sensor-bound particles were then detected using a highly sensitive giant magnetoresistive sensor chip. The detection limit achieved using this assay was 10 pM, and the assay time was 15 min. Overall, this technique facilitates rapid detection of protein analytes in the picomolar concentration range and in small sample volumes.

Magneto-immuno polymerase chain reaction (M-IPCR), a modified immuno-PCR technology for automatable highly sensitive antigen detection, has been recently developed.[700] This assay is based on antibody-functionalized biogenic magnetosomes (i.e., MNPs isolated from magnetotactic bacteria; for more details, see section 2.1.13). The general principle of the M-IPCR is similar to that of a sandwich immunoassay described previously in this section. Antibody-functionalized magnetosomes are employed for the immobilization and magnetic enrichment of the signal-generating detection complex (i.e., immunocomplex formed between the antibody functionalized onto the magnetic particles and the antigen to be detected). For example, the detection of recombinant hepatitis B surface antigen (HBsAg) in human

dx.doi.org/10.1021/cr300068p | *Chem. Rev.* 2012, 112, 5818–5878

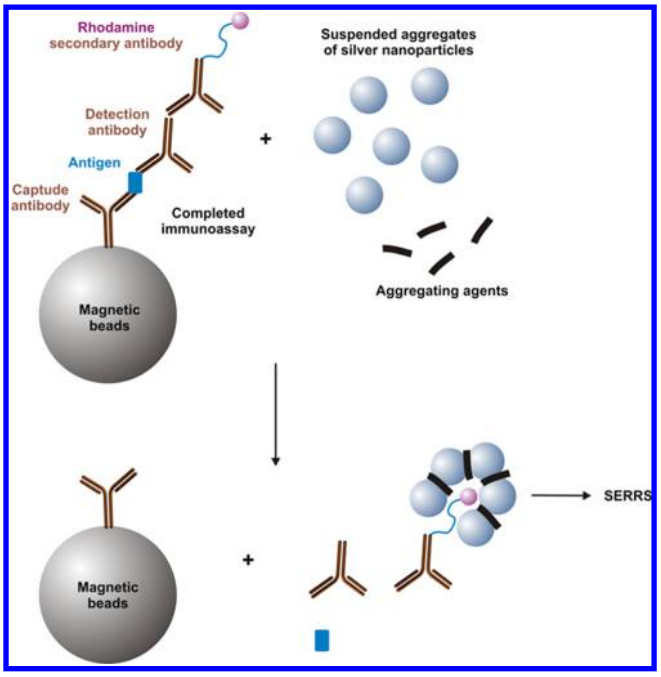

Figure 40. Schematic showing the assay complex dissociating from the surface of the beads upon addition of aggregating agents.[698] SERRS is then obtained from the aggregated colloid.

serum samples has been carried out by using M-IPCR with a detection limit of 320 pg/mL of HBsAg, which was ~100-fold more sensitive than the corresponding magneto-ELISA.

10.5. Separation of Heavy Metal Contaminants from Mixtures

Magnetic field-based separations using magnetic particles have received considerable attention for the separation/elimination of metallic impurities. These separation methods enable fast, cost-effective, and easy magnetic removal of these substances from complex heterogeneous reaction mixtures, both on small and pilot-plant scale.[159,701−707] In addition, this methodology can be automatized and miniaturized, and no dilution of the sample or loss of the magnetic carrier occurs during this purification procedure. For example, γ-Fe_2O_3 NPs surface-coated with poly(L-cysteine) as an ion-exchange system for binding to soft metal acids (e.g., Cd^{2+}, Pb^{2+}, etc.), and Fe_3O_4 NPs surface-coated with poly(acrylic acid) that binds to cations, have been used as selective heavy metal chelators.[708,709] When surface-functionalized with DMSA, these IONPs were found to be an effective sorbent material for toxic metals such as Hg, Ag, Pb, Cd, and Ti, which effectively bind to the DMSA ligands in addition to the iron oxide lattices (Figure 41). The NPs loaded with the adsorbed metals could be easily separated by a magnetic field.[710]

11. CONCLUSIONS

The possibility of tailoring the physicochemical properties of MNPs to fit with the desired applications in the pharmaceutical and biomedical fields has opened up new avenues. For in vivo applications such as disease therapy, MRI, imaging of transplanted cells, or tissue reconstruction, the safety and biocompatibility of those magnetically responsive nanodevices are of crucial importance. As discussed in this review, toxicity of MNPs is multifactorial and depends upon their composition, physicochemical properties such as size and surface characteristics, route of administration, and dose. Also the benefit-to-risk ratio has to be balanced according to the intended medical or pharmaceutical application. Thus, from a regulatory standpoint, NPs safety has to be evaluated case-by-case.

MNPs possessing optimal physicochemical properties, eventually encapsulated into polymeric, lipidic, or inorganic shells and surface-coated with nonbiofouling materials (e.g., PEG), have been successfully exploited as carriers for the smart delivery of therapeutic substances into the body as well as for imaging. As discussed, the ability of the injected drug-loaded MNPs to respond to an external magnetic stimulus has facilitated their guidance to the intended diseased cells and tissues, where they can deliver their drug cargo in a specific and controlled manner. As a result, MNPs have been investigated for chemotherapy, immunotherapy, and gene therapy, at preclinic stage but also in patients. The heat-rising property

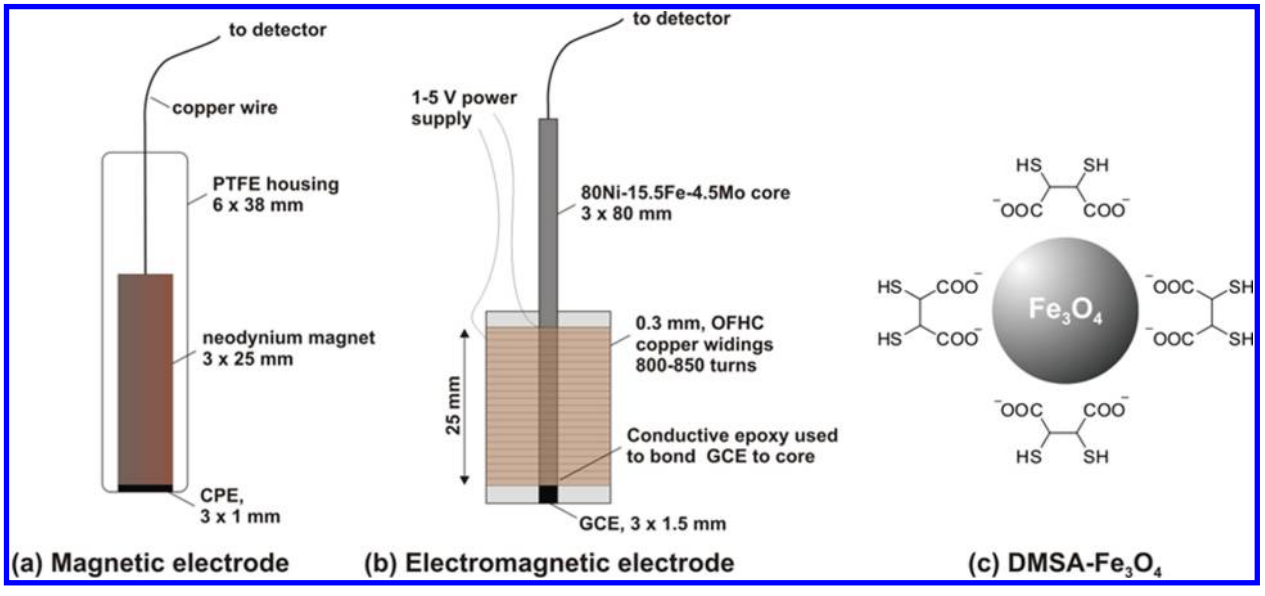

Figure 41. Representation of magnetic electrode (a) and electromagnetic electrode that preconcentrates metal ions (b) using DMSA−Fe_3O_4 NPs (c).[710]

dx.doi.org/10.1021/cr300068p | Chem. Rev. 2012, 112, 5818−5878

of these magnetic nanodevices upon exposure to an AMF has been used for hyperthermia and thermal ablation applications in clinical situations, especially for the treatment of neoplasic diseases. Of course, these approaches are generally limited to accessible tumor nodules (and not to metastasis or disseminated tumors), but they are of great benefit for nonsurgically removable neoplasia (i.e., brain cancers or hemorrhagic tumors). Therefore, the functionalization of the MNPs with homing devices has further improved drug addressage in the direction of disseminated diseases because of the specificity toward the target cells overexpressing unique surface receptors. Finally, the magnetic responsiveness of iron oxide nanocarriers coupled to their T_2 imaging properties make them a potential candidate for theranostic applications, as recently demonstrated by our group.

Although promising from a conceptual point of view, the use of MNPs for drug-delivery applications is, however, hampered by the complexity involved in the setup of external magnetic fields, which need adequate focusing and deep penetration into the tissues in order to reach the diseased area with sufficient strength. Intensive research to identify the best magnetic and irradiation technologies is therefore urgently needed. In addition, the emitters of such magnetic fields may be potentially expensive and, hence, is a major challenge for daily clinical practice. On the contrary, the use of MNPs for MRI is easier. It has improved the diagnosis of various diseases, especially for liver cancers (primary or metastasis) and for the visualization of sentinel lymph node invasion. It is noteworthy that some medicines are already on the market with diagnostics as the main indication.

Transplantation of cells or tissues as well as tissue engineering are other biomedical applications of MNPs allowing one to use imaging to follow the survival (or rejection) of the cell/tissue grafts and also taking advantage of a magnetic field to improve tissue construction. Although much progress has been made, there is still a long way to go for addressing numerous challenges to substantiate the application of MNPs in pharmacy and clinical medicine and to ensure the smooth transition of these concepts from bench to the bedside.

AUTHOR INFORMATION

Corresponding Author

*Phone: (+33) 1 46 83 53 96. Fax: (+33) 1 46 61 93 34. E-mail: patrick.couvreur@u-psud.fr.

Notes

The authors declare no competing financial interest.

Biographies

Dr. L. Harivardhan Reddy received his Master's degree in 1998 in Pharmaceutical Technology from Rajiv Gandhi University of Health Sciences, Bangalore, India. He obtained the Ph.D. in nanotechnology for drug delivery from The M. S. University of Baroda, India. He did 2 postdocs in the Université Paris-Sud XI and Centre Nationale de la Recherche Scientifique (CNRS) with the drug delivery expert Prof. Patrick Couvreur in France. Currently, he is the Head of Drug Delivery Technologies & Innovation-Nanotechnologies, in Pharmaceutical Sciences Department at Sanofi Research & Development, France. He is a coinventor of 5 patents, and especially of the lipid–drug conjugate nanotechnology discovered at Université Paris-Sud/CNRS, which received the most prestigious French award "Prix Galien" presented by Education Ministry of France in 2009. He has delivered various invited lectures on nanomedicine, including the one in most prestigious National Academy of Engineering U.S.A. and European Academies of Engineering conference in 2010 at Cambridge, U.K. He has co-edited a book entitled *Macromolecular Anticancer Therapeutics*, in 2009 published by Springer Science-Humana Press, U.S.A., and has published, as an author and co-author, more than 50 publications in various reputed international journals with high impact factors. He is also an editorial board member for a couple of international drug delivery/clinical journals. He is a member of The European Association for Cancer Research (EACR) and a board member of Groupe Thematique Recherche de la Vectorisation (GTRV), a French drug delivery and vectorization society. His principal research interests focus on nanotechnologies for health and diagnosis, drug delivery, and development to clinic.

Dr. José L. Arias received his Ph.D. in Pharmaceutical Technology from the University of Granada in 2003. He is currently a professor of Pharmaceutical Technology, Drug Delivery, as well as Biopharmacy and Pharmacokinetics, at the Department of Pharmacy and Pharmaceutical Technology in the University of Granada, Spain. He has also worked during the years 2007 and 2008 as Associate Researcher of UMR CNRS 8612 "Physico-chimie, Pharmacotechnie et Biopharmacie" under the direction of Prof. Patrick Couvreur at the Université Paris-Sud, France. He is the co-inventor of 3 patents and has published 44 peer-reviewed research articles in international journals and 15 book chapters. His research group is actively involved in the development of colloidal drug delivery systems against severe diseases (cancer, autoimmune diseases, infectious diseases, etc.). His area of specialization includes a focus on the formulation of advanced drug nanocarriers on the basis of passive and active targeting strategies (mainly, magnetic-sensitive nanoplatforms). More recently, he has commenced work on engineering strategies for the preparation of theranostic nanoparticles.

Dr. Julien Nicolas graduated from the Ecole Supérieure de Chimie Organique et Minérale (ESCOM), France, in 2001. He completed his Ph.D. in 2005 under the supervision of Prof. Bernadette Charleux at the University Pierre and Marie Curie, Paris, where he studied nitroxide-mediated polymerization in homogeneous and aqueous dispersed media. He then joined the group of Prof. David M. Haddleton at the University of Warwick, U.K., for a postdoctoral fellowship to design polymer–protein bioconjugates by controlled/living radical polymerization. In 2007, he was appointed permanent CNRS researcher in the group of Prof. Patrick Couvreur, University Paris-Sud, France, where his current research activities are focused on the synthesis of novel biomaterials and functionalized, biodegradable nanoparticles for active targeting and cell imaging purposes. He is the co-author of 50 peer-reviewed articles in international journals, 4 patents, and 7 book chapters.

Prof. Patrick Couvreur is Full Professor of Pharmacy at the Paris-Sud University and holder of the chair of "Innovation Technologique" (2009–2010) at the prestigious Collège de France. He is appointed as a Senior Member of the Institut Universitaire de France. He is the recipient of an "ERC Advanced Grant" (2009). Prof. Couvreur's contributions in the field of drug delivery and targeting are highly recognized around the world with more than 450 peer-reviewed research publications. His research is interdisciplinary, at the interface between Physico-Chemistry of Colloids, Polymer Chemistry, Material Science, and Pharmacology. Prof. Couvreur's research has led to the funding of two start-up companies (Bioalliance and Medsqual). The major scientific contribution of Patrick Couvreur to the Pharmaceutical Sciences is also recognized by numerous international awards, including the "2004 Pharmaceutical Sciences World Congress Award" (Kyoto, Japon), the prestigious "Host Madsen Medal" (Beijin, 2007), and very recently the "European Pharmaceutical Scientist Award" (European Federation of Pharmaceutical Sciences). In 2009, he was also awarded by the "Prix Galien", the highest French distinction in therapeutics. His appointment as a member of four academies (Académie des Technologies, Académie de Médecine, Académie de Pharmacie in France, and Académie Royale de Médecine in Belgium) is another recognition of the major scientific and scholarly contributions of Prof. Couvreur.

ACKNOWLEDGMENTS

Some results described in this review were obtained thanks to the ERC Advanced Grant TERNANOMED (European Research Council under the European Community's Seventh Framework Programme FP7/2007-2013; grant agreement no. 249835), and project FIS 11/02571 (Instituto de Salud Carlos III, Spain).

ABBREVIATIONS

ABC	accelerated blood clearance
ADXD	angular dispersive X-ray diffraction
AFM	atomic force microscopy
AI-2	autoinducer-2
AMF	alternating magnetic field
AMNPs	anionic γ-Fe_2O_3 nanoparticles
AODN	antisense oligodeoxynucleotides
ASPIONs	amino-functionalized SPIONs
α-Fe_2O_3	hemeatite
B	magnetic induction
BA	*n*-butyl acrylate
BBB	blood–brain barrier
β-FeOOH	akaganeite
BMs	bacterial magnetosomes
CD	β-cyclodextrin
CFM	chemical force microscopy
Cis	cisplatin
CLIO	cross-linked iron oxide
CNS	central nervous system
CT	computed tomography
dextran-*g*-P(NIPAAm-*co*-DMAAm)	dextran-*g*-poly(*N*-isopropylacrylamide-*co*-*N*,*N*-dimethylacrylamide)
DLPC	dilauroylphosphatidylcholine
DLS	dynamic light scattering
DMSA	dimercaptosuccinic acid
DOPE	1,2-dioleoyl-3-*sn*-phosphatidyl ethanolamine
DOTAP	1,2-dioleoyl-3-trimethylammonium propane
Dox	doxorubicin
Dox@TCL-SPIONs	doxorubicin-loaded thermally cross-linked superparamagnetic iron oxide nanoparticles
Dox-BMs	doxorubicin-loaded BMs
DSC	differential scanning calorimetry

dx.doi.org/10.1021/cr300068p | *Chem. Rev.* 2012, 112, 5818–5878

DSPE-PEG_{2000}	phospholipid-PEG derivative distearoyl phosphatidyl ethanolamine
*ds*RNA	double-stranded RNA
DTT	1,4-dithiothreitol
e-beam	electron beam
EBRT	external beam radiation therapy
EDXD	energy-dispersive X-ray diffraction
EPR	enhanced permeability and retention
FA	folic acid
FA-CD-SPIONs	FA- and CD-decorated SPIONs
FDA	Food and Drug Administration
feGM-CSF	feline granulocyte-macrophage colony-stimulating factor
γ-Fe_2O_3	maghemite
Fe_3O_4	magnetite
FeSEM	field emission scanning electron microscopy
FF-TEM	freeze-fracture TEM
FITC	fluorescence isothiocyanate
FTIR	Fourier transform infrared spectroscopy
Gd^{3+}	gadolinium
Gd^{3+}−DTPA	Gd^{3+}−diethylenetriaminopentaacetic acid
Gem	gemcitabine
GFP	green fluorescent protein
H	magnetic field
HAECs	human aortic endothelial cells
HBsAg	hepatitis B surface antigen
HBV	hepatitis B viral
HCV	hepatitis C viral
HES	human embryonic stem
HFMF	high-frequency magnetic field
HPPH	2-[1-hexyloxyethyl]-2-devinyl pyropheophorbide-a
*hr*GFP	humanized recombinant GFP
HRTEM	high-resolution transmission electron microscopy
HSPs	heat shock proteins
IC_{50}	half-maximal inhibitory concentration
IONPs	iron oxide nanoparticles
Ir	iridium
i.v	intravenous
K	drug's partitioning coefficient
LCST	lower critical solution temperature
LD_{50}	median lethal dose
LLC	Lewis lung carcinoma
LuxS	*S*-ribosylhomocysteinase
MAb's	monoclonal antibodies
Mag-TE	magnetic force-based tissue engineering
MCLs	magnetic cationic liposomes
MePEGMA	methoxyPEG methacrylate
MFe_2O_4	spinel metal ferrites
MFH	magnetic fluid hyperthermia
M-IPCR	magneto-immuno polymerase chain reaction
MMA	methyl methacrylate
MNPs	magnetic nanoparticles
MRI	magnetic resonance imaging
Nd−Fe	neodymium−iron
Nd−Fe−B	neodymium iron boron
NGF	nerve growth factor
NPs	nanoparticles
OA	oleic acid
PACA	poly(alkyl cyanoacrylate)
PBS	phosphate-buffered saline
PCL	poly(ε-caprolactone)
PCS	photon correlation spectroscopy
PEG	poly(ethylene glycol)
PEI	poly(ethylene imine)
Pfs	*S*-adenosylhomocysteine nucleosidase
PGA	poly(glycolide)
PHPP	2,7,12,18-tetramethyl-3,8-di-(1-propoxyethyl)-13,17-bis-(3-hydroxypropyl) porphyrin
p.i.	peritoneal injection
PLA	poly(D,L-lactide)
PLGA	poly(D,L-lactide-*co*-glycolide)
PMMA	polymethylmethacrylate
PNIPAAm	poly(*N*-isopropylacrylamide)
poly(TMSMA-*co*-PEGMA)	poly(3-(trimethoxysilyl)-propyl methacrylate-*co*-poly(ethylene glycol)-methacrylate)
Ptx	paclitaxel
PS	polystyrene
PVA	poly(vinyl alcohol)
PVB	poly(vinyl butyral)
PVP	polyvinylpyrrolidone
QELS	quasi-elastic light scattering
RES	reticuloendothelial system
RFA	radiofrequency ablation
RGD	arginine-glycine-aspartate sequence
RGD-MCLs	MCLs surface-functionalized with the RGD sequence
ROS	reactive oxygen species
RT	room temperature
rt-PA	recombinant tissue plasminogen activator

dx.doi.org/10.1021/cr300068p | *Chem. Rev.* 2012, 112, 5818−5878

Ru(bpy)	tris(2,2′-bipyridine) ruthenium
SAH	*S*-adenosylhomocysteine
SANS	small-angle neutron scattering
SAXS	small-angle X-ray scattering
SCF	supercritical fluid
SEM	scanning electron microscopy
SERRS	surface-enhanced resonance Raman spectroscopy
SERS	surface-enhanced Raman spectroscopy
SiO_2	silica
*si*RNA	small interfering ribonucleic acids
SPDP	*N*-succinimidyl 3-(2-pyridyldithio)propionate
SPIONs	superparamagnetic iron oxide nanoparticles
SQcis	squalenoyl cisplatin
SQdFdC (or SQgem)	squalenoyl gemcitabine
SQdox	squalenoyl doxorubicin
$SQGd^{3+}$	squalenoyl gadolinium
SQptx	squalenoyl paclitaxel
SRH	*S*-ribosyl homocysteine
SSIMS	statistic secondary ion mass spectra
T	Tesla
T	transverse relaxation
TAT	transactivator of transcription
TEM	transmission electron microscope
TGA	thermogravimetric analysis
TMX	tamoxifen
TSPP	*meso*-tetra(4-sulfonatophenyl) porphyrin dihydrochloride
u_e	electrophoretic mobility
ζ	zeta potential
ΔG_{SLS}	surface free energy change (per unit area) quantity
8-QMA	8-quinolinyl methacrylate

REFERENCES

(1) Laurent, S.; Forge, D.; Port, M.; Roch, A.; Robic, C.; Elst, L. V.; Muller, R. N. *Chem. Rev.* **2008**, *108*, 2064.
(2) Sun, C.; Lee, J. S. H.; Zhang, M. *Adv. Drug Delivery Rev.* **2008**, *60*, 1252.
(3) Shubayev, V. I.; Pisanic, T. R., II; Jin, S. *Adv. Drug Delivery Rev.* **2009**, *61*, 467.
(4) Gupta, A. K.; Gupta, M. *Biomaterials* **2005**, *26*, 3995.
(5) Durán, J. D. G.; Arias, J. L.; Gallardo, V.; Delgado, A. V. *J. Pharm. Sci.* **2008**, *97*, 2948.
(6) King, J. G.; Williams, W.; Wilkinson, C. D. W.; McVitie, S.; Chapman, J. N. *Geophys. Res. Lett.* **1996**, *23*, 2847.
(7) Rishton, A.; Lu, Y.; Altman, R. A.; Marley, A. C.; Bian Hahnes, C.; Viswanathan, R.; Xiao, G.; Gallagher, W. J.; Parkin, S. S. P. *Microelectron. Eng.* **1997**, *35*, 249.
(8) Lee, C. S.; Lee, H.; Westervelt, R. M. *Appl. Phys. Lett.* **2001**, *79*, 3308.
(9) Mathur, S.; Barth, S.; Werner, U.; Hernandez-Ramirez, F.; Romano-Rodriguez, A. *Adv. Mater.* **2008**, *20*, 1550.
(10) da Costa, G. M.; de Grave, E.; de Bakker, P. M. A.; Vandenberghe, R. E. *J. Solid State Chem.* **1994**, *113*, 405.
(11) Itoh, H.; Sugimoto, T. *J. Colloid Interface Sci.* **2003**, *265*, 283.
(12) Amemiya, Y.; Arakaki, A.; Staniland, S. S.; Tanaka, T.; Matsunaga, T. *Biomaterials* **2007**, *28*, 5381.
(13) Vereda, F.; Rodríguez-González, B.; de Vicente, J.; Hidalgo-Álvarez, R. *J. Colloid Interface Sci.* **2008**, *318*, 520.
(14) Massart, R. *IEEE Trans. Magn.* **1981**, *17*, 1247.
(15) Wu, J. H.; Ko, S. P.; Liu, H. L.; Kim, S.; Ju, J. S.; Kim, Y. K. *Mater. Lett.* **2007**, *61*, 3124.
(16) Khollam, Y. B.; Dhage, S. R.; Potdar, H. S.; Deshpande, S. B.; Bakare, P. P.; Kulkarni, S. D.; Date, S. K. *Mater. Lett.* **2002**, *56*, 571.
(17) Chen, F.; Gao, Q.; Hong, G.; Ni, J. *J. Magn. Magn. Mater.* **2008**, *320*, 1775.
(18) Salazar-Alvarez, G.; Muhammed, M.; Zagorodni, A. A. *Chem. Eng. Sci.* **2006**, *61*, 4625.
(19) Cabrera, L.; Gutierrez, S.; Menendes, N.; Morales, M. P.; Herrasti, P. *Electrochem. Acta* **2008**, *53*, 3436.
(20) Marques, R. F. C.; Garcia, C.; Lecante, P.; Ribeiro, J. L.; Noé, L.; Silva, N. J. O.; Amaral, V. S.; Millan, A.; Verelst, M. *J. Magn. Magn. Mater.* **2008**, *320*, 2311.
(21) González-Carreño, T.; Morales, M. P.; Gracia, M.; Serna, C. J. *Mater. Lett.* **1993**, *18*, 151.
(22) Strobel, R.; Pratsinis, S. E. *Adv. Powder Technol.* **2009**, *20*, 190.
(23) Enomoto, N.; Akagi, J.; Nakagawa, Z. *Ultrason. Sonochem.* **1996**, *3*, S97.
(24) Dang, F.; Enomoto, N.; Hojo, J.; Enpuku, K. *Ultrason. Sonochem.* **2009**, *16*, 649.
(25) Eckert, C. A.; Knutson, B. L.; Debenedetti, P. G. *Nature* **1996**, *383*, 313.
(26) Teng Lam, U.; Mammucari, R.; Suzuki, K.; Foster, N. R. *Ind. Eng. Chem. Res.* **2008**, *47*, 599.
(27) Breulmann, M.; Colfen, H.; Hentze, H. P.; Antonietti, M.; Walsh, D.; Mann, S. *Adv. Mater.* **1998**, *10*, 237.
(28) Bakar, M. A.; Tan, W. L.; Bakar, N. H. H. A. *J. Magn. Magn. Mater.* **2007**, *314*, 1.
(29) Narayanan, K. B.; Sakthivel, N. *Adv. Colloid Interface Sci.* **2010**, *156*, 1.
(30) Moon, J. W.; Roh, Y.; Lauf, R. J.; Vali, H.; Yeary, L. W.; Phelps, T. J. *J. Microbiol. Methods* **2007**, *70*, 150.
(31) Moon, J. W.; Rawn, C. J.; Rondinone, A. J.; Love, L. J.; Roh, Y.; Everett, S. M.; Lauf, R. J.; Phelps, T. J. *J. Ind. Microbiol. Biotechnol.* **2010**, *37*, 1023.
(32) Liu, X. M.; Yang, G.; Fu, S. Y. *Mater. Sci. Eng., C* **2007**, *27*, 750.
(33) Gunjakar, J. L.; More, A. M.; Shinde, V. R.; Lokhande, C. D. *J. Alloys Compd.* **2008**, *465*, 468.
(34) Naidek, K. P.; Bianconi, F.; da Rocha, T. C. R.; Zanchet, D.; Bonacin, J. A.; Novak, M. A.; Vaz, M. G. F.; Winnischofer, H. *J. Colloid Interface Sci.* **2011**, *358*, 39.
(35) Ketteler, G.; Weiss, W.; Ranke, W.; Schloegel, R. *Phys. Chem. Chem. Phys.* **2001**, *3*, 1114.
(36) Cannas, C.; Gatteschi, D.; Musinu, A.; Piccaluga, G.; Sangregorio, C. *J. Phys. Chem.* **1998**, *102*, 7721.
(37) Ennas, G.; Musinu, A.; Piccaluga, G.; Zedda, D.; Gatteschi, D.; Sangregorio, C.; Stanger, J. L.; Concas, G.; Spano, G. *Chem. Mater.* **1998**, *10*, 495.
(38) Byrappa, K.; Ohara, S.; Adschiri, T. *Adv. Drug Delivery Rev.* **2008**, *60*, 299.
(39) Feldmann, C.; Jungk, H. O. *Angew. Chem., Int. Ed.* **2001**, *40*, 359.
(40) Ding, J.; Tao, K.; Li, J.; Song, S.; Sun, K. *Colloids Surf., B* **2010**, *79*, 184.
(41) Cheng, C.; Xu, F.; Gu, H. *New J. Chem.* **2011**, *35*, 1072.
(42) Toneguzzo, P.; Viau, G.; Acher, O.; Fiévet-Vincent, F.; Fiévet, F. *Adv. Mater.* **1998**, *10*, 1032.

(43) Viau, G.; Fiévet-Vincent, F.; Fiévet, F. *J. Mater. Chem.* **1996**, *6*, 1047.
(44) Sugimoto, T.; Matijević, E. *J. Colloid Interface Sci.* **1980**, *74*, 227.
(45) Arias, J. L.; Gallardo, V.; Gómez-Lopera, S. A.; Plaza, R. C.; Delgado, A. V. *J. Controlled Release* **2001**, *77*, 309.
(46) Plaza, R. C.; Arias, J. L.; Espín, M.; Jiménez, M. L.; Delgado, A. V. *J. Colloid Interface Sci.* **2002**, *245*, 86.
(47) Bee, A.; Massart, R. *J. Magn. Magn. Mater.* **1995**, *149*, 6.
(48) López-López, M. T.; Durán, J. D. G.; Delgado, A. V.; González-Caballero, F. *J. Colloid Interface Sci.* **2005**, *291*, 144.
(49) Viota, J. L.; Durán, J. D. G.; González-Caballero, F.; Delgado, A. V. *J. Magn. Magn. Mater.* **2007**, *314*, 80.
(50) Ge, S.; Shi, X.; Sun, K.; Li, C.; Baker, J. R.; Banaszak Holl, M. M.; Orr, B. G. *J. Phys. Chem. C* **2009**, *113*, 13593.
(51) Piao, Y.; Kim, J.; Na, H. B.; Kim, D.; Baek, J. S.; Ko, M. K.; Lee, J. H.; Shokouhimehr, M.; Hyeon, T. *Nat. Mater.* **2008**, *7*, 242.
(52) Pascal, C.; Pascal, J. L.; Favier, F.; Moubtassim, M. L.; Elidrissi, P. C. *Chem. Mater.* **1999**, *11*, 141.
(53) Ocaña, M.; Rodríguez-Clemente, R.; Serna, C. J. *Adv. Mater.* **1995**, *7*, 212.
(54) Morales, M. P.; Veintemillas-Verdaguer, S.; Montero, M. I.; Serna, C. J. *Chem. Mater.* **1999**, *11*, 3058.
(55) Veintemillas-Verdaguer, S.; Leconte, Y.; Costo, R.; Bomati-Miguel, O.; Bouchet-Fabre, B.; Morales, M. P.; Bonville, P.; Pérez-Rial, S.; Rodriguez, I.; Herlin-Boime, N. *J. Magn. Magn. Mater.* **2007**, *311*, 120.
(56) Puntes, V. F.; Krisnan, K. M.; Alivisatos, A. P. *Science* **2001**, *291*, 2115.
(57) Sun, S.; Zeng, H. *J. Am. Chem. Soc.* **2002**, *124*, 8204.
(58) Sun, S. H.; Zeng, H.; Robinson, D. B.; Raoux, S.; Rice, P. M.; Wang, S. X.; Li, G. X. *J. Am. Chem. Soc.* **2004**, *126*, 273.
(59) Behrens, S.; Bönnemann, H.; Matoussevitch, N.; Gorschinski, A.; Dinjus, E.; Habicht, W.; Bolle, J.; Lee, J. H.; Huh, Y. M.; Jun, Y. W.; Seo, J. W.; Jang, J. T.; Song, H. T.; Kim, S.; Cho, E. J.; Yoon, H. G.; Suh, J. S.; Cheon, J. *Nat. Med.* **2007**, *13*, 95.
(60) Lee, J. H.; Huh, Y. M.; Jun, Y. W.; Seo, J. W.; Jang, J. T.; Song, H. T.; Kim, S.; Cho, E. J.; Yoon, H. G.; Suh, J. S.; Cheon, J. *Nat. Med.* **2007**, *13*, 95.
(61) Vijayakumar, R.; Koltypin, Y.; Felner, I.; Gedanken, A. *Mater. Sci. Eng., A* **2000**, *286*, 101.
(62) Xu, C. J.; Sun, S. H. *Polym. Int.* **2007**, *56*, 821.
(63) Cote, L. J.; Teja, A. S.; Wilkinson, A. P.; Zhang, Z. J. *J. Mater. Res.* **2002**, *17*, 2410.
(64) Chattopadhyay, P.; Gupta, R. B. *Ind. Eng. Chem. Res.* **2002**, *41*, 6049.
(65) Hao, Y.; Teja, A. S. *J. Mater. Res.* **2003**, *18*, 415.
(66) Santra, S.; Tapec, R.; Theodoropoulou, N.; Dobson, J.; Hebard, A.; Tan, W. *Langmuir* **2001**, *17*, 2900.
(67) Hou, Y.; Kondoh, H.; Shimojo, M.; Sako, E. O.; Ozaki, N.; Kogure, T. J.; Ohta, T. *J. Phys. Chem. B* **2005**, *109*, 4845.
(68) Strable, E.; Bulte, J. W. M.; Moskowitz, B.; Vivekanandan, K.; Allen, M.; Douglas, T. *Chem. Mater.* **2001**, *13*, 2201.
(69) Sangregorio, C.; Wiemann, J. K.; O'Connor, C. J.; Rosenzweig, Z. *J. Appl. Phys.* **1999**, *85*, 5699.
(70) Uchida, M.; Flenniken, M. L.; Allen, M.; Willits, D. A.; Crowley, B. E.; Brumfield, S.; Willis, A. F.; Jackiw, L.; Jutila, M.; Young, M. J.; Douglas, T. *J. Am. Chem. Soc.* **2006**, *128*, 16626.
(71) Rivas, J.; Sánchez, R. D.; Fondado, A.; Izco, C.; García-Bastida, A. J.; García-Otero, J.; Mira, J.; Baldomir, D.; González, A.; Lado, I.; López-Quintela, M. A.; Oseroff, S. B. *J. Appl. Phys.* **1994**, *76*, 6564.
(72) López-Pérez, J. A.; López-Quintanela, M. A.; Mira, J.; Rivas, J. *IEEE Trans. Magn.* **1997**, *33*, 4359.
(73) Carpenter, E. E. *J. Magn. Magn. Mater.* **2001**, *225*, 17.
(74) Lee, S. W.; Bae, S.; Takemura, Y.; Shim, I. B.; Kim, T. M.; Kim, J.; Lee, H. J.; Zurn, S.; Kim, C. S. *J. Magn. Magn. Mater.* **2007**, *310*, 2868.
(75) Choi, J. S.; Jun, Y. W.; Yeon, S. I.; Kim, H. C.; Shin, J. S.; Cheon, J. *J. Am. Chem. Soc.* **2006**, *128*, 15982.
(76) Kim, S.; Shibata, E.; Sergiienko, R.; Nakamura, T. *Carbon* **2008**, *46*, 1523.
(77) Cao, H.; Huang, G.; Xuan, S.; Wu, Q.; Gu, F.; Li, C. *J. Alloys Compd.* **2008**, *448*, 272.
(78) Gupta, A. K.; Curtis, A. S. G. *J. Mater. Sci. Mater. Med.* **2004**, *15*, 493.
(79) Ma, D. L.; Guan, J. W.; Normandin, F.; Denommee, S.; Enright, G.; Veres, T.; Simard, B. *Chem. Mater.* **2006**, *18*, 1920.
(80) Chen, S.; Li, Y.; Guo, C.; Wang, J.; Ma, J.; Liang, X.; Yang, L. R.; Liu, H. Z. *Langmuir* **2007**, *23*, 12669.
(81) de Cuyper, M.; Soenen, S. J. H.; Coenegrachts, K.; Beek, L. T. *Anal. Biochem.* **2007**, *367*, 266.
(82) Liu, H.; Guo, J.; Jin, L.; Yang, W.; Wang, C. *J. Phys. Chem. B* **2008**, *112*, 3315.
(83) Bulte, J. W.; Hoekstra, Y.; Kamman, R. L.; Magin, R. L.; Webb, A. G.; Briggs, R. W.; Go, K. G.; Hulstaert, C. E.; Miltenyi, S.; The, T. H.; Leij, L. D. *Magn. Reson. Med.* **1992**, *25*, 148.
(84) Berry, C. C.; Wells, S.; Charles, S.; Curtis, A. S. G. *Biomaterials* **2003**, *24*, 4551.
(85) Briley-Saebo, K. C.; Johansson, L. O.; Hustvedt, S. O.; Haldorsen, A. G.; Bjørnerud, A.; Fayad, Z. A.; Ahlstrom, H. K. *Invest. Radiol.* **2006**, *41*, 560.
(86) Liu, T. Y.; Hu, S. H.; Liu, K. H.; Liu, D. M.; Chen, S. Y. *J. Controlled Release* **2008**, *126*, 228.
(87) Butterworth, M. D.; Illum, L.; Davis, S. S. *Colloids Surf. A Physicochem. Eng. Aspects.* **2001**, *179*, 93.
(88) Lutz, J. F.; Stiller, S.; Hoth, A.; Kaufner, L.; Pison, U.; Cartier, R. *Biomacromolecules* **2006**, *7*, 3132.
(89) Jeong, J.; Ha, T. H.; Chung, B. H. *Anal. Chim. Acta* **2006**, *569*, 203.
(90) Seo, W. S.; Lee, J. H.; Sun, X.; Suzuki, Y.; Mann, D.; Liu, Z.; Terashima, M.; Yang, P. C.; McConnell, M. V.; Nishimura, D. G.; Dai, H. *Nat. Mater.* **2006**, *5*, 971.
(91) Chastellain, M.; Petri, A.; Gupta, A.; Rao, K. V.; Hofmann, H. *Adv. Eng. Mater.* **2004**, *6*, 235.
(92) Arias, J. L.; Gallardo, V.; Linares-Molinero, F.; Delgado, A. V. *J. Colloid Interface Sci.* **2006**, *299*, 599.
(93) Arias, J. L.; López-Viota, M.; Sáez-Fernández, E.; Ruiz, M. A.; Delgado, A. V. *Colloids Surf., A* **2011**, *384*, 157.
(94) Lecommandoux, S.; Sandre, O.; Chécot, F.; Perzynski, R. *Prog. Solid State Chem.* **2006**, *34*, 171.
(95) Kuznetsov, A. A.; Filippov, V. I.; Alyautdin, R. N.; Torshina, N. L.; Kuznetsov, O. A. *J. Magn. Magn. Mater.* **2001**, *225*, 95.
(96) Peira, E.; Marzola, P.; Podio, V.; Aime, S.; Sbarbati, A.; Gasco, M. R. *J. Drug Target.* **2003**, *11*, 19.
(97) Gonzales, M.; Krishnan, K. M. *J. Magn. Magn. Mater.* **2005**, *293*, 265.
(98) Lang, C.; Schüler, D. *J. Phys.: Condens. Matter* **2006**, *18*, S2815.
(99) Hsu, M. H.; Su, Y. C. *Biomed. Microdevices* **2008**, *10*, 785.
(100) Weissleder, R.; Bogdanov, A.; Neuwelt, E. A.; Papisov, M. *Adv. Drug Delivery Rev.* **1995**, *16*, 321.
(101) Barratt, G. *Cell. Mol. Life Sci.* **2003**, *60*, 21.
(102) Kim, D. K.; Mikhaylova, M.; Zhang, Y.; Muhammed, M. *Chem. Mater.* **2003**, *15*, 1617.
(103) Portet, D.; Denizot, B.; Rump, E.; Rump, E.; Lejeune, J. J.; Jallet, P. *J. Colloid Interface Sci.* **2001**, *238*, 37.
(104) Kreller, D. I.; Gibson, G.; Novak, W.; van Loon, G. W.; Horton, J. H. *Colloids Surf., A* **2003**, *212*, 249.
(105) Sahoo, Y.; Pizem, H.; Fried, T.; Golodnitsky, D.; Burstein, L.; Sukenik, C. N.; Markovich, G. *Langmuir* **2001**, *17*, 7907.
(106) Kim, E. H.; Lee, H. S.; Kwak, B. K.; Kim, B. K. *J. Magn. Magn. Mater.* **2005**, *289*, 328.
(107) Woo, K.; Hong, J.; Ahn, J. P. *J. Magn. Magn. Mater.* **2005**, *293*, 177.
(108) Selim, K. M. K.; Ha, Y. S.; Kim, S. J.; Chang, Y.; Kim, T. J.; Lee, G. H.; Kang, I. K. *Biomaterials* **2007**, *28*, 710.
(109) Hodenius, M.; De Cuyper, M.; Desender, L.; Muller-Schulte, D.; Steigel, A.; Lueken, H. *Chem. Phys. Lipids* **2002**, *120*, 75.

(110) Roberts, D.; Zhu, W. L.; Fromenn, C. M.; Rosenzweig, Z. *J. Appl. Phys.* **2000**, *87*, 6208.
(111) Bautista, M. C.; Bomati-Miguel, O.; Morales, M. D.; Serna, C. J.; Veintemillas-Verdaguer, S. *J. Magn. Magn. Mater.* **2005**, *293*, 20.
(112) Morales, M. A.; Fitonelli, P. V.; Coaquira, J. A. H.; Rocha-Leão, M. H. M.; Diaz-Aguila, C.; Baggio-Saitovitch, E. M.; Rossi, A. M. *Mater. Sci. Eng., C* **2008**, *28*, 253.
(113) Jia, Z.; Yujun, W.; Yangcheng, L.; Jingyu, M.; Guangsheng, L. *React. Funct. Polym.* **2006**, *66*, 1552.
(114) Shinkai, M. S.; Suzuki, M.; Iijima, S.; Kobayashi, T. *Biotechnol. Appl. Biochem.* **1994**, *21*, 125.
(115) Huth, S.; Lausier, J.; Gersting, S. W.; Rudolph, C.; Plank, C.; Welsch, U.; Rosenecker, J. *J. Gene Med.* **2004**, *6*, 923.
(116) Fauconnier, N.; Pons, J. N.; Roger, J.; Bee, A. *J. Colloid Interface Sci.* **1997**, *194*, 427.
(117) Mornet, S.; Vasseur, S.; Grasset, F.; Veverka, P.; Goglio, G.; Demourgues, A.; Portier, J.; Pollert, E.; Duguet, E. *Prog. Solid State Chem.* **2006**, *34*, 237.
(118) Zhang, C.; Wangler, B.; Morgenstern, B.; Zentgraf, H.; Eisenhut, M.; Untenecker, H.; Kruger, R.; Huss, R.; Seliger, C.; Semmler, W.; Kiessling, F. *Langmuir* **2007**, *23*, 1427.
(119) Bazile, D.; Prud'homme, C.; Bassoullet, M. T.; Marlard, M.; Spenlehauer, G.; Veillard, M. *J. Pharm. Sci.* **1995**, *84*, 493.
(120) Gupta, A. K.; Curtis, A. S. G. *Biomaterials* **2004**, *25*, 3029.
(121) Guowei, D.; Adriane, K.; Chen, X. Z.; Jie, C.; Yinfeng, L. *Int. J. Pharm.* **2007**, *328*, 78.
(122) Kievit, F. M.; Veiseh, O.; Bhattarai, N.; Fang, C.; Gunn, J. W.; Lee, D.; Ellenbogen, R. G.; Olson, J. M.; Zhang, M. *Adv. Funct. Mater.* **2009**, *19*, 2244.
(123) Zhang, M.; Ferrari, M. *J. Biomed. Microdev.* **1998**, *1*, 81.
(124) Gref, R.; Luck, M.; Quellec, P.; Marchand, M.; Dellacherie, E.; Harnisch, S.; Blunk, T.; Müller, R. H. *Colloids Surf., B* **2000**, *18*, 301.
(125) Shang, H.; Chang, W. S.; Kan, S.; Majetich, S. A.; Lee, G. U. *Langmuir* **2006**, *22*, 2516.
(126) Flesch, C.; Unterfinger, Y.; Bourgeat-Lami, E.; Duguet, E.; Delaite, C.; Dumas, P. *Macromol. Rapid Commun.* **2005**, *26*, 1494.
(127) Gupta, A. K.; Naregalkar, R. R.; Vaidya, V. D.; Gupta, M. *Nanomedicine (London)* **2007**, *2*, 23.
(128) Larsen, E. K.; Nielsen, T.; Wittenborn, T.; Birkedal, H.; Vorup-Jensen, T.; Jakobsen, M. H.; Ostergaard, L.; Horsman, M. R.; Besenbacher, F.; Howard, K. A.; Kjems, J. *ACS Nano* **2009**, *3*, 1947.
(129) Pilloni, M.; Nicolas, J.; Marsaud, V.; Bouchemal, K.; Frongia, F.; Scano, A.; Ennas, G.; Dubernet, C. *Int. J. Pharm.* **2010**, *401*, 103.
(130) Zhang, Y.; Kohler, N.; Zhang, M. Q. *Biomaterials* **2002**, *23*, 1553.
(131) Zhang, Y.; Sun, C.; Kohler, N.; Zhang, M. Q. *Biomed. Microdev.* **2004**, *6*, 33.
(132) Kohler, N.; Fryxell, G. E.; Zhang, M. Q. *J. Am. Chem. Soc.* **2004**, *126*, 7206.
(133) Veiseh, O.; Sun, C.; Gunn, J.; Kohler, N.; Gabikian, P.; Lee, D.; Bhattarai, N.; Ellenbogen, R.; Sze, R.; Hallahan, A.; Olson, J.; Zhang, M. Q. *Nano Lett.* **2005**, *5*, 1003.
(134) Lee, H.; Lee, E.; Kim, D. K.; Jang, N. K.; Jeong, Y. Y.; Jon, S. *J. Am. Chem. Soc.* **2006**, *128*, 7383.
(135) Shen, T.; Weissleder, R.; Papisov, M.; Bogdanov, A., Jr.; Brady, T. J. *Magn. Reson. Med.* **1993**, *29*, 599.
(136) Josephson, L.; Tung, C. H.; Moore, A.; Weissleder, R. *Bioconjugate Chem.* **1999**, *10*, 186.
(137) Corot, C.; Robert, P.; Idee, J. M.; Port, M. *Adv. Drug Delivery Rev.* **2006**, *58*, 1471.
(138) Schellenberger, E. A.; Bogdanov, A., Jr.; Hogemann, D.; Tait, J.; Weissleder, R.; Josephson, L. *Mol. Imaging* **2002**, *1*, 102.
(139) Wunderbaldinger, P.; Josephson, L.; Weissleder, R. *Bioconjugate Chem.* **2002**, *13*, 264.
(140) Bain, C. D.; Toughton, E. B.; Tao, Y. T.; Evall, J.; Whitesides, G. M.; Nuzzo, R. G. *J. Am. Chem. Soc.* **1989**, *111*, 321.
(141) Prime, K. L.; Whitesides, G. M. *Science* **1991**, *252*, 1164.
(142) Yu, H.; Chen, M.; Rice, P. M.; Wang, S. X.; White, R. L.; Sun, S. *Nano Lett.* **2005**, *5*, 379.
(143) Lu, A. H.; Salabas, E. L.; Schuth, F. *Angew. Chem., Int. Ed.* **2007**, *46*, 1222.
(144) Lu, Y.; Yin, Y. D.; Mayers, B. T.; Xia, Y. N. *Nano Lett.* **2002**, *2*, 183.
(145) Tan, W. H.; Wang, K. M.; He, X. X.; Zhao, X. J.; Drake, T.; Wang, L.; Bagwe, R. P. *Med. Res. Rev.* **2004**, *24*, 621.
(146) Tada, D. B.; Vono, L. L. R.; Duarte, D. L.; Itri, R.; Kiyohara, P. K.; Baptista, M. S.; Rossi, L. M. *Langmuir* **2007**, *23*, 8194.
(147) Bi, S.; Wei, X.; Li, N.; Lei, Z. *Mater. Lett.* **2008**, *62*, 2963.
(148) Peng, S.; Wang, C.; Xie, J.; Sun, S. *J. Am. Chem. Soc.* **2006**, *128*, 10676.
(149) Qiang, Y.; Antony, J.; Sharma, A.; Nutting, J.; Sikes, D.; Meyer, D. *J. Nanoparticle Res.* **2006**, *8*, 489.
(150) Popovici, E.; Dumitrache, F.; Morjan, I.; Alexandrescu, R.; Ciupina, V.; Prodan, G.; Vekas, L.; Bica, D.; Marinica, O.; Vasile, E. *Appl. Surf. Sci.* **2007**, *254*, 1048.
(151) Tartaj, P.; González-Carreño, T.; Serna, C. J. *Adv. Mater.* **2001**, *13*, 1620.
(152) Tartaj, P.; González-Carreño, T.; Serna, C. J. *Langmuir* **2002**, *18*, 4556.
(153) Arruebo, M.; Galán, M.; Navascues, N.; Téllez, C.; Marquina, C.; Ibarra, M. R.; Santamaría, J. *Chem. Mater.* **2006**, *18*, 1911.
(154) Arruebo, M.; Fernández-Pacheco, R.; Hirsuta, S.; Arbiol, J.; Ibarra, M. R.; Santamaría, J. *Nanotechnology* **2006**, *17*, 4057.
(155) Carja, G.; Chiriac, H.; Lupu, N. *J. Magn. Magn. Mater.* **2007**, *311*, 26.
(156) Fernández-Pacheco, R.; Arruebo, M.; Marquina, C.; Ibarra, R.; Arbiol, J.; Santamaría, J. *Nanotechnology* **2006**, *17*, 1188.
(157) Chatterjee, J.; Haik, Y.; Chen, C. J. *J. Magn. Magn. Mater.* **2001**, *225*, 21.
(158) Aurich, K.; Schwalbe, M.; Clement, J. H.; Weitschies, W.; Buske, N. *J. Magn. Magn. Mater.* **2007**, *311*, 1.
(159) Liang, Y. Y.; Zhang, L. M.; Jiang, W.; Li, W. *ChemPhysChem* **2007**, *8*, 2367.
(160) Saravanan, M.; Bhaskar, K.; Mahajaran, G.; Pillai, K. S. *Int. J. Pharm.* **2004**, *283*, 71.
(161) Alexiou, C.; Schmid, R. J.; Jurgons, R.; Kremer, M.; Wanner, G.; Bergemann, C.; Huenges, E.; Nawroth, T.; Arnold, W.; Parak, F. G. *Eur. Biophys. J.* **2006**, *35*, 446.
(162) Kim, D. H.; Lee, S. H.; Im, K. H.; Kim, K. N.; Kim, K. M.; Shim, I. B.; Lee, M. H.; Lee, Y. K. *Curr. Appl. Phys.* **2006**, *6*, e242.
(163) Ma, H. L.; Xu, Y. F.; Qi, X. R.; Maitani, Y.; Nagai, T. *Int. J. Pharm.* **2008**, *354*, 217.
(164) Viota, J. L.; Delgado, A. V.; Arias, J. L.; Durán, J. D. G. *J. Colloid Interface Sci.* **2008**, *324*, 199.
(165) Lin, P. C.; Chou, P. H.; Chen, S. H.; Liao, H. K.; Wang, K. Y.; Chen, Y. J.; Lin, C. C. *Small* **2006**, *2*, 485.
(166) Balakrishnan, S.; Bonder, M. J.; Hadjipanayis, G. C. *J. Magn. Magn. Mater.* **2009**, *321*, 117.
(167) Gómez-Lopera, S. A.; Plaza, R. C.; Delgado, A. V. *J. Colloid Interface Sci.* **2001**, *240*, 40.
(168) Gómez-Lopera, S. A.; Arias, J. L.; Gallardo, V.; Delgado, A. V. *Langmuir* **2006**, *22*, 2816.
(169) Hamoudeh, M.; Faraj, A. A.; Canet-Soulas, E.; Bessueille, F.; Léonard, D.; Fessi, H. *Int. J. Pharm.* **2007**, *338*, 248.
(170) Kumagai, M.; Imai, Y.; Nakamura, T.; Yamasaki, Y.; Sekino, M.; Ueno, S.; Hanaoka, K.; Kikuchi, K.; Nagano, T.; Kaneko, E.; Shimokado, K.; Kataoka, K. *Colloids Surf., B* **2007**, *56*, 174.
(171) Fan, Q. L.; Neoh, K. G.; Kang, E. T.; Shuter, B.; Wang, S. C. *Biomaterials* **2007**, *28*, 5426.
(172) Ren, J.; Hong, H. Y.; Ren, T. B.; Teng, X. R. *Mater. Lett.* **2005**, *59*, 2655.
(173) Nasongkla, N.; Bey, E.; Ren, J. M.; Ai, H.; Khemtong, C.; Guthi, J. S.; Chin, S. F.; Sherry, A. D.; Boothman, D. A.; Gao, J. M. *Nano Lett.* **2006**, *6*, 2427.
(174) Okassa, L. N.; Marchais, H.; Douziech-Eyrolles, L.; Cohen-Jonathan, S.; Soucé, M.; Dubois, P.; Chourpa, I. *Int. J. Pharm.* **2005**, *302*, 187.

(175) Okassa, L. N.; Marchais, H.; Douziech-Eyrolles, L.; Hervé, K.; Cohen-Jonathan, S.; Munnier, E.; Soucé, M.; Linassier, C.; Dubois, P.; Chourpa, I. *Eur. J. Pharm. Biopharm.* **2007**, *67*, 31.
(176) Liu, X.; Kaminski, M. D.; Chen, H.; Torno, M.; Taylor, L.; Rosengart, A. J. *J. Controlled Release* **2007**, *119*, 52.
(177) Holgado, M. A.; Álvarez-Fuentes, J.; Fernández-Arévalo, M.; Arias, J. L. *Curr. Drug Targets* **2011**, *12*, 1096.
(178) Pérez-Artacho, B.; Gallardo, V.; Ruiz, M. A.; Arias, J. L. *J. Nanopart. Res.* **2012**, *14*, 768.
(179) Arias, J. L.; Gallardo, V.; Gómez-Lopera, S. A.; Delgado, A. V. *J. Biomed. Nanotechol.* **2005**, *1*, 214.
(180) Arias, J. L.; Gallardo, V.; Ruiz, M. A.; Delgado, A. V. *Eur. J. Pharm. Biopharm.* **2008**, *69*, 54.
(181) Arias, J. L.; Ruiz, M. A.; Gallardo, V.; Delgado, A. V. *J. Controlled Release* **2008**, *125*, 50.
(182) Arias, J. L.; Linares-Molinero, F.; Gallardo, V.; Delgado, A. V. *Eur. J. Pharm. Sci.* **2008**, *33*, 252.
(183) Yang, J.; Lee, H.; Hyung, W.; Park, S. B.; Haam, S. *J. Microencapsulation* **2006**, *23*, 203.
(184) Arias, J. L.; Sáez-Fernández, E.; López-Viota, M.; Biedma-Ortiz, R. A.; Ruiz, M. A. *Med. Chem.* **2012**, *8*, 516.
(185) Wang, S. F.; Tan, Y. M. *Anal. Bioanal. Chem.* **2007**, *387*, 703.
(186) Arias, J. L.; Reddy, L. H.; Couvreur, P. *J. Mater. Chem.* **2012**, *22*, 7622.
(187) Santos, D. P.; Ruiz, M. A.; Gallardo, V.; Zanoni, M. V. B.; Arias, J. L. *J. Nanoparticle Res.* **2011**, *13*, 4311.
(188) Flesch, C.; Bourgeat-Lami, E.; Mornet, S.; Duguet, E.; Delaite, C.; Dumas, P. *J. Polym. Sci., Part A: Polym. Chem.* **2005**, *43*, 3221.
(189) Yang, J.; Park, S. B.; Yoon, H. G.; Huh, Y. M.; Haam, S. *Int. J. Pharm.* **2006**, *324*, 185.
(190) Arias, J. L.; López-Viota, M.; Ruiz, M. A.; López-Viota, J.; Delgado, A. V. *Int. J. Pharm.* **2007**, *339*, 237.
(191) Arias, J. L.; López-Viota, M.; Delgado, A. V.; Ruiz, M. A. *Colloids Surf., B* **2010**, *77*, 111.
(192) Yang, C.; Guan, Y.; Xing, J.; Liu, H. *Langmuir* **2008**, *24*, 9006.
(193) Gass, J.; Poddar, P.; Almand, J.; Srinath, S.; Srikanth, H. *Adv. Funct. Mater.* **2006**, *16*, 71.
(194) Yuan, J. J.; Armes, S. P.; Takabayashi, Y.; Prassides, K.; Leite, C. A. P.; Galembeck, F.; Lewis, A. L. *Langmuir* **2006**, *22*, 10989.
(195) Dey, T. *J. Nanosci. Nanotechnol.* **2006**, *6*, 2479.
(196) Hu, S. H.; Liu, T. Y.; Liu, D. M.; Chen, S. Y. *J. Controlled Release* **2007**, *121*, 181.
(197) Boissière, M.; Allouche, J.; Brayner, R.; Chanéac, C.; Livage, J.; Coradin, T. *J. Nanosci. Nanotechnol.* **2007**, *7*, 4649.
(198) Phanapavudhikul, P.; Shen, S.; Ng, W. K.; Tan, R. B. H. *Drug Delivery* **2008**, *15*, 177.
(199) Lee, J.; Isobe, T.; Senna, M. *J. Colloid Interface Sci.* **1996**, *177*, 490.
(200) Mikhaylova, M.; Jo, Y. S.; Kim, D. K.; Bobrysheva, N.; Anderson, Y.; Eriksson, T.; Osmolowsky, M.; Semenov, V.; Muhammed, M. *Hyperfine Interact.* **2004**, *156*, 257.
(201) Mikhaylova, M.; Kim, D. K.; Bobrysheva, N.; Osmolowsky, M.; Semenov, V.; Tsakalakos, T.; Muhammed, M. *Langmuir* **2004**, *20*, 2472.
(202) Arias, J. L.; Clares, B.; Morales, M. E.; Gallardo, V.; Ruiz, M. A. *Curr. Drug Targets* **2011**, *12*, 1151.
(203) Sabaté, R.; Barnadas-Rodríguez, R.; Callejas-Fernández, J.; Hidalgo-Álvarez, R.; Estelrich, J. *Int. J. Pharm.* **2008**, *347*, 156.
(204) Martina, M. S.; Fortin, J. P.; Menager, C.; Clement, O.; Barratt, G.; Gabrielle-Madelmont, C.; Gazeau, F.; Cabuil, V.; Lesieur, S. *J. Am. Chem. Soc.* **2005**, *127*, 10676.
(205) Hergt, R.; Dutz, S.; Müller, R.; Zeisberger, M. *J. Phys. Cond. Mater.* **2006**, *18*, S2919.
(206) Lang, C.; Schüler, D.; Faivre, D. *Macromol. Biosci.* **2007**, *7*, 144.
(207) Xiang, L.; Wei, J.; Jianbo, S.; Guili, W.; Feng, G.; Ying, L. *Lett. Appl. Microbiol.* **2007**, *45*, 75.
(208) Bergemann, C.; Müller-Schulte, D.; Oster, J.; Brassardm, L.; Lübbe, A. S. *J. Magn. Magn. Mater.* **1999**, *194*, 45.
(209) Bulte, J. W. M.; de Cuyper, M.; Despres, D.; Frank, J. A. *J. Magn. Magn. Mater.* **1999**, *194*, 204.
(210) Yoshino, T.; Hirabe, H.; Takahashi, M.; Kuhara, M.; Takeyama, H.; Matsunaga, T. *Biotechnol. Bioeng.* **2008**, *101*, 470.
(211) Huang, X.; Bronstein, L. M.; Retrum, J.; Dufort, C.; Tsvetkova, I.; Aniagyei, S.; Stein, B.; Stucky, G.; McKenna, B.; Remmes, N.; Baxter, D.; Kao, C. C.; Dragnea, B. *Nano Lett.* **2007**, *7*, 2407.
(212) Di Marco, M.; Port, M.; Couvreur, P.; Dubernet, C.; Ballirano, P.; Sadun, C. *J. Am. Chem. Soc.* **2006**, *128*, 10054.
(213) Weissleder, R.; Reimer, P.; Lee, A. S.; Wittenberg, J.; Brady, T. *Am. J. Roentgenol.* **1990**, *155*, 1161.
(214) Weissleder, R.; Elizondo, G.; Wittenberg, J.; Rabito, C. A.; Bengele, H. H.; Josephson, L. *Radiology* **1990**, *175*, 489.
(215) Donegá, C. M.; Liljeroth, P.; Vanmaekelbergh, D. *Small* **2005**, *12*, 1152.
(216) Arias, J. L.; Reddy, L. H.; Couvreur, P. *Langmuir* **2008**, *24*, 7512.
(217) Di Marco, M.; Sadun, C.; Port, M.; Guilbert, I.; Couvreur, P.; Dubernet, C. *Int. J. Nanomed.* **2007**, *2*, 609.
(218) Jung, C. W. *Magn. Reson. Imaging* **1995**, *13*, 675.
(219) Jung, C. W.; Jacobs, P. *Magn. Reson. Imaging* **1995**, *13*, 661.
(220) Moeser, G. D.; Green, W. H.; Laibinis, P. E.; Linse, P.; Hatton, T. A. *Langmuir* **2004**, *20*, 5223.
(221) Sadun, C.; Bucci, R.; Magri, A. L. *J. Am. Chem. Soc.* **2002**, *124*, 3036.
(222) Miser, D. E.; Shin, E. J.; Hajaligol, M. R.; Rasouli, F. *Appl. Catal., A* **2004**, *258*, 7.
(223) Brice-Profeta, S.; Arrio, M. A.; Tronc, E.; Menguy, N.; Letard, I.; Cartier dit Moulin, C.; Noguès, M.; Chanéac, C.; Jolivet, J. P.; Sainctavit, Ph. *J. Magn. Magn. Mater.* **2005**, *288*, 354.
(224) Yee, C.; Kataby, G.; Ulman, A.; Prozorov, T.; White, H.; King, A.; Rafailovich, M.; Sokolov, J.; Gedanken, A. *Langmuir* **1999**, *15*, 7111.
(225) Roger, J.; Pons, J. N.; Massart, R.; Halbreich, A.; Bacri, J. C. *Eur. Phys. J.: Appl. Phys.* **1999**, *5*, 321.
(226) Nooney, M. G.; Corneille, J. S.; Murrell, T. S.; Lin, X. F.; Hossner, L. R.; Chusuei, C. C.; Goodman, D. W. *Langmuir* **1998**, *14*, 2750.
(227) Hunter, R. J. *Foundations of Colloid Science*, 2nd ed.; Clarendon Press: Oxford, U.K., 2001.
(228) Joly, L.; Ybert, C.; Trizac, E. *Phys. Rev. Lett.* **2004**, *93*, 257805.
(229) Xu, R. *Langmuir* **1998**, *14*, 2593.
(230) Delgado, A. V.; Arroyo, F. J. In *Interfacial Electrokinetics and Electrophoresis*; Delgado, A. V., Ed.; Marcel Dekker: New York, 2002.
(231) O'Brien, R. W.; White, L. R. *J. Chem. Soc., Faraday Trans. II* **1978**, *74*, 1607.
(232) Matijević, E. In *Interfacial Electrokinetics and Electrophoresis*; Delgado, A. V., Ed.; Marcel Dekker: New York, 2002.
(233) El-Gholabzouri, O.; Cabrerizo-Vılchez, M. A.; Hidalgo-Alvarez, R. *Colloids Surf., A* **2006**, *291*, 30.
(234) Dukhin, A. S.; Ohshima, H.; Shilov, V. N.; Goetz, P. J. *Langmuir* **1999**, *15*, 3445.
(235) Di Marco, M.; Guilbert, I.; Port, M.; Robic, C.; Couvreur, P.; Dubernet, C. *Int. J. Pharm.* **2007**, *331*, 197.
(236) Delgado, A. V.; González-Caballero, F.; Hunter, R. J.; Koopal, L. K.; Lyklema, J. *Pure Appl. Chem.* **2005**, *77*, 1753.
(237) Ohshima, H.; Healy, T. W.; White, L. R. *J. Chem. Soc., Faraday Trans. II* **1983**, *2*, 1613.
(238) Ohshima, H. *J. Colloid Interface Sci.* **1997**, *188*, 481.
(239) Ohshima, H. *Colloids Surf., A* **2005**, *267*, 50.
(240) van Oss, C. J. *Interfacial Forces in Aqueous Media*, 2nd ed.; CRC Press: Boca Raton, FL, 2006.
(241) Neuberger, T.; Schöpf, B.; Hotmann, H.; Hofmann, M.; von Rechenberg, B. *J. Magn. Magn. Mater.* **2005**, *293*, 483.
(242) Sjögren, C. E.; Johansson, C.; Nævestad, A.; Sontum, P. C.; Briley-Sæbø, K.; Fahlvik, A. K. *Magn. Reson. Imaging* **1997**, *15*, 55.
(243) Schütt, W.; Grüttner, C.; Häfeli, U.; Zborowski, M.; Teller, J.; Putzar, H.; Schümichen, C. *Hybridoma* **1997**, *16*, 109.

(244) Sun, S. H.; Murray, C. B.; Weller, D.; Folks, L.; Moser, A. *Science* **2000**, *287*, 1989.
(245) Charles, S. W.; Popplewell, J. *Endeavour* **1982**, *6*, 153.
(246) Lin, X. M.; Samia, A. C. S. *J. Magn. Magn. Mater.* **2006**, *305*, 100.
(247) Janssen, J. J. M.; Baltussen, J. J. M.; van Gelder, A. P.; Perenboom, J. A. A. J. *J. Phys. D, Appl. Phys.* **1990**, *23*, 1455.
(248) Ortega-Vinuesa, J. L.; Martin-Rodriguez, A.; Hidalgo-Alvarez, R. *J. Colloid Interface Sci.* **1996**, *184*, 259.
(249) Romero-Cano, M. S.; Martín-Rodríguez, A.; de las Nieves, F. J. *Langmuir* **2001**, *17*, 3505.
(250) Valle-Delgado, J. J.; Molina-Bolıvar, J. A.; Galisteo-Gonzalez, F.; Gálvez-Ruiz, M. J. *Colloid Polym. Sci.* **2003**, *81*, 708.
(251) Ishikawa, Y.; Katoh, Y.; Ohshima, H. *Colloids Surf., B* **2005**, *42*, 53.
(252) Thode, K.; Muller, R. H.; Kresse, M. *J. Pharm. Sci.* **2000**, *89*, 1317.
(253) López-López, M. T.; de Vicente, J.; Bossis, G.; González-Caballero, F.; Durán, J. D. G. *J. Mater. Res.* **2005**, *20*, 874.
(254) Holthoff, H.; Egelhaaf, S. U.; Borkovec, M.; Schurtenberger, P.; Sticher, H. *Langmuir* **1996**, *12*, 5541.
(255) Schudel, M.; Behrens, S. H.; Holthoff, H.; Kretzschmar, R.; Borkovec, M. *J. Colloid Interface Sci.* **1997**, *196*, 241.
(256) Viota, J. L.; de Vicente, J.; Durán, J. D. G.; Delgado, A. V. *J. Colloid Interface Sci.* **2005**, *284*, 527.
(257) Blunk, T.; Hochstrasser, D. F.; Sanchez, J.; Müller, B. W.; Müller, R. H. *Electrophoresis* **1993**, *14*, 1382.
(258) Borchard, G.; Kreuter, J. *J. Drug Targeting* **1993**, *1*, 15.
(259) Borchard, G.; Kreuter, J. *Pharm. Res.* **1996**, *13*, 1055.
(260) Armstrong, T. I.; Davies, M. C.; Illum, L. *J. Drug Targeting* **1997**, *4*, 389.
(261) Arruebo, M.; Fernández-Pacheco, R.; Ibarra, M. R.; Santamaría, J. *Nano Today* **2007**, *2*, 22.
(262) Decuzzi, P.; Ferrari, M. *Biomaterials* **2006**, *27*, 5307.
(263) Gref, R.; Minamitake, Y.; Peracchia, M. T.; Trubetskoy, V.; Torchilin, V.; Langer, R. *Science* **1994**, *263*, 1600.
(264) Farokhzad, O. C.; Cheng, J.; Teply, B. A.; Sherifi, I.; Jon, S.; Kantoff, P. W.; Richie, J. P.; Langer, R. *Proc. Natl. Acad. Sci. U.S.A.* **2006**, *103*, 6315.
(265) Matsumura, Y. *Adv. Drug Delivery Rev.* **2008**, *60*, 899.
(266) Oussoren, C.; Storm, G. *J. Liposome Res.* **1999**, *9*, 349.
(267) Coins, B.; Phillips, W. T.; Klipper, R. *J. Liposome Res.* **1998**, *8*, 265.
(268) Laverman, P.; Carstens, M. G.; Boerman, O. C.; Dams, E. M.; Oyen, W. J. G.; van Rooijen, N.; Corstens, F. M.; Storm, G. *J. Pharmacol. Exp. Ther.* **2001**, *298*, 607.
(269) Ishida, T.; Kiwada, H. *Int. J. Pharm.* **2008**, *354*, 56.
(270) Ishida, T.; Harada, M.; Wang, X. Y.; Ichihara, M.; Irimura, K.; Kiwada, H. *J. Controlled Release* **2005**, *105*, 305.
(271) Ishida, T.; Atobe, K.; Wang, X.; Kiwada, H. *J. Controlled Release* **2006**, *115*, 251.
(272) Ishihara, T.; Takeda, M.; Sakamoto, H.; Kimoto, A.; Kobayashi, C.; Takasaki, N.; Yuki, K.; Tanaka, K.; Takenaga, M.; Igarashi, R.; Maeda, T.; Yamakawa, N.; Okamoto, Y.; Otsuka, M.; Ishida, T.; Kiwada, H.; Mizushima, Y.; Mizushima, T. *Pharm. Res.* **2009**, *26*, 2270.
(273) Ishihara, T.; Maeda, T.; Sakamoto, H.; Takasaki, N.; Shigyo, M.; Ishida, T.; Kiwada, H.; Mizushima, Y.; Mizushima, T. *Biomacromolecules* **2010**, *11*, 2700.
(274) Maeda, H. *Adv. Enzyme Reg.* **2001**, *41*, 189.
(275) Maeda, H. *Bioconjugate Chem.* **2010**, *21*, 797.
(276) Dobson, J. *Drug Dev. Res.* **2006**, *67*, 55.
(277) Senyei, A.; Widder, K.; Czerlinski, G. *J. Appl. Phys.* **1978**, *49*, 3578.
(278) Fang, C.; Shi, B.; Pei, Y. Y.; Hong, M. H.; Wu, J.; Chen, H. Z. *Eur. J. Pharm. Sci.* **2006**, *27*, 27.
(279) Moghimi, M. M.; Hunter, A. C.; Murray, J. C. *Pharmacol. Rev.* **2001**, *53*, 283.
(280) Majumdar, S.; Zoghbi, S. S.; Gore, J. C. *Invest. Radiol.* **1990**, *25*, 771.
(281) Varallyay, P.; Nesbit, G.; Muldoon, L. L.; Nixon, R. R.; Delashaw, J.; Cohen, J. I.; Petrillo, A.; Rink, D.; Neuwelt, E. A. *Am. J. Neuroradiol.* **2002**, *23*, 510.
(282) Bourrinet, P.; Bengele, H. H.; Bonnemain, B.; Dencausse, A.; Idee, J. M.; Jacobs, P. M.; Lewis, J. M. *Invest. Radiol.* **2006**, *41*, 313.
(283) Chouly, C.; Pouliquen, D.; Lucet, I.; Jeune, J. J.; Jallet, P. *J. Microencapsulation* **1996**, *13*, 245.
(284) Maaßen, S.; Fattal, E.; Müller, R. H.; Couvreur, P. *STP Pharma Sci.* **1993**, *3*, 11.
(285) Iannone, A.; Magin, R. L.; Walczack, T.; Federico, M.; Swartz, H. M.; Tomasi, A.; Vannini, V. *Magn. Reson. Med.* **1991**, *22*, 435.
(286) Wilhelm, C.; Gazeau, F.; Roger, J.; Pons, J. N.; Bacri, J. C. *Langmuir* **2002**, *18*, 8148.
(287) Billotey, C.; Wilhelm, C.; Devaud, M.; Bacri, J. C.; Bittoun, J.; Gazeau, F. *Magn. Reson. Med.* **2003**, *49*, 646.
(288) Wilhelm, C.; Billotey, C.; Roger, J.; Pons, J. N.; Bacri, J. C.; Gazeau, F. *Biomaterials* **2003**, *24*, 1001.
(289) Fujita, T.; Nishikawa, M.; Ohtsubo, Y.; Ohno, J.; Takakura, Y.; Sezaki, H.; Hashida, M. *J. Drug Targeting* **1994**, *2*, 157.
(290) Papisov, M. I.; Bogdanov, A.; Schaffer, B.; Nossiff, N.; Shen, T.; Weissleder, R.; Brady, T. J. *J. Magn. Magn. Mater.* **1993**, *122*, 383.
(291) Kwon, J. T.; Hwang, S. K.; Jin, H.; Kim, D. S.; Minai-Tehrani, A.; Yoon, H. J.; Choi, M.; Yoon, T. J.; Han, D. Y.; Kang, Y. W.; Yoon, B. I.; Lee, J. K.; Cho, M. H. *J. Occup. Health* **2008**, *50*, 1.
(292) Kim, J. S.; Yoon, T. J.; Yu, K. N.; Kim, B. G.; Park, S. J.; Kim, H. W.; Lee, K. H.; Park, S. B.; Lee, J. K.; Cho, M. H. *Toxicol. Sci.* **2006**, *89*, 338.
(293) Choi, H. S.; Liu, W.; Misra, P.; Tanaka, E.; Zimmer, J. P.; Ipe, B. I.; Bawendi, M. G.; Frangioni, J. V. *Nat. Biotechnol.* **2007**, *25*, 1165.
(294) Briley-Saebo, K.; Bjørnerud, A.; Grant, D.; Ahlstrom, H.; Berg, T.; Kindberg, G. M. *Cell Tissue Res.* **2004**, *316*, 315.
(295) Briley-Saebø, K.; Hustvedt, S. O.; Haldorsen, A.; Bjørnerud, A. *J. Magn. Reson. Imaging* **2004**, *20*, 622.
(296) Dupas, B.; Berreur, M.; Rohanizadeh, R.; Bonnemain, B.; Meflah, K.; Pradal, G. *Biol Cell.* **1999**, *91*, 195.
(297) Hillaireau, H.; Couvreur, P. *Cell. Mol. Life Sci.* **2009**, *66*, 2873.
(298) Raynal, I.; Prigent, P.; Peyramaure, S.; Najid, A.; Rebuzzi, C.; Corot, C. *Invest. Radiol.* **2004**, *39*, 56.
(299) Schulze, E.; Ferrucci, J. T., Jr.; Poss, K.; Lapointe, L.; Bogdanova, A.; Weissleder, R. *Invest Radiol.* **1995**, *30*, 604.
(300) Singh, N.; Jenkins, G. J. S.; Asadi, R.; Doak, S. H. *Nano Rev.* **2010**, *1*, 5358.
(301) Absolom, D. R.; Zingg, W.; Neumann, A. W. *J. Biomed. Mater. Res.* **1987**, *21*, 161.
(302) Haas, T. A.; Plow, E. F. *Curr. Opin. Cell Biol.* **1994**, *6*, 656.
(303) Berry, C. C.; Wells, S.; Charles, S.; Aitchison, G.; Curtis, A. S. G. *Biomaterials* **2004**, *25*, 5405.
(304) Simioni, A. R.; Martins, O. P.; Lacava, Z. G.; Azevedo, R. B.; Lima, E. C.; Lacava, B. M.; Morais, P. C.; Tedesco, A. C. *J. Nanosci. Nanotechnol.* **2006**, *6*, 2413.
(305) Müller, K.; Skepper, J. N.; Posfai, M.; Trivedi, R.; Howarth, S.; Corot, C.; Lancelot, E.; Thompson, P. W.; Brown, A. P.; Gillard, J. H. *Biomaterials* **2007**, *28*, 1629.
(306) Karlsson, H. L.; Gustafsson, J.; Cronholm, P.; Möller, L. *Toxicol. Lett.* **2009**, *188*, 112.
(307) Mahmoudi, M.; Simchi, A.; Imani, M.; Shokrgozar, M. A.; Milani, A. S.; Häfeli, U. O.; Stroeve, P. *Colloids Surf B Biointerfaces* **2010**, *75*, 300.
(308) Pisanic, T. R., II; Blackwell, J. D.; Shubayev, V. I.; Fiñones, R. R.; Jin, S. *Biomaterials* **2007**, *28*, 2572.
(309) de Freitas, E. R.; Soares, P. R.; Santos, R. P.; dos Santos, R. L.; da Silva, J. R.; Porfirio, E. P.; Báo, S. N.; Lima, E. C.; Morais, P. C.; Guillo, L. A. *J. Nanosci. Nanotechnol.* **2008**, *8*, 2385.
(310) Weissleder, R.; Stark, D. D.; Engelstad, B. L.; Bacon, B. R.; Compton, C. C.; White, D. L.; Jacobs, P.; Lewis, J. *Am. J. Roentgenol.* **1989**, *152*, 167.
(311) Klausner, R. D.; Ronault, T. A.; Harford, J. B. *Cell* **1993**, *72*, 19.
(312) Elias, A.; Tsourkas, A. *Hematology Am. Soc. Hematol. Educ. Program* **2009**, *2009*, 720.

(313) Glickstein, H.; El, R. B.; Link, G.; Breuer, W.; Konijn, A. M.; Hershko, C.; Nick, H.; Cabantchik, Z. I. *Blood* **2006**, *108*, 3195.
(314) Jain, T. K.; Reddy, M. K.; Morales, M. A.; Leslie-Pelecky, D. L.; Labhasetwar, V. *Mol. Pharmaceutics* **2008**, *5*, 316.
(315) Gajdosíková, A.; Gajdosík, A.; Koneracká, M.; Závisová, V.; Stvrtina, S.; Krchnárová, V.; Kopcanský, P.; Tomasovicová, N; Stolc, S; Timko., M. *Neuroendocrinol. Lett.* **2006**, *27*, 96.
(316) Lübbe, A. S.; Bergemann, C.; Huhnt, W.; Fricke, T.; Riess, H.; Brock, J. W.; Huhn, D. *Cancer Res.* **1996**, *56*, 4694.
(317) Lübbe, A. S.; Bergemann, C.; Riess, H.; Schriever, F.; Reichardt, P.; Possinger, K.; Matthias, M.; Dörken, B.; Herrmann, F.; Gürtler, R.; Hohenberger, P.; Haas, N.; Sohr, R.; Sander, B.; Lemke, A. J.; Ohlendorf, D.; Huhnt, W.; Huhn, D. *Cancer Res.* **1996**, *56*, 4686.
(318) Lemke, A. J.; Senfft von Pilsach, M. I.; Lübbe, A.; Bergemann, C.; Riess, H.; Felix, R. *Eur. Radiol.* **2004**, *14*, 1949.
(319) Reimer, P.; Balzer, T. *Eur. Radiol.* **2003**, *13*, 1266.
(320) Reimer, P.; Marx, C.; Rummeny, E. J.; Müller, M.; Lentschig, M.; Balzer, T.; Dietl, K. H.; Sulkowski, U.; Berns, T.; Shamsi, K.; Peters, P. E. *J. Magn. Reson. Imaging* **1997**, *7*, 945.
(321) Kopp, A. F.; Laniado, M.; Dammann, F.; Stern, W.; Grönewäller, E.; Balzer, T.; Schimpfky, C.; Claussen, C. D. *Radiology* **1997**, *204*, 749.
(322) Kehagias, D. T.; Gouliamos, A. D.; Smyrniotis, V.; Vlahos, L. J. *J. Magn. Reson. Imaging* **2001**, *14*, 595.
(323) Muldoon, L. L.; Sándor, M.; Pinkston, K. E.; Neuwelt, E. A. *Neurosurgery* **2005**, *57*, 785.
(324) Aillon, K. L.; Xie, Y.; El-Gendy, N.; Berkland, C. J.; Forrest, M. L. *Adv. Drug Delivery Rev.* **2009**, *61*, 457.
(325) Alexis, F.; Pridgen, E.; Molnar, L. K.; Farokhzad, O. C. *Mol. Pharmaceutics* **2008**, *5*, 505.
(326) Lacava, Z. G. M.; Azevedo, R. B.; Martins, E. V.; Lacava, L. M.; Freitas, M. L. L.; Garcia, V. A. P.; Rehbula, C. A.; Lemos, A. P. C.; Sousa, M. H.; Tourinho, F. A.; Da Silva, M. F.; Morais, P. C. *J. Magn. Magn. Mater.* **1999**, *201*, 431.
(327) Yu, Z.; Xiaoliang, W.; Xuman, W.; Hong, X.; Hongchen, G. *J. Biomed. Mater. Res.* **2008**, *85*, 582.
(328) Liu, S.; Han, Y.; Yin, L.; Long, L.; Liu, R. *Adv. Mater. Res.* **2008**, *47*−*50*, 1097.
(329) Kingsley, J. D.; Dou, H.; Morehead, J.; Rabinow, B.; Gendelman, H. E.; Destache, C. J. *J. Neuroimmune Pharmacol.* **2006**, *1*, 340.
(330) Couvreur, P.; Vauthier, C. *Pharm. Res.* **2006**, *23*, 1417.
(331) Arias, J. L. *Mini-Rev. Med. Chem.* **2011**, *11*, 1.
(332) Ibrahim, A.; Couvreur, P.; Roland, M.; Speiser, P. *J. Pharm. Pharmacol.* **1983**, *35*, 59.
(333) Gallo, J. M.; Gupta, P. K.; Hung, C. T.; Perrier, D. G. *J. Pharm. Sci.* **1989**, *78*, 190.
(334) Gallo, J. M.; Häfeli, U. *Cancer Res.* **1997**, *57*, 3063.
(335) Alexiou, C.; Schmidt, A.; Klein, R.; Hulin, P.; Bergemann, C. *J. Magn. Magn. Mater.* **2002**, *252*, 363.
(336) Alexiou, C.; Jurgons, R.; Schmid, R. J.; Bergemann, C.; Henke, J.; Erhardt, W.; Huenges, E.; Parak, F. *J. Drug Targeting* **2003**, *11*, 139.
(337) Alexiou, C.; Jurgons, R.; Schmid, R.; Hilpert, A.; Bergemann, C.; Parak, F.; Iro, H. *J. Magn. Magn. Mater.* **2005**, *293*, 389.
(338) Kohler, N.; Sun, C.; Wang, J.; Zhang, M. Q. *Langmuir* **2005**, *21*, 8858.
(339) Gupta, R.; Bajpai, A. K. *J. Biomater. Sci., Polym. Ed.* **2011**, *22*, 893.
(340) Arias, J. L. *Molecules* **2008**, *13*, 2340.
(341) Barry, S. E. *Int. J. Hyperthermia* **2008**, *24*, 451.
(342) Závišová, V.; Koneracká, M.; Štrbák, O.; Tomašovičová, N.; Kopčanský, P.; Timko, M.; Vavra, I. *J. Magn. Magn. Mater.* **2007**, *311*, 379.
(343) Weissleder, R.; Tung, C. H.; Mahmood, U.; Bogdanov, A., Jr. *Nat. Biotechnol.* **1999**, *17*, 375.
(344) Tung, C. H.; Mahmood, U.; Bredow, S.; Weissleder, R. *Cancer Res.* **2000**, *60*, 4953.
(345) Lübbe, A. S.; Bergemann, C.; Brock, J.; McClure, D. G. *J. Magn. Magn. Mater.* **1999**, *194*, 149.
(346) Grief, A. D.; Richardson, G. *J. Magn. Magn. Mater.* **2005**, *293*, 455.
(347) Scott, G.; Peterson, C.; Hohn, C.; Bittner, C. *J. Magn. Magn. Mater.* **1999**, *194*, 132.
(348) Pankhurst, Q. A.; Connolly, J.; Jones, S. K.; Dobson, J. *J. Phys. D: Appl. Phys.* **2003**, *36*, R167.
(349) Chen, H. T.; Ebner, A. D.; Rosengart, A. J.; Kaminski, M. D.; Ritter, J. A. *J. Magn. Magn. Mater.* **2004**, *284*, 181.
(350) Avilés, M. O.; Ebner, A. D.; Ritter, J. A. *J. Magn. Magn. Mater.* **2008**, *320*, 2640.
(351) Fernández-Pacheco, R.; Marquina, C.; Valdivia, J. G.; Gutiérrez, M.; Romero, M. S.; Cornudella, R.; Laborda, R.; Vitoria, A.; Higuera, T.; García, A.; de Jalón, J. A. G.; Ibarra, M. R. *J. Magn. Magn. Mater.* **2007**, *311*, 318.
(352) Gang, J.; Park, S. B.; Hyung, W.; Choi, E. H.; Wen, J.; Kim, H. S.; Shul, Y. G.; Haam, S.; Song, S. Y. *J. Drug Targeting* **2007**, *15*, 445.
(353) Yu, M. K.; Jeong, Y. Y.; Park, J.; Park, S.; Kim, J. W.; Min, J. J.; Kim, K.; Jon, S. *Angew. Chem., Int. Ed.* **2008**, *47*, 5362.
(354) Zhang, J. Q.; Zhang, Z. R.; Yang, H.; Tan, Q. Y.; Qin, S. R.; Qiu, X. L. *Pharm. Res.* **2005**, *22*, 573.
(355) Fortin-Ripoche, J. P.; Martina, M. S.; Gazeau, F.; Menager, C.; Wilhelm, C.; Bacri, J. C.; Lesieur, S.; Clement, O. *Nanomedicine* **2010**, *5*, 1173.
(356) Gultepe, E.; Reynoso, F. J.; Jhaveri, A.; Kulkarni, P.; Nagesha, D.; Ferris, C.; Harisinghani, M.; Campbell, R. B.; Sridhar, S. *Nanomedicine (London)* **2010**, *5*, 1173.
(357) Torchilin, P. *Nat. Rev. Drug Discovery* **2005**, *4*, 145.
(358) Martina, M. S.; Wilhelm, C.; Lesieur, S. *Biomaterials* **2008**, *29*, 4137.
(359) Viroonchatapan, E.; Sato, H.; Ueno, M.; Adachi, I.; Tazawa, K.; Horikoshi, I. *Life Sci.* **1996**, *58*, 2251.
(360) Lübbe, A. S.; Alexiou, C.; Bergemann, C. *J. Surg. Res.* **2001**, *95*, 200.
(361) Peer, D.; Karp, J. M.; Hong, S.; Farokhzad, O. C.; Margalit, R.; Langer, R. *Nat. Nanotechnol.* **2007**, *2*, 751.
(362) Holgado, M. A.; Martín-Banderas, L.; Álvarez-Fuentes, J.; Fernández-Arévalo, M.; Arias, J. L. *Curr. Med. Chem.* **2012**, *19*, 3188.
(363) Clares, B.; Ruiz, M. A.; Gallardo, V.; Arias, J. L. *Curr. Med. Chem.* **2012**, *19*, 3203.
(364) Weissleder, R.; Bogdanov, A.; Papisov, M. *Magn. Reson. Q* **1992**, *8*, 55.
(365) Varner, J. A.; Cheresh, D. A. *Curr. Opin. Cell Biol.* **1996**, *8*, 724.
(366) Vandewalle, B.; Granier, A. M.; Peyrat, J. P.; Bonneterre, J.; Lefebvre, J. *J. Cancer Res. Clin. Oncol.* **1985**, *110*, 71.
(367) Farokhzad, O. C.; Jon, S.; Khademhosseini, A.; Tran, T. N.; Lavan, D. A.; Langer, R. *Cancer Res.* **2004**, *64*, 7668.
(368) Herr, J. K.; Smith, J. E.; Medley, C. D.; Shangguan, D.; Tan, W. *Anal. Chem.* **2006**, *78*, 2918.
(369) Smith, J. E.; Medley, C. D.; Tang, Z.; Shangguan, D.; Lofton, C.; Tan, W. *Anal. Chem.* **2007**, *79*, 3075.
(370) Yigit, M. V.; Mazumdar, D.; Kim, H. K.; Lee, J. H.; Odintsov, B.; Lu, Y. *ChemBioChem* **2007**, *8*, 1675.
(371) Yigit, M. V.; Mazumdar, D.; Lu, Y. *Bioconjugate Chem.* **2008**, *19*, 412.
(372) Cerdan, S.; Lotscher, H. R.; Kunnecke, B.; Seelig, J. *Magn. Reson. Med.* **1989**, *12*, 151.
(373) Weissleder, R.; Lee, A. S.; Fischman, A. J.; Reimer, P.; Shen, T.; Wilkinson, R.; Callahan, R. J.; Brady, T. J. *Radiology* **1991**, *181*, 245.
(374) Tiefenauer, L. X.; Kuhne, G.; Andres, R. Y. *Bioconjugate Chem.* **1993**, *4*, 347.
(375) Artemov, D.; Mori, N.; Okollie, B.; Bhujwala, Z. M. *Magn. Reson. Med.* **2003**, *49*, 403.
(376) Artemov, D.; Mori, N.; Ravi, R.; Bhujwalla, Z. M. *Cancer Res.* **2003**, *63*, 2723.
(377) Huh, Y. M.; Jun, Y. W.; Song, H. T.; Kim, S.; Choi, J. S.; Lee, J. H.; Yoon, S.; Kim, K. S.; Shin, J. S.; Suh, J. S.; Cheon, J. *J. Am. Chem. Soc.* **2005**, *127*, 12387.

(378) Foon, K. A. *Cancer Res.* **1989**, *49*, 1621.
(379) Huang, G.; Diakur, J.; Xu, Z.; Wiebe, L. I. *Int. J. Pharm.* **2008**, *360*, 197.
(380) Banerjee, R.; Tyagi, P.; Li, S.; Huang, L. *Int. J. Cancer* **2004**, *112*, 693.
(381) Low, P. S.; Antony, A. C. *Adv. Drug Delivery Rev.* **2004**, *56*, 1055.
(382) Quintana, A.; Raczka, E.; Piehler, L.; Lee, I.; Myc, A.; Majaros, I.; Patri, A. K.; Thomas, T.; Mule, J.; Baker, J. R. *Pharm. Res.* **2002**, *19*, 1310.
(383) Weissleder, R.; Kelly, K.; Sun, E. Y.; Shtatland, T.; Josephson, L. *Nat. Biotechnol.* **2005**, *23*, 1418.
(384) Zhang, J.; Rana, S.; Srivastava, R. S.; Misra, R. D. K. *Acta Biomater.* **2008**, *4*, 40.
(385) Yang, X.; Chen, Y.; Yuan, R.; Chen, G.; Blanco, E.; Gao, J.; Shuai, X. *Polymer* **2008**, *49*, 3477.
(386) Lewin, M.; Carlesso, N.; Tung, C. H.; Tang, X. W.; Cory, D.; Scadden, D. T.; Weissleder, R. *Nat. Biotechnol.* **2000**, *18*, 410.
(387) Koch, A. M.; Reynolds, F.; Kircher, M. F.; Merkle, H. P.; Weissleder, R.; Josephson, L. *Bioconjugate Chem.* **2003**, *14*, 1115.
(388) Wadia, J. S.; Dowdy, S. F. *Adv. Drug Delivery Rev.* **2005**, *57*, 579.
(389) Wang, H.; Zhang, S.; Liao, Z.; Wang, C.; Liu, Y.; Feng, S.; Jiang, X.; Chang, J. *Biomaterials* **2010**, *31*, 6589.
(390) Arias, J. L. *Expert Opin. Drug Delivery* **2011**, *8*, 1589.
(391) Kohler, N.; Sun, C.; Fichtenholtz, A.; Gunn, J.; Fang, C.; Zhang, M. Q. *Small* **2006**, *2*, 785.
(392) Santra, S.; Kaittanis, C.; Grimm, J.; Perez, J. M. *Small* **2009**, *5*, 1862.
(393) Maeng, J. H.; Lee, D. H.; Jung, K. H.; Bae, Y. H.; Park, I. S.; Jeong, S.; Jeon, Y. S.; Shim, C. K.; Kim, W.; Kim, J.; Lee, J.; Lee, Y. M.; Kim, J. H.; Kim, W. H.; Hong, S. S. *Biomaterials* **2010**, *31*, 4995.
(394) Arias, J. L.; Reddy, L. H.; Othman, M.; Gillet, B.; Desmaële, D.; Zouhiri, F.; Dosio, F.; Gref, R.; Couvreur, P. *ACS Nano* **2011**, *5*, 1513.
(395) Rowe, M. D.; Thamm, D. H.; Kraft, S. L.; Boyes, S. G. *Biomacromolecules* **2009**, *10*, 983.
(396) Bagalkot, V.; Zhang, L.; Levy-Nissenbaum, E.; Jon, S.; Kantoff, P. W.; Langer, R.; Farokhzad, O. C. *Nano Lett.* **2007**, *7*, 3065.
(397) Kim, J.; Kim, H. S.; Lee, N.; Kim, T.; Kim, H.; Yu, T.; Song, I. C.; Moon, W. K.; Hyeon, T. *Angew. Chem., Int. Ed.* **2008**, *47*, 8438.
(398) Camilleri-Broet, S.; Hardy-Bessard, A. C.; Le Tourneau, A.; Paraiso, D.; Levrel, O.; Leduc, B.; Bain, S.; Orfeuvre, H.; Audouin, J.; Pujade-Lauraine, E. *Ann. Oncol.* **2004**, *15*, 104.
(399) Tovey, S. M.; Brown, S.; Doughty, J. C.; Mallon, E. A.; Cooke, T. G.; Edwards, J. *Br. J. Cancer* **2009**, *100*, 680.
(400) Yang, J.; Lee, C. H.; Ko, H. J.; Suh, J. S.; Yoon, H. G.; Lee, K.; Huh, Y. M.; Haam, S. *Angew. Chem., Int. Ed.* **2007**, *46*, 8836.
(401) Schmieder, A. H.; Caruthers, S. D.; Zhang, H.; Williams, T. A.; Robertson, J. D.; Wickline, S. A.; Lanza, G. M. *FASEB J.* **2008**, *22*, 4179.
(402) Alexiou, C.; Arnold, W.; Klein, R.; Parak, F. G.; Hulin, P.; Bergemann, C.; Erhardt, W.; Wagenpfeil, S.; Lübbe, A. S. *Cancer Res.* **2000**, *60*, 6641.
(403) Chertok, B.; David, A. E.; Yang, V. C. *Biomaterials* **2010**, *31*, 6317.
(404) Poore, G. A.; Senyei, A. E. *Eur. J. Cancer Clin. Oncol.* **1983**, *19*, 141.
(405) Widder, K. J.; Morris, R. M.; Poore, G. A.; Howard, D. P.; Senyei, A. F. *Eur. J. Cancer Clin. Oncol.* **1983**, *19*, 135.
(406) Blakemore, R. B. *Science* **1975**, *190*, 377.
(407) Fischer, H.; Mastrogiacomo, G.; Lofflerb, J. F.; Warthmann, R. F.; Weidlerd, P. G.; Gehring, A. U. *Earth Planet Sci. Lett.* **2008**, *270*, 200.
(408) Schuler, D. *J. Mol. Microbiol. Biotechnol.* **1999**, *1*, 79.
(409) Gorby, Y. A.; Beveridge, T. J.; Blakemore, R. P. *J. Bacteriol.* **1988**, *170*, 834.
(410) Grünberg, K.; Müller, E. C.; Otto, A.; Reszka, R.; Linder, D.; Kube, M.; Reinhardt, R.; Schüler, D. *Appl. Environ. Microbiol.* **2004**, *70*, 1040.
(411) Matsunaga, T.; Maeda, Y.; Yoshino, T.; Takeyama, H.; Takahashi, M.; Ginya, H.; Aasahina, J.; Tajima, H. *Anal. Chim. Acta* **2007**, *597*, 331.
(412) Takeyama, H.; Yamazawa, A.; Nakamura, C.; Matsunaga, T. *Biotechnol. Tech.* **1995**, *9*, 355.
(413) Sun, J. B.; Duan, J. H.; Dai, S. L.; Ren, J.; Zhang, Y. D.; Tian, J. S.; Li, Y. *Cancer Lett.* **2007**, *258*, 109.
(414) Chen, H.; Langer, R. *Pharm. Res.* **1997**, *14*, 537.
(415) Zhang, J.; Misra, R. D. *Acta Biomater.* **2007**, *3*, 838.
(416) Yuan, Q.; Venkatasubramanian, R.; Hein, S.; Misra, R. D. *Acta Biomater.* **2008**, *4*, 1024.
(417) Gaharwar, A. K.; Wong, J. E.; Müller-Schulte, D.; Bahadur, D.; Richtering, W. *J. Nanosci. Nanotechnol.* **2009**, *9*, 5355.
(418) Willmott, N. *Cancer Treat. Rev.* **1987**, *14*, 143.
(419) Ma, Y. H.; Hsu, Y. W.; Chang, Y. J.; Hua, M. Y.; Chen, J. P.; Wu, T. *J. Magn. Magn. Mater.* **2007**, *311*, 342.
(420) Torchilin, V. P.; Paptov, M. I.; Orekova, N. M.; Belyaev, A. A.; Petrov, A. D.; Ragimov, S. E. *Haemostasis* **1988**, *18*, 113.
(421) Larsen, C.; Østergaard, J.; Larsen, S. W.; Jensen, H.; Jacobsen, S.; Lindegaard, C.; Andersen, P. H. *J. Pharm. Sci.* **2008**, *97*, 4622.
(422) Butoescu, N.; Jordan, O.; Petri-Fink, A.; Hofmann, H.; Doelker, E. *J. Microencapsulation* **2008**, *25*, 339.
(423) Arias, J. L.; López-Viota, M.; López-Viota, J.; Delgado, A. V. *Int. J. Pharm.* **2009**, *382*, 270.
(424) Karalezli, N.; Ogun, T. C.; Kartal, S.; Saracgil, S. N.; Yel, M.; Tuncay, I. *Clin. Rheumatol.* **2007**, *26*, 569.
(425) Dhalla, N. S.; Temsah, R. M.; Netticadan, T. *J. Hypertension* **2000**, *18*, 655.
(426) Chorny, M.; Hood, E.; Levy, R. J.; Muzykantov, V. R. *J. Controlled Release* **2010**, *146*, 144.
(427) Kopke, R. D.; Wassel, R. A.; Mondalek, F.; Grady, B.; Chen, K.; Liu, J.; Gibson, D.; Dormer, K. J. *Audiol. Neurotol.* **2006**, *11*, 123.
(428) Forbes, Z. G.; Yellen, B. B.; Halverson, D. S.; Fridman, G.; Barbee, K. A.; Friedman, G. *IEEE Trans. Biomed. Eng.* **2008**, *55*, 643.
(429) Goldberg, S. L.; Loussararian, A.; De Gregorio, J.; Di Mario, C.; Albiero, R.; Colombo, A. *J. Am. Coll. Cardiol.* **2001**, *37*, 1019.
(430) McDowell, G.; Slevin, M.; Krupinski, J. *Vasc. Cell.* **2011**, *3*, 8.
(431) Kempe, H.; Kempe, M. *Biomaterials* **2010**, *31*, 9499.
(432) Chorny, M.; Fishbein, I.; Yellen, B. B.; Alferiev, I. S.; Bakay, M.; Ganta, S.; Adamo, R.; Amiji, M.; Friedman, G.; Levy, R. J. *Proc. Natl. Acad. Sci. U.S.A.* **2010**, *107*, 8346.
(433) Mykhaylyk, O.; Antequera, Y. S.; Vlaskou, D.; Plank, C. *Nat. Protoc.* **2007**, *2*, 2391.
(434) Juliano, R. L.; Alahari, S.; Yoo, H.; Kole, R.; Cho, M. *Pharm. Res.* **1999**, *16*, 494.
(435) Brigger, I.; Dubernet, C.; Couvreur, P. *Adv. Drug Delivery Rev.* **2002**, *54*, 631.
(436) Toub, N.; Malvy, C.; Fattal, E.; Couvreur, P. *Biomed. Pharmacother.* **2006**, *60*, 607.
(437) Fattal, E.; Barratt, G. *Br. J. Pharmacol.* **2009**, *157*, 179.
(438) Li, W.; Szoka, F. C., Jr. *Pharm. Res.* **2007**, *24*, 438.
(439) Plank, C.; Scherer, F.; Schillinger, U.; Bergemann, C.; Anton, M. *J. Liposome Res.* **2003**, *13*, 29.
(440) Plank, C.; Anton, M.; Rudolph, C.; Rosenecker, J.; Krotz, F. *Expert Opin. Biol. Ther.* **2003**, *3*, 745.
(441) Nesbeth, D.; Williams, S. L.; Chan, L.; Brain, T.; Slater, N. K.; Farzaneh, F.; Darling, D. *Mol. Ther.* **2006**, *13*, 814.
(442) Hughes, C.; Galea-Lauri, J.; Farzaneh, F.; Darling, D. *Mol. Ther.* **2001**, *3*, 623.
(443) Schillinger, U.; Brill, T.; Rudolph, C.; Huth, S.; Gersting, S.; Krotz, F.; Hirschberger, J.; Bergemann, C.; Plank, C. *J. Magn. Magn. Mater.* **2005**, *293*, 501.
(444) Pan, B. F.; Cui, D. X.; Sheng, Y.; Ozkan, C. G.; Gao, F.; He, R.; Li, Q.; Xu, P.; Huang, T. *Cancer Res.* **2007**, *67*, 8156.
(445) Morishita, N.; Nakagami, H.; Morishita, R.; Takeda, S.; Mishima, F.; Terazono, B.; Nishijima, S.; Kaneda, Y.; Tanaka, N. *Biochem. Biophys. Res. Commun.* **2005**, *9*, 1121.
(446) Remy, J. S.; Abdallah, B.; Zanta, M. A.; Boussif, O.; Behr, J. P.; Demeneix, B. *Adv. Drug Delivery Rev.* **1998**, *30*, 85.

(447) Abdallah, B.; Hassan, A.; Benoist, C.; Goula, D.; Behr, J. P.; Demeneix, B. A. *Hum. Gene Ther.* **1996**, *7*, 1947.
(448) Akinc, A.; Thomas, M.; Klibanov, A. M.; Langer, R. *J. Gene Med.* **2005**, *7*, 657.
(449) Mykhaylyk, O.; Vlaskou, D.; Tresilwised, N.; Pithayanukul, P.; Moller, W.; Plank, C. *J. Magn. Magn. Mater.* **2007**, *311*, 275.
(450) Hirao, K.; Sugita, T.; Kubo, T.; Igarashi, K.; Tanimoto, K.; Murakami, T.; Yasunaga, Y.; Ochi, M. *Int. J. Oncol.* **2003**, *22*, 1065.
(451) Yang, S. Y.; Sun, J. S.; Liu, C. H.; Tsuang, Y. H.; Chen, L. T.; Hong, C. Y.; Yang, H. C.; Horng, H. E. *Artif. Organs* **2008**, *32*, 195.
(452) Ino, K.; Kawasumi, T.; Ito, A.; Honda, H. *Biotechnol. Bioeng.* **2008**, *100*, 168.
(453) Pan, X.; Guan, J.; Yoo, J. W.; Epstein, A. J.; Lee, L. J.; Lee, R. J. *Int. J. Pharm.* **2008**, *358*, 263.
(454) Bhattarai, S. R.; Kim, S. Y.; Jang, K. Y.; Lee, K. C.; Yi, H. K.; Lee, D. Y.; Kim, H. Y.; Hwang, P. H. *Nanomedicine* **2008**, *4*, 146.
(455) Lee, C. H.; Kim, E. Y.; Jeon, K.; Tae, J. C.; Lee, K. S.; Kim, Y. O.; Jeong, M. Y.; Yun, C. W.; Jeong, D. K.; Cho, S. K.; Kim, J. H.; Lee, H. Y.; Riu, K. Z.; Cho, S. G.; Park, S. P. *Stem Cells Dev.* **2008**, *17*, 133.
(456) Scherer, F.; Anton, M.; Schillinger, U.; Henke, J.; Bergemann, C.; Krüger, A.; Gänsbacher, B.; Plank, C. *Gene Ther.* **2002**, *9*, 102.
(457) Krotz, F.; de Wit, C.; Sohn, H. Y.; Zahler, S.; Gloe, T.; Pohl, U.; Plank, C. *Mol. Ther.* **2003**, *7*, 700.
(458) Jahnke, A.; Hirschberger, J.; Fischer, C.; Brill, T.; Köstlin, R.; Plank, C.; Küchenhoff, H.; Krieger, S.; Kamenica, K.; Schillinger, U. *J. Vet. Med. A: Physiol. Pathol. Clin. Med.* **2007**, *54*, 599.
(459) Hüttinger, C.; Hirschberger, J.; Jahnke, A.; Köstlin, R.; Brill, T.; Plank, C.; Küchenhoff, H.; Krieger, S.; Schillinger, U. *J. Gene Med.* **2008**, *10*, 655.
(460) Govindan, S. V.; Goldenberg, D. M. In *Macromolecular Anticancer Therapeutics*; Reddy, L. H., Couvreur, P., Eds.; Springer Science−Humana Press: New York, 2010.
(461) Natarajan, A.; Xiong, C. Y.; Gruettner, C.; DeNardo, G. L.; DeNardo, S. J. *Cancer Biother. Radiopharm.* **2008**, *23*, 82.
(462) Chen, J.; Wu, H.; Han, D.; Xie, C. *Cancer Lett.* **2006**, *231*, 169.
(463) Natarajan, A.; Gruettner, C.; Ivkov, R.; DeNardo, G. L.; Mirick, G.; Yuan, A.; Foreman, A.; DeNardo, S. J. *Bioconjugate Chem.* **2008**, *19*, 1211.
(464) Konan, Y. N.; Gurny, R.; Allemann, E. *J. Photochem. Photobiol. B* **2002**, *66*, 89.
(465) Park, S. I.; Hwang, Y. H.; Lim, J. H.; Kim, J. H.; Yun, H. I.; Kim, C. O. *J. Magn. Magn. Mater.* **2006**, *304*, e403.
(466) Primo, F. L.; Macaroff, P. P.; Lacava, Z. G. M.; Azevedo, R. B.; Morais, P. C.; Tedesco, A. C. *J. Magn. Magn. Mater.* **2007**, *310*, 2838.
(467) Primo, F. L.; Michieleto, L.; Rodrigues, M. A. M.; Macaroff, P. P.; Morais, P. C.; Lacava, Z. G. M.; Bentley, M. V. L. B.; Tedesco, A. C. *J. Magn. Magn. Mater.* **2007**, *311*, 354.
(468) Huang, P.; Li, Z.; Lin, J.; Yang, D.; Gao, G.; Xu, C.; Bao, L.; Zhang, C.; Wang, K.; Song, H.; Hu, H.; Cui, D. *Biomaterials* **2011**, *32*, 3447.
(469) Cinteza, L. O.; Ohulchanskyy, T. Y.; Sahoo, Y.; Bergey, E. J.; Pandey, R. K.; Prasad, P. N. *Mol. Pharmaceutics* **2006**, *3*, 415.
(470) Ding, J.; Zhao, J.; Cheng, K.; Liu, G.; Xiu, D. *J. Biomed. Nanotechnol.* **2010**, *6*, 683.
(471) Kopelman, R.; Koo, Y. E. L.; Philbert, M.; Moffat, B. A.; Reddy, G. R.; McConville, P.; Hall, D. E.; Chenevert, T. L.; Bhojani, M. S.; Buck, S. M.; Rehemtulla, A.; Ross, B. D. *J. Magn. Magn. Mater.* **2005**, *293*, 404.
(472) Chen, Z. L.; Sun, Y.; Huang, P.; Yang, X. X.; Zhou, X. P. *Nanoscale Res Lett.* **2009**, *4*, 400.
(473) Lai, C. W.; Wang, Y. H.; Lai, C. H.; Yang, M. J.; Chen, C. Y.; Chou, P. T.; Chan, C. S.; Chi, Y.; Chen, Y. C.; Hsiao, J. K. *Small* **2008**, *4*, 218.
(474) Lim, Y. T.; Cho, M. Y.; Kim, J. K.; Hwangbo, S.; Chung, B. H. *ChemBioChem* **2007**, *8*, 2204.
(475) Jordan, A.; Scholz, R.; Wust, P.; Fähling, H.; Felix, R. *J. Magn. Magn. Mater.* **1999**, *201*, 413.
(476) Ito, A.; Tanaka, K.; Honda, H.; Abe, S.; Yamaguchi, H.; Kobayashi, T. *J. Biosci. Bioeng.* **2003**, *96*, 364.
(477) Ito, A.; Shinkai, M.; Honda, H.; Kobayashi, T. *J. Biosci. Bioeng.* **2005**, *100*, 1.
(478) Hilger, I.; Hergt, R.; Kaiser, W. A. *J. Magn. Magn. Mater.* **2005**, *293*, 314.
(479) Campbell, R. B. *Nanomedicine (London)* **2007**, *2*, 649.
(480) Fortin, J. P.; Wilhelm, C.; Servais, J.; Ménager, C.; Bacri, J. C.; Gazeau, F. *J. Am. Chem. Soc.* **2007**, *129*, 2628.
(481) Fortin, J. P.; Gazeau, F.; Wilhelm, C. *Eur. Biophys. J.* **2008**, *37*, 223.
(482) Jordan, A.; Scholz, R.; Maier-Hauff, K.; Johannsen, M.; Wust, P.; Nadobny, J.; Schirra, H.; Schmidt, H.; Deger, S.; Loening, S.; Lanksch, W.; Felix, R. *J. Magn. Magn. Mater.* **2001**, *225*, 118.
(483) Moroz, P.; Jones, S. K.; Gray, B. N. *Int. J. Hyperthermia* **2002**, *18*, 267.
(484) Tanaka, K.; Ito, A.; Kobayashi, T.; Kawamura, T.; Shimada, S.; Matsumoto, K.; Saida, T.; Honda, H. *J. Biosci. Bioeng.* **2005**, *100*, 112.
(485) Glöckl, G.; Hergt, R.; Zeisberger, M.; Dutz, S.; Nagel, S.; Weitschies, W. *J. Phys. Cond. Matter.* **2006**, *18*, S2935.
(486) Huber, D. L. *Small* **2005**, *1*, 482.
(487) Hilger, I.; Andrä, W.; Hergt, R.; Hiergeist, R.; Schubert, H.; Kaiser, W. A. *Radiology* **2001**, *218*, 570.
(488) Jordan, A.; Scholz, R.; Wust, P.; Schirra, H.; Schiestel, T.; Schmidt, H.; Felix, R. *J. Magn. Magn. Mater.* **1999**, *194*, 185.
(489) Jordan, A.; Maier-Hauff, K. *J. Nanosci. Nanotechnol.* **2007**, *7*, 4604.
(490) Jordan, A.; Scholz, R.; Maier-Hauff, K.; van Landeghem, F. K. H.; Waldoefner, N.; Teichgraeber, U.; Pinkernelle, J.; Bruhn, H.; Neumann, F.; Thiesen, B.; von Deimling, A.; Felix, R. *J. Neurooncol.* **2006**, *78*, 7.
(491) Multhoff, G.; Bozler, C.; Wiesnet, M.; Müller, E.; Meier, T.; Wilmanns, W.; Issels, R. D. *Int. J. Cancer* **1995**, *61*, 272.
(492) Ito, A.; Shinkai, M.; Honda, H.; Wakabayashi, T.; Yoshida, J.; Kobayashi, T. *Cancer Immunol. Immunother.* **2001**, *50*, 515.
(493) Ito, A.; Shinkai, M.; Honda, H.; Yoshikawa, K.; Saga, S.; Wakabayashi, T.; Yoshida, J.; Kobayashi, T. *Cancer Immunol. Immunother.* **2003**, *52*, 80.
(494) Yan, S.; Zhang, D.; Gu, N.; Zheng, J.; Ding, A.; Wang, Z.; Xing, B.; Ma, M.; Zhang, Y. *J. Nanosci. Nanotechnol.* **2005**, *5*, 1185.
(495) Babincov, M.; Altanerov, V.; Altaner, C.; Bergemann, C.; Babinec, P. *IEEE Trans. Nanobiosci.* **2008**, *7*, 15.
(496) Ang, K. L.; Venkatraman, S.; Ramanujan, R. V. *Mater. Sci. Eng., C* **2007**, *27*, 347.
(497) Lehmann, J.; Natarajan, A.; Denardo, G. L.; Ivkov, R.; Foreman, A. R.; Catapano, C.; Mirick, G.; Ouang, T.; Gruettner, C.; Denardo, S. J. *Cancer Biother. Radiopharm.* **2008**, *23*, 265.
(498) Sonvico, F.; Mornet, S.; Vasseur, S.; Dubernet, C.; Jaillard, D.; Degrouard, J.; Hoebeke, J.; Duguet, E.; Colombo, P.; Couvreur, P. *Bioconjugate Chem.* **2005**, *16*, 1181.
(499) Rastogi, R.; Gulati, N.; Kotlana, R. K.; Sharma, U.; Jayasundar, R.; Koul, V. *Colloids Surf., B* **2011**, *82*, 160.
(500) Ito, A.; Kuga, Y.; Honda, H.; Kikkawa, H.; Horiuchi, A.; Watanabe, Y.; Kobayashi, T. *Cancer Lett.* **2004**, *212*, 167.
(501) Hayashi, K.; Ono, K.; Suzuki, H.; Sawada, M.; Moriya, M.; Sakamoto, W.; Yogo, T. *ACS Appl. Mater. Interfaces* **2010**, *2*, 1903.
(502) Hilger, I.; Hiergeist, R.; Hergt, R.; Winnefeld, K.; Schubert, H.; Kaiser, W. A. *Invest. Radiol.* **2002**, *37*, 580.
(503) Yukumi, S.; Watanabe, Y.; Horiuchi, A.; Doi, T.; Sato, K.; Yoshida, M.; Machara, T.; Aono, H.; Naohara, T.; Kawachi, K. *Anticancer Res.* **2008**, *28*, 69.
(504) DeNardo, S. J.; DeNardo, G. L.; Miers, L. A.; Natarajan, A.; Foreman, A. R.; Gruettner, C.; Adamson, G. N.; Ivkov, R. *Clin. Cancer Res.* **2005**, *11*, 7087s.
(505) Kong, G.; Braun, R. D.; Dewhirst, M. W. *Cancer Res.* **2000**, *60*, 4440.
(506) Needham, D.; Anyarambhatla, G.; Kong, G.; Dewhirst, M. W. *Cancer Res.* **2000**, *60*, 1197.
(507) Tashjian, J. A.; Dewhirst, M. W.; Needham, D.; Viglianti, B. L. *Int. J. Hyperthermia* **2008**, *24*, 79.
(508) Karino, T.; Koga, S.; Maeta, M. *Surg. Today* **1988**, *18*, 276.

(509) Horsman, M. R.; Overgaard, J. *Int. J. Hyperthermia* **1997**, *13*, 141.
(510) Kong, G.; Dewhirst, M. W. *Int. J. Hyperthermia* **1999**, *15*, 345.
(511) Cope, D.; Dewhirst, M.; Friedman, H.; Bigner, D.; Zalutsky, M. *Cancer Res.* **1990**, *50*, 1803.
(512) Hosono, M. N.; Hosono, M.; Endo, K.; Ueda, R.; Onoyama, Y. *J. Nucl. Med.* **1994**, *35*, 504.
(513) Johannsen, M.; Gneveckow, U.; Eckelt, L.; Feussner, A.; Waldöfner, N.; Scholz, R.; Deger, S.; Wust, P.; Loening, S. A.; Jordan, A. *Int. J. Hyperthermia* **2005**, *21*, 637.
(514) Johannsen, M.; Gneveckow, U.; Taymoorian, K.; Thiesen, B.; Waldöfner, N.; Scholz, R.; Jung, K.; Jordan, A.; Wust, P.; Loening, S. A. *Int. J. Hyperthermia* **2007**, *23*, 315.
(515) Johannsen, M.; Gneveckow, U.; Thiesen, B.; Taymoorian, K.; Cho, C. H.; Waldöfner, N.; Scholz, R.; Jordan, A.; Loening, S. A.; Wust, P. *Eur. Urol.* **2007**, *52*, 1653.
(516) Wust, P.; Gneveckow, U.; Johannsen, M.; Böhmer, D.; Henkel, T.; Kahmann, F.; Sehouli, J.; Felix, R.; Ricke, J.; Jordan, A. *Int. J. Hyperthermia* **2006**, *22*, 673.
(517) Maier-Hauff, K.; Rothe, R.; Scholz, R.; Gneveckow, U.; Wust, P.; Thiesen, B.; Feussner, A.; Deimling, A.; Waldoefner, N.; Felix, R.; Jordan, A. *J. Neurooncol.* **2007**, *81*, 53.
(518) Müller, S. *Nanomed. Nanotechnol. Biol. Med.* **2009**, *5*, 387.
(519) Sneed, P. K.; Stauffer, P. R.; McDermott, M. W.; Diederich, C. J.; Lamborn, K. R.; Prados, M. D.; Chang, S.; Weaver, K. A.; Spry, L.; Malec, M. K.; Lamb, S. A.; Voss, B.; Davis, R. L.; Wara, W. M.; Larson, D. A.; Phillips, T. L.; Gutin, P. H. *Int. J. Radiat. Oncol. Biol. Phys.* **1998**, *40*, 287.
(520) Kroft, L. J. M.; Doornbos, J.; van der Geest, R. J.; van der Laarse, A.; van der Meulen, H.; de Roos, A. *Magn. Reson. Imaging* **1998**, *16*, 755.
(521) Terreno, E.; Castelli, D. D.; Viale, A.; Aime, S. *Chem. Rev.* **2010**, *110*, 3019.
(522) Qiao, R.; Yang, C.; Gao, M. *J. Mater. Chem.* **2009**, *19*, 6274.
(523) Vogl, T. J.; Hammerstingl, R.; Schwarz, W.; Mack, M. G.; Muller, P. K.; Pegios, W.; Keck, H.; Eibl-Eibesfeldt, V.; Hoelzl, J.; Woessmer, B.; Bergman, V.; Felix, R. *Radiology* **1996**, *198*, 881.
(524) Oswald, P.; Clement, O.; Chambon, C.; Schouman-Claeys, E.; Frija, G. *Magn. Reson. Imaging* **1997**, *15*, 1025.
(525) Shamsi, K.; Balzer, T.; Saini, S.; Ros, P. R.; Nelson, R. C.; Carter, E. C.; Tollerfield, S.; Niendorf, H. P. *Radiology* **1998**, *206*, 365.
(526) Abe, Y.; Yamashita, Y.; Namimoto, T.; Tang, Y.; Takahashi, M. *Radiat. Med.* **2000**, *18*, 97.
(527) Reimer, P.; Tombach, B. *Eur. Radiol.* **1998**, *8*, 1198.
(528) Reddy, L. H.; Couvreur, P. *J. Hepatol.* **2011**, *55*, 1461.
(529) Lind, K.; Kresse, M.; Debus, N. P.; Müller, R. H. *J. Drug Target.* **2002**, *10*, 221.
(530) Mack, M. G.; Balzer, J. O.; Straub, R.; Eichler, V.; Vogl, T. J. *Radiology* **2002**, *222*, 239.
(531) Thorek, D. L. J.; Chen, A. K.; Czupryna, J.; Tsourkas, A. *Ann. Biomed. Eng.* **2006**, *34*, 23.
(532) Corot, C.; Petry, K. G.; Trivedi, R.; Saleh, A.; Jonkmanns, C.; Le Bas, J. F.; Blezer, E.; Rausch, M.; Brochet, B.; Foster-Gareau, P.; Baleriaux, D.; Gaillard, S.; Dousset, V. *Invest. Radiol.* **2004**, *39*, 619.
(533) Hauger, O.; Grenier, N.; Deminere, C.; Laseur, C.; Delmas, Y.; Merville, P.; Combe, C. *Eur. Radiol.* **2007**, *17*, 2898.
(534) Lefevre, S.; Ruimy, D.; Jehl, F.; Neuville, A.; Robert, P.; Sordet, C.; Ehlinger, M.; Dietemann, J. L.; Bierry, G. *Radiology* **2011**, *258*, 722.
(535) Guimaraes, R.; Clément, O.; Bittoun, J.; Carnot, F.; Frija, G. *Am. J. Roentgenol.* **1994**, *162*, 201.
(536) Harisinghani, M. G.; Saksena, M. A.; Hahn, P. F.; King, B.; Kim, J.; Torabi, M. T.; Weissleder, R. *Am. J. Roentgenol.* **2006**, *186*, 144.
(537) Islam, T.; Harisinghani, M. G. *Cancer Biomarkers* **2009**, *5*, 61.
(538) Anzai, Y.; Piccoli, C. W.; Outwater, E. K.; Stanford, W.; Bluemke, D. A.; Nurenberg, P.; Saini, S.; Maravilla, K. R.; Feldman, D. E.; Schmiedl, U. P.; Brunberg, J. A.; Francis, I. R.; Harms, S. E.; Som, P. M.; Tempany, C. M. *Radiology* **2003**, *228*, 777.
(539) Will, O.; Purkayastha, S.; Chan, C.; Athanasiou, T.; Darzi, A. W.; Gedrovc, W.; Tekkis, P. P. *Lancet Oncol.* **2006**, *7*, 52.
(540) Dousset, V.; Delalande, C.; Ballarino, L.; Quesson, B.; Seilhan, D.; Coussemacq, M.; Thiaudiére, D.; Brochet, B.; Canioni, P.; Caillé, J. M. *Magn. Reson. Med.* **1999**, *41*, 329.
(541) Müller, R. N.; Gillis, P.; Moiny, F.; Roch, A. *Magn. Reson. Med.* **1991**, *22*, 178.
(542) Chambon, C.; Clement, O.; Le Blanche, A.; Schouman-Claeys, E.; Frija, G. *Magn. Reson. Imaging* **1993**, *11*, 509.
(543) Schmitz, S. A.; Coupland, S. E.; Gust, R.; Winterhalter, S.; Wagner, S.; Kresse, M.; Semmler, W.; Wolf, K. J. *Invest. Radiol.* **2000**, *35*, 460.
(544) Ruehm, S. G.; Corot, C.; Vogt, P.; Kolb, S.; Debatin, J. F. *Circulation* **2001**, *103*, 415.
(545) Trivedi, R. A.; Mallawarachi, C.; U-King-Im, J. M.; Graves, M. J.; Horsley, J.; Goddard, M. J.; Brown, A.; Wang, L.; Kirkpatrick, P. J.; Brown, J.; Gillard, J. H. *Arterioscler. Thromb. Vasc. Biol.* **2006**, *26*, 1601.
(546) Virmani, R.; Kolodgie, F. D.; Burke, A. P.; Finn, A. V.; Gold, H. K.; Tulenko, T. N.; Wrenn, S. P.; Narula, J. *Arterioscler., Thromb., Vasc. Biol.* **2005**, *25*, 2054.
(547) Kooi, M. E.; Cappendijk, V. C.; Cleutjens, K.; Kessels, A. G. H.; Kitslaar, P.; Borgers, M.; Frederik, P. M; Daemen, M.; van Engelshoven, J. M. A. *Circulation* **2003**, *107*, 2453.
(548) Rausch, M.; Sauter, A.; Fröhlich, J.; Neubacher, U.; Radü, E. W.; Rudin, M. *Magn. Reson. Med.* **2001**, *46*, 1018.
(549) Saleh, A.; Schroeter, M.; Jonkmanns, C.; Hartung, H. P.; MoÈdder, U.; Jander, S. *Brain* **2004**, *127*, 1670.
(550) Neuwelt, E. A.; Varallyay, P.; Bago, A. G.; Muldoon, L. L.; Nesbit, G.; Nixon, R. *Neuropathol. Appl. Neurobiol.* **2004**, *30*, 456.
(551) Hunt, M. A.; Bago, A. G.; Neuwelt, E. A. *Am. J. Neuroradiol.* **2005**, *26*, 1084.
(552) Baeten, K.; Hendriks, J. J.; Hellings, N.; Theunissen, E.; Vanderlocht, J.; Ryck, L. D.; Gelan, J.; Stinissen, P.; Adriaensens, P. *Neuroimmunol.* **2008**, *195*, 1.
(553) Dousset, V.; Brochet, B.; Deloire, M. S.; Lagoarde, L.; Barroso, B.; Caille, J. M.; Petry, K. G. *Am. J. Neuroradiol.* **2006**, *27*, 1000.
(554) Zhang, Y.; Dodd, S. J.; Hendrich, K. S.; Williams, M.; Ho, C. *Kidney Int.* **2000**, *58*, 1300.
(555) Kanno, C.; Lee, P. C.; Dodd, S. J.; Williams, M.; Griffith, B. P.; Ho, C. *J. Thorac. Cardiovasc. Surg.* **2000**, *120*, 923.
(556) Bierry, G.; Jehl, F.; Neuville, A.; Lefevre, S.; Robert, P.; Kremer, S.; Dietemann, J. L. *Am. J. Roentgenol.* **2010**, *194*, W521.
(557) Lutz, A. M.; Seemayer, C.; Corot, C.; Gay, R. E.; Goepfert, K.; Michel, B. A.; Marincek, B.; Gay, S.; Weishaupt, D. *Radiology* **2004**, *233*, 149.
(558) Kanno, S.; Wu, Y. J.; Lee, P. C.; Dodd, S. J.; Williams, M.; Griffith, B. P.; Ho, C. *Circulation* **2001**, *104*, 934.
(559) Sosnovik, D. E.; Nahrendorf, M.; Weissleder, R. *Circulation* **2007**, *115*, 2076.
(560) Sosnovik, D. E.; Nahrendorf, M.; Deliolanis, N.; Novikov, M.; Aikawa, E.; Josephson, L.; Rosenzweig, A.; Weissleder, R.; Ntziachristos, V. *Circulation* **2007**, *115*, 1384.
(561) Sosnovik, D. E.; Nahrendorf, M.; Weissleder, R. *Basic Res. Cardiol.* **2008**, *103*, 122.
(562) Kou, G.; Wang, S.; Cheng, C.; Gao, J.; Li, B.; Wang, H.; Qian, W.; Hou, S.; Zhang, D.; Dai, J.; Gu, H; Guo, Y. *Biochem. Biophys. Res. Commun.* **2008**, *374*, 192.
(563) Li, X.; Du, X.; Huo, T.; Liu, X.; Zhang, S.; Yuan, F. *Acta Radiol.* **2009**, *50*, 583.
(564) Zhang, C. F.; Jugold, M.; Woenne, E. C.; Lammers, T.; Morgenstern, B.; Mueller, M. M.; Zentgraf, H.; Bock, M.; Eisenhut, M.; Semmler, W.; Kiessling, F. *Cancer Res.* **2007**, *67*, 1555.
(565) Yang, J.; Wadghiri, Y. Z.; Hoang, D. M.; Tsui, W.; Sun, Y.; Chung, E.; Li, Y.; Wang, A.; de Leon, M.; Wisniewski, T. *Neuroimage* **2011**, *55*, 1600.
(566) Sun, C.; Sze, R.; Zhang, M. Q. *J. Biomed. Mater. Res., Part A* **2006**, *78*, 550.

(567) Meier, R.; Henning, T. D.; Boddington, S.; Tavri, S.; Arora, S.; Piontek, G.; Rudelius, M.; Corot, C.; Daldrup-Link, H. E. *Radiology* **2010**, *255*, 527.
(568) Bulte, J. W.; Zhang, S.; van Gelderen, P.; Herynek, V.; Jordan, E. K.; Duncan, I. D.; Frank, J. A. *Proc. Natl. Acad. Sci. U.S.A.* **1999**, *96*, 15256.
(569) Bulte, J. W. M. *J. Magn. Magn. Mater.* **2005**, *289*, 423.
(570) Bulte, J. W. *Methods Mol. Med.* **2006**, *124*, 419.
(571) Zhang, C.; Liu, T.; Gao, J.; Su, Y.; Shi, C. *Mini-Rev. Med. Chem.* **2010**, *10*, 193.
(572) Jendelová, P.; Herynek, V.; DeCroos, J.; Glogarová, K.; Andersson, B.; Hájek, M.; Syková, E. *Magn. Reson. Med.* **2003**, *50*, 767.
(573) Metz, S.; Bonaterra, G.; Rudelius, M.; Settles, M.; Rummeny, E. J.; Daldrup-Link, H. E. *Eur. Radiol* **2004**, *14*, 1851−1858.
(574) Shapiro, E. M.; Skrtic, S.; Koretsky, A. P. *Magn. Reson. Med.* **2005**, *53*, 329.
(575) Zhao, M.; Kircher, M. F.; Josephson, L.; Weissleder, R. *Bioconjug. Chem.* **2002**, *13*, 840.
(576) Xie, J.; Wang, J.; Niu, G.; Huang, J.; Chen, K.; Li, X.; Chen, X. *Chem. Commun.* **2010**, *46*, 433.
(577) Arbab, A. S.; Yocum, G. T.; Wilson, L. B.; Parwana, A.; Jordan, E. K.; Kalish, H.; Frank, J. A. *Mol. Imaging* **2004**, *3*, 24.
(578) Arbab, A. S.; Yocum, G. T.; Kalish, H.; Jordan, E. K.; Anderson, S. A.; Khakoo, A. Y.; Read, E. J.; Frank, J. A. *Blood* **2004**, *104*, 1217.
(579) Arbab, A. S.; Yocum, G. T.; Rad, A. M.; Khakoo, A. Y.; Fellowes, V.; Read, E. J.; Frank, J. A. *NMR Biomed.* **2005**, *18*, 553.
(580) Janic, B.; Rad, A. M.; Jordan, E. K.; Iskander, A. S.; Ali, M. M.; Varma, N. R.; Frank, J. A.; Arbab, A. S. *PLoS One* **2009**, *4*, e5873.
(581) Wu, Y. J.; Muldoon, L. L.; Varallyay, C.; Markwardt, S.; Jones, R. E.; Neuwelt, E. A. *Am. J. Physiol., Cell Physiol.* **2007**, *293*, C1698.
(582) Walczak, P.; Kedziorek, D. A.; Gilad, A. A.; Lin, S.; Bulte, J. W. *Magn. Reson. Med.* **2005**, *54*, 769.
(583) Amsalem, Y.; Mardor, Y.; Feinberg, M. S.; Landa, N.; Miller, L.; Daniels, D.; Ocherashvilli, A.; Holbova, R.; Yosef, O.; Barbash, I. M.; Leor, J. *Circulation* **2007**, *116*, 138.
(584) Babič, M.; Horák, D.; Trchová, M.; Jendelová, P.; Glogarová, K.; Lesný, P.; Herynek, V.; Hájek, M.; Syková, E. *Bioconjugate Chem.* **2008**, *19*, 740.
(585) Chaleawlert-Umpon, S.; Mayen, V.; Manotham, K.; Pimpha, N. *J. Biomater. Sci., Polym. Ed.* **2010**, *21*, 1515.
(586) Daldrup-Link, H. E.; Rudelius, M.; Piontek, G.; Metz, S.; Bräuer, R.; Debus, G.; Corot, C.; Schlegel, J.; Link, T. M.; Peschel, C.; Rummeny, E. J.; Oostendorp, R. A. *Radiology* **2005**, *234*, 197.
(587) Tallheden, T.; Nannmark, U.; Lorentzon, M.; Rakotonirainy, O.; Soussi, B.; Waagstein, F.; Jeppsson, A.; Sjögren-Jansson, E.; Lindahl, A.; Omerovic, E. *Life Sci.* **2006**, *79*, 999.
(588) Neri, M.; Maderna, C.; Cavazzin, C.; Deidda-Vigoriti, V.; Politi, L. S.; Scotti, G.; Marzola, P.; Sbarbati, A.; Vescovi, A. L.; Gritti, A. *Stem Cells* **2008**, *26*, 505.
(589) Anderson, S. A.; Glod, J.; Arbab, A. S.; Noel, M.; Ashari, P.; Fine, H. A.; Frank, J. A. *Blood* **2005**, *105*, 420.
(590) Zhang, S.; He, H.; Lu, W.; Xu, Q.; Zhou, B.; Tang, X. *Pancreas* **2009**, *38*, 293.
(591) Evgenov, N. V.; Medarova, Z.; Dai, G.; Bonner-Weir, S.; Moore, A. *Nat. Med.* **2006**, *12*, 144.
(592) Toso, C.; Vallee, J. P.; Morel, P.; Ris, F.; Demuylder-Mischler, S.; Lepetit-Coiffe, M.; Marangon, N.; Saudek, F.; James-Saphiro, A. M.; Bosco, D.; Berney, T. *Am. J. Transplant.* **2008**, *8*, 701.
(593) de Vries, I. J.; Lesterhuis, W. J.; Barentsz, J. O.; Verdijk, P.; van Krieken, J. H.; Boerman, O. C.; Oyen, W. J.; Bonenkamp, J. J.; Boezeman, J. B.; Adema, G. J.; Bulte, J. W.; Scheenen, T. W.; Punt, C. J.; Heerschap, A.; Figdor, C. G. *Nat. Biotechnol.* **2005**, *23*, 1407.
(594) Kubinova, S.; Sykova, E. *Minim. Invasive Ther. Allied Technol.* **2010**, *19*, 144.
(595) Ito, A.; Takizawa, Y.; Honda, H.; Hata, K.; Kagami, H.; Ueda, M.; Kobayashi, T. *Tissue Eng.* **2004**, *10*, 833.
(596) Bock, N.; Riminucci, A.; Dionigi, C.; Russo, A.; Tampieri, A.; Landi, E.; Goranov, V. A.; Marcacci, M.; Dediu, V. *Acta Biomater.* **2010**, *6*, 786.
(597) Ishii, M.; Shibata, R.; Numaguchi, Y.; Kito, T.; Suzuki, H.; Shimuzu, K.; Ito, A.; Honda, H.; Murohara, T. *Arterioscler., Thromb., Vasc. Biol.* **2011**, *31*, 2210.
(598) Ito, A.; Ino, K.; Kobayashi, T.; Honda, H. *Biomaterials* **2005**, *26*, 6185.
(599) Hu, S. H.; Liu, T. Y.; Tsai, C. H.; Chen, S. Y. *J. Magn. Magn. Mater.* **2007**, *310*, 2871.
(600) Sasaki, T.; Iwasaki, N.; Kohno, K.; Kishimoto, M.; Majima, T.; Nishimura, S. I.; Minami, A. *J. Biomed. Mater. Res.* **2008**, *86A*, 969.
(601) Nedopil, A. J.; Mandrussow, L. G.; Daldrup-Link, H. E. *J. Vis. Exp.* **2010**, *38*, 1793.
(602) Shimuzu, K.; Ito, A.; Honda, H. *J. Biomed. Mater. Res., Part B: Appl. Biomater.* **2006**, *77B*, 265.
(603) Ito, A.; Akiyama, H.; Kawabe, Y.; Kamihira, M. *J. Biosci. Bioeng.* **2007**, *104*, 288.
(604) Ito, A.; Ino, K.; Hayashida, M.; Kobayashi, T.; Matsunuma, H.; Kagami, H.; Ueda, M.; Honda, H. *Tissue Eng.* **2005**, *11*, 1553.
(605) Mironov, V.; Rasyanov, M.; Markwald, R. R. *Trends Biotechnol.* **2008**, *26*, 338.
(606) Shimuzu, K.; Ito, A.; Arinobe, M.; Murase, Y.; Iwata, Y.; Narita, Y.; Kagami, H.; Ueda, M.; Honda, H. *J. Biosci. Bioeng.* **2007**, *103*, 472.
(607) Ito, A.; Hibino, E.; Kobayashi, C.; Terasaki, H.; Kagami, H.; Ueda, M.; Kobayashi, T.; Honda, H. *Tissue Eng.* **2005**, *11*, 489.
(608) Shimuzu, K.; Ito, A.; Yoshida, T.; Yamada, Y.; Ueda, M.; Honda, H. *J. Biomed. Mater. Res., Part B: Appl. Biomater.* **2007**, *82B*, 471.
(609) Shimuzu, K.; Ito, A.; Honda, H. *J. Biosci. Bioeng.* **2007**, *104*, 171.
(610) Oshima, S.; Ishikawa, M.; Mochizuki, Y.; Kobayashi, T.; Yasunaga, Y.; Ochi, M. *J. Bone Joint Surg. Br.* **2010**, *92*, 1606.
(611) Kobayashi, T.; Ochi, M.; Yanada, S.; Ishikawa, M.; Adachi, N.; Deie, M.; Arihiro, K. *Arthroscopy* **2008**, *24*, 69.
(612) Kobayashi, T.; Ochi, M.; Yanada, S.; Ishikawa, M.; Adachi, N.; Deie, M.; Arihiro, K. *Arthroscopy* **2009**, *25*, 1435.
(613) Shimuzu, K.; Ito, A.; Yoshida, T.; Miwa, K.; Ishiguro, H.; Numaguchi, Y.; Murohara, T.; Kodama, I.; Honda, H. *Biotechnol. Bioeng.* **2007**, *96*, 803.
(614) Li, Y. G.; Gao, H. S.; Li, W. L.; Xing, J. M.; Liu, H. Z. *Bioresour. Technol.* **2009**, *100*, 5092.
(615) Ansari, F.; Grigoriev, P.; Libor, S.; Tothill, I. E.; Ramsden, J. J. *Biotechnol. Bioeng.* **2009**, *102*, 1505.
(616) Di Corato, R.; Piacenza, P.; Musarò, M.; Buonsanti, R.; Cozzoli, P. D.; Zambianchi, M.; Barbarella, G.; Cingolani, R.; Manna, L.; Pellegrino, T. *Macromol. Biosci.* **2009**, *9*, 952.
(617) Kaittanis, C.; Naser, S. A.; Perez, J. M. *Nano Lett.* **2007**, *7*, 380.
(618) Sudeshna, P.; Alocilja, E. C. *Biosens. Bioelectron.* **2009**, *24*, 1437.
(619) Mandal, S. M.; Ghosh, A. K.; Mandal, M. *Prep. Biochem. Biotechnol.* **2009**, *39*, 20.
(620) Liu, H. L.; Sonn, C. H.; Wu, J. H.; Lee, K. M.; Kim, Y. K. *Biomaterials* **2008**, *29*, 4003.
(621) Hoshino, A.; Ohnishi, N.; Yasuhara, M.; Yamamoto, K.; Kondo, A. *Biotechnol. Prog.* **2007**, *23*, 1513.
(622) Kaittanis, C.; Santra, S.; Perez, J. M. *J. Am. Chem. Soc.* **2009**, *131*, 12780.
(623) Wang, G. P.; Song, E. Q.; Xie, H. Y.; Zhang, Z. L.; Tian, Z. Q.; Zuo, C.; Pang, D. W.; Wu, D. C.; Shi, Y. B. *Chem. Commun.* **2005**, *34*, 4276.
(624) Song, E. Q.; Wang, G. P.; Xie, H. Y.; Zhang, Z. L.; Hu, J.; Peng, J.; Wu, D. C.; Shi, Y. B.; Pang, D. W. *Clin. Chem.* **2007**, *53*, 2177.
(625) van Engeland, M.; Nieland, L. J. W.; Ramaekers, F. C. S.; Schutte, B.; Reutelingsperger, C. P. M. *Cytometry* **1998**, *31*, 1.
(626) Wang, Y.; Ravindranath, S.; Irudayaraj, J. *Anal. Bioanal. Chem.* **2011**, *399*, 1271.
(627) Pamme, N.; Eijkel, J. C. T.; Manz, A. *J. Magn. Magn. Mater.* **2006**, *307*, 237.
(628) Vergun, L.; Klimchuk, D. A.; Gorbik, P. P.; Bondar, L. A.; Perekhristenko, P. M. *Mikrobiol Z.* **2009**, *71*, 65.
(629) Perez, J. M.; Josephson, L.; O'Loughlin, T.; Högemann, D.; Weissleder, R. *Nat. Biotechnol.* **2002**, *20*, 816.

(630) Haun, J. B.; Yoon, T. J.; Lee, H.; Weissleder, R. *Nanomed. Nanobiotechnol.* **2010**, *2*, 291.
(631) Josephson, L.; Perez, J. M.; Weissleder, R. *Angew. Chem., Int. Ed.* **2001**, *40*, 3204.
(632) Perez, J. M.; Simeone, F. J.; Saeki, Y.; Josephson, L.; Weissleder, R. *J. Am. Chem. Soc.* **2003**, *125*, 10192.
(633) Lee, H.; Sun, E.; Ham, D.; Weissleder, R. *Nat. Med.* **2008**, *14*, 869.
(634) Kaittanis, C.; Nath, S.; Perez, J. M. *PLoS One* **2008**, *3*, e3253.
(635) Pinkse, M. W. H.; Uitto, P. M.; Hilhorst, M. J.; Ooms, B.; Heck, A. J. R. *Anal. Chem.* **2004**, *76*, 3935.
(636) Lin, H. Y.; Chen, W. Y.; Chen, Y. C. *J. Biomed. Nanotechnol.* **2009**, *5*, 215.
(637) Lin, H. Y.; Chen, W. Y.; Chen, Y. C. *Anal. Bioanal. Chem.* **2009**, *394*, 2129.
(638) Qi, D.; Lu, J.; Deng, C.; Zhang, X. *J. Chromatogr., A* **2009**, *1216*, 5533.
(639) Lo, C. Y.; Chen, W. Y.; Chen, C. T.; Chen, Y. C. *J. Proteome Res.* **2007**, *6*, 887.
(640) Zeng, Y. Y.; Chen, H. J.; Shiau, K. J.; Hung, S. U.; Wang, Y. I.; Wu, C. C. *Proteomics* **2012**, *12*, 380.
(641) Shukoor, M. I.; Natalio, F.; Tahir, M. N.; Ksenofontov, V.; Therese, H. A.; Theato, P.; Schröder, H. C.; Müller, W. E.; Tremel, W. *Chem. Commun.* **2007**, *44*, 4677.
(642) Hickstein, B.; Peuker, U. A. *Biotechnol. Prog.* **2008**, *24*, 409.
(643) Mohapatra, S.; Pal, D.; Ghosh, S. K.; Pramanik, P. *J. Nanosci. Nanotechnol.* **2007**, *7*, 3193.
(644) Yu, C.; Zhao, J.; Guo, Y.; Lu, C.; Ma, X.; Gu, Z. *J. Biomed. Mater. Res., A* **2008**, *87*, 364.
(645) Pereira, C.; Pereira, A. M.; Quaresma, P.; Tavares, P. B.; Pereira, E.; Araujo, J. P.; Freire, C. *Dalton Trans.* **2010**, *39*, 2842.
(646) Bacri, J. C.; Perzynski, R.; Salin, D.; Cabuil, V.; Massart, R. *J. Magn. Magn. Mater.* **1990**, *85*, 27.
(647) Mehta, R. V.; Upadhyay, R. V.; Charles, S. W.; Ramchand, C. N. *Biotechnol. Tech.* **1997**, *11*, 493.
(648) Saiyed, Z. M.; Sharma, S.; Godawat, R.; Telang, S. D.; Ramchand, C. N. *J. Biotechnol.* **2007**, *131*, 240.
(649) Chen, J. P.; Lin, W. S. *Enzym. Microb. Technol.* **2003**, *32*, 801.
(650) Dyal, A.; Loos, K.; Noto, M.; Chang, S. W.; Spagnoli, C.; Shafi, K. V. P. M.; Ulman, A.; Cowman, M.; Gross, R. A. *J. Am. Chem. Soc.* **2003**, *125*, 1684.
(651) Bai, S.; Guo, Z.; Liu, W.; Sun, Y. *Food Chem.* **2006**, *96*, 1.
(652) Zhang, H. L.; Lai, G. S.; Han, D. Y.; Yu, A. M. *Anal. Bioanal. Chem.* **2008**, *390*, 971.
(653) Lei, Z.; Bi, S.; Hu, B.; Yang, H. *Food Chem.* **2007**, *105*, 889.
(654) Korecká, L.; Ježová, J.; Bílková, Z.; Beneš, M.; Horák, D.; Hradcová, O.; Slováková, M.; Viovy, J. L. *J. Magn. Magn. Mater.* **2005**, *293*, 349.
(655) Hong, J.; Gong, P. J.; Yu, J. H.; Xu, D. M.; Sun, H. W.; Yao, S. *J. Mol. Catal. B: Enzym.* **2006**, *42*, 99.
(656) Hong, J.; Xu, D.; Gong, P. J.; Sun, H.; Dong, L.; Yao, S. *J. Mol. Catal. B: Enzym.* **2007**, *45*, 84.
(657) Hong, J.; Gong, P.; Xu, D.; Dong, L.; Yao, S. *J. Biotechnol.* **2007**, *128*, 597.
(658) Kwon, H. S.; Han, K. C.; Hwang, K. S.; Lee, J. H.; Kim, T. S.; Yoon, D. S.; Yang, E. G. *Anal. Chim. Acta* **2007**, *585*, 344.
(659) Betancor, L.; Fuentes, M.; Dellamora-Ortiz, G.; López-Gallego, F.; Hidalgo, A.; Alonso-Morales, N.; Mateo, C.; Guisán, J. M.; Fernández-Lafuente, R. *J. Mol. Catal. B: Enzym.* **2005**, *32*, 97.
(660) Qiu, J.; Peng, H.; Liang, R. *Electrochem. Commun.* **2007**, *9*, 2734.
(661) Rossi, L. M.; Quach, A. D.; Rosenzweig, Z. *Anal. Bioanal. Chem.* **2004**, *380*, 606.
(662) Lee, D. G.; Ponvel, K. M.; Kim, M.; Hwang, S.; Ahn, I. S.; Lee, C. H. *J. Mol. Catal. B: Enzym.* **2009**, *57*, 62.
(663) Li, G. Y.; Huang, K. L.; Jiang, Y. R.; Yang, D. L.; Ding, P. *Int. J. Biol. Macromol.* **2008**, *42*, 405.
(664) Kuroiwa, T.; Noguchi, Y.; Nakajima, M.; Sato, S.; Mukataka, S.; Ichikawa, S. *Proc. Biochem.* **2008**, *43*, 62.
(665) Lei, L.; Bai, Y.; Li, Y.; Yi, L.; Yang, Y.; Xia, C. *J. Magn. Magn. Mater.* **2009**, *321*, 252.
(666) Huang, J.; Liu, C.; Xiao, H.; Wang, J.; Jiang, D.; Gu, E. *Int. J. Nanomed.* **2007**, *2*, 775.
(667) Choi, S. H.; Kim, H. S.; Lee, I. S.; Lee, E. Y. *Biotechnol. Lett.* **2010**, *32*, 1685.
(668) Fernandes, R.; Tsao, C. Y.; Hashimoto, Y.; Wang, L.; Wood, T. K.; Payne, G. F.; Bentley, W. E. *Metab. Eng.* **2007**, *9*, 228.
(669) Fernandes, R.; Bentley, W. E. *Biotechnol. Bioeng.* **2009**, *102*, 390.
(670) Grimm, J.; Perez, J. M.; Josephson, L.; Weissleder, R. *Cancer Res.* **2004**, *64*, 639.
(671) Perrin, A.; Theretz, A.; Lanet, V.; Vialle, S.; Mandrand, B. *J. Immunol. Methods* **1999**, *224*, 77.
(672) Liu, G.; Lin, Y. *J. Nanosci. Nanotechnol.* **2005**, *5*, 1060.
(673) Fuentes, M.; Mateo, C.; Rodriguez, A.; Casqueiro, M.; Tercero, J. C.; Riese, H. H.; Fernández-Lafuente, R.; Guisán, J. M. *Biosens. Bioelectron.* **2006**, *21*, 1574.
(674) Ibraimi, F.; Kriz, D.; Lu, M.; Hansson, L. O.; Kriz, K. *Anal. Bioanal. Chem.* **2006**, *384*, 651.
(675) Gong, J. L.; Liang, Y.; Huang, Y.; Chen, J. W.; Jiang, J. H.; Shen, G. L.; Yu, R. Q. *Biosens. Bioelectron.* **2007**, *22*, 1501.
(676) Nichkova, M.; Dosev, D.; Gee, S. J.; Hammock, B. D.; Kennedy, I. M. *Anal. Biochem.* **2007**, *369*, 34.
(677) Fornara, A.; Johansson, P.; Petersson, K.; Gustajsson, S.; Qin, J.; Olsson, E.; Ilver, D.; Krozer, A.; Muhammed, M.; Johansson, C. *Nano Lett.* **2008**, *8*, 3423.
(678) Lacharme, F.; Vandevyer, C.; Gijs, M. A. M. *Anal. Chem.* **2008**, *80*, 2905.
(679) Wang, J.; Liu, G.; Wu, H.; Lin, Y. *Anal. Chim. Acta* **2008**, *610*, 112.
(680) Jain, K. K. *Expert. Rev. Mol. Diagn.* **2003**, *3*, 153.
(681) Kriz, K.; Ibraimi, F.; Lu, M.; Hansson, L. O.; Kriz, D. *Anal. Chem.* **2005**, *77*, 5920.
(682) Hahn, Y. K.; Jin, Z.; Kang, J. H.; Oh, E.; Han, M. K.; Kim, H. S.; Jang, J. T.; Lee, J. H.; Cheon, J.; Kim, S. H.; Park, H. S.; Park, J. K. *Anal. Chem.* **2007**, *79*, 2214.
(683) Tsai, H. Y.; Hsu, C. F.; Chiu, I. W.; Fuh, C. B. *Anal. Chem.* **2007**, *79*, 8416.
(684) Tsai, H. Y.; Chan, J. R.; Li, Y. C.; Cheng, F. C.; Fuh, C. B. *Biosens. Bioelectron.* **2010**, *25*, 2701.
(685) Tang, D.; Yuan, R.; Chai, Y. *Biotechnol. Lett.* **2006**, *28*, 559.
(686) Tang, D.; Yuan, R.; Chai, Y. *Bioprocess. Biosyst. Eng.* **2008**, *31*, 55.
(687) Ambrosi, A.; Castañeda, M. T.; Killard, A. J.; Smyth, M. R.; Alegret, S.; Merkoci, A. *Anal. Chem.* **2007**, *79*, 5232.
(688) Aurich, K.; Nagel, S.; Glöckl, G.; Weitschies, W. *Anal. Chem.* **2007**, *79*, 580.
(689) Tang, D.; Yuan, R.; Chai, Y. *Anal. Chem.* **2008**, *80*, 1582.
(690) Fu, X. H. *Biochem. Eng. J.* **2008**, *39*, 267.
(691) Kouassi, G. K.; Irudayaraj, J. *Anal. Chem.* **2006**, *78*, 3243.
(692) Chalmers, J. J.; Zaborowski, M.; Sun, L.; Moore, L. *Biotechnol. Prog.* **1998**, *14*, 141.
(693) Menik, K.; Nakamura, M.; Comella, K.; Lasky, L. C.; Zborowski, M.; Chalmers, J. J. *Biotechnol. Prog.* **2001**, *17*, 907.
(694) Ström, V.; Hultenby, K.; Grüttner, C.; Teller, J.; Xu, B.; Holgersson, J. *Nanotechnology* **2004**, *15*, 457.
(695) Kim, E. Y.; Stanton, J.; Korber, B. T.; Krebs, K.; Bogdan, D.; Kunstman, K.; Wu, S.; Phair, J. P.; Mirkin, C. A.; Wolinsky, S. M. *Nanomedicine (London)* **2008**, *3*, 293.
(696) Nie, L. B.; Wang, X. L.; Li, S.; Chen, H. *Anal. Sci.* **2009**, *25*, 1327.
(697) Ao, L.; Gao, F.; Pan, B.; He, R.; Cui, D. *Anal. Chem.* **2006**, *78*, 1104.
(698) Douglas, P.; Stokes, R. J.; Graham, D.; Smith, W. E. *Analyst* **2008**, *133*, 791.
(699) Dittmer, W. U.; de Kievit, P.; Prins, M. W. J.; Vissers, J. L. M.; Mersch, M. E. C.; Martens, M. F. W. C. *J. Immunol. Methods* **2008**, *338*, 40.

(700) Wacker, R.; Ceyhan, B.; Alhorn, P.; Schueler, D.; Lang, C.; Niemeyer, C. M. *Biochem. Biophys. Res. Commun.* **2007**, *357*, 391.
(701) Liu, X.; Xing, J.; Guan, Y.; Shan, G.; Liu, H. *Colloids Surf., A* **2004**, *238*, 127.
(702) Hórak, D.; Babič, M.; Machová, H.; Beneš, M. J. *J. Sep. Sci.* **2007**, *30*, 1751.
(703) Hung, C. W.; Holoman, T. R. P.; Kofinas, P.; Bentley, W. E. *Biochem. Eng. J.* **2008**, *38*, 164.
(704) Park, H. Y.; Schadt, M. J.; Wang, L.; Lim, I. I. S; Njoki, P. N.; Kim, S. H.; Jang, M. Y.; Luo, J.; Zhong, C. J. *Langmuir* **2007**, *23*, 9050.
(705) Yang, H.; Qu, L.; Wimbrow, A. N.; Jiang, X.; Sun, Y. *Int. J. Food Microbiol.* **2007**, *118*, 132.
(706) Gan, Z. F.; Jiang, J. S.; Yang, Y.; Du, B.; Qian, M.; Zhang, P. *J. Biomed. Mater. Res.* **2008**, *84A*, 10.
(707) Käpler, T. E.; Hickstein, B.; Peuker, U. A.; Posten, C. *J. Biosci. Bioeng.* **2008**, *105*, 579.
(708) Huang, S. H.; Chen, D. H. *J. Hazard. Mater.* **2009**, *163*, 174.
(709) White, B. R.; Stackhouse, B. T.; Holcombe, J. A. *J. Hazard. Mater.* **2009**, *161*, 848.
(710) Yantesse, W.; Hongsirikarn, K.; Warner, C. L.; Choi, D.; Sangvanich, T.; Toloczko, M. B.; Warner, M. G.; Fryxell, G. E.; Addleman, R. S.; Timchalk, C. *Analyst* **2008**, *133*, 348.